

Kwame Nkrumah University of Science and Technology, Kumasi

College of Engineering

Department of Agricultural Engineering

KNUST

Modelling the Irrigation Potential of Besease Wetlands



By

Thomas Atta-Darkwa

August 2012

Modelling the Irrigation Potential of Besease Wetlands

By

Thomas Atta-Darkwa

BSc (Hons.) Agricultural Engineering

KNUST

A Thesis submitted to the Department of Agricultural Engineering,
Kwame Nkrumah University of Science and Technology, Kumasi in
partial fulfillment of the requirements for the degree of

**DOCTOR OF PHILOSOPHY IN SOIL AND WATER
ENGINEERING**

College of Engineering

August 2012

DECLARATION

I hereby declare that this submission is my own work towards the PhD and that, to the best of my knowledge, it contains no material previously published by another person nor material which has been accepted for the award of any other degree of the university, except where due acknowledgement has been made in the text.

THOMAS ATTA-DARKWA

PG 9511706

Signature

Date

Students name and ID

Certified by:

PROF. NICHOLAS KYEI-BAFFOUR

Supervisor

Signature

Date

Certified by:

DR. EMMANUEL OFORI

Supervisor

Signature

Date

Certified by:

DR. WILSON AGYEI AGYARE

Supervisor

Signature

Date

Certified by:

PROF. EBENEZER MENSAH

Head of Department

Signature

Date

DEDICATION

To my: father, Stephen Kwabena Kyereh, my mother, Comfort Amankwaa, my siblings and friends who supported me all the way through my pursuit of higher education

KNUST



ABSTRACT

The harsh climate, shallow and erodible soils of low fertility uplands have led to farmers extending their cultivable areas to wetlands for optimal crop production since these systems have the potential for irrigation in the dry season. Inland valleys have been cited as having a high potential for the development of rice-based, small-holder farming systems at the village level, due to their specific hydrological conditions and relatively high soil fertility. To ensure its sustainable use, the physico-chemical and the hydrological processes of the valley bottom should be ascertained. The irrigation potential of wetlands was studied at Ejisu-Besease in the Ashanti Region of Ghana by analysing the hydrodynamics of the valley bottom through a groundwater flow modelling process using MODFLOW. Groundwater recharge estimates from the water table fluctuation method was used as the recharge input into the model. The results showed that annual water level rise ranged from 1105–3115 mm in 2009 and from 397–3070 mm in 2010. A range of specific yields were extracted from the values determined from the soil textural classification triangle. The estimated recharge for the study area ranged from 133–467 mm for the fourteen (14) piezometers, representing 9–31% of 2009 annual rainfall and 47.6–427.9 mm in 2010 representing 4–34 % of the annual rainfall. Groundwater recharge was also estimated using the Kalman filter method. Using the mathematical model developed, the infiltration parameters were determined. The infiltration factor for the years 2009 and 2010 varied from 0.0–16.70 % of the incident rainfall. The results from the groundwater flow model showed that groundwater levels ranged from 259.10–259.97 m in the wet season and 258.19–258.86 m in the dry season of the simulation period. It also exhibited a form of interaction between the inland valley wetland and the Oda River which varied from period to period depending on the river stage. Sensitivity analysis was performed, and model outputs were found to be highly sensitive to the parameters such as horizontal hydraulic conductivity, specific yield and specific storage. The hydrochemical study of the area revealed that alkaline earths exceed alkalis and weak acids exceed strong acids in groundwater which presented a CaHCO_3 groundwater type. Results from the groundwater chemistry of the two boreholes indicated that the groundwater is of good quality for irrigation. The Inland Valley Bottom was also classified into three hydrological regimes as a management tool for developing wetlands for crop production. The regimes are WTF Class I acute slopes segment varying from 0–30 %, WTF Class II acute slopes segment varying from 30–45% and WTF Class III acute slope segment > 45 %. The study unravelled the relationship between recurrent spatial and temporal patterns of watertable response within the inland valley bottom and their controlling factors. It is concluded that a controlled water table offers a distinguishing criterion for the development of Inland Valley Bottoms for year round crop production.

TABLE OF CONTENTS

<i>TITLE PAGE</i>	
<i>DECLARATION</i>	i
<i>DEDICATION</i>	ii
<i>ABSTRACT</i>	iii
<i>TABLE OF CONTENTS</i>	iv
<i>LIST OF TABLES</i>	x
<i>LIST OF FIGURES</i>	xii
<i>LIST OF ABBREVIATIONS AND SYMBOLS</i>	xvi
<i>ACKNOWLEDGEMENTS</i>	xvii
CHAPTER ONE: INTRODUCTION	1
1.1 Background.....	1
1.2 Problem Statement.....	3
1.3 Justification.....	4
1.4 Aims of the Project.....	5
1.4.1 Specific Objectives	5
1.5 Hypothesis of the Study.....	5
1.6 Structure of the Thesis	6
CHAPTER TWO: BACKGROUND AND LITERATURE REVIEW	8
2.1 Introduction to Wetlands	8
2.2 Wetland Occurrence and Extent.....	8
2.3 Wetland Types	9
2.3.1 Marshes.....	9
2.3.2 Swamps.....	11
2.3.3 Peatlands.....	12
2.3.3.1 Bog	13
2.3.3.2 Fens	14

2.3.4	Inland Valley Bottoms.....	15
2.4	Inland Valley Suitability and Factors Affecting Wetland Rice Production.....	15
2.4.1	Geographic Factors.....	16
2.4.2	Climatic Factors.....	16
2.4.3	Land and Soil Factors.....	17
2.4.4	Land Preparation.....	22
2.5	Water Balance.....	23
2.6	Hydrologic Processes in Wetlands.....	24
2.7	Models Used for Wetlands Studies.....	25
2.7.1	The DITCH Model.....	26
2.7.2	The MODFLOW Model.....	27
2.7.3	The USEPA SWMM Model.....	28
2.7.4	The SLURP Model.....	29
2.7.5	The HYDRUS-2D Model.....	29
2.7.6	The UNSATI Model.....	30
2.7.7	The MIKE SHE/MIKE 11 Model.....	30
2.7.8	The WETLANDS Model.....	30
2.7.9	The IWAN Model.....	31
2.7.10	The DEMON Model.....	31
2.7.11	The HEC Model.....	31
2.7.12	The Kalman Filter Model.....	31
2.8	Water Quality.....	32
CHAPTER THREE: MATERIALS AND METHODS.....		38
3.1	Study Area.....	38
3.1.1	Location.....	38
3.1.2	Climate.....	38

3.1.3	Rainfall	39
3.1.4	Temperature.....	39
3.1.5	Relative Humidity.....	39
3.1.6	Evapotranspiration.....	39
3.1.7	Land Use and Vegetation	40
3.1.8	Soils and Geology.....	41
3.1.9	Relief and Drainage	41
3.2	Data Identification and Source	44
3.3	Wetland Vegetation Identification.....	44
3.4	Installation of Piezometers	44
3.5	Watertable Depth.....	45
3.6	Soil Physical Properties	46
3.6.1	Bulk Density	46
3.6.2	Total Porosity	46
3.6.3	Water Content.....	47
3.6.4	Soil Texture	47
3.6.5	Hydraulic Conductivity	48
3.6.5.1	Laboratory Measurement (Falling-Head Method)	48
3.6.5.2	Field Methods	49
3.6.6	Infiltration Rate.....	49
3.6.7	Evaporation Estimates	50
3.6.8	Soil Sampling	51
3.6.9	Groundwater Recharge	52
CHAPTER FOUR: SOIL PHYSICO-CHEMICAL PROPERTIES		54
4.1	Dynamics of Soil Physical Properties	54
4.2	Soil Bulk Density and Porosity	55
4.3	Watertable Depth.....	60

4.4	Computation of Hydraulic Conductivity	60
4.5	Infiltration characteristics of Besease Inland Valley Bottom	66
4.6	Characteristics of the Soil Chemical Properties	68
4.7	Discussion of Physico-Chemical Properties.....	71
CHAPTER FIVE: ESTIMATING GROUNDWATER RECHARGE USING WATERTABLE FLUCTUATION METHOD		72
5.1	Overview of Groundwater Recharge Estimation.....	72
5.2	Water Level Rise Estimation	73
5.2.1	Determination of Specific Yield.....	74
5.3	Results and Discussions.....	76
5.3.1	Water Level Rise	77
5.3.2	Groundwater Recharge Estimation.....	79
5.4	Conclusions	83
CHAPTER SIX:ESTIMATING GROUNDWATER RECHARGE USING THE LINEAR KALMAN FILTER.....		85
6.1	Introduction	85
6.1.1	Model.....	86
6.1.2	The Kalman Filter.....	88
6.1.3	Kalman Filtering Scheme	89
6.2	Results and Discussions.....	93
6.3	Conclusions	107
CHAPTER SEVEN: HYDROCHEMISTRY OF THE BESEASE INLAND VALLEY BOTTOM.....		109
8.1	Introduction	109
8.2	Water Sampling	109
8.3	Results and Discussions.....	110
8.3.1	Chemical Constituents of Groundwater Samples.....	110
8.3.2	Hydrochemistry	110

8.3.3	Graphical Representation of Hydrochemical Data	110
8.4	Groundwater Quality Analysis for Irrigation	114
8.5	Conclusions	115
CHAPTER EIGHT: WATERTABLE FLUCTUATION AND INLAND VALLEY BOTTOMS CLASSIFICATION		
116		
9.1	Introduction	116
9.2	Piezometric Hydrograph.....	117
9.2.1	Shapes and Classifications of Piezometric Hydrographs	117
9.3	Results and Discussions.....	119
9.3.1	Results	119
9.3.1.1	Segmented Watertable Slopes for Different Piezometers	119
9.3.1.2	Slopes of Piezometric Hydrograph.....	126
9.4	Discussions	127
9.4.1	Hydrograph Representation.....	127
9.4.2	Watertable Slopes Segment Fluctuation and Areal Extent.....	128
9.4.3	Watertable Fluctuation and Classification of Inland Valley Bottom ...	128
9.4.4	Watertable Fluctuation Classes	130
9.5	Conclusions	131
CHAPTER NINE: GROUNDWATER FLOW MODELLING USING MODFLOW.....		
133		
10.1	Introduction	133
10.2	Conceptual Model.....	133
10.3	Layer Type and Boundary Conditions.....	135
10.4	Model Boundaries.....	136
10.5	Model Code Selection	137
10.6	Numerical Model.....	138
10.7	Spatial Discretisation.....	138
10.8	Aquifer Geometry.....	139

10.9	Recharge	139
10.10	Hydraulic Conductivity	140
10.11	River Package	140
10.12	Results and Discussions.....	143
10.12.1	Model Calibration.....	143
10.12.2	Model Calibration Evaluation	160
10.12.3	Mass Balance	162
10.13	Uncertainty and Sensitivity Analysis	171
10.14	Groundwater Flow Prediction	175
10.15	Conclusions	178
CHAPTER TEN:GENERAL CONCLUSIONS AND		
RECOMMENDATIONS.....		179
11.1	Introduction	179
11.2	Conclusions	179
11.3	Suggestions for Practicalising Research Results	181
11.4	Recommendations	181
REFERENCES.....		183
APPENDICES.....		202

LIST OF TABLES

Table 2.1	Selected Crop Yield from the Safford Field Experiment Station as Compared to Average Farm Yields (Source: Dutt <i>et al</i> , 1984).....	35
Table 2.2	Red Mountain Farms Lint Cotton Yields (t/ha)	35
Table 2.3	Effect of Irrigation Method on Sodium and Chloride Concentration of the Foliage of Lemon.....	37
Table 4.1	Piezometric Watertable Depth.....	59
Table 4.2	Spatial Saturated Hydraulic Conductivity of the Site from Falling Head Method	63
Table 4.3	Spatial Saturated Hydraulic Conductivity of the Site from Falling Head Method	63
Table 4.4	Hydraulic Conductivity of the Site Using the Mini Disc Infiltrometer.....	64
Table 4.5	Infiltration Rates of the Besease Wetland Site	66
Table 4.6	Chemical Properties of Soils	69
Table 5.1	Values of Specific Yield (Sy) Determined by Type-Curve Matching for 18 Aquifer Tests (Prickett, 1965; cited in Healy and Cook, 2002)	75
Table 5.2	Hydraulic Parameters for Alluvial Deposits, U.K (after Bradford and Acreman, 2003).....	76
Table 5.3	Recharge Values in the Ejisu-Besease Oda River Basin of Ghana, in 2009/2010	76
Table 5.4	Percentage of Groundwater Seasonal Recharge (RC).....	78
Table 6.1	Recharge Values Based on the Present Day Rainfall.....	101
Table 6.2	Values of the Diagonal Elements of the Matrix Q	103
Table 6.3	Recharge Values Based on the Seven Days Previous Rainfall	106
Table 8.1	Percentages of Slopes Exhibited by the Hydrographs.....	126
Table 9.1	Adjusted Parameters for the Groundwater Flow Model.....	144
Table 9.2	Model Fit Statistics for the Transient Run Monthly Values of Observed and Simulated Hydraulic Heads	160
Table 9.3	Volumetric Water Budget.....	165

Table 9.4 Cumulative Water Budget for Different Components in the Model
Area 171

KNUST



LIST OF FIGURES

Figure 2.1	Hydrological Water Balance in Wetlands (Mitsch and Gosselink, 2002)	24
Figure 3.1	Vegetation Map of Ghana [Source: Menz and Bethke, 2000 (Cited in Nyarko, 2007)].....	42
Figure 3.2	Map of the Besease Project Site Showing the Location Piezometric Network	43
Figure 3.3	Piezometer for Monitoring Groundwater Fluctuations.....	45
Figure 4.1	Relationship between Bulk Density and Water Content for Site P13-P 4.....	55
Figure 4.2	Graph of Porosity with Depth for Site P 13-P 4	56
Figure 4.3	Relationship between Bulk Density and Water Content for Site P 11-P 14.....	56
Figure 4.4	Graph of Porosity with Depth for Site P 11-P 14	57
Figure 4.5	Relationship between Bulk Density and Water Content for Site P1-P2.....	57
Figure 4.6	Graph of Porosity with Depth for Site P 1 - P 2	58
Figure 4.7	Relationship between Bulk Density and Water Content for Site P7-P8.....	58
Figure 4.8	Graph of Porosity with Depth for Site P 7 - P 8	59
Figure 4.9	Cumulative Infiltration Versus the Square Root of Time for P1-P2	61
Figure 4.10	Cumulative Infiltration Versus the Square Root of Time for P6-P9.....	61
Figure 4.11	Cumulative Infiltration Versus the Square Root of Time for P6-P7.....	62
Figure 4.12	Cumulative Infiltration Versus the Square Root of Time for P13-P4.....	62
Figure 4.13	Infiltration in Besease Wetland Site P1-P9.....	67
Figure 4.14	Infiltration in Besease Wetland Site P11-P14.....	67
Figure 4.15	Infiltration in Besease Wetland Site P7-P8.....	68
Figure 4.16	Soil pH, Organic Matter (OM), Total Nitrogen (TN) and ECEC of the Wetland.....	70

Figure 4.17	Electrical Conductivity for the different Sampling Points.....	70
Figure 4.18	SAR for the Different Sampling Points	70
Figure 5.1	Graphical Approach for Estimating Recharge for P1	78
Figure 5.2a	Quarterly Recharge Estimate for Piezometer 2	81
Figure 5.2b	Quarterly Recharge Estimate for Piezometer 4	82
Figure 5.2c	Quarterly Recharge Estimate for Piezometer 8	82
Figure 5.3 d	Quarterly Recharge Estimate for Piezometer 14	83
Figure 6.1	Rainfall and Watertable Level During the Years 2009 and 2010 for $Q = 0$	93
Figure 6.20	Parameter Variation with $Q = 0$	94
Figure 6.21	Parameter Variation with $Q = 0.01$ for the Diagonal Element a_2	97
Figure 6.22	Parameter Variation with $Q = 0.01$ for all the Diagonal Elements a_1 , a_2 and a_3	98
Figure 6.23	Comparison of Simulated and Observed Heads in the Besease Inland Valley Wetland	100
Figure 6.3a	Rainfall and Watertable level During the Years 2009 and 2010 for a_2 , $Q = 0.01$	102
Figure 6.3b	Rainfall and Watertable Level During the Years 2009 and 2010 for a_1 , a_2 , a_3 , and $Q = 0.01$	102
Figure 6.4a	Parameter Estimate for a_1 and a_2 with Variable Q Matrix	104
Figure 6.4b	Parameter Estimate for a_3 and a_4 with Variable Q Matrix	104
Figure 6.4c	Parameter Estimate for a_5 and a_6 with Variable Q Matrix	104
		105
Figure 6.4d	Parameter Estimate for a_7 and a_9 with Variable Q Matrix	105
Figure 6.4e	Parameter Estimate for a_9 and Error with Variable Q Matrix.....	105
Figure 6.5	Rainfall and Observed and Simulated Watertable Level During the Years 2009 and 2010 for Previous Seven Days Rainfall, $Q = \text{Variable}$	106
Figure 7.1	Piper Plots for Groundwater Samples.....	112
Figure 7.2	US Salinity Diagram for Groundwater Samples at Besease Inland Valley Bottom.....	113

Figure 8.1	Classification Scheme of Hydrograph by Slopes (Source: Raj, 2004)	118
Figure 8.2a	Hydrograph of P1 dominated by Acute Slopes.....	119
Figure 8.2b	Hydrograph of P2 dominated by Acute Slopes.....	119
Figure 8.2c	Hydrograph of P3 dominated by Acute Slopes.....	120
Figure 8.2d	Hydrograph of P4 dominated by Acute Slopes.....	120
Figure 8.2e	Hydrograph of P5 dominated by Acute Slopes.....	121
Figure 8.2f	Hydrograph of P6 dominated by Acute Slopes.....	121
Figure 8.2g	Hydrograph of P7 dominated by Acute Slopes.....	122
Figure 8.2h	Hydrograph of P8 dominated by Acute Slopes.....	122
Figure 8.2i	Hydrograph of P9 dominated by Acute Slopes.....	123
Figure 8.2j	Hydrograph of P10 dominated by Acute Slopes.....	123
Figure 8.2k	Hydrograph of P11 dominated by Obtuse Slopes.....	124
Figure 8.2l	Hydrograph of P12 dominated by Acute Slopes.....	124
Figure 8.2m	Hydrograph of P13 dominated by Acute Slopes.....	125
Figure 8.3n	Hydrograph of P14 dominated by Flat Slopes	125
Figure 9.1	Conceptual Diagram of Besease Inland Valley Bottom Study Site.	134
Figure 9.2	Monthly Recharge from Watertable Fluctuation	140
Figure 9.3	River Gauge Heights at Ejisu-Besease Station	142
Figure 9.4	Simulated and Observed Heads in the Besease Inland Valley Bottom.....	147
Figure 9.5a	Depth of Estimated Hydraulic Head (m) of Inland Valley in January 2009	150
Figure 9.5b	Depth of Estimated Hydraulic Head (m) of Inland Valley in June 2009.....	151
Figure 9.5c	Depth of Estimated Hydraulic Head (m) of Inland Valley in September 2009	152
Figure 9.5d	Depth of Estimated Hydraulic Head (m) of Inland Valley in October 2009.....	153
Figure 9.5e	Depth of Estimated Hydraulic Head (m) of Inland Valley in March 2010	154
Figure 9.5f	Depth of Estimated Hydraulic Head (m) of Inland Valley in June 2010	155

Figure 9.5g	Depth of Estimated Hydraulic Head (m) of Inland Valley in August 2010	156
Figure 9.5h	Depth of Estimated Hydraulic Head (m) of Inland Valley in September 2010	157
Figure 9.5i	Depth of Estimated Hydraulic Head (m) of Inland Valley in October 2010.....	158
Figure 9.5j	Depth of Estimated Hydraulic Head (m) of Inland Valley in December 2010	159
Figure 9.6	Comparison of Simulated and Observed Heads in the Besease Inland Valley Wetland for a Period of two Years (January 2009 to December 2010).....	161
Figure 9.7	Graph of Sensitivity Analysis for Hydraulic Conductivity	173
Figure 9.8	Graph of Sensitivity Analysis for Specific Yield	174
Figure 9.9	Graph of Sensitivity Analysis for Specific Storage	174
Figure 9.10	Calculated Heads (m) for the Dry Period	176
Figure 9.11	Calculated Heads (m) for the Wet Period.....	177



LIST OF ABBREVIATIONS AND SYMBOLS

Abbreviations	Description
GIS	Geographic Information Systems
IFPRI	International Food Policy Research Institute
IVs	Inland Valleys
MOFA	Ministry of Food and Agriculture
CRI	Crops Research Institute
CSIR	Council for Scientific and Industrial Research
AHT	Agrar-und Hydrotechnik
FAO	Food and Agriculture Organisation
NRC	National Research Council (USA)
USEPA	United States Environmental Protection Agency
TCTC	Tropic of Cancer and the Topic of Capricorn
CEC	Cation exchange capacity
IRRI	International Rice Research Institute
IITA	International Institute of Tropical Agriculture
SWI	Surface water inflow
SWO	Surface water outflow
GWI	Groundwater inflow
GWO	Groundwater outflow
EC	Electrical Conductivity
SAR	Sodium Absorption Ratio
K_{sat}	Saturated Hydraulic Conductivity
PWT	Piezometric watertable
AWT	Actual watertable
NR	Near River
NU	Near Upland
MRC	Master recession curve
APHA	American Public Health Association
WTF	Watertable fluctuation
USSLS	United State Salinity Laboratory Staff

ACKNOWLEDGEMENTS

Above all else, I would like to thank the Almighty GOD for all his guidance, provision and mercies throughout my life, and for helping me to get to this point.

I would like to express my sincere gratitude to my supervisors, Prof. Nicholas Kyei-Baffour and Dr. Emmanuel Ofori for their supervision, formulating the subject of the thesis, fruitful discussions, encouragements and support throughout the period from the first stage to its completion.

I am also grateful to the Department of Agricultural Engineering for their support during the study. Special thanks are extended to Dr. Benjamin Kofi Nyarko at the University of Cape Coast, Department of Tourism and Geography and Mr. Emmanuel Owusu Ansah of the Department of Mathematics, KNUST, for their invaluable assistance and scientific advice in the construction of groundwater flow and the Kalman filter model.

I pay tribute to George Doda, Isaac Yankson, Appiah Kubi, George Ashiagbor and Adu Poku Adarkwa at the Department of Geomatic Engineering, for the surveying and GIS work. Special thanks are due to Mr Robert Ebo Ghunney, the Ashanti Regional Manager of the Meteorological Services Agency for providing climate information of the area. My sincere thanks go to Mr. Anthony Kpetepe, and Mr. Sadiq Adams of the Soil Research Institute, Kumasi for their laboratory assistance. My great thanks go to Inusah Seidu, Fuseini Adama and Aziz Zakari of Besease for their continuous support during my study.

I would like to express my sincere gratitude to the authorities of the Kwame Nkrumah University of Science and Technology and the Ministry of Food and Agriculture for sponsoring this research. I am also grateful to my brothers and sisters

and my friends Francis Kumi, Collins Bonsu, George Addo, Gaston Edem Awashie and Olivia Afriyie for the encouragement they gave me during tough times. Finally, many thanks go to the ones who gave me diverse support but I forgot to mention them.

Thomas Atta-Darkwa

August 2012

KNUST



CHAPTER ONE

INTRODUCTION

1.1 Background

There is growing concern about food security in Africa especially in sub-Saharan Africa. Whilst the aggregate global food supply/demand picture is relatively good, it is projected that there will be a worsening in food security in sub-Saharan Africa and cereal imports are projected to treble by 2020 (IFPRI, 1995). To arrest this, agricultural productivity should keep pace with population increase and the cultivated area has to be increased to achieve high production growth. To increase yield, both rain-fed and irrigated agriculture will have to be intensified. Irrigated agriculture offers a higher potential for intensification. Global estimates indicate that irrigated agriculture produces nearly 40 % of food and agricultural commodities on 17% of agricultural land (IFPRI, 1995). The harsh climate and shallow erodible and low fertility of uplands soil have led to farmers extending their cultivable areas to wetlands for optimal crop production since these systems have the potential for irrigation in the dry season. Inland valleys (IVs) have been cited as having high potential for development of rice-based, small-holder farming systems at the village level, due to their specific hydrological conditions and relatively high soil fertility. Farmers along the Oda River in Ejisu-Besease in the Ashanti Region of Ghana practice floodplain cultivation as a form of supplementary irrigation. The Government of Ghana through the Ministry of Food and Agriculture (MoFA) and the Crops Research Institute (CRI) of the Council for Scientific and Industrial Research (CSIR) is actively encouraging floodplain cultivation, which can be practiced in the dry season using pumped river water as a source of irrigation. This has led to improve

food production for surrounding communities. Flood plains, swamps and lakes provide a range of ecological resources and economic opportunities. Without wetlands, the dry lands of the West African Sahel would be both less productive and more hazardous as a place for people to live (FAO, 1995). Owing to the importance of wetlands they are included as waters and sites for preservation in most countries around the world. Wetlands have important functions: they serve as infiltration basins, route floods, and store water which fluctuate over time and space which is discharged gradually to adjacent streams, thereby influencing runoff in a catchment. Therefore runoff, a component of the hydrological cycle, is considered an important process in the study of hydrology. Knowledge about runoff and storage components of the hydrological cycle is limited and the water balance for the floodplain has not been modelled in Ghana. Therefore understanding the spatial and temporal distribution of runoff and storage components is a key to capturing the behaviour of the catchment (Nyarko, 2007). Initial storage, antecedent moisture, volume and intensity of rainfall, surface cover will help to further understand the behaviour of unconfined aquifers as well. Information about catchment behaviour (response to rainfall input) is fundamental to the understanding of the overall hydrological processes in the Ejisu-Besease Oda River Basin. For instance, in scheduling the irrigation water requirement for the Besease wetlands, Serrano and Unny (1987) reported that, it is necessary to calculate an optimal estimate of the groundwater table elevation due to an available weather forecast in order to determine an adequate irrigation depth for maximum crop yield. The changes in permeability of adjacent uplands have effect on runoff contribution to wetlands which in turn have ramifications on groundwater table variation. In this vein, researchers are challenged to model adequately and understand the contribution of runoff on wetlands to groundwater flow processes in the

hydrological meso-macro scale in order to meet the water demands of both wet and dry season crops. As noted by Nyarko (2007), subsurface water of the floodplain wetlands in the White Volta Basin plays a vital role as it acts as a major source of water for agricultural activities for farming communities. However, there is a growing concern about the sustainable use and management of this resource. In other words, an understanding of the recharge characteristics of floodplain wetland to rainfall inputs is necessary for viable sustainable floodplain agriculture. For any policy formulation, it is important to assess how sustainable wetland water supply will be able to meet the demand of a unit area of floodplain under cultivation.

1.2 Problem Statement

The people of Besease normally use the swamp land for rice cultivation. During high rainfall intensities, the runoff and overflow of the river run over the cultivated area causing it to be flooded. The flood damages the crops, stays on the field for few weeks leading to subsequent leaching of fertiliser applied to the field. Also rainfall delay coupled with short periods of rainfall results in crop loss with associated economic hardship to the people of Besease. In Zimbabwe and Mozambique, Marneweck and Batchelor (2002) noted that many poor people depending on agriculture for their living utilise wetlands to mitigate problems of low crop yields associated with droughts across the region, and the low rainfall that is characteristic of the basin. The soil moisture regime in the dry periods and also periods between rainfall events has not been studied and for that matter not known to the farmers. The water balance of the valley bottom in Besease has not been modelled to know the water input and output to the wetland and the key terms that can contribute to the sustenance of dry season crop cultivation.

1.3 Justification

The growing population of Besease needs fresh water for agricultural production. There is the need to improve the natural resources of water and land by providing structures for control and distribution of runoff water. In Ghana, the perennial shortages of water in several regions as a result of the drying-up of raw water storage reservoirs and flows in streams and rivers from late November to early March is an indication that water will have to be harnessed to meet the demands in these periods. The management of water could often ensure its absorptions as clean water into the soil and thus control, to some extent, its flow towards the ocean, its storage and distribution. Dry season crop production and livestock production are some of the uses of *dambos* and riverine wetlands in Mozambique (Gomes *et al.*, 1998). In drought years, wetlands often have sufficient moisture to sustain crop production, mitigating the potential impacts of drought on food availability. Irrigation in the wetlands provides the means to intensify food production, and alleviates constraints resulting from short drought spells or mid-season droughts. In Ghana, there are large wetland areas but most of them are still unexploited or underutilised. Recently, in recognition of the limitations of upland production systems to provide sustainable food security to the populations, many Sub-Saharan Africa countries have promoted the development of wetland areas for agricultural production (Andriessse *et al*, 1993). In Sub-Sahara Africa, most rice production increases during the last two decades as a result of the expansion of area under cultivation, principally is in the upland production systems. Even with this rapid expansion of area under cultivation, total annual growth in rice output is still inferior to growth in demand for rice in several countries including Ghana.

The outcome of the study could be used as a reference document by government or private entities/enterprises especially NGO's for consideration to develop wetlands for food production. The water balance for the area has been developed to assist in designing the agricultural potential of the area for rice, vegetable and other crop production activities.

1.4 Aims of the Project

The main objective of this study was to model the hydrological possibilities of developing the Besease wetlands into a sustainable crop production area.

1.4.1 Specific Objectives

The specific objectives of the study were:

1. To establish baseline information about the conditions of the Besease wetlands for developing it for crop production,
2. To assess the physico-chemical properties of the Besease inland valley bottom soil and water,
3. To determine the response of wetland watertable to rainfall events,
4. To estimate the groundwater recharge of the inland valley bottom and finally
5. To model the water balance for the area.

1.5 Hypothesis of the Study

The specific objectives were used in the formulation of hypotheses to guide the study and these hypotheses were formulated around the achievement of good experimental results.

The null hypotheses (H_0) are;

Wetlands are not conducive landforms for development of crop production.

Wetland watertables do not fluctuate under variable rainfall conditions.

Numerical Groundwater flow models are not the options for modelling the water balance of wetlands.

The alternate hypotheses (H_1) are;

Wetlands are conducive landforms for development of crop production.

Wetland watertables fluctuate under variable rainfall conditions.

Numerical groundwater flow models are the best options for modelling wetland water balance.

1.6 Structure of the Thesis

The thesis is organised into ten chapters. Chapter 1 captures the introduction, statement of the problem, justification and research objectives. Chapter 2 presents a review of wetland types, characteristics of inland valley bottoms, models used in wetland studies and water quality criteria for irrigation. Chapter 3 deals with the materials and methods of the research work. The physico-chemical properties of the soils in the study area are discussed in Chapter 4. Chapter 5 and chapter 6 talk about the estimation of groundwater recharge using the Watertable Fluctuation and the Kalman Filter Methods respectively. Chapter 7 dwells on the hydrochemistry of the Besease wetlands. Chapter 8 is devoted to the classification of Besease valley bottom for crop production. Numerical groundwater flow modelling of the catchment of River Oda at Ejisu-Besease is presented in Chapter 9. Finally, Chapter 10 gives a

synthesis of this work. It summarises the findings of the research by converging outcomes from the different approaches used in the study.

KNUST



CHAPTER TWO

BACKGROUND AND LITERATURE REVIEW

2.1 Introduction to Wetlands

Studies of wetlands in Africa with respect to hydrology, status of appropriate databases and analytical techniques are yet to be consolidated, and this is frequently hampered by the lack of reliable hydrological records (Bonell and Balek, 1993). Currently, there have been little or no attempts to collate and integrate findings of those few existing studies in a comprehensive manner. However, efforts are being made by the Centre for Africa Wetlands located at the University of Ghana to collate studies on African wetlands as a first step in creating appropriate databases. These studies can be put into three main categories:

- Detailed investigations of individual wetlands,
- Regional hydrological studies concerned with the relationships between wetland extent and river flow regimes, and
- Monitoring and modelling of internal wetland hydrology for developmental purposes.

An understanding of the dynamics of floodplain wetland hydrology in Africa is a key step toward their management (Nyarko, 2007).

2.2 Wetland Occurrence and Extent

Wetlands are dynamic landforms characterised by periods of saturation that produce a recognizable wetland substrate and biota (NRC, 1995). Wetlands typically occur in low-lying areas that receive fresh water at the edges of lakes, ponds, streams, and rivers, or salt water from tides in coastal areas protected from waves. In wetlands, the surface of the water, called the watertable, is usually at, above, or just below the land

surface for enough time to restrict the growth of plants to those that are adapted to wet conditions and promote the development of soils characteristic of a wet environment (Wilcox, 2002). These lands have hydromorphic soils and they normally support hydrophytes, halophytes and mesophytes. By implication they can either be under permanent or intermittent flooding. They normally occur in valleys, lowlands, floodplains, coastal plains and depressions. Accurate data on actual land use is often hard to come by. Wetlands are, however, estimated to cover 900 million hectares (Burrow, 1990) which is quite substantial compared with global estimates of arable land under cultivation. According to other estimates, wetlands cover 6×10^6 km² of actual land cover and this is about 4% of land cover (Fresco, 1994; cited in Kyei-Baffour and Agodzo, 1996). The aggregate extent of small wetlands has probably been under-estimated in world level inventories.

2.3 Wetland Types

The wetlands in Ghana are of two types: the coastal zone wetlands, non-coastal inlands. These can be further classified by water regimes, topography, soils, vegetation, animal life and resource potential and use (Anderson, 1997). Coastal wetlands are among the most biologically productive ecosystems in the world. However, more than two-thirds of the population lives along the coast and they are under heavy pressure to be drained and filled for urban and industrial development (Mitsch and Gosselink, 2000).

2.3.1 Marshes

Marshes are defined as wetlands frequently or continually inundated with water, characterized by emergent soft-stemmed vegetation adapted to saturated soil conditions. There are many different kinds of marshes, ranging from the prairie potholes to the everglades, coastal to inland, freshwater to saltwater. All types receive

most of their water from surface water, and many marshes are also fed by groundwater. Nutrients are plentiful and the pH is usually neutral leading to an abundance of plant and animal life. Non-tidal marshes are the most prevalent and widely distributed wetlands in North America. They are mostly freshwater marshes, although some are brackish or alkaline. They frequently occur along streams in poorly drained depressions, and in the shallow water along the boundaries of lakes, ponds, and rivers. Water levels in these wetlands generally vary from a few centimetres to 60 or 90 cm, and some marshes, like prairie potholes, may periodically dry out completely. It is easy to recognize a non-tidal marsh by its characteristic soils, vegetation and wildlife.

Highly organic, mineral rich soils of sand, silt, and clay underlie these wetlands, while lily pads, cattails, reeds, and bulrushes provide excellent habitat for waterfowl and other small mammals, such as red-winged blackbirds, great blue herons, otters, and muskrats. Prairie potholes, playa lakes, vernal pools, and wet meadows are all examples of non-tidal marshes. Tidal wetlands provide a wide range of ecosystem services. As transitional zones between uplands and estuaries, they mediate the exchange of sediments, nutrients, organic matter, and pollutants between terrestrial and aquatic ecosystems and are important factors in determining the quality of surface waters and the viability of local fisheries. Tidal marshes are found along protected coastlines in middle and high latitudes worldwide. They are most prevalent in the United States on the eastern coast from Maine to Florida and continuing on to Louisiana and Texas along the Gulf of Mexico (USEPA, 2007). Some Tidal marshes are freshwater marshes, brackish, and saline, but they are all influenced by the motion of ocean tides. Tidal marshes are normally categorized into two distinct zones, the lower or intertidal marsh and the upper or high marsh. In saline tidal marshes, the

lower marsh is normally covered and exposed daily by the tide. It is predominantly covered by the tall form of smooth cordgrass (*Spartina alterniflora*). The saline marsh is covered by water only sporadically, and is characterized by short smooth cordgrass, spike grass, and black grass (*Juncus gerardii*). Saline marshes support a highly specialized set of life adapted for saline conditions. Brackish and fresh tidal marshes are also associated with specific plants and animals, but they tend to have a greater variety of plant life than saline marshes.

2.3.2 Swamps

A swamp is any wetland dominated by woody plants. There are many different kinds of swamps, ranging from the forested red maple (*Acer rubrum*), swamps of the Northeast USA, to the extensive bottomland hardwood forests found along the sluggish rivers of the Southeast USA. Swamps are characterized by saturated soils during the growing season and standing water during certain times of the year. The highly organic soils of swamps form a thick, black, nutrient-rich environment for the growth of water-tolerant trees such as cypress (*Taxodium* spp.), Atlantic white cedar (*Chamaecyparis thyoides*), and tupelo (*Nyssa aquatica*).

Some swamps are dominated by shrubs, such as buttonbush or smooth alder. Plants, birds, fish, and invertebrates such as freshwater shrimp, crayfish, and clams require the habitats provided by swamps. Many rare species, such as the endangered American crocodile depend on these ecosystems. Forested swamps are often inundated with floodwater from nearby rivers and streams. Sometimes, they are covered by many metres of very slowly moving or standing water. In very dry years, they may represent the only shallow water for kilometres and their presence is critical to the survival of wetland-dependent species like wood ducks (*Aix sponsa*), river otters (*Lutra canadensis*), and cottonmouth snakes (*Agkistrodon piscivorus*). Some of

the common species of trees found in these wetlands are red maple and pin oak (*Quercus palustris*) in the Northern United States, overcup oak (*Quercus lyrata*) and cypress in the South, and willows (*Salix* spp.) and western hemlock (*Tsuga* sp.) in the Northwest of USA. Bottomland hardwood swamp is a name commonly given to forested swamps in the south central United States.

Mangrove swamps are coastal wetlands found in tropical and subtropical regions. They are characterised by halophytic (salt loving) trees, shrubs and other plants growing in brackish to saline tidal waters. These wetlands are often found in estuaries, where fresh water meets salt water and are infamous for their impenetrable maze of woody vegetation. In North America, they are found from the southern tip of Florida along the Gulf Coast to Texas. Florida's southwest coast supports one of the largest mangrove swamps in the world.

2.3.3 Peatlands

The formation of Newfoundland's peatlands was initiated about 5000-10000 years ago following the most recent glacial retreat (Rayment, 1993) in Canada. A peatland is a wetland on which extensive organic material has accumulated. Peat soils are almost entirely organic matter, about 93-97 %. A soil that is more than 30 % organic matter is considered an organic soil. Johnson and Bernard (1984) observed that a minimum depth of 40 cm of peat is required before the wetland can be defined as an organic soil. In general, peat accumulation results when the primary peat production exceeds its decomposition for a prolonged period. On average, the rate of peat formation is about 0.6-0.7 mm per year. It is the relatively slow rate of decomposition, rather than the rate of production, that is responsible for the accumulation. The decomposition rate is slow because the peatland environment is unfavourable for growth and activity of many organisms capable of breaking down the peat. The older, deeper peat is more

highly decomposed than the near-surface peat. Peat that is decomposed to a limited extent is called fibric, while increased decomposition is classified as mesic and advanced decomposition as humic.

2.3.3.1 Bog

When the peatland and its surface vegetation obtain their water and nutrients primarily from precipitation, the peatland is termed ombrotrophic. Bogs are ombrotrophic peatlands in which the water table occurs at or near the surface. Bogs are nutrient-poor with an extremely acid reaction (pH 3.5-4.5) resulting in a limited diversity of naturally occurring plant species. Bogs are one of North America's most distinctive kinds of wetlands. They are characterized by spongy peat deposits, acidic waters, and a floor covered by a thick carpet of sphagnum moss. Peat bogs develop because there is an excess of water within the landscape due to climate (i.e. high precipitation and cool temperatures) and restricted drainage. Newfoundland's mean annual precipitation varies from about 500 mm in the northwest to 1500 mm on the Avalon Peninsula. Most of this precipitation ends up as moisture surpluses. This has contributed to the formation of bogs up to 4-5 m in depth over much of Newfoundland's poorly drained landscapes. Bogs receive all or most of their water from precipitation rather than from runoff, groundwater or streams. As a result, bogs are low in the nutrients needed for plant growth, a condition that is enhanced by acid forming peat mosses.

There are two primary ways that a bog can develop: bogs can form as sphagnum moss grows over a lake or pond and slowly fills it (terrestrialisation), or bogs can form as sphagnum moss blankets dry land and prevents water from leaving the surface (paludification). Because of their ubiquity and extent, sphagnum peat bogs are the peatlands that are most commonly developed for vegetable production.

Over time, many metres of acidic peat deposits build up in bogs of either origin. The unique and demanding physical and chemical characteristics of bogs result in the presence of plant and animal communities that demonstrate many special adaptations to low nutrient levels, waterlogged conditions, and acidic waters, such as carnivorous plants.

2.3.3.2 Fens

When the vegetation obtains its nutrients from the groundwater, the peatland is termed minerotrophic. Fens are minerotrophic peatlands with the watertable at or just above the surface of the peat. In general, the pH of a fen is very acid to alkaline (about 4.5-7.5) with the watertable at or just above the surface of the peat. Fens are peat-forming wetlands that receive nutrients from sources other than precipitation: usually from upslope sources through drainage from surrounding mineral soils and from groundwater movement. Fens differ from bogs because they are less acidic and have higher nutrient levels. They are therefore able to support a much more diverse plant and animal community. These systems are often covered by grasses, sedges, rushes, and wildflowers. Some fens are characterized by parallel ridges of vegetation separated by less productive hollows. The ridges of these patterned fens are perpendicular to the downslope direction of water movement. Over time, peat may build up and separate the fen from its groundwater supply. When this happens, the fen receives fewer nutrients and may become a bog. Like bogs, fens are mostly a northern hemisphere phenomenon, occurring in the northeastern United States, the Great Lakes region, the Rocky Mountains, and much of Canada, and are generally associated with low temperatures and short growing seasons, where ample precipitation and high humidity cause excessive moisture to accumulate (Penny *et al*, 1991).

2.3.4 Inland Valley Bottoms

Inland Valley Systems (IVs) are abundant in Ghana, as in other West African countries. According to Wakatsuki *et al.* (1998), the estimated potential area for small-scale, irrigated sawah in inland valley watersheds in Ghana is 700,000 ha. Inland valley systems are complex landforms of the upper parts of river watersheds. They comprise the toposequence of valley bottoms, which may be submerged for most parts of the year, their hydromorphic fringes and contiguous upland slopes and crests extending over an area that contributes runoff and seepage to the valley bottom (Windmeijer and Andriessse, 1993). In Ghana, as in other West African countries, IVs are heterogeneous in morphology, soil type, vegetation, hydrology and agronomic practices. Within the agro-ecological zones, various crops are grown under a range of distinct ecological condition that is determined by both topography (that is, position in the inland valley) and human modifications. Given their assured water supply and relatively fertile soils, IVs can contribute to an increase in and stabilization of food production, resulting in a consolidation of food security. Effective utilization of these ecologies can boost Ghana's food production.

2.4 Inland Valley Suitability and Factors Affecting Wetland Rice Production

The suitability of inland valleys for rice cultivation depends on parameters that are valley-related and non-valley-related. Non-valley-related parameters include climatological conditions, socio-economic factors and cultivation methods. In the Savanna Zones, the main climatological constraints are the rainfall distribution and its irregularity, high temperatures during the second crop cycle, and the seasonally low night temperatures. In the Equatorial Forest Zone, the main climatological constraints are the high air humidity and the low solar radiation. The socio-economic conditions at present prevailing in West Africa have a strong negative impact on agricultural

production. The rapid population growth, rural-urban migration, results in labour shortages in the rural areas and decreasing rice production per caput and changing food preferences. The shortage of labour also results in inappropriate farming and cropping methods because the optimum cropping calendar cannot be followed. Furthermore, compared with crops like maize and millet, the low net return of the rice-cropping systems to labour does not stimulate the farmers to increase their rice production. At valley scale, the main constraints to rice production result from the soils, hydrology, and valley shape. If these constraints are not too severe, they can be improved by relatively simple technical interventions.

2.4.1 Geographic Factors

Wetland rice cultivation extends from 45° North to 40° South in Japan. In general, yields of wetland rice planted in the areas between the Tropic of Cancer and the Tropic of Capricorn (TCTC) zone are lower than those of rice planted in areas outside of this zone.

2.4.2 Climatic Factors

Temperature regimes greatly influence not only the growth duration but also the growth pattern of rice plants. Rice varieties from Japan which has low temperatures during the cropping season when grown in Indonesia has moderate to high temperatures during the cropping season. They generally mature early whereas Indonesian varieties when grown in Japan generally extend growth duration. In temperate countries, generally, low temperature regimes limit rice cropping to only one season. On the other hand, it is known that respiration is low at low temperatures. The low respiration, due to low night temperatures during the grain development

phases of rice plants grown in areas outside the TCTC zone may favour grain development and filling, thus guaranteeing high yields.

Solar radiation is essential for photosynthetic activity. As such, the growth, development and yield of rice plants are affected by the level of solar radiation. Rice yields are closely correlated with solar radiation during the reproductive and ripening phases of rice plants. Day-length is an important factor affecting wetland rice production. With the availability of an increasing number of high yielding and non-photoperiod-sensitive rice varieties, the effect of day-length on wetland rice production is becoming less and less important. However, the long day and short night regimes coupled with high level of solar radiation during reproductive and ripening phases of rice, planted in countries having temperate climate, are generally favourable for high yields.

Winds and relative humidity may affect growth and production of rice plants. Winds at high speeds during the typhoons are very detrimental to the growth and production of rice, especially when they occur during the flowering and ripening phases.

2.4.3 Land and Soil Factors

Most of the wetland rice fields are developed in river valleys, basins, deltas, estuaries, lake fringes and coastal plains. The topography of most of these areas is either level or gently undulating with slopes varying from 0-8 %. Rice being a semi-aquatic plant, poor to moderately-well drained conditions are best suited for hydromorphic and wetland rice cultivation. Wetland rice is grown on practically all types of soils, from sandy loam to heavy clay. However, it is well established that the heavy soil characteristic of river valleys and deltas are better suited to wetland rice production

than lighter soils. An ideal rice soil should contain up to 50-60% of finer fractions of silt and clay. Well-drained and excessively well-drained soils carry a drought risk. Such a risk may be overcome by levelling and by constructing bunds around the fields to retain the water. Continuous saturation is not suitable for rice because some alternating oxidation and reduction of the (top) soils is required for good rice growth. Coarse-textured soils generally are less productive than soils with a fine texture. This is due to the lower inherent fertility of the former, but also due to their higher percolation rates, by which nutrients (including fertilisers) are easily leached beyond the rootzone. On sandy soils, therefore, fertilizers should be applied in several small doses rather than in one or two large applications. The higher percolation of sandy soils implies that it is difficult to retain water on the field. Also, coarse-textured soils lend themselves less well for the construction of bunds, dykes, and drains than do loams or clays. The inherent fertility of sandy soils in general is very low. In such soils, the cation exchange capacity (CEC) depends largely on the organic matter. This serves as storage for plant nutrients, but it is a source of nutrients too, mainly of nitrogen.

In clayey soils, the fertility is generally higher. Here, the CEC depends not only on the organic matter and clay content, but also on the clay mineralogy. Kaolinitic clays, which dominate the clay fraction of alluvium derived from granitic Basement Complex rocks and which prevail in the humid parts of West Africa, have a low CEC compared with illite, vermiculite, and smectite. The latter clay minerals are slightly more abundant in alluvium derived from the metamorphic Basement Complex rocks (schists, greenstones, and amphibolites). Alternatively, they are formed *in situ* in the drier zones of the inventory area. In general, a high base saturation is favourable for plant growth. It is of limited relevance, however, if the total amount of bases available

to the plant is low (i.e. if the CEC is low), as is the case in many valley bottom soils. Soil reaction (pH) in the valley bottoms of West Africa ranges from extremely acid (pH 4.0-4.5) to slightly acid (pH 6.1-6.5). For rice production, this is a suitable range, considering that, upon reduction of the (top) soil following submergence; the pH tends to change towards neutral (pH 6.5-7.0). Most plant nutrients are most readily available for uptake by roots in a slightly-acid to near-neutral environment (IRRI, 1978).

The deficiency of nitrogen is the most common constraint to wetland rice production. Uncertainty, however, exists as to factors affecting the nitrogen supply capacity of rice soils under flooded conditions. It had been commonly believed that the total soil nitrogen could be an adequate guide to nitrogen release. Recently, however, results from long-term experiments have provided evidence that soil (N) supply is governed more by the chemical qualities than the amounts of soil organic matter and soil N (Cassman *et al*, 1998). Although the availability of phosphorus is generally improved under flooded conditions, phosphorus deficiency is the next commonly observed constraint to wetland rice production, especially in acidic soils with light texture. Increasing evidences of potash, zinc, sulphur deficiencies have been observed in wetland areas under continuous cropping with high yielding rice varieties. In the valley bottoms, however, the fertility of the soils is also governed by the hydrology of the valley. Because of submergence, the pH becomes near neutral, and phosphate, for instance, becomes more readily available. To increase the productivity of these soils, fertiliser applications are necessary. The efficiency of the fertilizers depends on the management level of the farms. Soil and fertilizer nutrients are lost by different processes. On the uplands, large amounts of nutrients are lost by leaching, erosion, or fixation (phosphate). The extent of these losses depends on the soil texture and the

content of sesquioxides in the soil. On the (colluvial) footslopes, besides leaching (N and K) and fixation (P), losses of nitrogen by volatilization and denitrification are high. In the valley bottom, loss of nitrogen by denitrification and volatilisation is the main problem. Nitrogen in the soil is susceptible to various loss mechanisms, including leaching, denitrification and volatilisation. These loss mechanisms act most severely in strongly alternating wet and dry environments, as occur in the (colluvial) footslopes. Moormann *et al* (1977) found that nitrogen deficiency was highest in these phreatic zones of the inland valleys. On the uplands, nitrogen is lost mainly by leaching. Leaching is highest in the most humid zone of West Africa (i.e. the Equatorial Forest Zone).

In the drier Guinea Savanna and Sudan Savanna Zones, the recovery of nitrogen is higher. In lowland rice cultivation, the major loss of nitrogen is due initially to NH_4^+ volatilization, followed by denitrification. Any management techniques aiming at a more efficient use of nitrogen fertilizer and a reduction of N-loss must necessarily look for ways to delay nitrification (Goswami *et al*, 1986). Iron toxicity is one major constraint of wetland rice production, especially in inland valley swamps in West Africa (Jamin and Andriessse, 1993). In the Equatorial Forest and Guinea Savanna Zones, wetland and hydromorphic rice cultivation faces the problem of iron toxicity. Iron toxicity is mostly found in the lower parts of the colluvial footslopes and in the adjacent parts of the valley bottoms. This problem, which has been reported from many West African countries, appears to be most severe in areas where Ferralsols dominate (Sierra Leone, Liberia, southeastern Nigeria, and Cameroon). Ferrous iron (Fe^{2+}) is either formed in the soil by the reduction under acid conditions of ferric iron (Fe^{3+}), already present *in situ*, or it is brought into the rootzone by subsurface flow

from the uplands. Under reduced conditions, ferrous iron affects the development of the rice crop in two ways:

- By coating the plant roots with iron oxide and thus reducing the absorption capacity of the plant for other nutrients, such as P, K, Ca, and Mg (Fe^{2+} -induced deficiency), or
- By direct iron toxicity through excessive Fe^{2+} absorption by the plant.

Iron toxicity in rice plants shows as a characteristic orange discolouration (bronzing) of the leaves (Howeler, 1973). Possible remedies, apart from the use of tolerant rice varieties, include seasonal drying of affected fields (oxidation of Fe^{2+} to insoluble Fe^{3+}) or interception of the subsurface water flow containing ferrous iron (IITA, 1982). The availability of soil nutrients, however, changes with the moisture regimes of soils. The damage to rice crops varies with the developmental stage during which water deficiency occurs and the duration of the water deficiency. Damage is usually heavy and irreparable when intensive water deficiency occurs during the reproductive and flowering phases of rice crop. Yield losses of one t/ha or more may occur after 10 days with continuous water deficiency during these phases. Although rice plants are well known for their ability to transport oxygen from air to their root systems, flooding with consequent crop submergence may severely damage rice crop. Most of wetland rice cultivars, including deep-water ones, can stand complete submergence for at least 6 days before 50% of crops die, whereas 100% mortality occurs in all cultivars within 14 days of complete submergence (Setter *et al*, 1995).

Adequate and controllable water supply to wetland rice is possible only with the development of irrigation and drainage infrastructures. Run-off water from watershed areas can be stored with the construction of dams and reservoirs and then supplied to rice

fields. Water from major rivers can be diverted to rice fields with the construction of diversion dams and/or be lifted to rice field using either modern or traditional water lifting devices. Water in underground aquifers can be lifted through installation of tube/deep wells and utilisation of pumps. Therefore, the availability of water sources and their potentials for irrigation development for wetland rice cultivation are important factors affecting the development of wetland rice production. In fact, it is well recognized that the development of irrigation infrastructure is one of the main pillars of successful green revolutions in many Asian rice producing countries during the 1970s and 1980s.

2.4.4 Land Preparation

Land preparation by itself may not be necessary for successful wetland rice production. However, land preparation indirectly affects rice yield through resultant better field conditions. Land preparation is recognised as an effective weed control practice. Also, good land preparation facilitates better water management and to a lesser extent fertilizer management in wetland rice production. Land preparation using the hand hoe is widely practiced by women in small inland swamps in West Africa whereas animal traction and/or small motorcultors/tractors are popular in tropical Asian and African developing countries where the area of wetland rice fields per household varies from a few thousand square metres to a few hectares. On the other hand, in many areas in America, Australia, and Europe, where the wetland rice area per household ranges from several tens to several hundreds of hectares, land preparation and levelling are mainly done with the use of laser-guided tractors and weed control is done with herbicides. The available tools and equipment, the sex of the person who is responsible for the land preparation and the size of the fields interactively affect the quality of land preparation and thus the performance and yield of wetland rice.

2.5 Water Balance

In studies of wetland hydrology, the water balance is a central concept. It expresses the movement of water into, through and out of the wetland, and the storage of water within it and the relative significance of the different terms of this balance underlie the hydrological functions, water quality functions and the management of the wetland for conservation (Gilman, 1994). The input for a floodplain wetland (and indeed every riparian zone) is made up of precipitation, influent river seepage, over bank floods and groundwater inflow. The output consists of evapotranspiration, effluent river seepage, surface runoff and groundwater outflow (Burt and Haycock, 1996). The storage of water takes place in different forms, e.g. as snow or surface films on plants but the most important factor is storage in the soil (Ingram, 1983).

Changes in the hydrologic regime of a wetland can be characterized by analysing measured water-budget components or by simulating them (Smakhtin and Piyankarage, 2003). One of the hardest components of the water budget is to quantify groundwater flow to a wetland, especially as wetlands may form areas of either groundwater recharge or discharge (Siegel, 1988). In groundwater discharge areas, groundwater inflow may be a more significant water source than precipitation (Roulet, 1990). However, difficulties in measuring subsurface flow have led to the application of groundwater models to determine the relationship between of groundwater flow and surface water features of wetlands (Gilvear *et al*, 1993).

2.6 Hydrologic Processes in Wetlands

Hydrologic processes occurring in wetlands are the same processes that occur outside of wetlands and collectively are referred to as the hydrologic cycle.



Figure 2.1 Hydrological Water Balance in Wetlands (Mitsch and Gosselink, 2002)

Components of the wetland water budget are:

- $P + SWI + GWI = ET + SWO + GWO + \Delta S$ (1)

where P is precipitation, SWI is surface-water inflow, SWO is surface-water outflow, GWI is ground-water inflow, GWO is ground-water outflow, ET is evapotranspiration, and ΔS is change in storage.

Constructing a water balance for a wetland is not a simple task, since the wetland system is not delineated by no-flow boundaries (Gilman, 1994). Estimates are needed for the fluxes to and from groundwater and to and from surface water. Owen (1995)

quantified the hydrologic budget for an urban wetland using the loss/gain of water from the river as a residual term to close the balance, but recognised the large uncertainties in the different terms and the considerable error associated with the budget. Bendjoudi *et al.* (2002) studied the functioning of riparian wetland of the middle reaches of the River Seine, and found that water levels were controlled by the river level. Internal vertical fluxes arose from the swiftness of the reaction of different layers to changes in river stage. They used the evapotranspiration to close the water balance and found it to be 95% of the potential evapotranspiration. Conceptual wetland models have also been developed to describe the interactions between a wetland, the surrounding catchments and local groundwater. Numerical evaluation of a wetland water balance can be achieved by applying a bucket model, which requires little calibration, and uses physically based catchment properties and recorded climatic data sets (Krasnostein and Oldham, 2004).

2.7 Models Used for Wetlands Studies

In wetland studies, model applications are considered to be an option to understand the role wetlands play and ascribe the appropriate management procedure or application. Numerous wetland models exist, but scientists have not been able to come to a consensus as to which model is the best to apply to specific problems (Janssen and Hemke, 2004). Among the numerous models, two types of models for studying wetlands can be distinguished. These are models based on data and models based on processes. Models based on data, known as stochastic models are considered as a black box system that uses mathematical and statistical techniques to link model inputs to outputs. Common techniques are regression, transfer function and neural networks. In this case, wetlands are treated as a black box, where time series of input data are related to outputs. The internal processes and controls are not made reference

to, it is only the overall behaviour that is considered. Wetlands themselves are superb simplifiers, converting a spatial complexity of patterns and processes into a relatively simple and well understood output like a hydrograph (Mulligan, 2004). Models based on process description, commonly called deterministic models, can be sub-divided into single event models and continuous simulation models. This type of model represents physical processes observed in the wetland and typically contains representations of surface runoff, evapotranspiration and sub-surface flow. However, the use of this kind of model can be complicated, due to the large number of parameters that usually are required to be estimated from limited data input-output observation (Young, 2001). Application of models in this category require very good understanding of the nature of the system and internal working of and connection and interaction between its subsystems and components of the subsystem, together with knowledge of the physical laws governing the processes occurring in the system to formulate. Most wetland modelling studies so far have focused on predicting watertable levels.

2.7.1 The DITCH Model

The DITCH (Drain Interaction with Channel Hydrology) model, a water balance model based on basic drainage theory, has been applied in the UK to examine the consequences of various ditch management regimes (Armstrong and Rose, 1998). It simulates the fluxes of water moving between the soil and the peripheral ditches (both recharge and drainage) and so estimates the position of the watertable in the field. The model has been applied to uniform soils as well as soils with decreasing hydraulic conductivity, layered soil profiles and soils with presence of macropores (Armstrong and Rose, 1998; Armstrong and Rose, 1999; Armstrong, 2000).

2.7.2 The MODFLOW Model

Groundwater flow models like MODFLOW, a physical based numerical groundwater flow model, has been applied in many aspects of wetland hydrology research because it can represent a wide range of drainage situations, geometry, configurations and different hydraulic settings. MODFLOW has been used to predict watertables in several wetland modelling studies.

Bradley (1996, 2002) simulated the annual watertable variations in a British floodplain wetland that is the Naborough Bog. Bradley (2002) simulated the annual watertable using MODFLOW. The model estimate diffuse water fluxes such as seepage flows to and from the adjacent river. The technique of model analysis employed in his research indicated the precise effects of individual precipitation and evapotranspiration events on watertable variations. The tabulated water budget indicates the quantities of water that are estimated to flow from the wetland to the river. The pattern of water drawdown in periods of low or infrequent rainfall illustrated how the river marginal wetland may sustain river base flow, while the river level represents a base level to which the wetland watertable adjusts and that demonstrated the need for rivers and floodplain wetlands to remain closely integrated.

According to Bradley (2002) water budget can be modelled as:

$$P + \text{Inf}_{\text{RIV}} + S_{\text{OUT}} = E + \text{Effl}_{\text{RIV}} + S_{\text{IN}} \dots\dots\dots (2)$$

Where inflows comprises:

- Precipitation (P), influent seepage from the river (Inf_{RIV}), water movement from storage (S_{OUT}), equal outflows of evapotranspiration (E), Effluent seepage (Effl_{RIV}) and water movement to storage input (S_{IN}).

Bradford and Acreman (2003) applied a 3D groundwater flow model, MODFLOW, to simulate groundwater levels within a single field in wet coastal grassland underlain by a low permeability sequence located in the central part of Pevensey Levels, Sussex, UK. It was noted that Rainfall and evaporation have the most influence on watertable fluctuations and in-field wetness in wet grasslands with low permeability clay soils. At the field-scale, it was considered necessary only to model the surface clay layer as vertical groundwater leakage to or from the deeper, more permeable part of the sequence and regional groundwater flow within this part of the sequence can generally be neglected.

Nyarko (2007) established the interaction that goes on between the main river and floodplain wetlands within the White Volta Basin. The HYDRUS-ID bottom flux was used as groundwater recharge which served as an input into the PM-WIN (MODFLOW) model. The PM-WIN (MODFLOW) simulation showed a systematic variation in hydraulic head of the wetland to changes in rainfall pattern, the observed interaction between floodplain wetlands and the White Volta Basin was bi-directional in terms of horizontal direction with most of the flow coming out of the river.

2.7.3 The USEPA SWMM Model

Obropta *et al* (2006) utilised the USEPA SWMM model to characterise water movement through 46 sub-basins for the Teaneck Creek Conservancy urban wetland site in USA. Studies revealed that the amount of water in the wetland at the end of simulation period was roughly the same as at the beginning. It was concluded that the model could be used to analyse each wetland basin, separately or in combination, and to evaluate the effects of various restoration options, such as grading changes or installing water-control structures.

2.7.4 The SLURP Model

Su *et al* (2000) applied SLURP, a semi-distributed model developed for simulating streamflow, to calculate water levels in a prairie wetland in Saskatchewan, Canada. The model calculates the daily vertical water balance using four tanks in each ASA (aggregated simulation area) to represent the capacities of canopy interception, snowpack, surface storage and soil moisture storage. Release from the 'slow' soil moisture storage tank was calculated using a water transfer coefficient of the subsurface soil. Unsaturated-saturated flow models solving the Richards' equation have been used to predict transient responses of the watertable in floodplains to in-bank floods (Burt *et al*, 2002; Bates *et al*, 2000). The aim of these models, however, were to examine the role of the floodplain in the buffering or mitigation of floods, and no verification to root zone conditions was carried out (nor was this the goal of the modelling exercise).

2.7.5 The HYDRUS-2D Model

Schot *et al* (2004) applied Hydrus-2D, a numerical finite element code that solves the Richards' equation for water flow in a saturated-unsaturated domain (Šimúnek *et al.*, 1999), to a fen drained by ditches to simulate the formation of rainwater lenses on top of the groundwater system and investigate the effect of upward seepage of groundwater, drainage, presence of a semi-confining layer, seasonal recharge fluctuations and spells of dry and wet years. Although the aim of the study was eco-hydrological and the developed model had a high spatial resolution, the simulations were rather general in nature and served to identify factors important for the dynamics of rainwater lens formation without field verification.

2.7.6 The UNSATI Model

Bradley and Gilvear (2000) used UNSATI, a Hermitian finite-element model that can simulate water movement in a one-dimensional, saturated and unsaturated non-homogeneous soil profile. Van Genuchten (1978) modelled the unsaturated water contents of a floodplain wetland. It was noted that water dynamics within both the saturated and unsaturated zones are highly variable, and could be reproduced given satisfactory identification of the wetland profile, and determination of the appropriate hydraulic parameters. The results for the unsaturated model simulations demonstrated the significance of evapotranspiration, especially in the near-surface deposits, and demonstrated the need to incorporate and measure appropriate hydrometeorological variables when studying wetland moisture dynamics.

2.7.7 The MIKE SHE/MIKE 11 Model

Thompson *et al* (2004) applied the coupled MIKE SHE/MIKE 11 model, a deterministic, fully distributed and physically based modelling system with one-dimensional unsaturated flow described by the Richards' equation, to Elmley Marshes in southeastern England to model ditch water levels and groundwater dynamics. The unsaturated zone was represented by a single soil profile comprising alluvial clay to a depth of 2 m.

2.7.8 The WETLANDS Model

Mansell *et al* (2000) used WETLANDS, a multi-dimensional water flow and solute transport numerical model, to calculate water levels and pond water level for a cypress pond located within a relatively flat Coastal Plain pine forest landscape in southeastern United State . The model combines the Richards' equation, an equation for the rate of change of water volume in the pond providing a dynamic linkage between pond water, groundwater and unsaturated soil zones.

2.7.9 The IWAN Model

Krause and Bronstert (2005) applied the IWAN model to simulate the water balance of the Havel floodplain in Southwestern Germany. The simulation results proved the tight interaction between river and floodplain. It was shown that the spatially and temporally variable influences of the connected floodplain on the river discharge were only important during low discharge in summer.

2.7.10 The DEMON Model

Brown *et al* (2003) used DEMON to quantify lateral flow into wetlands, with a stream tube flow routing model and compared the results with those of the model D8 (a model that uses DEM to define flow directions). They found that D8 produced unrealistic results, while DEMON incorporated with storage term predicted observed changes from storage-dominated flow to catchment topography-dominated flow as rainfall increased.

2.7.11 The HEC Model

Sui and Maggio (1999), in an attempt to delineate floodplain wetland boundaries, developed a new approach by integrating GIS with hydrological/hydraulic modelling via a loose coupling approach. The approach involved the use of a GIS package (arc info) and a hydrological modelling programme, HEC. The model has a four phase approach, namely, database creation, hydrological modeling using HEC -1 (rainfall-runoff).

2.7.12 The Kalman Filter Model

Adamowski *et al* (1986) developed a linear groundwater model incorporating snowmelt and evapotranspiration based on mass balance of water fluxes to predict groundwater levels for the Castor River watershed in Ontario, Canada. Parameter

estimation was performed by ordinary least squares (OLS), weighted least squares (WLS), generalized least squares (GLS) and the Extended Kalman Filter (EKF). It was concluded that the WLS and the EKF methods provide the best prediction results.

2.8 Water Quality

In many wetlands, the inflowing water provides a major pathway for the import of elements. It helps to determine the availability of essential plant nutrients as well as regulating other components of the chemical environment of the root zone, such as pH (Wheeler, 1999). Hydrological variables influence soil conditions by modifying or changing chemical and physical properties of the soil such as nutrient availability, degree of substrate anoxia, soil salinity, sediment properties and pH (Mistch and Gosselink, 2000). In a study of an alluvial ecosystem in a regularly flooded area of the Rhine floodplain, Takatert *et al* (1999) found that variations in groundwater level regulate spatio-temporal variations in nutrient concentrations in groundwater as a result of the oxidation-reduction status of the soil, which creates favourable or unfavourable conditions for nutrient bio-availability. Their findings were supported by a comparative study between two alluvial forests in the Rhine floodplain, one flooded and one unflooded. This study revealed that the alternation of wet and dry cycles in the flooded sector stimulated biochemical transformations of nitrogen, while in the unflooded sector the soil-root filter for nitrate provided by mineralisation and nitrification was less efficient.

Another example of the important effects of hydrology on root zone chemistry and wetland vegetation is given in Lucassen *et al* (2004) who compared groundwater fed wetlands with inflow of sulphate-rich groundwater containing low or high amount of nitrate. They found that while the increased sulphate concentrations in the groundwater may negatively affect groundwater fed wetlands because of mobilisation

of phosphate through the interaction of sulphide (from reduction of SO_4^{2-}) with iron-phosphate complexes, high nitrate concentrations in groundwater inhibited eutrophication of wetlands. The wetlands with high NO_3 inflow showed lower SO_4^{2-} reduction and lower PO_4^{3-} concentrations, and this was reflected in the occurrence of plant species characteristic of clear water.

Henry and Hogg (2002) evaluated the effects of irrigation on soil chemical and physical properties. Twelve paired irrigation and dryland sites within the SSRID No. 1 were sampled, specifically non-saline soils. The results suggested no significant difference in bulk density or pH between irrigated and dryland treatments. Annual application of ammonia-based fertilisers such as urea and anhydrous ammonia did not reduce soil pH. The dryland treatment maintained significantly higher water aggregate stability (WAS) than the irrigated treatment. They also revealed that irrigation management altered nutrient availability. The irrigation treatment contained significantly higher $\text{NO}_3\text{-N}$ than the dryland soil (23 ug g^{-1} versus 9 ug g^{-1} respectively). The significant difference in $\text{NO}_3\text{-N}$ levels may be attributed to:

- Greater amount of ammonia-based fertilizer application on irrigated land,
- Annual fertilizer application on irrigated land and
- Greater mineralisation of N in irrigated land than dryland.

USGS (1974) transported irrigation water from the San Joaquin River, an exceptionally low salinity water through a Friant-Kern Canal, to farms along the east side of the San Joaquin Valley, California, USA. Analysis showed that salinity was exceptionally low with the EC_w ranging between 0.05 and 0.01 dS/m which often causes severe water infiltration problems on soils planted to moisture sensitive crops like potatoes and citrus. The water SAR by itself was not high enough to account for

the poor rates of infiltration observed ($SAR = 0.5$). For a potato crop, gypsum applied and disked into the soil at rates as high as 10 t/ha/y has resulted in a greatly improved rate of infiltration. Likewise, water-applied gypsum administered nearly continuously at a rate sufficient to raise the water calcium content to 2-3 meq/l Ca was also effective.

In a survey of 47 farms in Bahrain Island of Saudi Arabia, Amer (1983) irrigated the farms which were mostly devoted for vegetable production with groundwater. The irrigation water salinity test was generally high and ranged from 3.25-4.95 dS/m. Boron test was low to moderate (0.4–1.2 mg/l). It was concluded that owing to the salinity, maximum yields of vegetable crops were not possible, but better yields could be obtained if proper attention were given to leaching and more frequent irrigation.

Dutt *et al* (1984) made some trials at the Safford Experimental Station of the University of Arizona. Soils in the experimented station are clayey and saline. The groundwater used for irrigation during the cropping season ranged in quality from $EC_w = 3.1-3.5$ dS/m and an SAR of 14. Crop yields reported from tests conducted at the station with cotton, barley, sugarbeets and sorghum are as reported in Table 2.1. They compare with statewide averages and found that in most cases the yields from the experimental trials equalled or exceeded the average yield for these crops grown on commercial farms throughout Arizona.

Table 2.1 Selected Crop Yield from the Safford Field Experiment Station as Compared to Average Farm Yields (Source: Dutt *et al*, 1984)

Crop	Year	Yield (t/ha)	Statewide Average (t/ha)
Cotton	1970	1,258	1,120
Barley	1972	4,117	3,214
Sorghum	1971	7,820	4,892
Sugarbeet	1972	56	57

Table 2.2 Red Mountain Farms Lint Cotton Yields (t/ha)

Field	44	10	14	29
Replication	Yield (t/ha)			
1	1.507	1.076	1.022	1.022
2	1.668	1.076	0.807	1.13
3	1.345	0.861	0.807	1.213
4	1.937	0.967	0.7	1.076
Average	1.614	0.995	0.834	1.076
Statewide Average (t/ha)	1.238			
Applied Water Salinity EC _w dS/m	6.2	4.5	4	11.1

From Table 2.2, water with EC_w = 6.2 dS/m would be capable of producing a better than 90 % yield and a water of EC_w of 11 dS/m would be capable of at least a 50 % yield. On that basis, a full yield from Field 4 would be about 1.800 t/ha and from Field 29 about 2.200 t/ha. Both these projected maximum yields were approaching reported good near maximum lint cotton yield from other areas where there are no limiting factors to production (2.3–2.5) t/ha of lint cotton.

Soil conditions and high salinity of the irrigation water make the lower Medjerda Valley of Tunisia difficult to farm. The heavy clay soils have a very low infiltration rate and the low salinity winter rainfall may stand on the surface for extended periods of time. (Van't Leven and Haddad, 1968) tested the soil quality and found it to vary

considerably in the wet and dry seasons within the two year period. The monthly mean salinity (EC_w) during 1962 (Wet season) and 1963 (Dry season) ranged from 1.3-4.7 dS/m. During much of the year, the Medjerda River water can be used for irrigation of medium to high salt tolerant crops such as date palm, sorghum, forage barley and alfalfa. The soil conditions in summer (large cracks) make efficient leaching difficult, while in winter the rainfall only partially leaches salts from the top soil layer of the clayey soils (15cm). The main recommendation of the study was for proper timing of leaching to save water and the use of cropping patterns which included crops tolerant to the expected salinity build-up.

Savva *et al* (1981) adopted two different irrigation methods to improve the yields of tomatoes by using high salinity water for the trial. The tomato production employing drip and furrow irrigation methods yielded 10.9 t/ha and 6.5 t/ha respectively. These differences were consistent regardless of whether the tomatoes were field seeded or transplanted. They also treated Lemon trees with four different irrigation methods. The new lemon plantings showed that sprinkling reduced growth during the first 16 months as compared to bubbler, drip and basin irrigation. Extensive leaf burn and defoliation were caused by the concentrations of sodium and chloride in the irrigation water. Table 2.3 shows the differences in sodium and chloride concentrations in the lower leaves on trees irrigated by the four different methods. The higher sodium and chloride with sprinklers was attributed to the adsorption through leaves wetted by low angle sprinklers during the early growth stages. Eventually, the trees grew above the reach of these low angle sprinklers and growth accelerated.

Table 2.3 Effect of Irrigation Method on Sodium and Chloride Concentration of the Foliage of Lemon

Trees (Dry Weight Bases)		
Irrigation System	Percent Sodium in lower leaves	Percent Chloride in lower leaves
Basin	0.39	0.88
Bubbler	0.28	0.84
Drip	0.39	0.61
Sprinkler	1.5	1.43

KNUST



CHAPTER THREE

MATERIALS AND METHODS

3.1 Study Area

3.1.1 Location

Besease is a predominant farming area in the Ejisu Municipal Area of the Ashanti Region in Ghana. The site lies within Latitude $1^{\circ} 15' N$ and $1^{\circ} 45' N$ and Longitude $6^{\circ} 15' W$ and $7^{\circ} 00' W$. The Besease Inland Valley Bottom Wetland has an area extent of 1.6 km^2 and is bisected by the Oda River. Due to the limited scope of the study, it was not possible to investigate the whole catchment. Therefore, a section along the right side of the river with an area of 72 ha, which is under cultivation by small holder farmers, was demarcated for the research work (Fig 3.1).

3.1.2 Climate

The climate of the study area is mostly related to the semi-humid type. The region is characterised with two distinct seasons, the wet season which begins from April and ends in October whilst the dry season extends from the month of November to March. The wet seasons can be categorised under two rainy seasons. The major rainy season which ranges from mid April to July and the minor rainy season from September to mid November. The dry season is characterised with rapid rise in temperature and low relative humidity. In a semi-humid climate, the annual potential evaporation is estimated to exceed precipitation in 6-9 months of the year

3.1.3 Rainfall

Rainfall is the main water source of the catchment. It is also the most important parameter in the water balance and aquifer recharge. Nearly 74% of the annual rainfall occurs in the wet season. The mean annual rainfall is 1420 mm.

3.1.4 Temperature

The average monthly temperature values for the study area is 26.5°C, and the maximum average is 33.3°C in July, while the minimum is 22°C in January.

3.1.5 Relative Humidity

Relative humidity is one of the most important factors directly affecting evapotranspiration. Relative humidity is a measure of the water vapour content of the air at a given temperature. The variation in relative humidity results from the fact that the saturation vapour pressure is determined by the change of air temperature, and the relative humidity which is a cyclic variable. It is thus related to temperature and evaporation. The average maximum and minimum relative humidity in the study area is (84 %) and (64 %) in August and January respectively.

3.1.6 Evapotranspiration

Evapotranspiration in an area can be analysed in two ways as potential evapotranspiration and actual evapotranspiration. Potential evapotranspiration describes the water loss that will occur under a given climatic condition with no deficiency of water for vegetation. Since the actual evaporation accounts for the field conditions, it depends on the availability of water (Seneviratne, 2007). As evaporation proceeds, and if water is not limited, the surrounding air becomes gradually saturated and the process slows down and might stop if the wet air is not transferred to the atmosphere. The replacement of the saturated air with drier air depends greatly on

wind speed (Allen *et al*, 2006). Major studies have also been undertaken by the American Society of Civil Engineers and a consortium of European Research Institutes to evaluate the performance of the different evapotranspiration estimation procedures under different climatological conditions. Both have indicated that the FAO Penman–Monteith approach of reference crop evapotranspiration is relatively accurate and have consistent performance in both arid and humid climates. Reference crop evapotranspiration is recommended as the sole standard method in the evapotranspiration estimation (Allen *et al*, 2006). The only factors affecting evapotranspiration (ET) are climatic parameters and ET_o as a climatic parameter can be computed from weather data. The average monthly maximum and minimum evapotranspiration (ET_o) for the study area is 127.5 mm and 64.7 mm and has an annual ET_o of 1230 mm.

3.1.7 Land Use and Vegetation

Ghana has two main vegetation patterns, tropical forest occupies the southern portion, and savanna the northern and some parts of southeastern Ghana. Taxonomically, the two are very distinct and very few plant species occur naturally in both ecosystem. Besease is located in the moist semi-deciduous forest zone Fig 3.1. Grass species prominently found in the valley bottom are *Sanrocema trifolia*, *Chromolaena odorata*, *Imperata cylindrical*, *Mimosa pigra*, *Ceiba patendra*, *Centrosema pubescens* and *Mariscus flabelliformis*. Plant species like *Raphia hookeri* (*Raphia palm*), *Alstonia boonei*, *Malotus oppositifolius* and *Pseudospondias microcarpa* extends are found along the margins of the Oda River. The Valley bottom is developed by small holder farmers and they cultivate rice in the wet season and also grow vegetables like cabbage, lettuce, sweet pepper, cauliflower, cucumber and okro and cereals like maize in the dry season when the watertable is low.

3.1.8 Soils and Geology

Soils of the Ejisu-Besease area can be found in the soil map of the Kumasi area. Soils of the study area lies in the Offin soil series which are grey to light brownish grey, poorly drained alluvial sands and clays developed within nearly flat but narrow valley bottoms along streams. The series have very slow internal drainage, very slow runoff, very rapid permeability and moderate water holding capacity. The profile consist of dark grey to dark brown loamy sand and sandy loam humous-stained top soil about 20-30 cm thick and it is underlain by loose grey to brownish grey coarse sand which is a few to several centimetres tick and mottled brown.

The geology of the watershed is relatively heterogeneous and mainly composed of phyllites, quartzite, shale, Tarkwaian and Voltaian sandstone and limestone. The phyllites which underlie 59% of the area consist of upper and lower Birimian rocks. Very few rock outcrops were encountered in the survey as the rocks are deeply weathered. The weathered phyllite is soft and easily broken, recognizable pieces and is typically found at 2-3 m below surface. Soils found within the Oda River catchment are grouped as those derived from granites, sandstones, alluvial materials, greenstone, andesite, schist and amphibolities. Specifically the soils are Orthic-Ferric Acrisol, Eutric Fluvisol, Gleyic Arenosols, Eutric Gleysols and Dystri-Haplic Nitisol.

3.1.9 Relief and Drainage

The topography of the study area (Fig 3.2) is generally gently undulating. The area is drained by the Oda River which is seasonal and whose basin is about 143 km² (Kankam Yeboah *et al*, 1997) and its tributaries are rather small streamlets flowing from nearby uplands. The tributaries as well as the main stream dry up during the dry season. The main stream, however, leaves pools of water at various places within the river bed. It flows from the north to south within the project area. The tributaries flow

from northwest and north eastern directions into the main stream forming a dentritic pattern around the area bordering the Oda River.

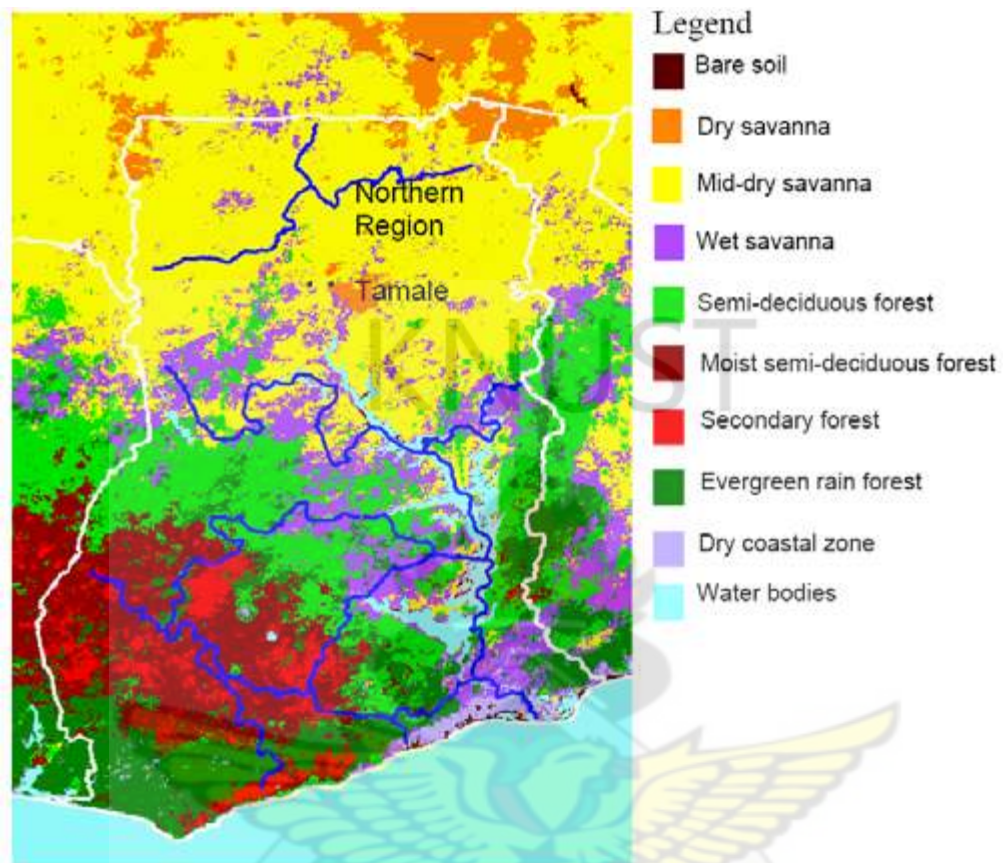


Figure 3.1 Vegetation Map of Ghana [Source: Menz and Bethke, 2000 (Cited in Nyarko, 2007)]

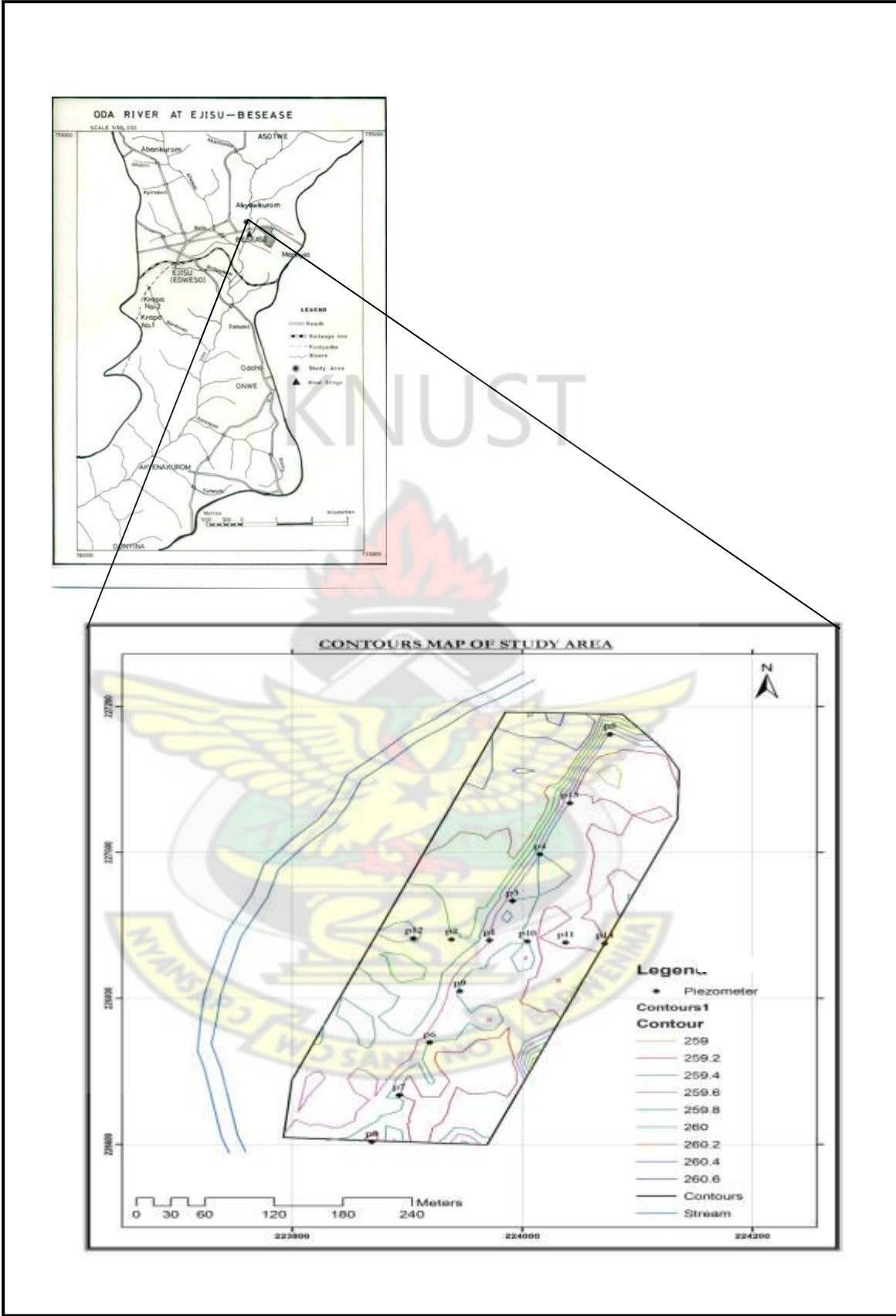


Figure 3.2 Map of the Besease Project Site Showing the Location Piezometric Network

3.2 Data Identification and Source

Data collected for the study were based on field observations, field measurements and laboratory analysis. Field observation techniques assisted in cross checking predictions derived from models based on data obtained from measurements and secondary sources. The field data collection involved measurement of soil infiltration, hydraulic conductivity and river cross sections. Groundwater was also sampled to determine its suitability for agriculture within the catchment. Laboratory analysis were carried out for physico-chemical properties at the Soils Research Institute, Kumasi. Data collected were used to describe the hydro-dynamics of the wetlands that served as input into the KALMAN FILTER and MODFLOW models for this study.

3.3 Wetland Vegetation Identification

Vegetation survey was conducted using a 1m×1m quadrat placed randomly at 10-30 m intervals along transects (200-600 m). Vegetation within each quadrat was identified with experts and others were collected and sent to the Forestry Research Institute, Fumesua for identification.

3.4 Installation of Piezometers

Wetland groundwater level fluctuations were monitored through a network of 14 vertical piezometers installed using a hand auger along a longitudinal transect spaced at 75 m and transverse transect also spaced at 33 m at the Besease site as shown in Fig 3.2. The piezometers consisted of PVC pipes of 7.62 cm (3 inches) diameter screened over the bottom 20 cm with holes of 0.3 cm diameter ranging from 1.8-3 m in depth. Sand was packed around the screens as an envelope and the rest of the annulus hole was backfilled with auger cuttings and then grout placed on the top to prevent surface water entry. The cup covering the top of the pipes were not hermetically closed to prevent build-up of pressure in the piezometer during phases of groundwater rise.

Depth to watertable was measured every two days with greater frequency of one day during rainfall events by inserting a measuring tape down into the piezometers (Fig 3.3) and observing when it encountered the water surface. The elevations of the piezometers were surveyed to benchmarks to allow adjusting the water levels in the wells to the local datum.



Figure 3.3 Piezometer for Monitoring Groundwater Fluctuations

3.5 Watertable Depth

The actual watertable depth on the swampy land was determined from hand augured hole by pushing core samplers of 8.3 cm diameter and 10 cm long into the ground till it hits the watertable. The centre point of pipes P13-P4, P11-P14, P1-P2 and P7-P8

were sited for the watertable depth determination. The content of the core samplers were packaged and sent to the laboratory for soil physical analysis.

3.6 Soil Physical Properties

3.6.1 Bulk Density

Dry soil bulk density refers to the weight (mass) of soil per unit *in situ* volume. This relates primarily to the physical ability of the soil to hold water to sustain plant growth. Bulk density was measured by taking a soil sample of known volume. The mass was obtained after oven-drying the soil for 24 h at 105°C, and dividing it by the internal volume of the cylinder that was used to collect the sample. The following equation was used to estimate bulk density:

$$\rho_b = \frac{M_s}{V_t} \dots\dots\dots (3)$$

Where ρ_b [g/cm³] represents bulk density, M_s [g] mass of sample, V_t [cm³] is the Volume of sample.

3.6.2 Total Porosity

The number of pores and their size distribution (as reflected in estimates of total pore space, coarse porosity and air-filled porosity) are general indicators of the physical condition of the soil. However, the tortuosity and continuity of soil pores are important features influencing aeration, water movement and root penetration. Total porosity can be estimated from bulk density and particle density as specified in the following equation:

$$\text{Porosity} = (1- \rho_b/\rho_s) \times 100 \dots\dots\dots (4)$$

Where, ρ_b [g/cm³] is bulk density and ρ_s is particle density (2.65g/cm³).

3.6.3 Water Content

Water content is a measure of the ratio of water volume to soil volume. The soil samples were collected by taking soil with a ring volume of 100 cm³. The sample was weighed for its initial wetness and later dried in the oven at 105°C for 24 h to remove inter-particle absorbed water, but not structural water trapped within the soil lattices known as crystallization water. The difference between the wet and the dry weights is the mass of water held in the initial sample:

$$\theta = \frac{M_w - M_d}{\rho_w V_t} \dots\dots\dots (5)$$

Where, θ [cm³/cm³] represents water content, M_w [g] is mass of wet sample, M_d [g] is mass of dried sample, and ρ_w is density of water [g/cm³]

3.6.4 Soil Texture

Soil texture describes the mass proportions of the various sizes of the soil particles. The three primary soil particles are sand, silt and clay. In this study, the hydrometric method was used in analysing particle size fractions. This involved the removal of organic matter by adding a chemical dispersing agent (sodium hexametaphosphate) after which the sample was mechanically agitated through shaking overnight for complete dispersion of soil floccules. The bouyoucos hydrometer was then used to determine the density of the solution at timed settling increments. The density of the soil solution was used to determine the concentration percentages for sand and clay particles. For the determination of sand and clay size fractions, the Stokes' Law relationship between the diameter of suspended particles and their rate of settlement in liquid at constant temperature was used. After particle size determination, the texture was determined using the USDA textural triangle.

3.6.5 Hydraulic Conductivity

3.6.5.1 Laboratory Measurement (Falling-Head Method)

The saturated hydraulic conductivity (K_{sat}) measurements were made on core samples with a length of 10.0 cm and diameter of 8.3 cm in the laboratory using the falling head method developed by Klute and Dirksen (1986). This method operates according to Darcy's law with a one-dimensional, saturated column of soil with a uniform cross-sectional area. The falling-head method differs from the constant-head method in that the water that percolates through the saturated column is kept at an unsteady-state flow regime in which both the head and the discharged volume vary during the test. As described by Agyare (2004), the soil in the core is held in place by a fine nylon cloth tied with a rubber band and soaked in water until it was saturated. The soaked soil is fitted with another cylinder of the same diameter but of 40 cm length at the top of the core to allow imposition of a hydraulic head. A large metallic box and plastic with a perforated bottom is filled with gravel (<2 cm). A fast filtration filter paper is placed between the soil core and the reservoir. With the core placed on the gravel box, water is gently added to the core to give a hydraulic head in the extended reservoir. The water then flows through the soil and is collected in the box and drained off by plastic pipe tubing. The fall of the hydraulic head at the soil surface is measured as a function of time using a water manometer with a meter scale. However, time was allowed for water to flow through the soil to ensure uniform flow. The saturated hydraulic conductivity of the soil samples was calculated by the equation:

$$K_{sat} = \left(\frac{AL}{A_t}\right) \ln\left(\frac{H_1}{H_2}\right) \dots \dots \dots (6)$$

Where, K_{sat} is the hydraulic conductivity (LT^{-1}), A is the cross-sectional area of the sample, H_1/H_2 is the difference in the hydraulic head between the up gradient end of

the sample and the down gradient end, L is the length of the sample or the distance over which the head is lost, and t is time.

3.6.5.2 Field Methods

A number of methods are used for the *in-situ* determination of saturated and unsaturated hydraulic conductivity of soil. The mini disk infiltrometer was also used to determine the unsaturated hydraulic conductivity. The infiltrometer has an adjustable suction (0.5-6 cm). When infiltrating water is under tension or suction, it will not enter macropores such as cracks or wormholes, but will only move into and through the soil as determined by the hydraulic forces in the soil. Based on the procedure (Zhang, 1997), the upper chamber of the mini disk infiltrometer was filled by running down water through the suction control tube. The infiltrometer is inverted and the bottom elastometer with the porous disk was removed and the water reservoir filled. The position of the end of the marriote tube with respect to the porous disk is carefully set to ensure a zero suction offset while the tube bubbles. The elastometer is replaced with the porous disk firmly in place. The infiltrometer was slid down vertically to make contact with the soil surface at time zero. The volume was recorded at regular time intervals of 30 seconds as the water infiltrated into the soil at a suction rate of 2 cm which is suitable for most soils.

3.6.6 Infiltration Rate

Double ring infiltrometers, consisting of two concentric rings, were used to measure the infiltration rate. Rings were 250 mm deep and were made from 12-gauge steel with sharpened bottom edges. They were driven into the ground to 50 mm depth. Grass was cut to near soil level and a pad was placed inside the inner ring to prevent puddling. The inner and outer edges were tamped to seal possible cracking. Generally the water level was kept at or above 50 mm depth. The difference in height between

the inner and outer rings was kept to a minimum. The rate of fall of water was measured in the inner ring while a pool of water was maintained at approximately the same level in the outer ring to reduce the amount of lateral flow from the inner ring. The rate of fall of the water level in the inner cylinder was measured at 2, 3, 5, 10, 15, 20, 30, 45 and 60 minutes and at 30-minute intervals thereafter. The accumulated volume of water entering the soil was converted to the infiltration rate (mm/h) and was plotted against elapsed time whereby a declining slope was obtained. The aim of the measurements was to obtain a steady-state infiltration rate. This is achieved when the amount of infiltrated water is constant in time, i.e. when the infiltration curve (instantaneous infiltration against time) levels out. To estimate the infiltration rate at steady state, the terminal infiltration rate (i.e. the infiltration rate obtained at the end of the experiment in about 2 h), was used as an approximation of the steady state infiltration rate.

3.6.7 Evaporation Estimates

The Penman (1963) Equation which was used is expressed as:

$$ET_o = 0.8 \left[0.408 \frac{\Delta}{\Delta + \gamma} R_n + 7.5 \frac{\gamma}{\gamma + \Delta} E_a \right] \dots \dots \dots (7)$$

Where,

ET_o is reference evapotranspiration (mm day^{-1}); R_n the net radiation measured at 2 m above the crop surface ($\text{MJm}^{-1}\text{day}^{-1}$); T the daily mean air temperature ($^{\circ}\text{C}$) at 2 m above ground; U_2 the wind speed at 2 m high (ms^{-2}); e_a the actual vapour pressure (kPa); $(e_s - e_a)$ the saturation vapour pressure deficit at temperature T (kPa); γ the psychrometric constant ($0.0677 \text{ kPa } ^{\circ}\text{C}^{-1}$); and e_s the saturation vapour pressure (kPa), estimated as follows:

$$e_s = 0.5[e^{\circ}(T_{\max}) + e^{\circ}(T_{\min})] \dots \dots \dots (8)$$

Where,

$e^{\circ}(T_{\max})$ and $e^{\circ}(T_{\min})$ are the saturated vapour pressure at maximum and minimum temperatures, respectively. The actual vapour pressure, e_a , can be calculated as follows when the measurements are missing $e_a = e^{\circ}(T_{\min})$ which assumes the dew point temperature equals minimum temperature in humid regions. The function to calculate saturated vapour pressure at a particular temperature (T) is:

$$e^{\circ}(T) = 0.6108 \exp\left[\frac{17.27T}{T + 237.3}\right] \dots\dots\dots(9)$$

Where,

e_a is vapour pressure (kPa) and T is the mean daily temperature ($^{\circ}\text{C}$). Δ is slope of vapour pressure curve ($\text{kPa}^{\circ}\text{C}^{-1}$) given by:

$$\Delta = \frac{4098[0.6108 \exp\left[\frac{17.27T}{T+237.3}\right]]}{(T+237.3)^2} \dots\dots\dots(10)$$

Where,

E_a is aerodynamic term (mm day^{-1}), given by:

$$E_a = 0.35(1 + 0.00438U_2)(e_s - e_a) \dots\dots\dots(11)$$

Where,

T is the mean daily Temperature.

3.6.8 Soil Sampling

Soil samples were collected using core samplers first on the four points in between the P1-P2, P4-P13, P7-P8 and PP11-P14 from the topsoil (0–10). Also samples were

collected from the profile pits in P11-P14 demarcated portion of the valley system from the topsoil 10 cm to the subsoil 80 cm. The samples were air-dried, ground and passed through a 2 mm mesh sieve. Soil pH was determined by using a pH meter (with a glass electrode) with a soil-water ratio of 1:1, according to the methods described by IITA (1979). Total carbon (TC) and nitrogen (TN) contents were determined by the dry combustion method using an N-C analyzer (Sumigraph NC-90A) as described by Geiger and Hardy (1971). Available phosphorus (P) was determined by the Bray No.1 method. Exchangeable cations [calcium (Ca), magnesium (Mg), potassium (K), sodium (Na)] were first extracted with ammonium acetate (1.0 M NH₄OAc) and the contents were then determined by inductively coupled plasma-atomic emission spectroscopy. Exchangeable acidity was determined by first extracting with potassium chloride (1M KCl) and then titrating the extract with sodium hydroxide as described by McLean (1965). Effective cation exchange capacity (eCEC) was calculated as the sum of exchangeable cations (Ca, Mg, K, Na) and exchangeable acidity. Electrical conductivity was also determined using the electrical conductivity meter and probe.

3.6.9 Groundwater Recharge

The watertable fluctuation method (Meinzer, 1923; Hall *et al*, 1993; Ramussen and Andreasen; 1959; Healy and Cook, 2002; Risser *et al*, 2005;) was used for estimating recharge based on the premise that the rise in groundwater levels in unconfined aquifers was due to recharging water arriving at the watertable. Recharge was calculated using the following formula:

$$R = S_y \frac{dh}{dt} = S_y \frac{\Delta h}{\Delta t} \dots\dots\dots (12)$$

Where,

R = Recharge (mm/month)

S_y = Specific yield

dh or Δh = Change in watertable height (mm)

dt or Δt = Time interval (month)

KNUST



CHAPTER FOUR

SOIL PHYSICO-CHEMICAL PROPERTIES

4.1 Dynamics of Soil Physical Properties

Characteristically, the textures of the soils at the Besease Wetlands vary markedly from silt loam to sand both vertically in each profile and among the soils (Appendix 1). Variability in soil texture was attributed to the variable and complex nature of the parent material. This is largely due to the pre-Cambrian igneous and metamorphic rocks of the basement complex. The rocks vary widely in texture and mineral composition from very coarse pegmatite to fine grained schist, and from acid quartzite to basic rocks consisting largely of amphibolites (Smyth and Montgomery, 1962; Hekstra and Andriessse, 1983). Hekstra and Andriessse (1983) specifically reported that the metamorphosed rocks (schists, amphibolites, etc.) tend to form relatively fine-textured soils, while the soils formed over granitic material have coarser textures.

Bulk density was lower in the surface soil layers, increasing with depth in all profiles. The bulk density and the moisture content on the field increased with depth in all profiles as shown from Figs 4.1, 4.3, 4.5, 4.7. High bulk density values at depths may indicate presence of compact layers that could restrict root growth. However, generally low bulk densities in the topsoil layers indicated low soil strength and resistance to root penetration, so that, the only factor that may limit root growth is the depth of the ground-watertable, which is either perennially near the soil surface or fluctuates between the rainy season (when rainfall recharges the groundwater and rise to highest level) and dry season (when the watertable recedes to lower depths). Porosity was, however, greater in the surface layers decreasing to lower values with depth. This demonstrated that lateral water movement in the soils may dominate

compared to the vertical movement as depicted from Figures 4.2, 4.4, 4.6, 4.8 which shows that a well aggregated, fine textured soil, high in organic matter would have high pore space than a massive, or compact soil which would have low pore space. Understanding the mechanisms that control the rate of water movement through and out of the soil system are of considerable importance as these are the main determining factors that will influence overland flow and runoff. The average volumetric water content at pit P8-P7 was 0.27 in March which was greater than 0.26 in February at site P11-P14 though site P11-P14 is attributed to be a discharge area. This is so because the rainfall amount of 120 mm in March was greater than the rainfall amount of 49 mm in February. It is surmised that the moisture content in the vadoze zone depends on the time since the last rainfall event, storage capacity, temperature, wind and evapotranspiration occurred.

4.2 Soil Bulk Density and Porosity

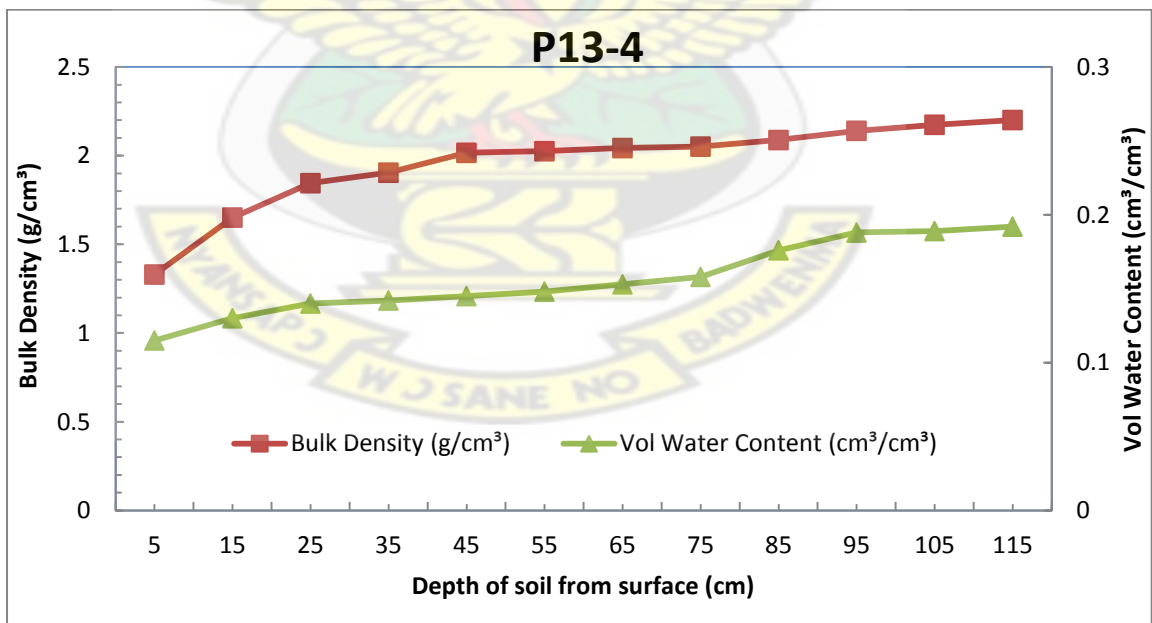


Figure 4.1 Relationship between Bulk Density and Water Content for Site P13-P 4

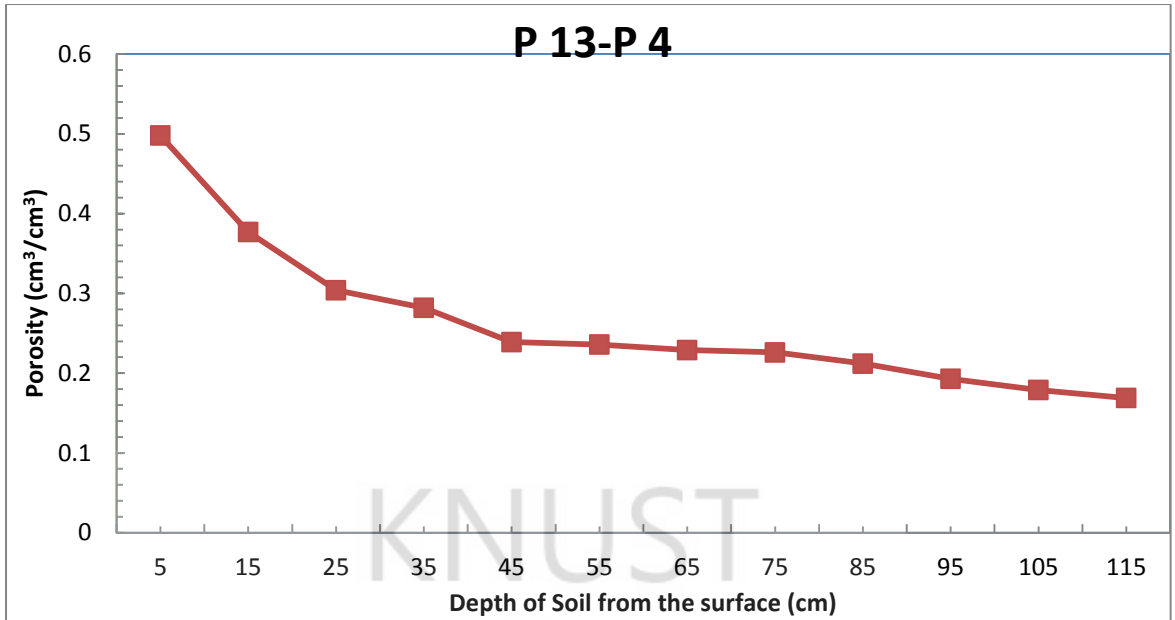


Figure 4.2 Graph of Porosity with Depth for Site P 13-P 4

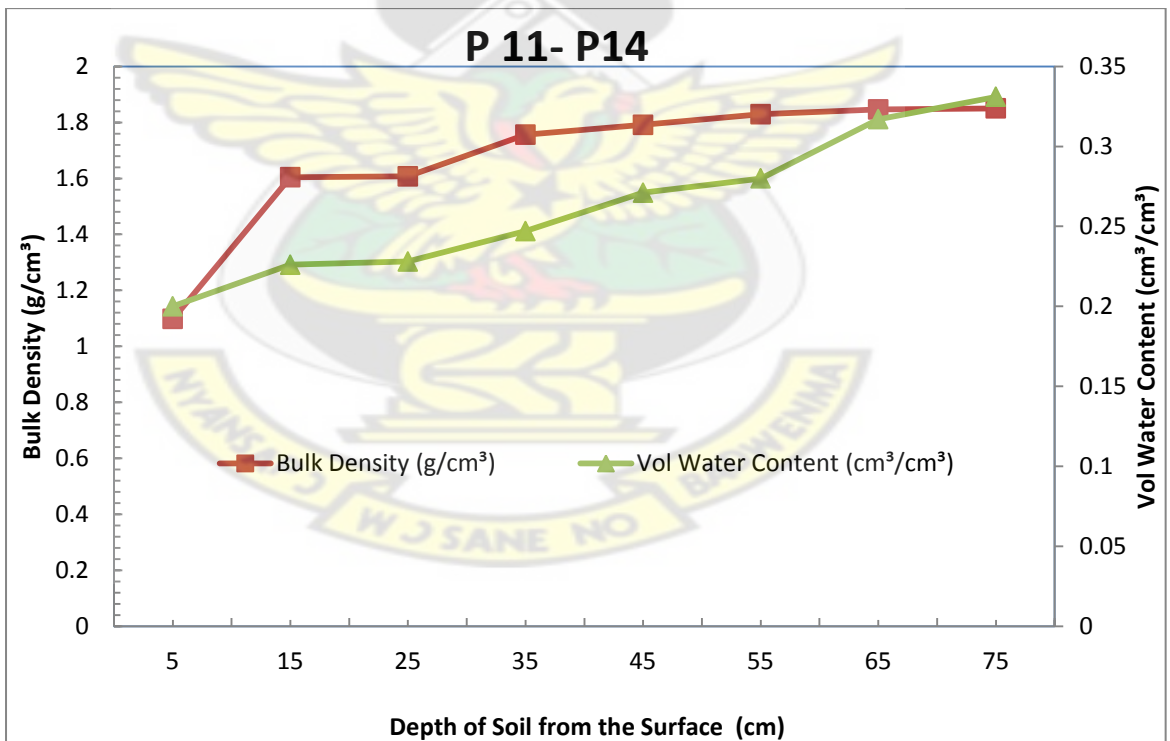


Figure 4.3 Relationship between Bulk Density and Water Content for Site P 11-P 14

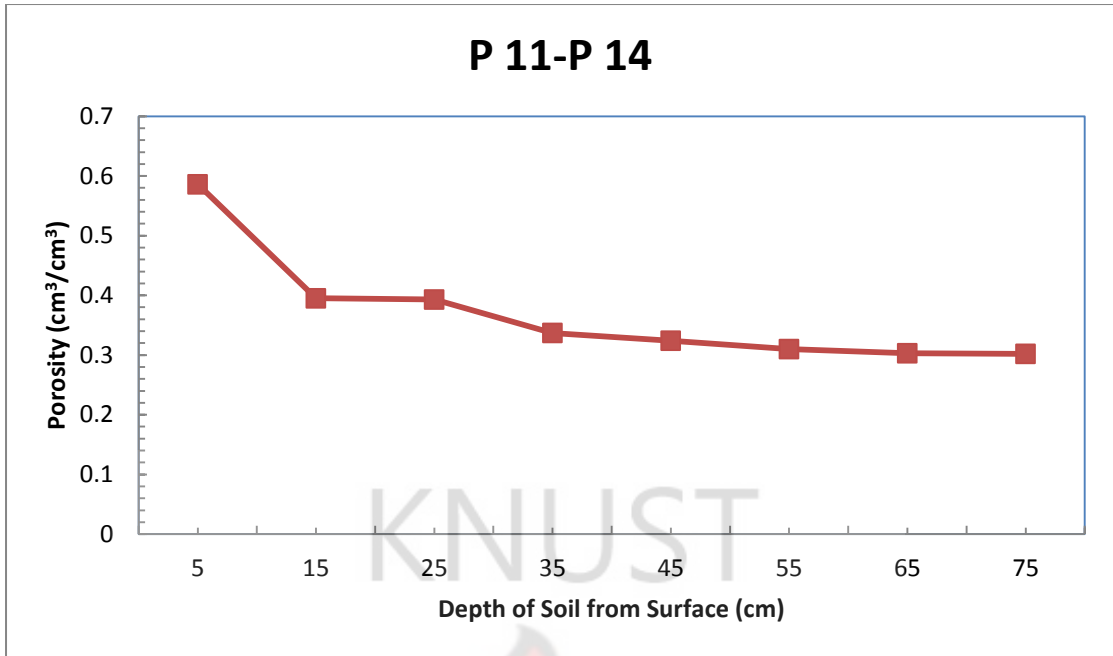


Figure 4.4 Graph of Porosity with Depth for Site P 11-P 14

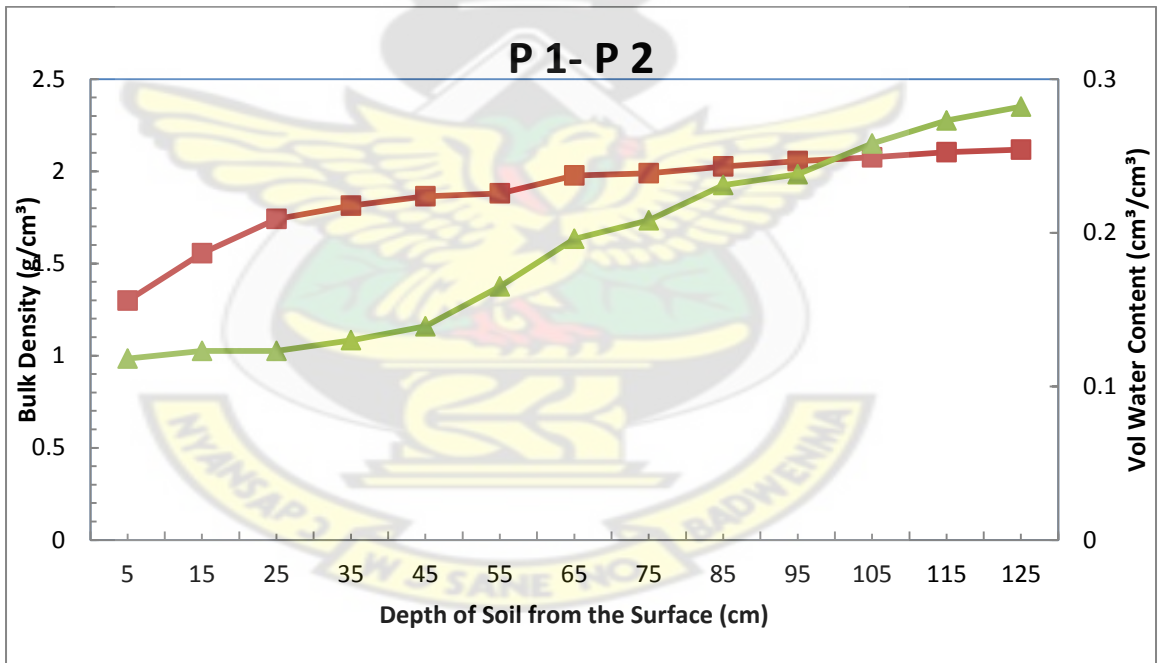


Figure 4.5 Relationship between Bulk Density and Water Content for Site P1-P2

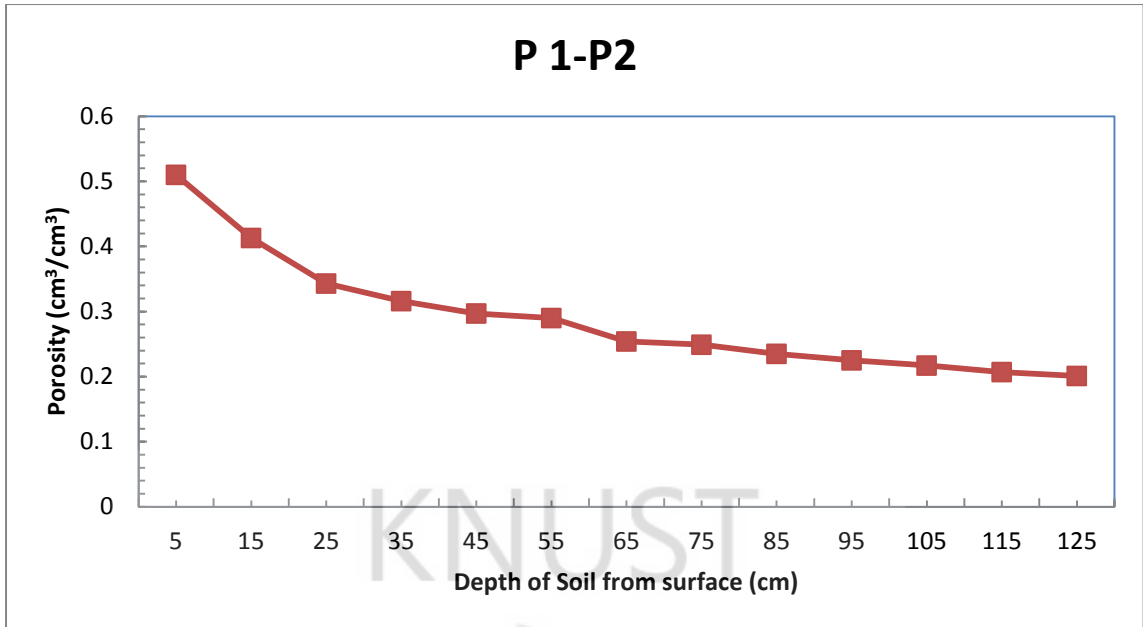


Figure 4.6 Graph of Porosity with Depth for Site P 1 - P 2

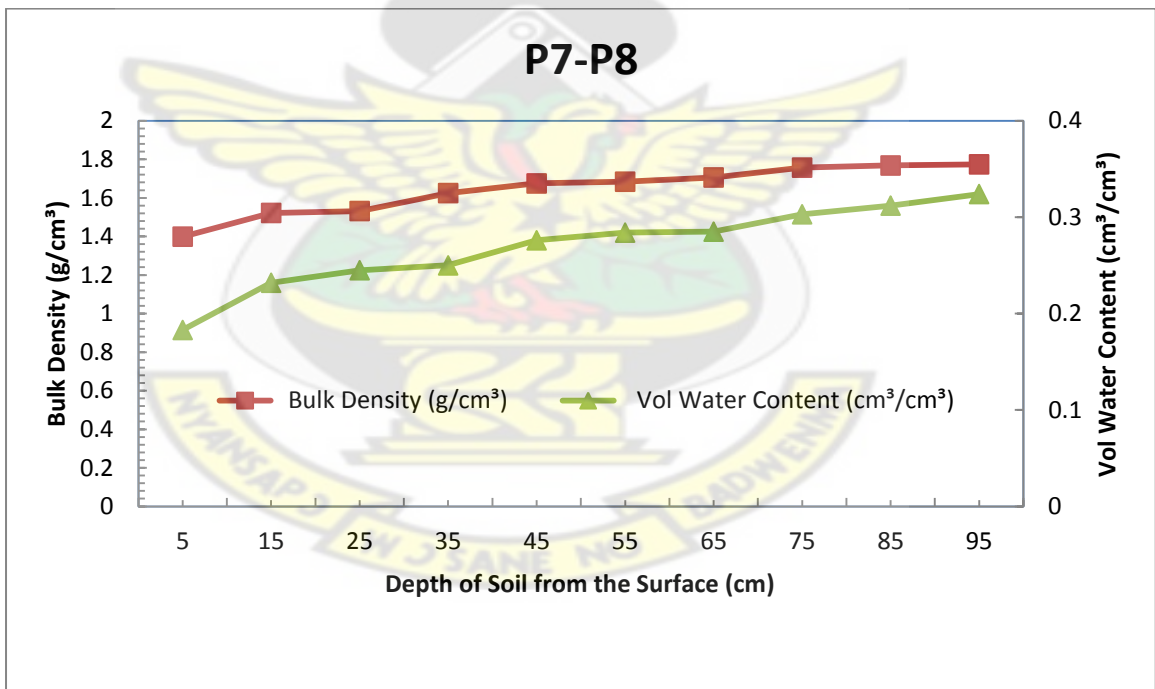


Figure 4.7 Relationship between Bulk Density and Water Content for Site P7-P8

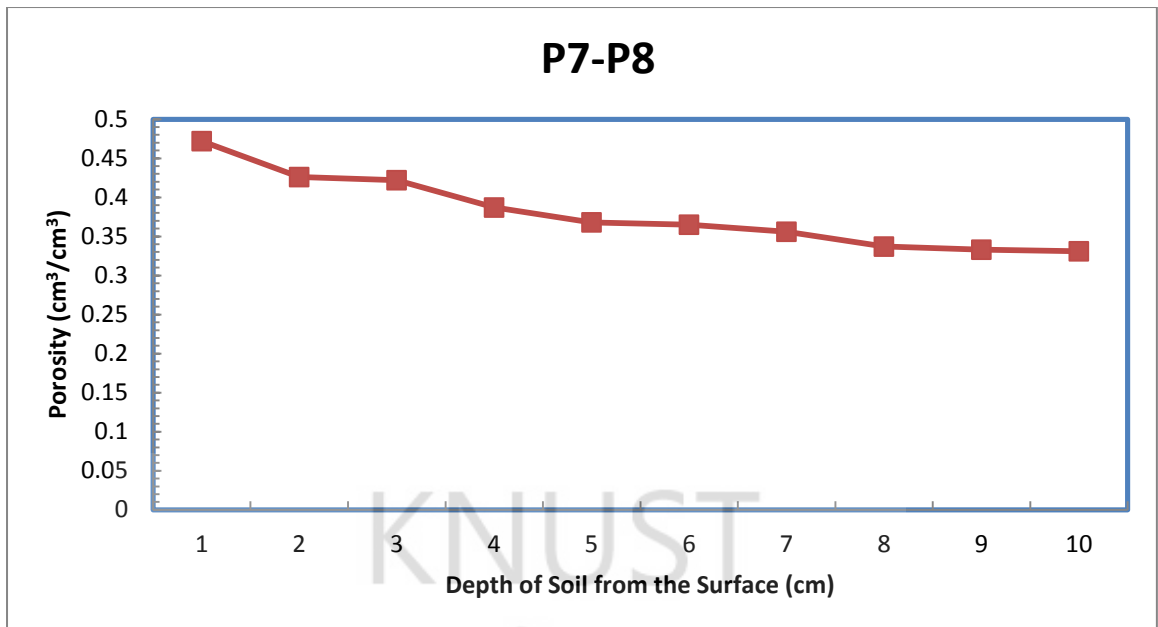


Figure 4.8 Graph of Porosity with Depth for Site P 7 - P 8

Table 4.1 Piezometric Watertable Depth

Site	Depth to WT bgl(m)	AWT - PWT(m)
Pit P13-P4	1.2	-
P 13	0.53	0.67
P 4	1.07	0.13
Pit P11-P14	0.8	-
P 11	0.2	0.6
P 14	0.57	0.23
Pit P1-P2	1.3	-
P 1	1	0.3
P 2	1.3	0
Pit 7-P8	1	-
P7	1.03	0.03
P8	empty	-

4.3 Watertable Depth

The wetland watertable depths are indicated in Table 4.1 as the depth of the four pits dug at the site in the month of February and March 2009. The piezometric watertable (PWT) below ground level (bgl) of piezometer P4 (1.07 m) and P13 (0.53 m) were lower as compared to the actual water table depth (Pit P13-P4) of 1.2 m. The same scenario was observed for the site of Pit P11 - P14. And it was the pit with a shallow watertable depth of 0.8 m which suggests that the place is a discharge area. For site Pit P1-P2 the PWT for P1 was 1 m but the PWT of P2 coincided with the actual watertable depth (AWT) of 1.3 m. At site Pit P7-P8, piezometer eight (P8) was empty P7 had a water table depth of 1.0 m which was close to the AWT of 1.03 m. This shows the spatial and temporal variations of the watertable on the field.

4.4 Computation of Hydraulic Conductivity

Excel was used to calculate the slope of the curve of the cumulative infiltration versus the square root of time from the infiltrated volume of water recorded. Zhang (1997) formulated an equation for determining the hydraulic conductivity of soil. Infiltration is calculated using the equation:

$$I = C_1 t + C_2 \sqrt{t}$$

Where,

C_1 (ms^{-1}) and C_2 ($\text{ms}^{-1/2}$), and C_1 is related to hydraulic conductivity and it is the soil sorptivity. The hydraulic conductivity of the soil (k) was then computed from:

$$k = \frac{C_1}{A}$$

Where,

C_1 is the slope of the curve of the cumulative infiltration versus the square root of time, and A is a value relating the van Genuchten parameters for a given soil type to the suction rate and radius of the infiltrometer disk.

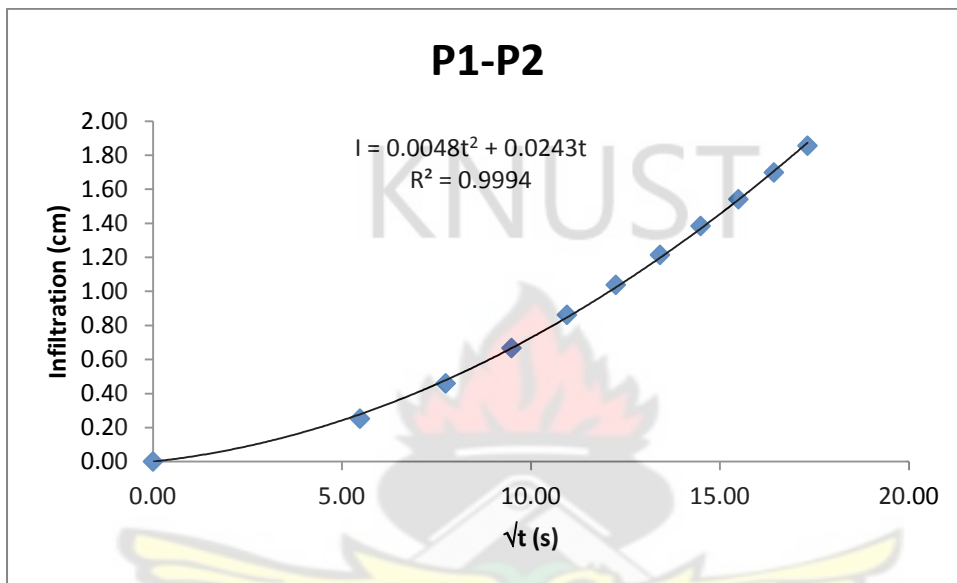


Figure 4.9 Cumulative Infiltration Versus the Square Root of Time for P1-P2

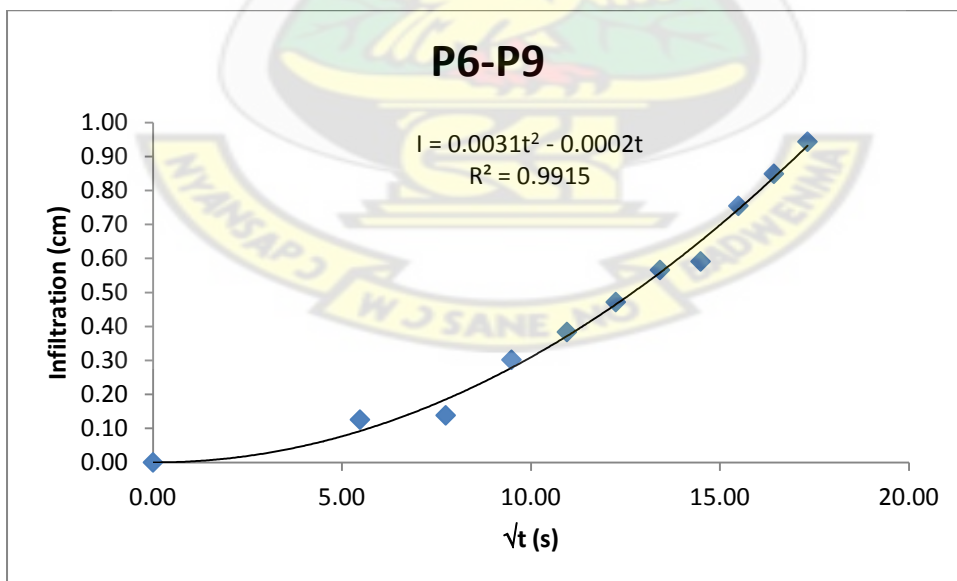


Figure 4.10 Cumulative Infiltration Versus the Square Root of Time for P6-P9

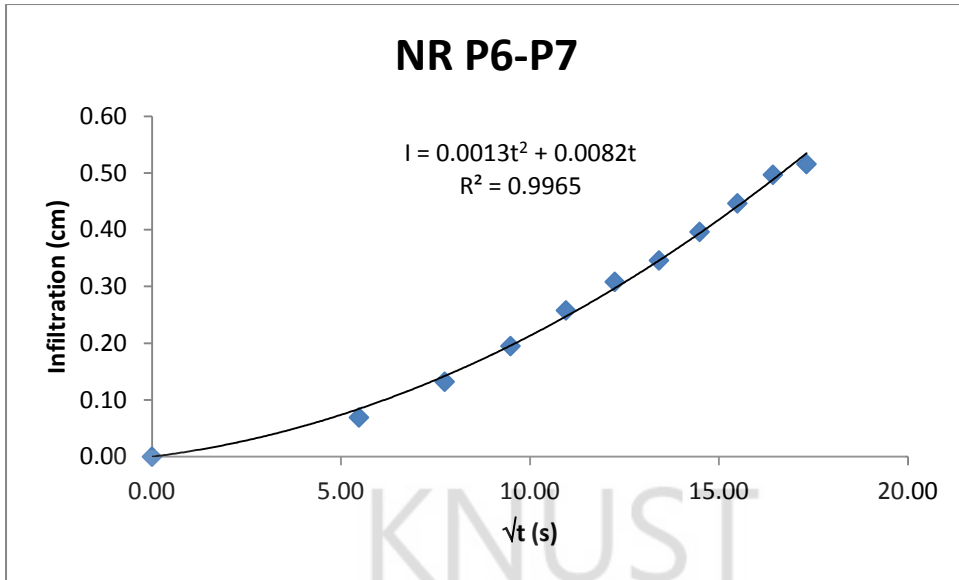


Figure 4.11 Cumulative Infiltration Versus the Square Root of Time for P6-P7

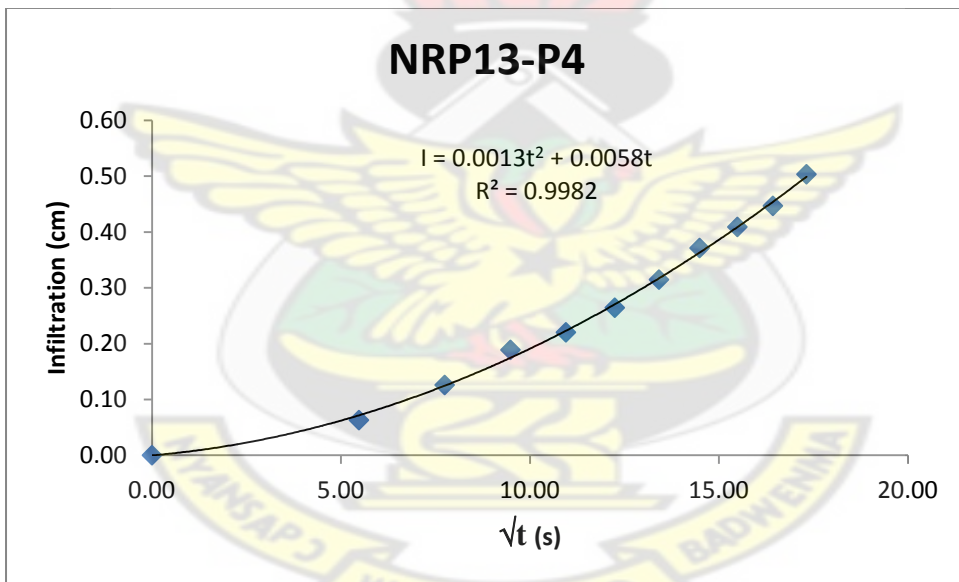


Figure 4.12 Cumulative Infiltration Versus the Square Root of Time for P13-P4

Table 4.2 Spatial Saturated Hydraulic Conductivity of the Site from Falling Head Method

location	Depth of Soil	
	10 cm	20 cm
	K (cm/d)	
P1-P2	6.0212	4.896
P6-P9	4.885	1.438
P7-P8	0.1983	0.3649
P3-P4	5.5016	5.1784
P5-P13	1.0905	0.1554
P11-14	0.1069	0.1012
NU P6-P7	0.3196	1.033
NRP4-P13	1.3458	1.123
NUP4-P13	0.4628	0.4651

NR- Near river UP- Near Upland

Table 4.3 Spatial Saturated Hydraulic Conductivity of the Site from Falling Head Method

Depth (cm)	K_{sat} (cm/d) for P1-P2 Profile
10	6.0212
20	4.896
30	0.4633
40	0.87733
50	0.620048
60	0.106516
70	0.00156
80	0.11914

Table 4.4 Hydraulic Conductivity of the Site Using the Mini Disc Infiltrometer

Location	Hydraulic Conductivity (cm/d)
NU P7-P8	88.3
NR P4-P13	22
NR P7-P8	2.2
P1-P2	66.3
P7-P8	5.44
P3-P1	44.24
P6-P7	66.3
P11-P14	2
P6-P9	66.3
P10-P11	54.52
P4-P13	18.144
P1-P9	16.69
NR- Near river	UP- Near Upland

The saturated hydraulic conductivity (K_{sat}), is the quantitative measure of a saturated soil ability to transmit water when subjected to a hydraulic gradient. Spatial variability of soil hydraulic conductivity must be considered in distributed hydrological models if they are to represent patterns of infiltration and runoff generation via surface and subsurface pathways correctly within a drainage basin. This variability in turn may be governed to some extent by diversity in the size, geometries and distributions of soil macropores, which are pore spaces significantly larger than those of the soil matrix. A unit volume of water passing through a unit cross sectional area of soil in inland valley bottoms reflect differences in hydraulic properties of soils because as fluid flow increases, inter-aggregate pores reduce the possibility of obtaining equilibrated pore water pressure profiles. Hence, macropore

continuity and the more tortuous pore system found at the western portion of the valley bottom where faunal activity and high root density dominated enable preferential flow particularly at saturation, thereby giving high conductivity values (Table 4.2, 4.3 and 4.4). Although macropores make up a relatively small fraction of a soil's total porosity (Watson and Luxmoore, 1986), they can have a disproportionate effect on the soil's infiltration properties. For example, German and Beven (1981) demonstrated that small amounts of macropores could increase saturated hydraulic conductivity by more than an order of magnitude in soils with low-to-moderate matrix conductivity.

The vertical K_{sat} measured in Besease sites were not the same for each depth of sample collected. Conductivity tests revealed that K_{sat} varied spatially within the site, and that each layer possesses different conductivity values. For instance, over the first 20 cm of depth, K_{sat} ranged from 0.01-4.9 cm/day and in the lower depth of 70 cm was 0.002 cm/day. The vertical flow direction within layers was likely to be different, because layers show marked differences in vertical hydraulic conductivity. Particle size also affects conductivity of soils. Soils constituted by clay can have different infiltration characteristics depending on the amount of aggregation present. The presence of clay mostly indicate a low K_{sat} , but may on the other hand be subjected to cracks and macropores (in comparison to a coarser grained soil), and thus give rise to higher K_{sat} . Profile P11-P14 pit had higher clay content than the other pit sampled which experienced a lower K_{sat} (Appendix 1). Such a site undergoes longevity in the hydro-period which also lowers hydraulic conductivity. Soils with high clay content subjected to decreasing water content govern the conditions for crack formation. The cracks form a network of macropores which will be of great importance for water infiltration (Vogel *et al*, 2005). The flow in the unsaturated soil at the study sites is

more complicated than flow through a continuously saturated pore space. Within unsaturated soils, macropores are filled with air leaving the finer pores to accommodate water movement. Therefore, gravity does not dictate the movement of water through the soil but rather differences in matric potential. Sobieraj *et al* (2004) attributed the differences in K_{sat} to microbial processes, especially in cases with clay rich soils at shallow depth. They also suggest that the classical theory of K_{sat} being mostly influenced by particle size is only true for soils consisting of more than 80% sand. Topography and slope greatly influence the microclimatic properties in the soil, and hence also the physical properties (Casanova *et al*, 2000). Fine textured soils are often found at the bottom of slopes, and have small water intake and large runoff potential (Casanova *et al*, 2000). The process of erosion should be greater at higher slopes and thus give rise to a deposition of finer particles at gentle slopes (Casanova *et al*, 2000). Therefore profile pit at P1-P2 at a higher elevation showed a high K_{sat} .

4.5 Infiltration characteristics of Besease Inland Valley Bottom

Table 4.5 Infiltration Rates of the Besease Wetland Site

Site	Infiltration capacity (cm/min)
P1-P2	0.78
P1-P9	0.625
P6-P9	0.047
P7-P8	0.06
P4-P13	0.15
P11-P14	0.02

Infiltration processes represent a wide range of mechanisms of vertical water movement in the soil in Besease under gravity and capillary forces. Before taking the infiltration measurement, the soil was wetted to obtain uniform water content and reduce the soil hydro-phobicity. Each point presented different infiltration rates that decreased with time for any given point. The infiltration experiment conducted at the

Besease Wetland sites mostly exhibited a high infiltration rate at the start of the measurement (Fig 4.13, 4.14, 4.15,) which declined gradually over time. The initially high rate in the Besease Wetlands is usually due to the capillary potential drawing

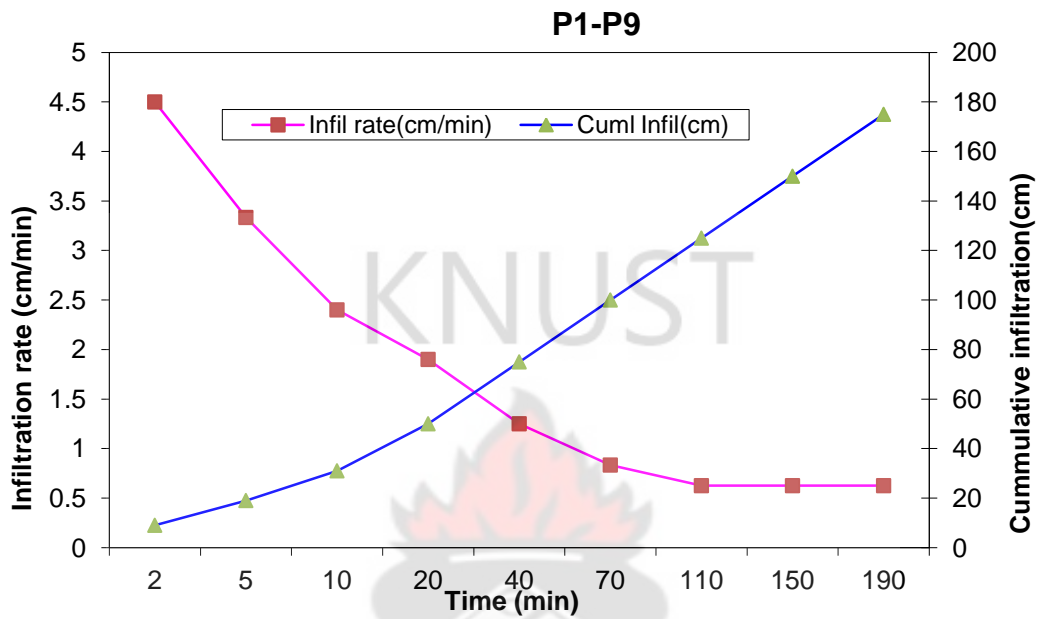


Figure 4.13 Infiltration in Besease Wetland Site P1-P9

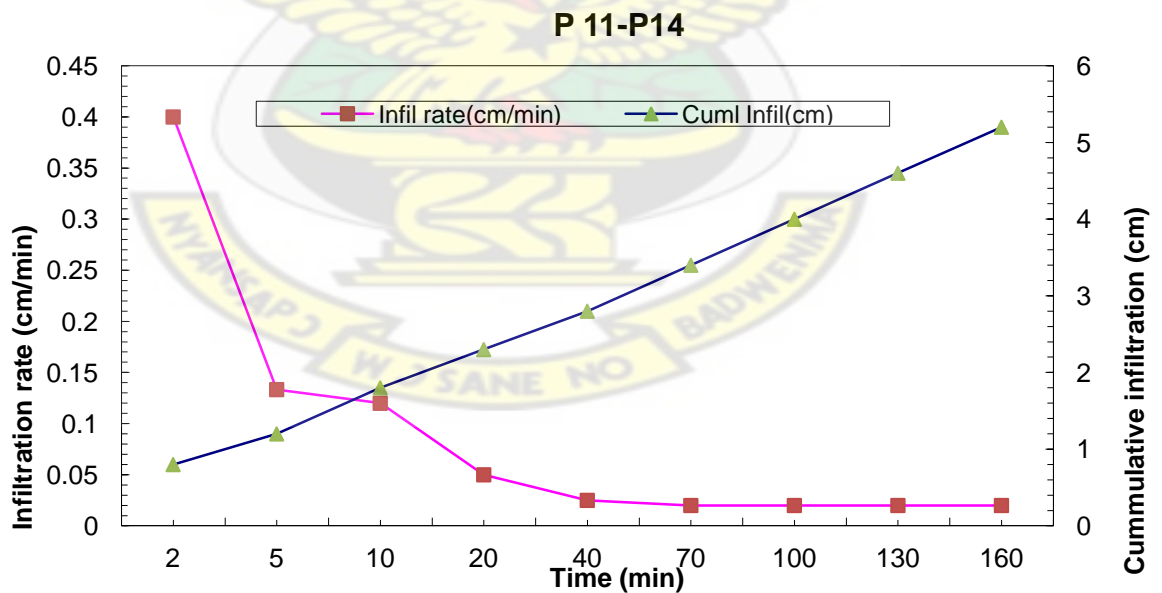


Figure 4.14 Infiltration in Besease Wetland Site P11-P14

water into the dry soil, and the effect of gravity. Variations in infiltration rates are facilitated by extensive root system and animals burrowing in the soil, inadequate prewetting, and soil disturbance by the infiltration ring. The infiltration rate on the studied floodplain ranged from 0.02-0.78 cm/min. The average infiltration rate for the entire population was 0.28 cm/min. Site P1-P2 with high percent sand fraction had the highest infiltration rate of 0.78cm/min. Site P11-P14 and site P8-P7 at lower elevation with low percent sand and moderate clay content (Fig 4.13, 4.14, 4.15,) exhibited a low infiltration rate of 0.02cm/min and 0.06cm/min respectively. This shows that water level ponding could elongate which will result in increased water storage under rice cultivation in the valley bottom.

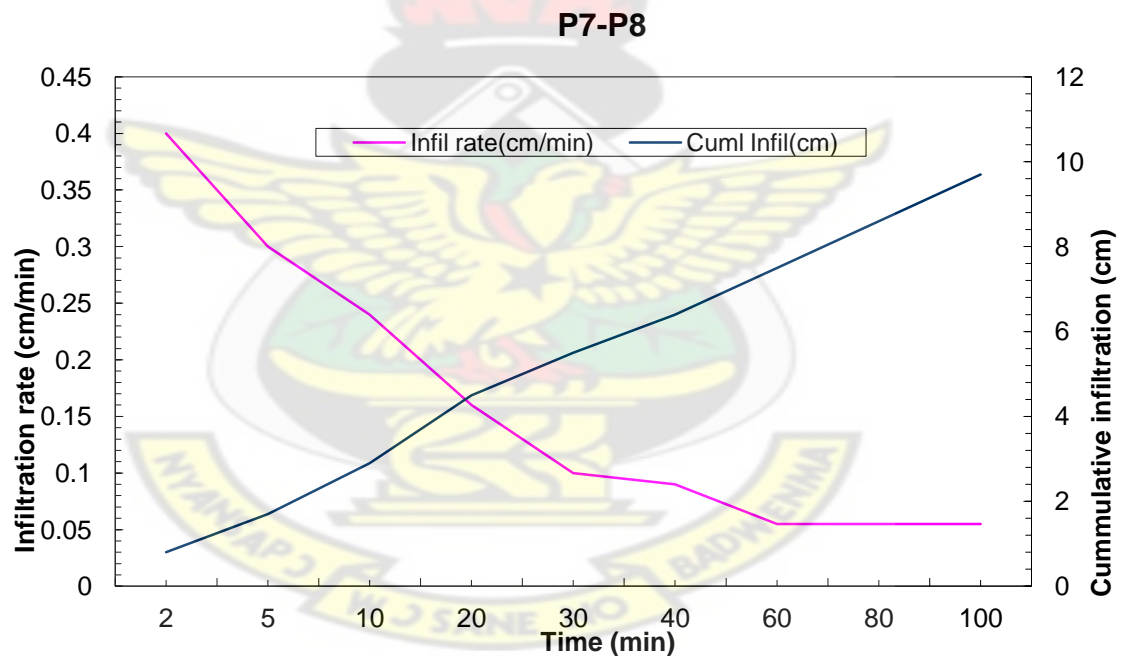


Figure 4.15 Infiltration in Besease Wetland Site P7-P8

4.6 Characteristics of the Soil Chemical Properties

The soil pH was higher at site P11-P14 followed by P4-P3, P7-P8 and P1-P2 (Fig 5.16). The OM content of the soils was highest (6.38%) in the P7-P8 area. A relatively higher value was recorded at P11-P14 (4.69%) and the lowest values were observed at P4-P13 and P1-P2 (Fig 5.17). Also the highest level of total nitrogen was

recorded at P7-P8 followed by P11-P14, P4-P13 and P1-P2. Site P11-P14 had the highest eCEC which was slightly higher than that of P1-P2 (Fig 5.16). This was followed by P7-P8 and P4-P13 in decreasing order. Again the electrical conductivity (EC) was higher at site P11-P14 followed by P4-P3, P1-P2 and P7-P8 (Fig 4.17). The sodium absorption ratio (SAR) also varied in the wetland for which 0.376 mg/l was observed at P7-P8, as the highest. P11-P14, P4-P13 and P1-P2 followed in decreasing order (Figure 4.18). The soil profile distribution for the site from the top 10 cm to the bottom 80 cm horizon showed that pH, total nitrogen and organic matter decreased slightly with depth. However, the exchangeable cations decreased with depth and there was a slight change at the 40 cm depth and continued to decrease again except Ca and Mg which showed some variations from high to low and vice versa from the 40 cm to the bottom 80 cm.

Table 4.6 Chemical Properties of Soils

Horizon	pH	Org.	Total	Org.	Exchangeable Cations me/100g				C.E.C me/100g
		C %	N %	M %	Ca	Mg	K	Na	
0-10	6.9	2.72	0.2	4.69	4.81	3.2	0.5	0.39	9
10-20	6.5	0.6	0.05	1.03	2.94	1.87	0.45	0.24	5.85
20-30	5.6	0.41	0.03	0.7	1.87	1.34	0.28	0.18	4.22
30-40	5.3	0.21	0.03	0.36	1.34	0.94	0.24	0.15	3.32
40-50	5.5	0.18	0.03	0.31	1.6	1.2	0.31	0.15	3.76
50-60	4.7	0.14	0.01	0.25	0.8	0.27	0.2	0.1	2.27
60-70	5.1	0.11	0.01	0.19	1.07	0.53	0.15	0.08	2.58
70-80	4.6	0.11	0.01	0.19	0.8	0.53	0.15	0.07	2.6

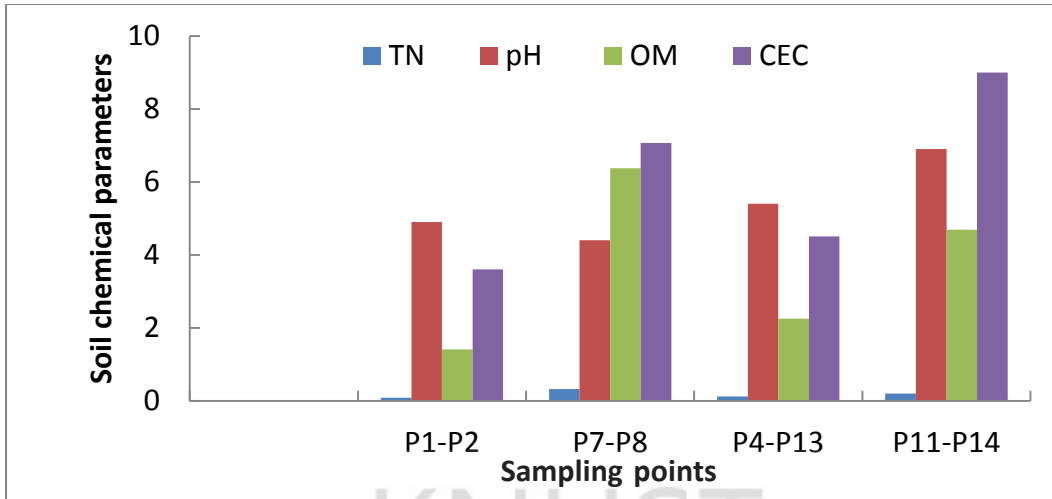


Figure 4.16 Soil pH, Organic Matter (OM), Total Nitrogen (TN) and ECEC of the Wetland

* Soil chemical parameters – pH, Organic matter (OM) and ECEC

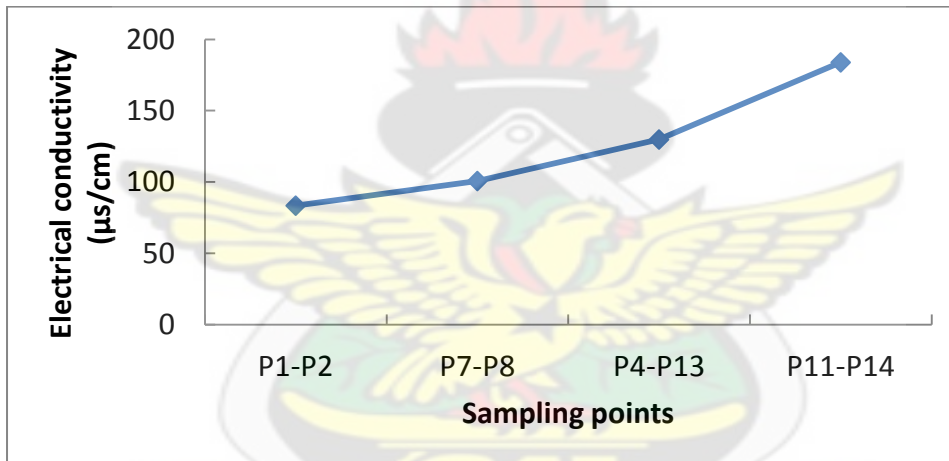


Figure 4.17 Electrical Conductivity for the different Sampling Points

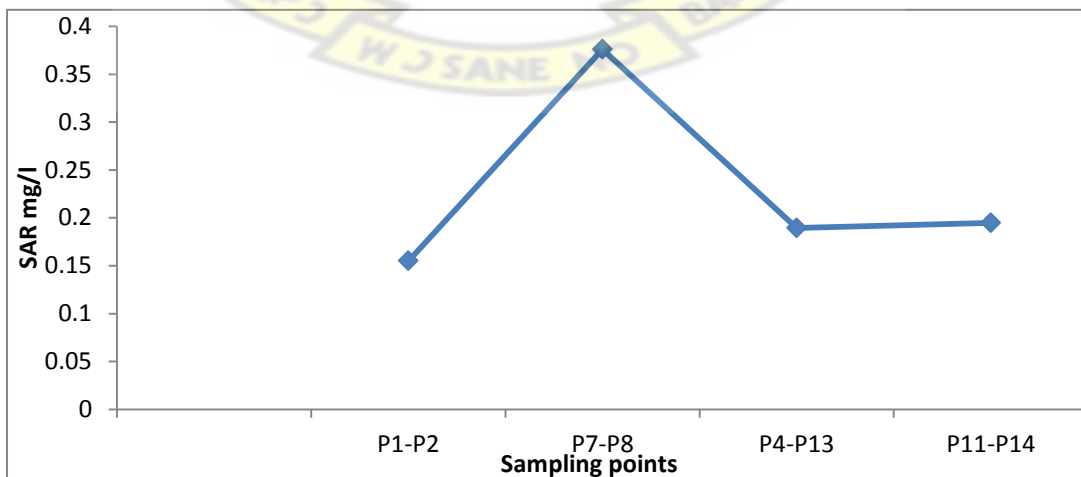


Figure 4.18 SAR for the Different Sampling Points

4.7 Discussion of Physico-Chemical Properties

The valley system exhibit a slightly acidic to a moderate acidity and this was also replicated in the profile pit P11-P14 ranging from slightly acid in the topsoil to moderately acid in the bottom horizon. A lower soil pH may occur as a result of soil leaching and/or weathering (Kawaguchi and Kyuma, 1977). For rice production, the results obtained is suitable, considering that, upon reduction of the (top) soil following submergence, the pH tends to change towards neutral (pH 6.5-7.0). Most plant nutrients are most readily available for uptake by roots in a slightly-acid to near-neutral environment (IRRI, 1978). The high organic matter content and total nitrogen in the surface layers of P7-P8 and P11-P14 were attributed to concentration of vegetation litter and that decomposition processes are usually slow in hydromorphic soils. However, in waterlogging conditions as it is always experienced in valley systems, it reduces N, availability due to low mineralization rates and the risk of denitrification under alternating wet and dry conditions (Annan-Afful *et al*, 2005). These loss mechanisms act most severely in strongly alternating wet and dry environments such as the Besease Wetland. During the soil drying phase, reduced forms of N, particularly NH_4^+ , are nitrified to NO_3^- (Sanchez, 1976). After soil flooding, NO_3^- may be lost by leaching or by denitrification to N gasses. To ameliorate the losses of N, efficient use of fertiliser application must be employed. The higher eCEC at site P11-P14 and P7-P8 was as a result of higher clay content (Appendix 1) and organic matter coupled with sedimentation and less leaching. The higher EC observed at P11-P14 may be due to possible groundwater discharge and evaporation associated with the area. The SAR observed from the four sampling points (Figure 5.18) shows the valley systems suitability for crop production.

CHAPTER FIVE

ESTIMATING GROUNDWATER RECHARGE USING WATERTABLE FLUCTUATION METHOD

5.1 Overview of Groundwater Recharge Estimation

Estimation of the rate of groundwater recharge is a basic prerequisite for efficient groundwater resource management (Sophocleous, 1991). This constitutes a major issue in regions with large demands for groundwater supplies, such as in semi-arid areas, where such resources are the key to agricultural development (Marèchal *et al*, 2006). The determination of groundwater recharge rates is an inherently difficult task because of uncertainties and assumptions associated with different methods of analysis and because various quantifying methods differ in the type of recharge and the space and time scales represented (Scanlon *et al*, 2002). A multitude of methods have been used to estimate recharge. According to Sophocleous (1991), the main techniques used to estimate groundwater recharge rates can be divided into physical methods and chemical methods (Allison, 1988; Foster, 1988). These methods produce estimates over various time and space scales and encompass a wide range of complexity and expense. Information on different methods is contained in references such as Simmers (1988, 1997), Sharma (1989), Lerner *et al*. (1990), Scanlon *et al*. (2002) and Marèchal *et al*, (2006). Among the physical methods, the watertable fluctuation technique (WTF) links the change in groundwater storage with resulting watertable fluctuations through the storage parameter (specific yield in unconfined aquifer). This method is applied likely due to the abundance of available groundwater-level data and the simplicity of estimating recharge rates from temporal fluctuations or spatial patterns of groundwater levels. The primary advantage of this method is

ease of use and low cost of application in semi-arid areas (Beekman and Xu, 2003). Groundwater recharge is critical hydrological parameter that, depending on the applications, may need to be estimated at a variety of spatial and temporal scales (Sophocleous and Perry, 1985; Hendrickx and Walker, 1997). Thus there is the need to develop a method to quantify both the spatial and temporal distribution of groundwater recharge for input to groundwater models.

5.2 Water Level Rise Estimation

To account for drainage from the watertable that takes place during rises in water levels, water level rise is generally computed as the difference between the peak of a water level rise and the value of the extrapolated antecedent recession curve at the time of the peak. The recession curve is the trace that the well hydrograph would have followed had there not been any recharge (Delin *et al*, 2007). There are various approaches for estimating the water level rise. They include the master recession curve (MRC) and the graphical extrapolation approach. The MRC approach is an automated or semi-automated procedure for estimating change in water level per time from water level records. The MRC for a given site is a characteristic watertable recession hydrograph, which represents the average behaviour for a declining water table for the site and can be used to predict what the watertable decline should be in the absence of recharge. Once the master recession curve is determined, the water level rise is calculated as the difference between the predicted and the measured elevations (Obuobie, 2008). In this study, the rise in water level (dh) was computed with the graphical approach as the difference between the peak water level during a recharge event and the extrapolated level to which water levels would have declined if the recharge event had not occurred. This was done by visually examining the entire

water level records for each piezometer and manually extrapolating the antecedent recession curves. The rise in water level during the recharge period was obtained as the difference between the peak of the rise and the low point of the extrapolated antecedent recession curve at the time of the peak. The extrapolations are represented by the dashed lines in Fig. 5.1

5.2.1 Determination of Specific Yield

The specific yield, S_y , is the fraction of water that will drain by gravity from a volume of soil or rock. It is defined as the difference between total porosity and the water content at field capacity. According to Martin (2006) the high variability of specific yield even within the same textural class causes the main uncertainty in the determination of recharge rates by means of the watertable fluctuation method. Healy and Cook (2002) list values of S_y from different studies. They recommend using the usually smaller S_y values determined from pumping tests rather than those determined from laboratory experiments. However, these values also vary over a large range. For fine to medium sand, Healy and Cook (2002) list values for S_y ranging from 0.005 to 0.19. The value depends on the grain size, shape and distribution of pores and compaction of the strata (Gupta and Gupta, 1999 cited in Martin, 2006). In this study, a soil profile was constructed by pushing core samplers of 8.3 cm diameter and 10 cm height into the ground till it hits the watertable. The centre point of piezometers P13-P4, P11-P14, P1-P2, and P7-P8 were sited for the profiling. The content of the core samplers were packaged and sent to the laboratory for soil physical analysis. The soil textures for all the layers were determined using the hydrometer method. Johnson (1967) developed a relation between particle size and specific yield from a soil classification triangle. The results of percent sand, silt and clay obtained from the soil analysis were used to determine the specific yield from the soil textural classification

triangle. The specific yield used for the recharge estimation is a parameter which is difficult to estimate accurately. Lerner *et al.* (1990) ascribed standard specific yield values to be taken from literature (Tables 5.1 and 5.2) rather than field test measurements when values from laboratories are unavailable. Owing to that, the values obtained were compared with standard values of soil specific yields from Prickett (1965), Johnson (1967), Todd (1980), and Sinha and Sharma (1988 ; cited in Lerner, 1990), Bradford and Acreman (2003) from which a range of specific yield values were used to quantify the annual groundwater recharge at the study site (Table 5.3). The specific yields in the recharge estimation were the average values of the specific yields of the soil texture at each station considering the profile of the soil layer textures and the corresponding specific yields from the surface to the water level.

Table 5.1 Values of Specific Yield (S_y) Determined by Type-Curve Matching for 18 Aquifer Tests (Prickett, 1965; cited in Healy and Cook, 2002)

Material	S_y	Material	S_y
Sand, medium to coarse	0.2	Sand, medium to coarse	0.25
Sand, medium	0.161	Sand, fine	0.113
Sand, medium	0.166	Sand, silty to medium	0.014
Sand, medium	0.181	Sand, fine to medium	0.192
Sand, fine to medium	0.032	Sand, fine to coarse	0.014
Sand, medium, silty	0.051	Sand, fine with clay	0.021
Sand, fine to medium	0.005	Sand, fine with clay	0.206
Sand, fine to medium	0.007	Sand, fine with silt	0.018
Sand, fine	0.09	Clay, silt, fine sand	0.039

Table 5.2 Hydraulic Parameters for Alluvial Deposits, U.K (after Bradford and Acreman, 2003)

Hydraulic Parameters	Clay	Silty sand
Specific Yield (%)	1-10	10-30
Specific Storage (m^{-1})	10^{-3} - 10^{-2}	10^{-5} - 10^{-3}

5.3 Results and Discussions

Table 5.3 Recharge Values in the Ejisu-Besease Oda River Basin of Ghana, in 2009/2010

Piezometer	Soil Texture	Specific yield	Year	h(mm)	Recharge (mm)	% of Rainfall
P1	Sandy Loam	0.12 - 0.18	2009	1933	232-348 (290)	15-23 (19)
	Sandy Loam	0.12 - 0.18	2010	1519	182.3-273.2 (227.9)	15-22 (18.5)
P2	Sandy Loam	0.12 - 0.18	2009	3055	366.6-550 (458.3)	24-36 (30)
	Sandy Loam	0.12 - 0.18	2010	2835	340.2-510.3 (425.3)	27-41 (34)
P3	Sandy Loam	0.12 - 0.18	2009	2288	247.5-411.8 (343.1)	16-27 (22)
	Sandy Loam	0.12 - 0.18	2010	1950	234-351 (292.5)	19-28 (24)
P4	Sandy Loam	0.12 - 0.18	2009	1624	194.9-292.3 (243.6)	13-19 (16)
	Sandy Loam	0.12 - 0.18	2010	1464	175.7-263.5 (219.6)	14-21 (18)
P5	Sandy Loam	0.12 - 0.18	2009	2495	299.4-449.1 (374.25)	20-29 (25)
	Sandy Loam	0.12 - 0.18	2010	2734	328.1-492.1 (410.1)	26-40 (33)
P6	Sandy Loam	0.12 - 0.18	2009	3115	373.7-560.6 (467.2)	24-37 (31)
	Sandy Loam	0.12 - 0.18	2010	2205	264.6-396.9 (330.8)	21-32 (27)
P7	Silt Loam	0.10 - 0.14	2009	3070	307-429.8 (368.4)	20-28 (24)
	Silt Loam	0.10 - 0.14	2010	2853	285.3-399.42 (342.4)	23-32 (28)
P8	Silt Loam	0.10 - 0.14	2009	2784	278.4-389.8 (334.1)	18-25 (22)
	Silt Loam	0.10 - 0.14	2010	1623	162.3-227.2 (194.8)	13-18 (16)
P9	Sandy Loam	0.12 - 0.18	2009	2725	327-490.5 (408.8)	21-32 (27)
	Sandy Loam	0.12 - 0.18	2010	2223	266.8-400.2 (333.5)	21-32 (27)
P10	Silt Loam	0.10 - 0.14	2009	2230	223-312.2 (267.6)	14 -20 (17)
	Silt Loam	0.10 - 0.14	2010	2154	215.4-301.6 (258.5)	17-24 (21)
P11	Silt Loam	0.10 - 0.14	2009	1105	110.5-154.7 (132.6)	7-10 (9)
	Silt Loam	0.10 - 0.14	2010	397	39.7-55.6 (47.7)	3-5 (4)
P12	Sandy Loam	0.12 - 0.18	2009	2995	359.4-539.6 (449.3)	23-35 (29)
	Sandy Loam	0.12 - 0.18	2010	2435	292.2-438.4 (365.3)	23-35 (29)
P13	Sandy Loam	0.12 - 0.18	2009	2125	255-382.6 (318.8)	17-25 (21)
	Sandy Loam	0.12 - 0.18	2010	1636	196.3-294.5 (245.4)	16-24 (20)
P14	Silt Loam	0.10 - 0.14	2009	2650	265-371 (318)	17-24 (21)
	Silt Loam	0.10 - 0.14	2010	1421	142.1-198.9 (170.5)	11-16 (14)

5.3.1 Water Level Rise

When one takes into account all observation boreholes, rise of water level in the study area is almost entirely from the seasonal rainfall, since water level rise occurred mostly in the rainfall period. Though there was some accumulation of recharge in the dry season possibly due to regional flow of groundwater, this was very small. The annual and spatial variations in water level were quite high as shown in the groundwater hydrographs. The total annual water level rise for the piezometric networked ranged from 1105-3115 mm for an annual rainfall of 1543.9 mm in 2009 and 397-3070 mm for an annual rainfall of 1247.5 mm in 2010 respectively. The degree to which water levels fluctuate in observation wells varied considerably within the study area. The variability in water level rise exhibited by these wells was mostly the result of the location of the wells. The highest and lowest water level rises in the piezometers were recorded at P6 and P11 respectively for 2009 and that of 2010 was recorded at P7 and P11 respectively. The water level rise measured at P12 and P2 were rather high and may have been influenced by lateral flow due to its close proximity 33 m and 66 m to the Oda River and P14 at a low topographic height also experienced a high water level rise.

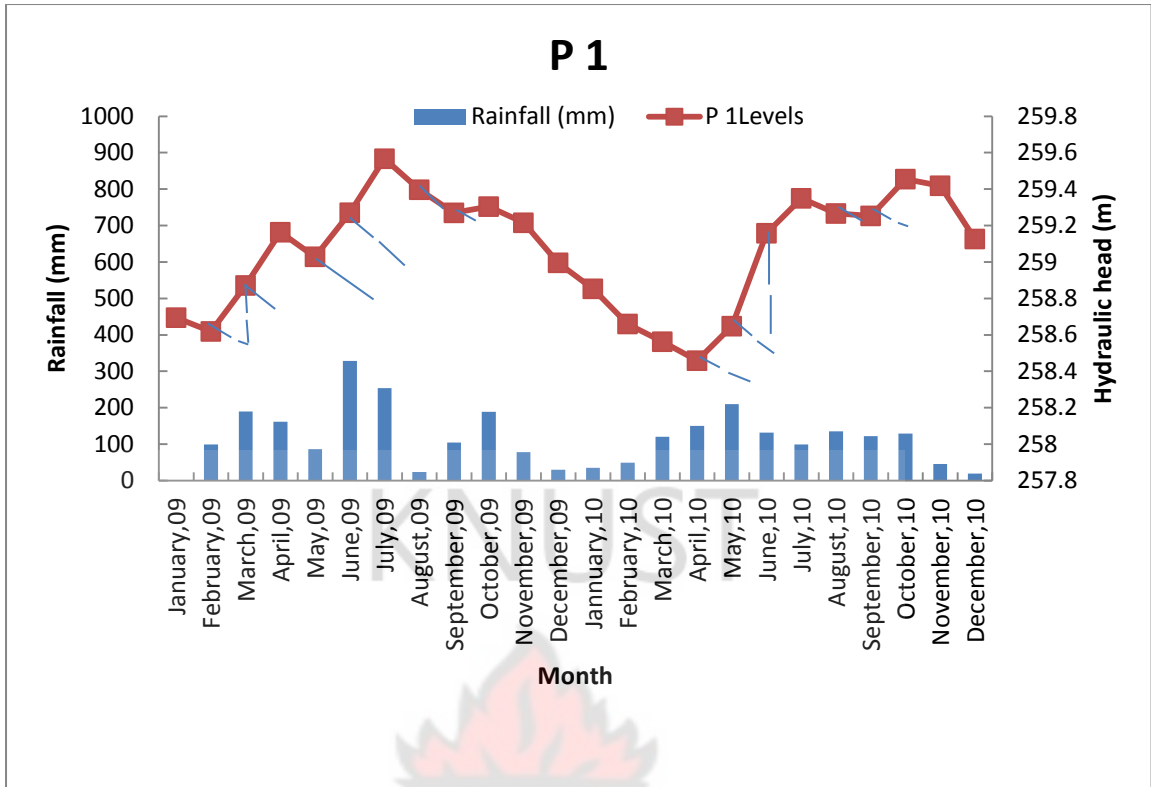


Figure 5.1 Graphical Approach for Estimating Recharge for P1

Table 5.4 Percentage of Groundwater Seasonal Recharge (RC)

Piezometers	Dry season	Major Rainy Season	Minor Rainy Season
	RC%	RC%	RC%
P 1	0.08	18.6	3.2
P 2	6.3	29	10.6
P 3	1.1	22	6.7
P 4	4.8	14.5	7.1
P 5	1.3	21.6	7.2
P 6	0.8	25.6	11.5
P 7	1.3	27.5	8.1
P 8	0.9	24.6	6.3
P 9	0.9	22.4	9.1
P 10	0	24.5	4
P 11	0	12.45	2
P 12	7.7	17.8	8.3
P 13	1.8	14.1	9.4
P 14	0	24.9	8.1

5.3.2 Groundwater Recharge Estimation

The groundwater recharge rate for each of the observation wells was calculated by multiplying the water level rise with the specific yield value of 12-18 %. The estimated recharge for the study area ranged from 166 mm to 467 mm for the 14 piezometers, representing 11-31 % of 2009 annual rainfall and 47.6-427.9 mm, in 2010 representing 5-34 % of the annual rainfall. The overall mean groundwater recharge in the Ejisu-Besease Oda River basin of Ghana was estimated to be 316 mm in 2009, representing 21 % of the mean annual rainfall for that year and 238 mm in 2010, representing 20 % of the mean annual rainfall. The difference in the recharge values for the two study years could be attributed to variability in the annual rainfall distribution and intensity. The recharge estimate obtained in this study is similar to estimates from groundwater studies done elsewhere in the world, using the watertable fluctuation method. Sibanda *et al.*, (2009) estimated the recharge rate of Nyamandhlovu aquifer in Zimbabwe to be 0.4% and 9% of the long term annual precipitation. Also Obuobie (2008) applied the method to the southern part of the White Volta Basin, Ghana and estimated recharge to range from 28.0–150.0 mm in 2006, representing 3.5 – 16.5 % of the mean annual rainfall and from 32.0–204.0 mm in 2007, representing 2.5–16.0 % of the mean annual rainfall with a specific yield range of 0.01–0.05. Similarly, Sanwidi (2007) used this method to the Kompienga Dam Basin, Burkina Faso, in 2005 and estimated the recharge to be from 5.3–29.4 % of the annual rainfall. Similarly, Martin (2006) applied the method in the Atankwidi catchment, Ghana and estimated the recharge to vary from 1.8 –12.5 % of the annual rainfall in 2003 and from 1.4–10.3 % of the annual rainfall in 2004. It can be concluded that differences in estimate of specific yield causes large relative differences in estimated recharge. Cumulative rainfall in January to February 2010

could not recharge the groundwater. This time lag occurred because rainfall takes some time to reach the groundwater table. That implied the rainfall infiltrated to replenish soil moisture deficit.

Recharge rate in the month of March was very high in all the observational piezometric networked. The highest recharge rate of 160 mm occurred in P14 which is located at a relatively low topographic height (259.2 m amsl) with a shallower watertable. However, the watertable fluctuation estimated recharge rate increased. One possible reason for this increase in recharge rate may be that it takes proportionately less time for water to travel through a thinner unsaturated zone, thus bringing the water to the saturated zone before it can be transpired by plants. The topographic low height at the site of P14 coupled with the horizontal movement of subsurface groundwater (West-East) at the location of piezometer P 14 gives the field a better point to locate a well to irrigate the field (Appendix 2).

Results of groundwater recharge (Figure 5.2 a,b,c and d) rate for three months period showed that March-May experienced a higher average recharge of 179 mm followed by February-April 167 mm and 121 mm for May-July representing 11.6 %, 8.4 % and 7.8 % of annual rainfall of 1543 mm for 2009 respectively. The May-July period which experienced a high rainfall but not the highest recharge suggesting that water levels were near or at ground surface and so recharge becomes minimal and that was caused by accumulated antecedent high moisture content from the previous quarter and excessive surface water runoff to the Oda River during heavy storms especially in the months of June and July. For 2010 where recharge was highest in the period of April-June, and May-July rather showed intermittent short dry periods in the rainy quarters. It can be inferred that rice which can withstand floodwater ponding could be planted and supported with controlled irrigation and drainage. In the periods of

February-April and March-May which had appreciable recharge increases indicating that moisture deficit had been replenished and so a high rise of water level could be experienced. This also suggests that high recharge rate leads to lower moisture stress by crops and an occurrence of an optimal watertable height to accommodate crops with different rooting depths. Therefore, there is the need to incorporate cumulative precipitation when accounting for groundwater recharge estimates. The lowest recharge rate were showcased from November-January with 26.4 mm and December-February with 26.9 mm representing 1.7 % of the annual rainfall. And it implies more irrigation water has to be applied to obtain optimal moisture content and watertable levels. Also from the graph of the quarterly recharge of the four piezometers it showed that recharge rate was lowest during the dry season followed by the minor rainy season and the highest in the major rainy seasons respectively, indicating a temporal variation of recharge in the seasons (Figure 5.1 and 5.2). This also suggests that seasonal rainfall (Table 5.4) causes variation in groundwater recharge.

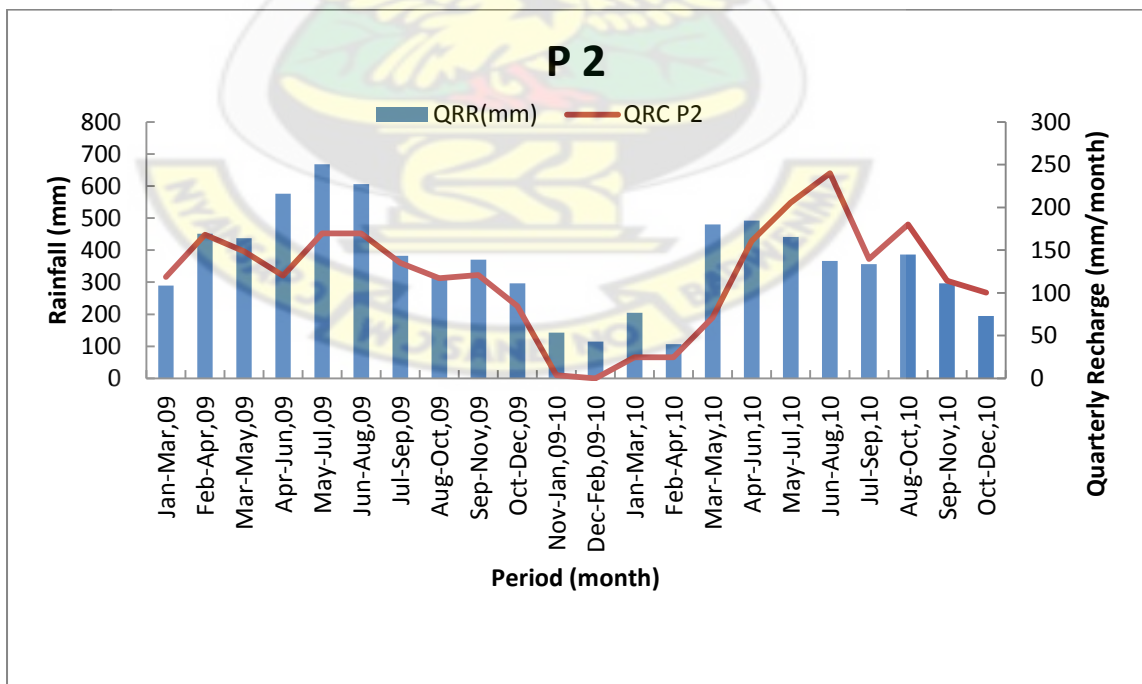


Figure 5.2a Quarterly Recharge Estimate for Piezometer 2

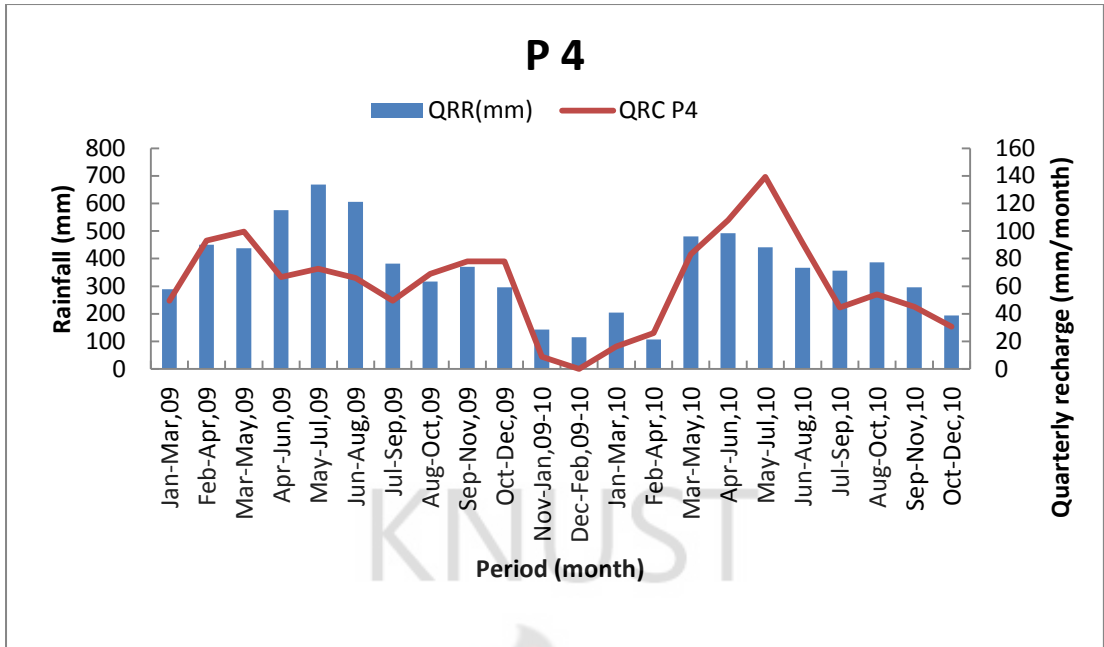
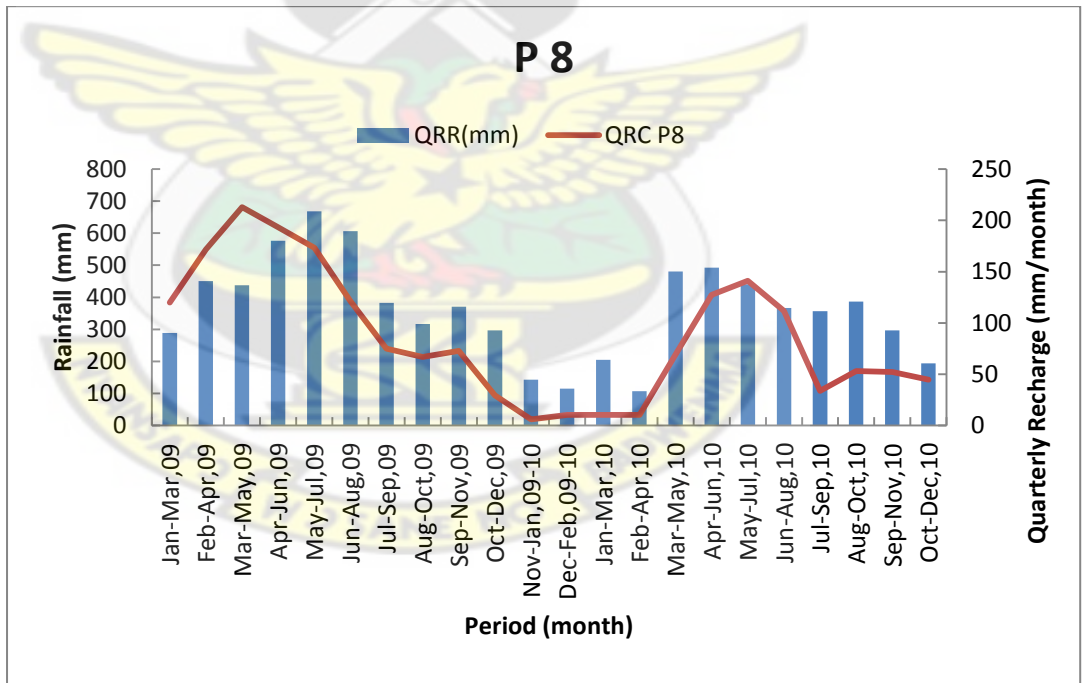


Figure 5.2b Quarterly Recharge Estimate for Piezometer 4

Figure 5.2c Quarterly Recharge Estimate for Piezometer 8



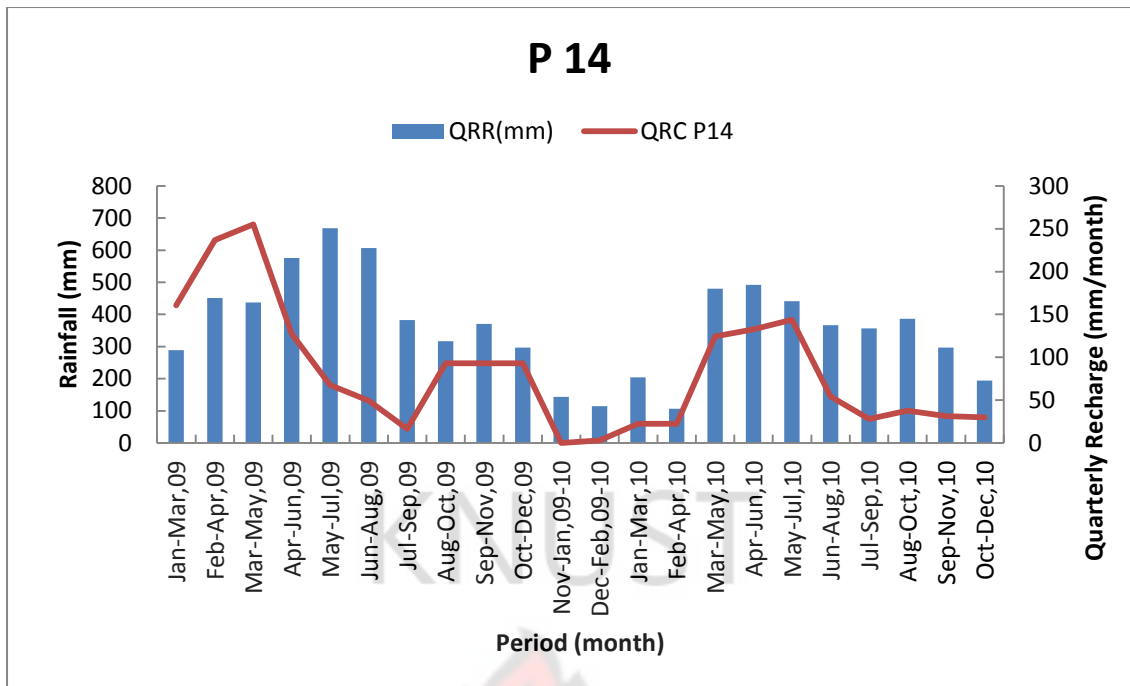


Figure 5.3 d Quarterly Recharge Estimate for Piezometer 14

5.4 Conclusions

The watertable fluctuation (WTF) method for estimating groundwater recharge requires data of specific yield and changes in the watertable over time. It is best applied to systems with shallow watertables that display sharp rises and declines. The method requires no assumption on the mechanisms for water movement through the unsaturated zone; hence the presence of preferential flow path does not restrict its use at a research site. The WTF method was applied to the Oda River Basin at Besease, Ghana in 2009 and 2010 to quantify groundwater recharge and to analyse the fluctuations in the watertable. Findings from the recharge estimation for the study area ranged from 133–467 mm for the fourteen (14) piezometers, representing 11–31% for 2009 annual rainfall and 47.6–427.9 mm, in 2010 representing 5–34 % of the annual rainfall. Results from the three (3) months successive periods show that the May-July period in 2009 experienced a minimal recharge because water levels were already near or at ground surface as a result of high rainfall in the period. The lowest

recharge rate in the dry periods of the two study years showed a decrease in groundwater storage and lowered the phreatic water level which meant that irrigation water needed to be applied to obtain optimal moisture content and watertable levels.

KNUST



CHAPTER SIX

ESTIMATING GROUNDWATER RECHARGE USING THE LINEAR KALMAN FILTER

6.1 Introduction

The maximum quantity of water that can be extracted from an aquifer usually depends on the recharge levels of the aquifer. One of the usual forms of recharge is by rainfall. In the case of unconfined aquifers such as that at Besease Wetlands, a fraction of the rainfall reaches the watertable and the rest is either lost as evapotranspiration or runoff. This fraction determines the safe yield of the aquifer and hence its estimation to a reasonable degree of accuracy is essential for the proper management of such aquifers. The infiltration due to rainfall depends upon several factors such as surface-level gradients, sand particle size in the unsaturated zone, depth of watertable level from the surface and intensity of rainfall. These factors not only vary spatially but also with respect to time. The infiltration rates could generally be determined by three methods namely experimental methods, conceptual and time series models.

Experimental methods often include the use of lysimeters. Conceptual models include mass-balance. For example, Caro and Eagleson (1981) estimated aquifer recharge due to rainfall from an annual water balance. Time series analysis offers a black-box approach for the determination of recharge parameters given a history of rainfall events and watertable readings. Stephenson and Zuzel (1981) noted that for a precipitation of 147 mm the net groundwater recharge was 71 mm which represented 48.3% of rainfall. It was concluded from the study that rainfall in excess of 20–30 mm or high intensity cloud bursts are major contributors to groundwater recharge. Rennolls *et al* (1980) used a first order auto-regressive model to describe the response

of the watertable level in a borehole to a series of rainfall events. The model parameters λ and α were estimated using maximum likelihood method to be 0.88 and 1.13 respectively. Viswanathan (1983) also developed a model for aquifer in order to estimate the groundwater levels from a history of rainfall observations and past groundwater levels to determine the recharge levels of unconfined aquifers. Matsumoto (1992) utilized a multiple regression analysis to eliminate not only the responses of barometric pressure and earth tide but also precipitation from the groundwater level variation.

Modelling groundwater flow faces the problem of modelling an invisible asset. In the field of groundwater studies, groundwater models manage to reproduce the dynamics of the variation of the piezometric heads, which tend to be biased. To circumvent this, it is possible to include the additional information contained in the observations by using data assimilation. Kalman filtering is the most popular approach to data assimilation in hydrological modelling because of its simplicity of implementation and the development of a number of sub-optimal schemes that can be used to deal with high dimensional systems (Riechle *et al*, 2002; Eigbe *et al*, 1998).

6.1.1 Model

The linear relationship (Viswanathan, 1983) between watertable level and rainfall is:

$$y_k = a_{1,k}y_{k-1} + a_{2,k}R_k + a_3 + \epsilon_k \quad (1)$$

Where,

y_t and R_t are water level in a borehole and rainfall on day “ k ” and y_{k-1} is the water level in a borehole in day “k-1”, a_1 , and a_3 represent the natural drainage characteristics of the aquifer and a_2 represents infiltration or recharge characteristics of the aquifer due to rainfall.

To simplify notation the following representations were made:

$$(y_{k-1}, R_k, 1) = (x_{1,k}, x_{2,k}, 1) \quad (2)$$

Then

$$y_k = a_{1,k}x_{1,k} + a_{2,k}x_{2,k} + a_3 + \epsilon_k \quad (3)$$

$$= H_k X_k + \epsilon_k \quad (4)$$

Where,

$$X_k^T = (a_{1,k}, a_{2,k}, a_3) \quad (5)$$

and

$$H_k = (x_{1,k}, x_{2,k}, 1) \quad (6)$$

For Recursive Formulation:

Let

$$\Delta a_{j,k} = v_{j,k}$$

$$a_{j,k} - a_{j,k-1} = v_{j,k} \quad (7)$$

$$a_{j,k} = a_{j,k-1} + v_{j,k} \quad (8)$$

Also let

$$x_{j,k} = v_{j,k}$$

Then,

$$x_{1,k} = x_{1,k-1} + v_{1,k}$$

$$x_{2,k} = x_{2,k-1} + v_{2,k}$$

$$x_{3,k} = x_{3,k-1} + v_{3,k} \quad (9)$$

Matrix Representation:

$$\begin{bmatrix} Z_{1,k} \\ Z_{2,k} \\ Z_{3,k} \end{bmatrix} = \begin{bmatrix} 1 & 0 & 0 \\ 0 & 1 & 0 \\ 0 & 0 & 1 \end{bmatrix} \begin{bmatrix} Z_{1,k-1} \\ Z_{2,k-1} \\ Z_{3,k-1} \end{bmatrix} + \begin{bmatrix} v_{1,k} \\ v_{2,k} \\ v_{3,k} \end{bmatrix} \quad (10)$$

The present problem is to estimate the parameters as a function of time, given R_k and y_k , and the estimation of the parameters a_1 , a_2 and a_3 is done using the Kalman Filter technique.

6.1.2 The Kalman Filter

The problem of estimating a set of parameters which varies according to a known parameter variation law as:

$$a_k = Fa_{k-1} + \varepsilon_k \quad (11)$$

Is similar to the problem of estimating the state vector

$$X_k = (X_1 \dots \dots X_n)_k^t$$

Of a linear discrete time stochastic system of the form:

$$X_k = FX_{k-1} + v_k \quad (12)$$

For a p dimensional vector of noisy measurement:

$$y_k = (y_1 \dots \dots y_p)_k^t$$

Linearly related to the state by an observational equation of the form:

$$y_k = H_k X_{k-1} + \epsilon_k \quad (13)$$

Where,

$F = I$ the linear Model operator, X_k is the state vector at time k , v_k the model error. The model error is assumed to be time-uncorrelated, normally distributed, with zero mean and covariance matrix Q_k (size $n \cdot n$), also named the model error covariance, y_k is the observation at time k , H_k the observation matrix and ϵ_k the observation error. The observation error is assumed to be time-uncorrelated, normally distributed with zero mean and covariance matrix R_k (size $q \cdot q$), also named the observation error covariance. Observation error and model error were assumed to be uncorrelated.

$$v_k \sim N(0, Q_k)$$

$$\epsilon_k \sim N(0, R_k)$$

Also F_k and H_k are respectively $n \times n$ and $p \times n$ matrices,

6.1.3 Kalman Filtering Scheme

Stage 1: Prediction - No knowledge from measurement

The predicted state vector is given by the deterministic model propagation

$$X_k = FX_{k-1} \quad (14)$$

The predicted covariance matrix is propagated through the following equation:

$$P_k^- = FP_{k-1}^+ F^T + Q_k \quad (15)$$

Stage 2: Data Assimilation (measurement information used)

The innovation vector is defined as the difference between the observations and the forecast state variables:

$$d_k = y_k - H_k X_k^- \quad (16)$$

and its covariance matrix is:

$$H_k P_{k-1}^+ H_k^T + R_k \quad (17)$$

The Kalman gain is derived by requiring that X_k^+ is the minimum variance estimate of X_k given the observation y_k :

$$K_k = P_k^- H_k^T (H_k P_{k-1}^+ H_k^T + R_k)^{-1} \quad (18)$$

The analysis step is:

$$X_k^+ = X_k + K_k (y_k - H_k X_k^-) \quad (19)$$

and

$$P_k^+ = (I - K_k H_k) P_k^- \quad (20)$$

Where:

X_k^- = *a priori* state estimate

X_k^+ = *a posteriori* state estimate

P_k^- = covariance matrix of the predicted error ($e_k - e_k^-$)

P_k^+ = covariance matrix of the updated error ($e_k - e_k^+$)

The analysis step is in fact a linear combination of the observations and the model forecast. The Kalman gain describes how the innovations are spread over the entire state space and weights how strong the correction should be. If the model forecast is

more certain than the observation, i.e. $P_k^- \ll R_k$, then the gain is close to zero and $X_k^+ \rightarrow X_k$. In case, $P_k^- \gg R_k$ then the gain is close to one, and the analysis is close to the observations.

SOLUTION

Let the parameter vector be:

$$a_k = \begin{bmatrix} a_1 \\ a_2 \\ a_3 \end{bmatrix}$$

and the matrix H becomes a vector of the following form:

$$H_k = (y_{k-1} \ R_k \ 1)_k^t$$

For a simple random walk model:

$$F_k = I$$

Where I is identity matrix

Therefore equations (14) and (15) become:

$$X_k = X_{k-1} \tag{21}$$

$$P_k^- = P_{k-1}^+ + Q_k \tag{22}$$

Hence Equations (21) and (22) are prediction algorithms and Equations (19) and (20) are also correction algorithms for the estimation of time dependent parameters a_1 , a_2 and a_3 . In equation (22), the Q matrix is chosen to be diagonal with the diagonal elements selected to represent the expected rate of variation of the parameters between the sample intervals. Differing expected rate of change can be specified for different parameters. Any parameter that is known to be time invariant can simply be handled by setting the appropriate diagonal element to zero (Young, 1974).

If the parameters a_1 , a_2 and a_3 are known in Equation 1, then the watertable level can be estimated (Fig 6.1, Fig 6.3a and Fig 6.5) using the equation;

$$y_k = a_{1,k}y_{k-1} + a_{2,k}R_k + a_3 \quad (23)$$

Where y_k is the estimate of level on day t in Equation (1) and there are three components that affect the watertable level on day k . These are water level y_{k-1} in a borehole on day “ $k-1$ ” and rainfall R_t on day “ k ” and unknown external influences exhibited by the parameter a_3 . In estimating the parameters, three scenarios that can exist with respect to the parameters that correspond to the above three components are:

- the parameters a_1 , a_2 and a_3 are all time invariant;
- the parameter a_2 was assumed to be time dependent with the value of the diagonal element that corresponds to a_2 was arbitrarily chosen as 0.01 and the parameters a_1 and a_3 were treated as time invariants;
- all the parameters are time dependent with equal weightage

6.2 Results and Discussions

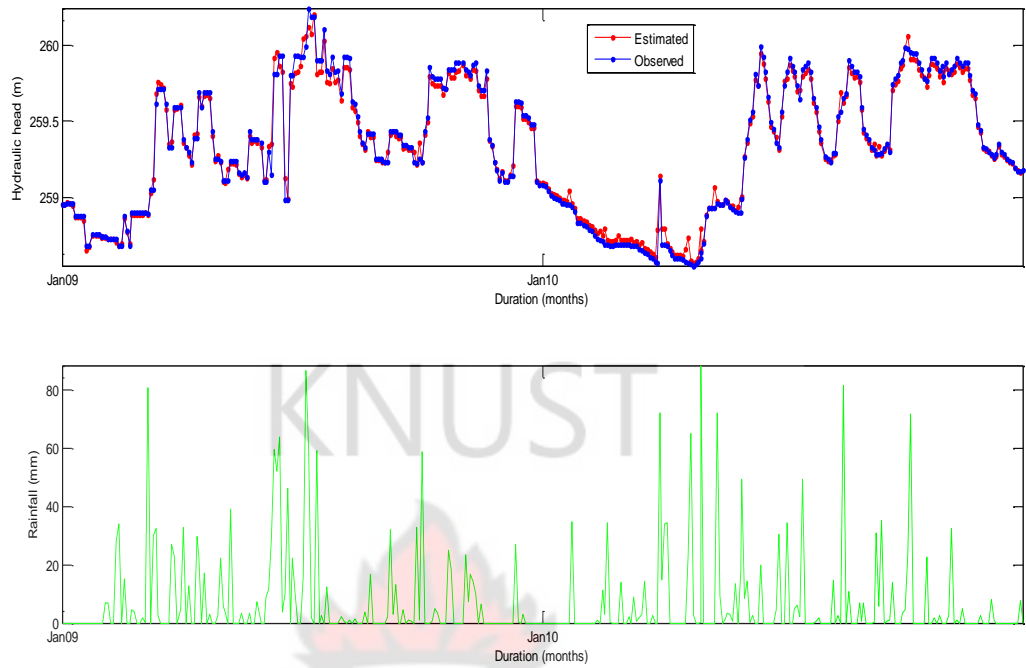
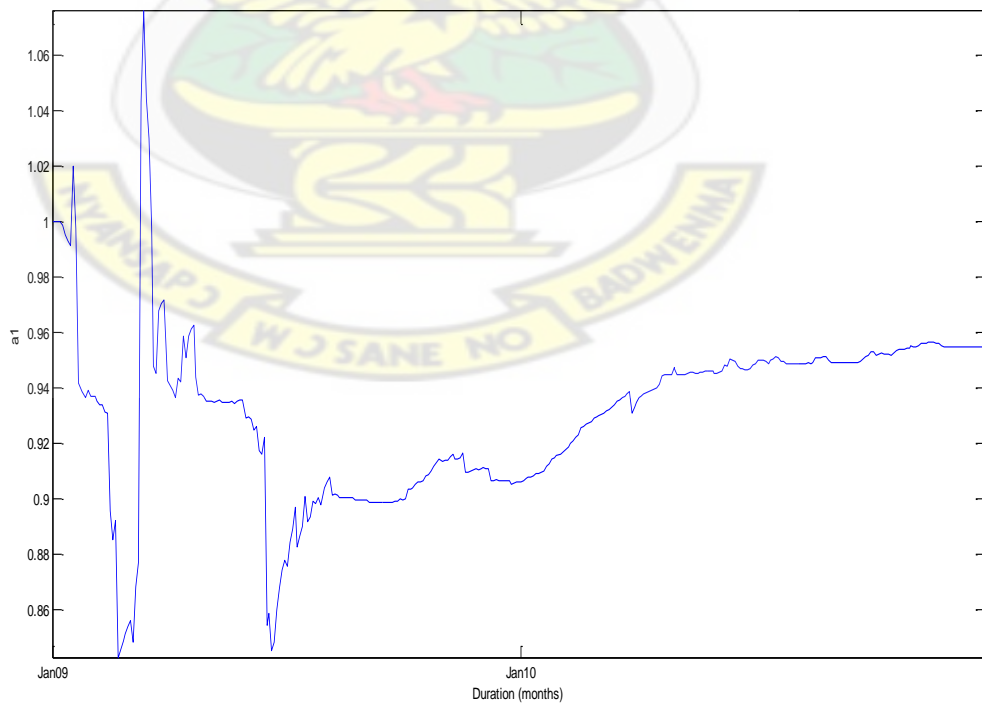


Figure 6.1 Rainfall and Watertable Level During the Years 2009 and 2010 for $Q = 0$



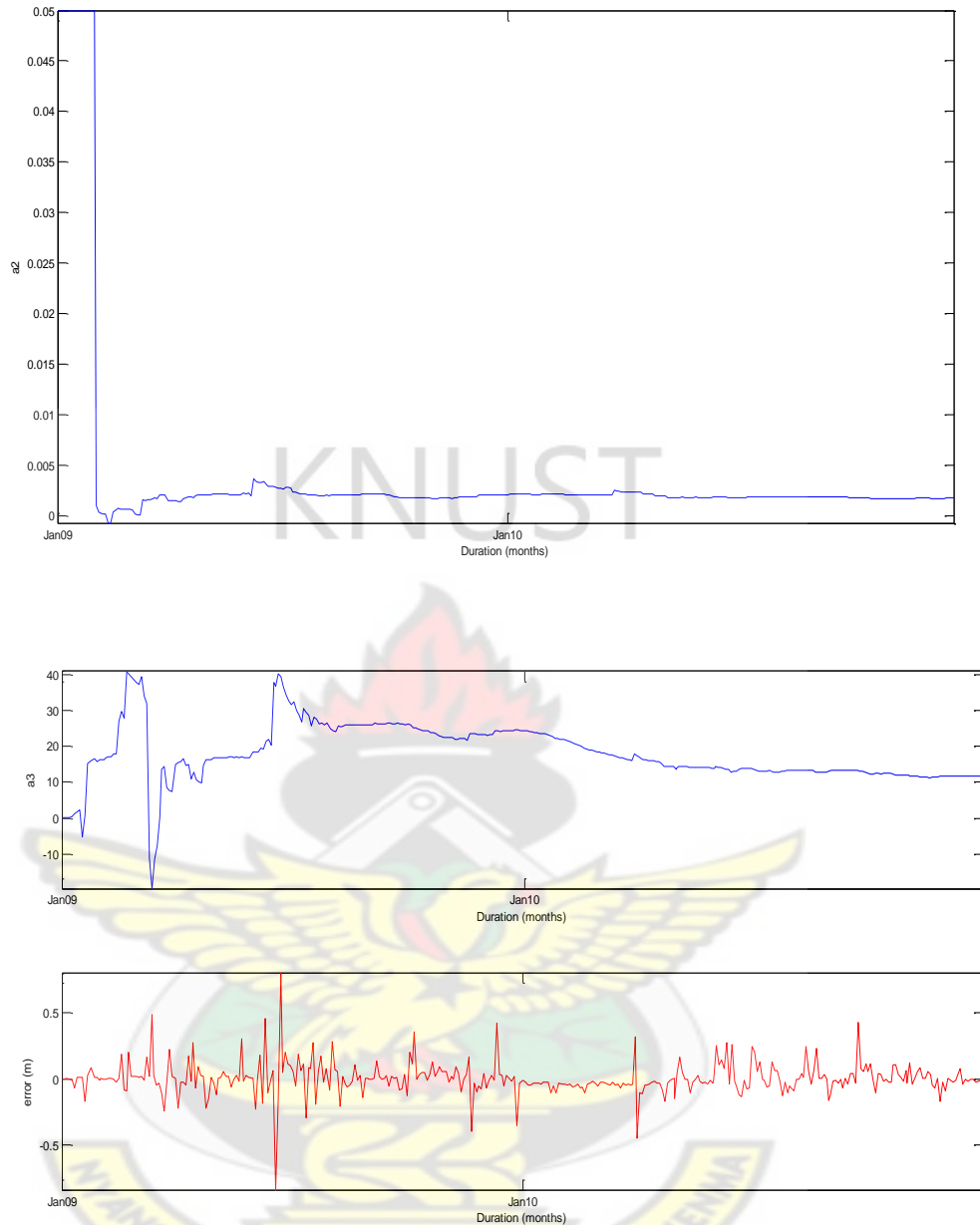


Figure 6.20 Parameter Variation with $Q = 0$.

Figure 6.20 shows the variation parameters a_1 , a_2 , a_3 and errors with the diagonals of the matrix Q in Equation (21) being taken as zero. This means that the parameters a_1 , a_2 and a_3 are assumed to be time invariant. Consequently, the variation in the parameters was extremely slow. The infiltration due to rainfall is given by the parameter a_2 which varied between 0.0 and 0.005. The rise in watertable level due to rainfall alone is :

$$\Delta h = a_2 R_t \quad (22)$$

Where,

α is given as the fraction of rainfall that reaches the watertable, then the rise in watertable could also be expressed as:

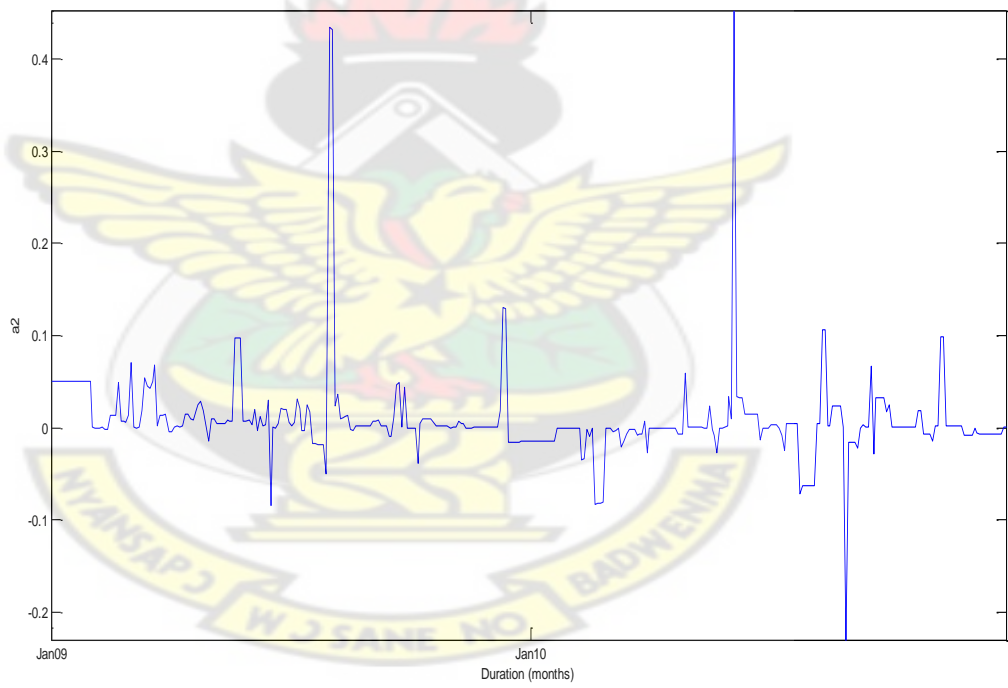
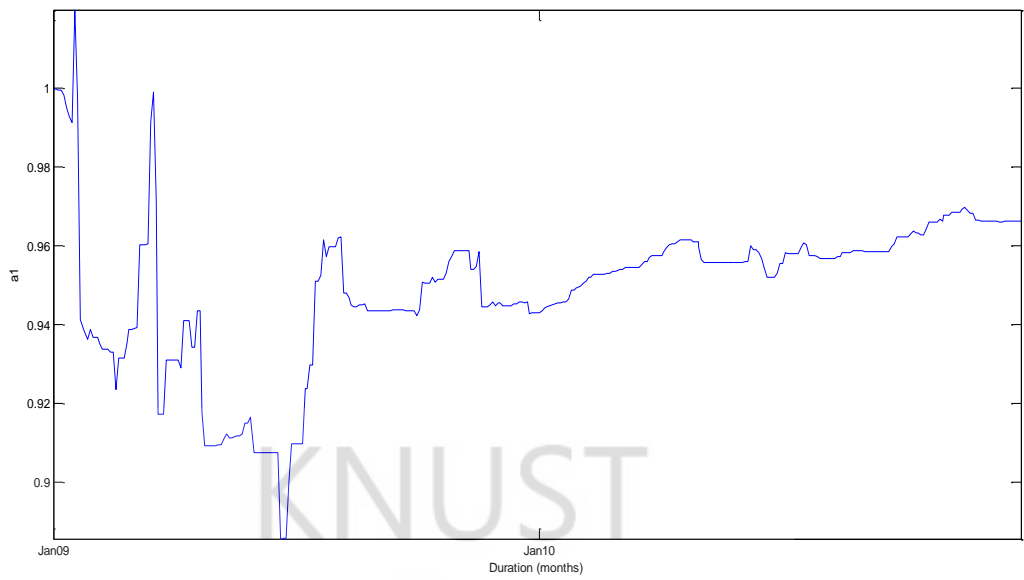
$$\Delta h = \frac{\alpha R_t}{S_y} \quad (23)$$

Where,

S_y is the specific yield. Combining Equation (22) and (23)

$$\alpha = a_2 \cdot S_y$$

With the average value of specific yield (S_y) for the field being 0.15, the infiltration factor α for the period 2009 and 2010 varied between 0.0 and 0.00075. However, the error between the estimated and actual watertable levels was substantially high owing to the assumption that the parameters are time invariant. In the next scenario the parameter corresponding to the rainfall a_2 was assumed to be time variant and the value of its diagonal element arbitrarily taken as 0.01. The value of 0.01 was chosen from trial and error, so that the error between the measured and calculated watertable levels is nearly equal to zero. The rest of the parameters a_1 and a_3 were assumed to be time independent.



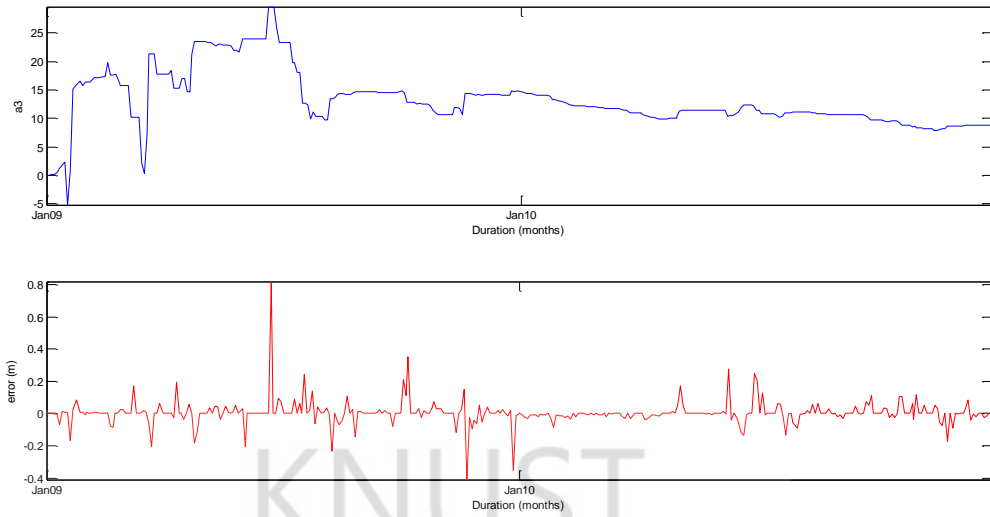
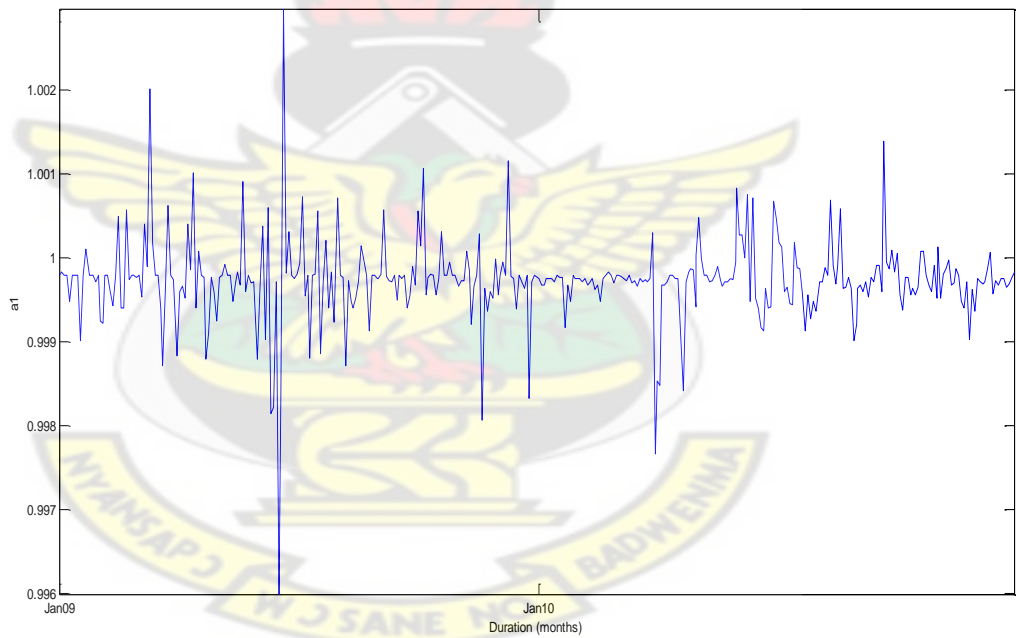


Figure 6.21 Parameter Variation with $Q = 0.01$ for the Diagonal Element a_2



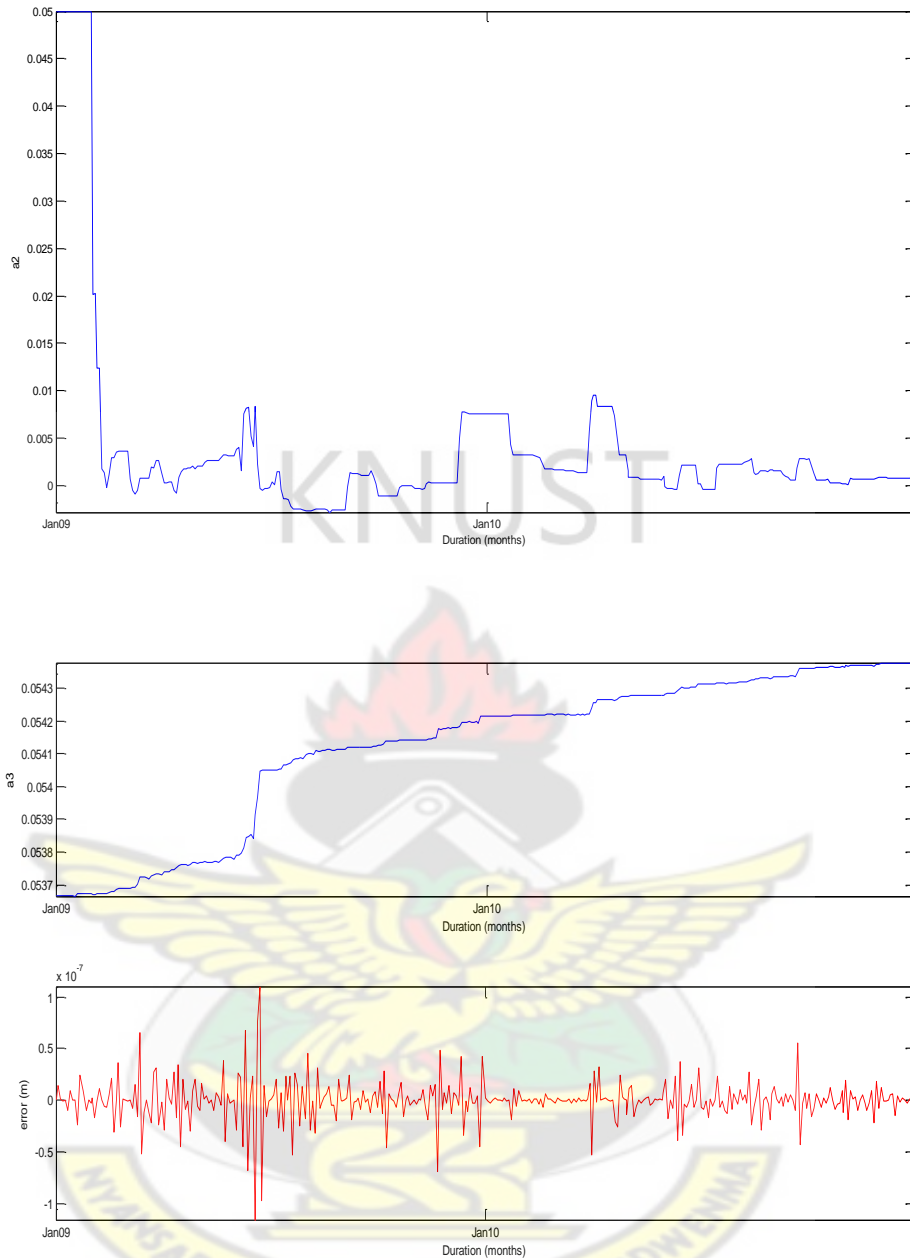
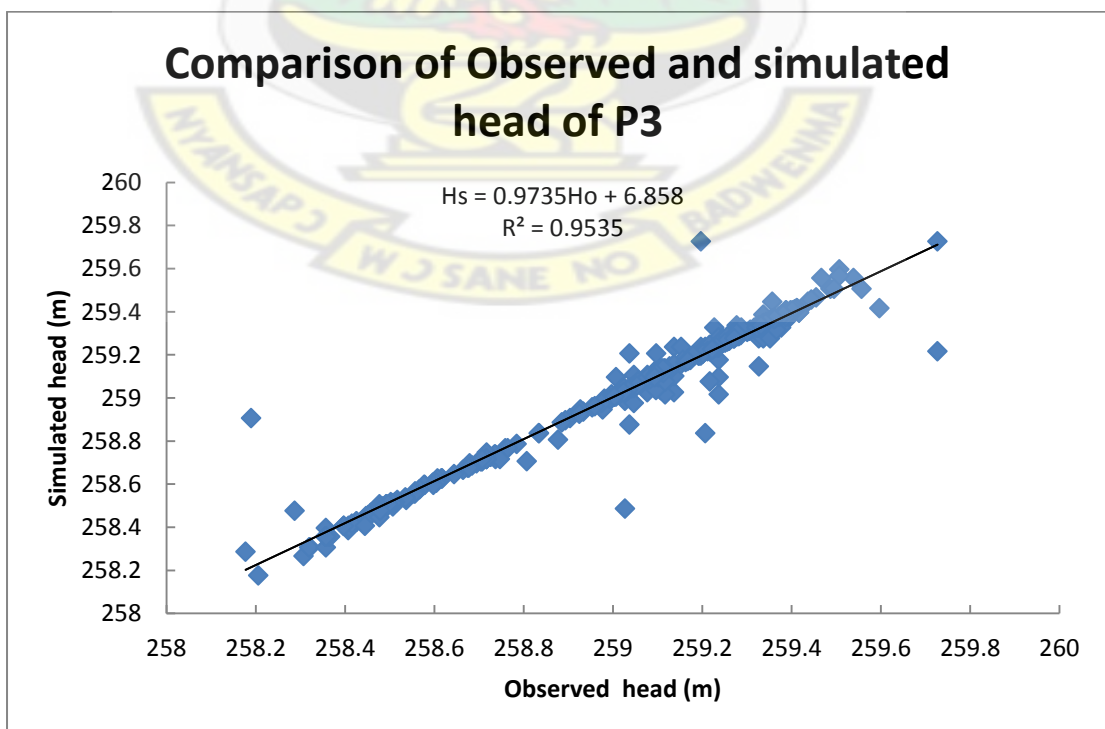
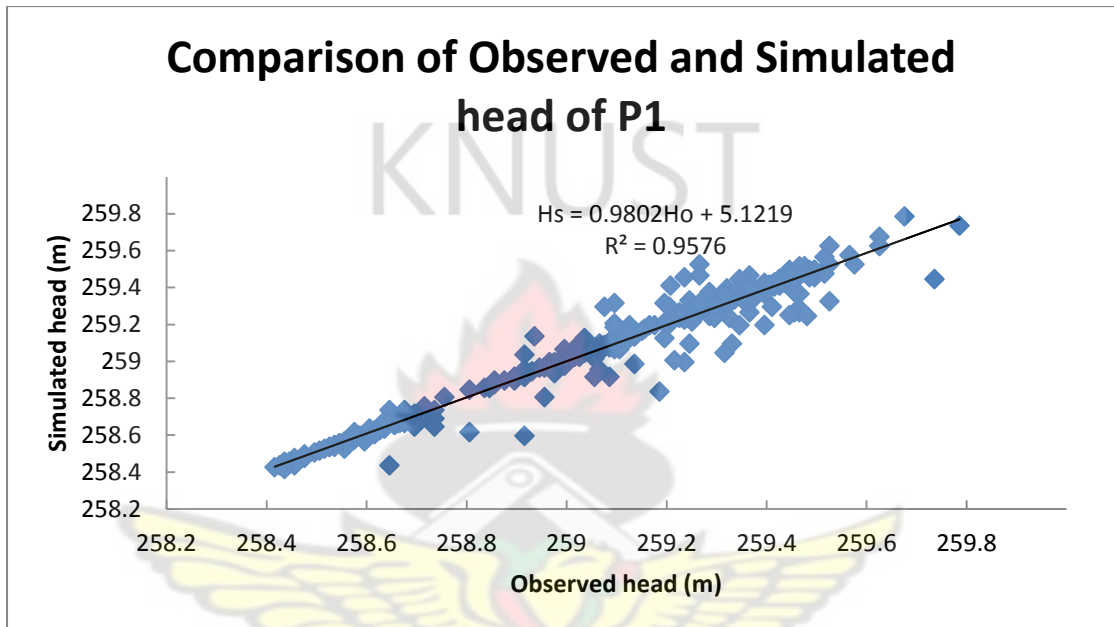


Figure 6.22 Parameter Variation with $Q = 0.01$ for all the Diagonal Elements a_1 , a_2 and a_3

From Figure 6.21 and Table 6.2 the results show that the parameter a_2 varied considerably over the period of time and the recharge values ranged between 0.0-1.27 % for P4 and 0-16.5 % for P14 of the incident rainfall. In the last analysis a constant value 0.01 was used for the diagonal elements for the matrix Q , which meant that all the parameters were time variant with equal weightage. Results also showed α

varying between 0.0 and 0.15 % of the annual rainfall for all the piezometers. The Kalman Filter method used as a recharge estimate resulted in a fit between the simulated hydraulic head and observed sub-surface water level fluctuation (Figure 6.23).



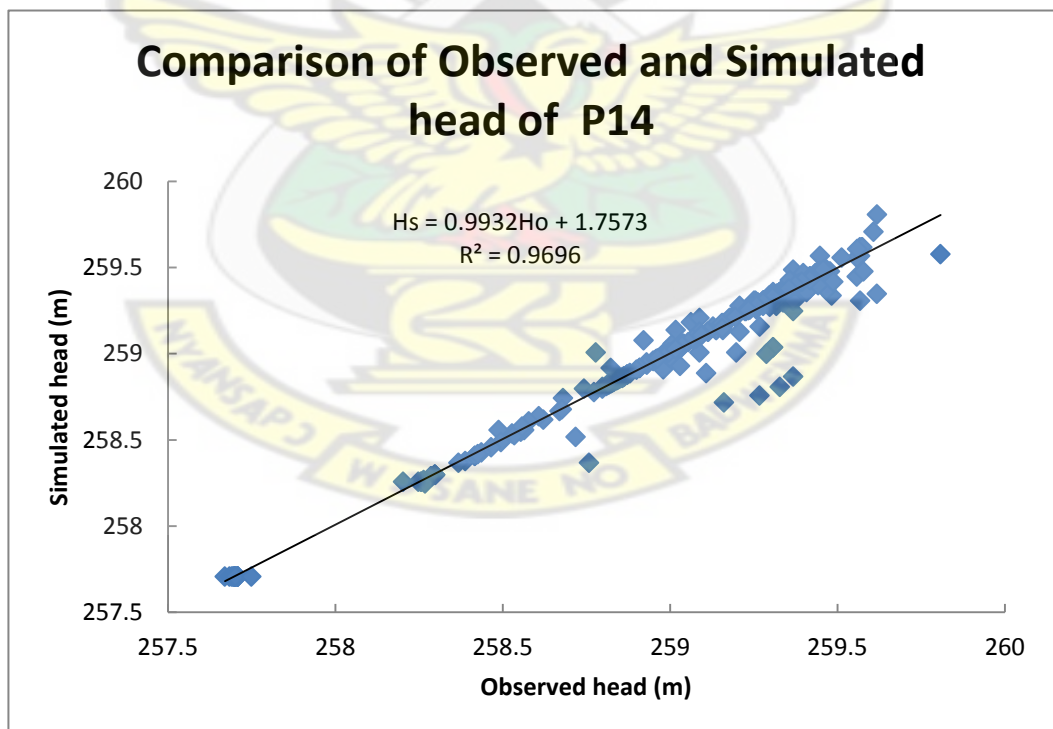
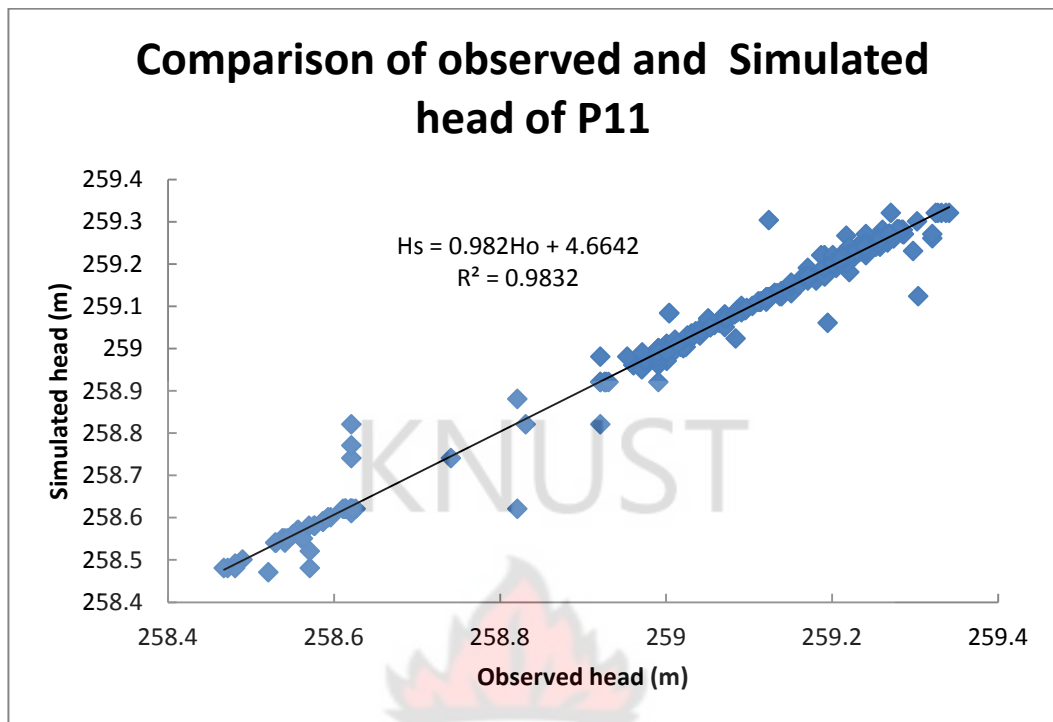


Figure 6.23 Comparison of Simulated and Observed Heads in the Besease Inland Valley Wetland

Table 6.1 Recharge Values Based on the Present Day Rainfall

Piezometer	Specific yield	Fraction of rainfall (α)	Recharge	% of Rainfall
P1	0.15	0-0.15	0-0.0225	0-2.25
P2	0.15	0-0.46	0-0.069	0-6.95
P3	0.15	0-0.22	0-0.033	0-3.3
P4	0.15	0-0.085	0-0.0127	0-1.27
P5	0.15	0-0.38	0-0.057	0-5.7
P6	0.15	0-0.97	0-0.1455	0-14.5
P7	0.15	0-0.98	0-0.147	0-14.7
P8	0.15	0-0.33	0-0.0495	0-4.95
P9	0.15	0-0.24	0-0.036	0-3.6
P10	0.15	0-0.12	0-0.018	0-1.8
P11	0.15	0-0.16	0-0.024	0-2.4
P12	0.15	0-0.7	0-0.105	0-10.5
P13	0.15	0-0.7	0-0.105	0-10.5
P14	0.15	0-1.1	0-0.165	0-16.5

The error between the calculated and the observed watertable level (Fig 6.22) was nearly equal to zero. It could be deduced from the assumption, that the time variant parameters of a_2 only was considerable in the parameter values estimated (Fig 6.21) was more appropriate and realistic than the time invariant assumptions and the time variant parameters with equal weightage. From Figures 6.21 and 6.22, when considerable rain fell during June 2009, October 2009, June and July 2010, the infiltration factor α was very high. However, during the periods December 2009 to April 2010, the infiltration factor was zero which indicated that infiltration could not reach the water table but was retained in the unsaturated zone to replenish moisture deficit.

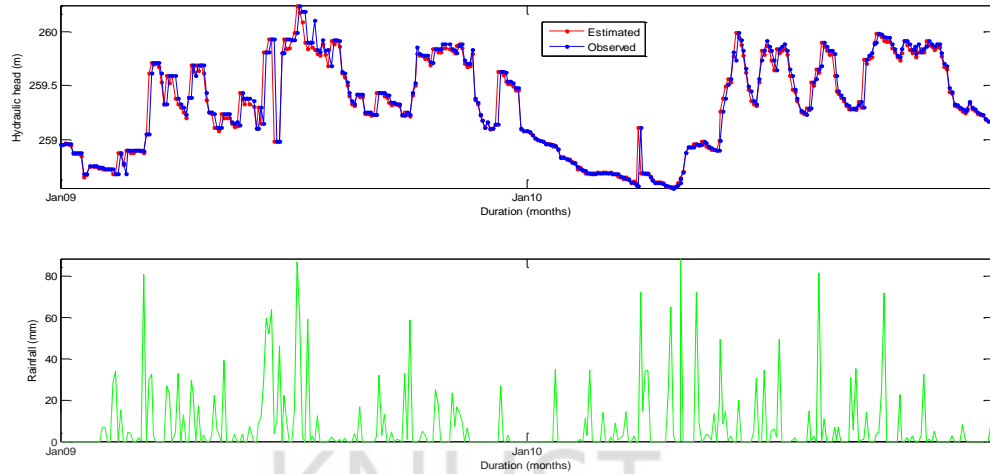


Figure 6.3a Rainfall and Watertable level During the Years 2009 and 2010 for a_2 , $Q = 0.01$

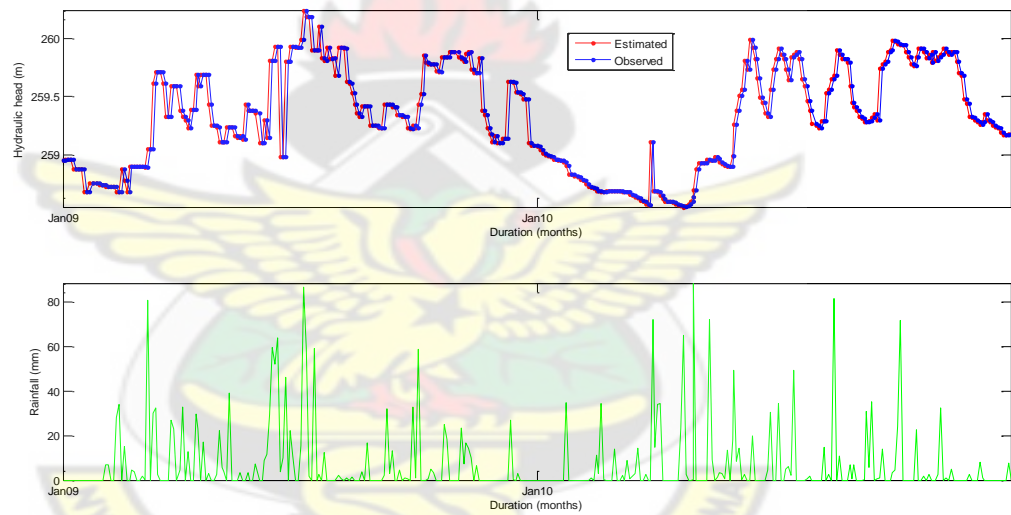


Figure 6.3b Rainfall and Watertable Level During the Years 2009 and 2010 for a_1, a_2, a_3 , and $Q = 0.01$

The effects of previous rainfalls to the order of seven days on the fluctuations of watertable levels were also ascertained. The linear relationship between watertable level and rainfall is:

$$y_k = a_{1,k}R_k + a_{2,k}R_{k-1} + \dots + a_{p,k}R_{k-p+1} + a_{p+1,k}y_{k-1} + a_{p+2,k}y_{k-2} + \dots + a_{p+1,k}y_{k-1} + a_{p+2,k}y_{k-2} + \dots + \epsilon_k \quad (24)$$

Where,

R_k and y_k are rainfall and watertable level at day k and $p = 7$

If the parameters $a_1 - a_9$ are known then the watertable levels can be estimated.

In Equation (24) as it has been said earlier, three factors directly affect the watertable level on day k . They are:

- the watertable level on day $k-1$;
- the rainfall on day $k, (k - 1), \dots, (k - 6)$ and
- unknown external influences reflected by the parameter a_9 .

In choosing a value for the parameter a_1 , it was assumed that a_1 would vary considerably with respect to time, and hence a high value of 0.02 for the corresponding diagonal element of the Q matrix. Similarly it was assumed that parameter a_2-a_4 will have less variation and a_5-a_7 even lesser variation with respect to time. Parameter a_8 was assumed to be time invariant and a very small variation (10^{-5}) was assumed (Table 6.2) for the parameter a_9 .

Table 6.2 Values of the Diagonal Elements of the Matrix Q

Parameters	Elements of diagonal element of matrix Q
a_1	0.02
a_2-a_4	0.01
a_5-a_7	0.001
a_8	0
a_9	0.00001

The results in Fig 6.4a show the scenario where the parameters were time dependents with different weights (Table 6.1).

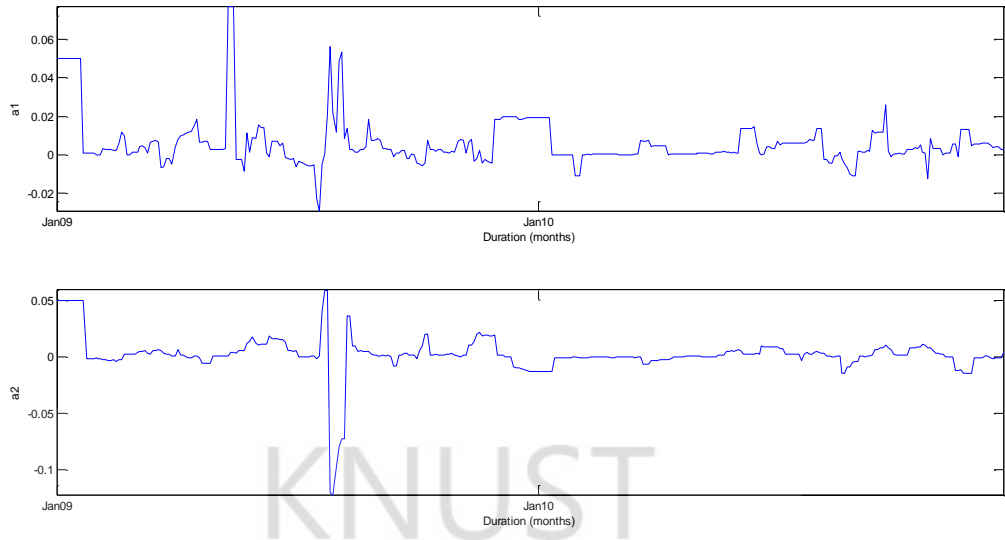


Figure 6.4a Parameter Estimate for a_1 and a_2 with Variable Q Matrix

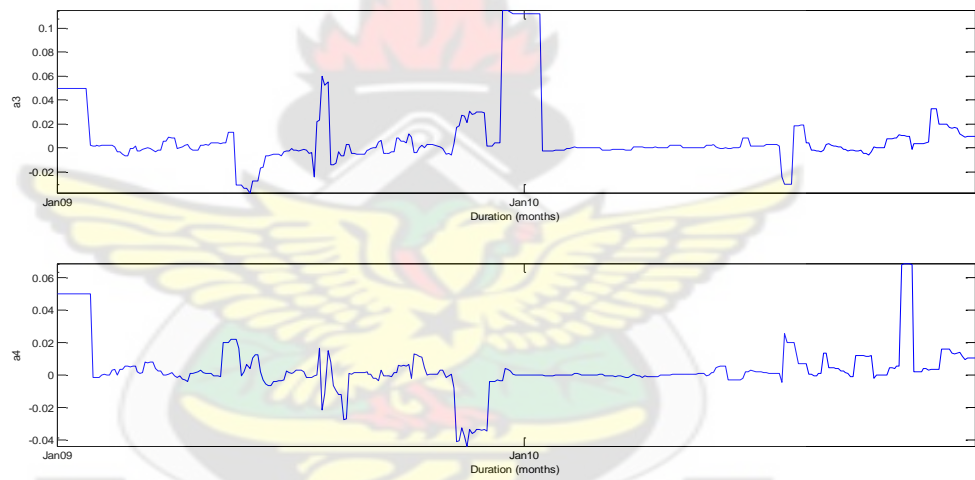


Figure 6.4b Parameter Estimate for a_3 and a_4 with Variable Q Matrix

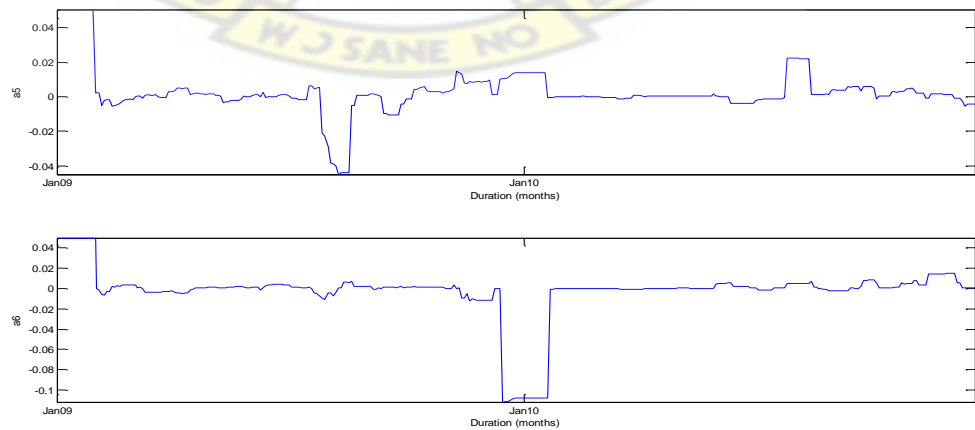


Figure 6.4c Parameter Estimate for a_5 and a_6 with Variable Q Matrix

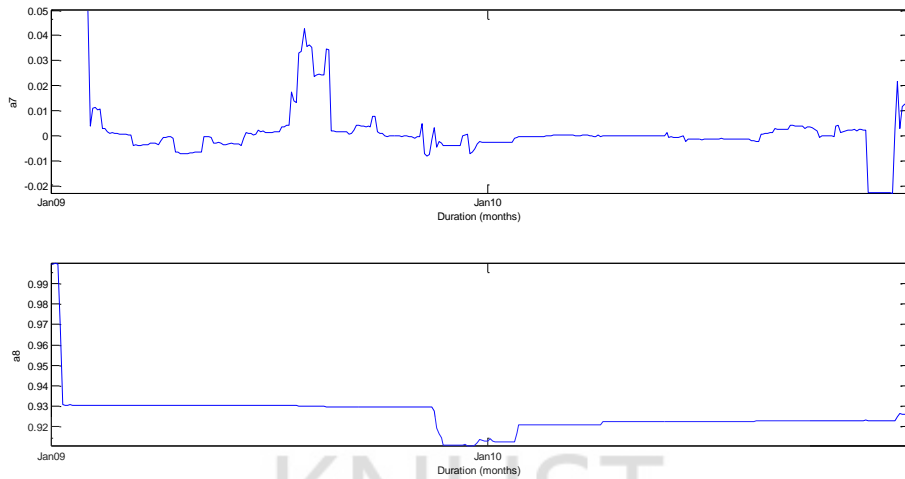


Figure 6.4d Parameter Estimate for a_7 and a_9 with Variable Q Matrix

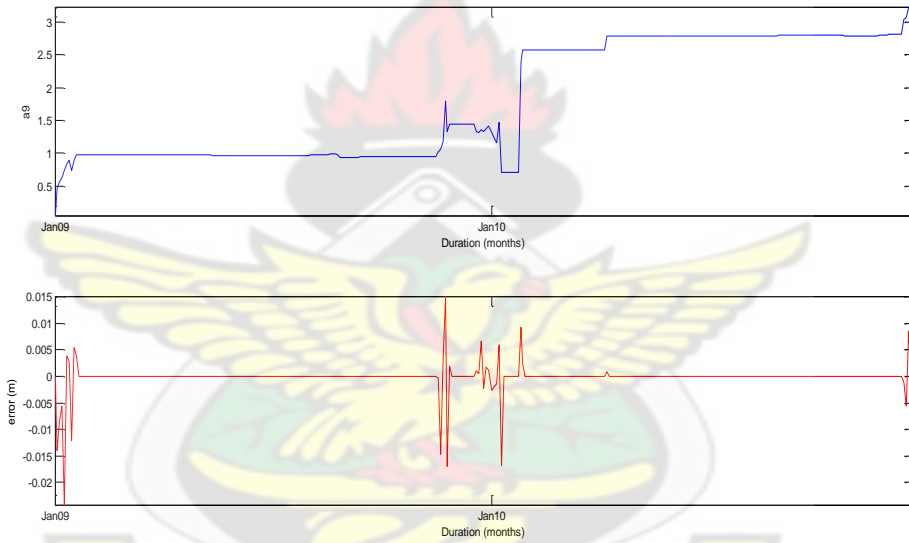


Figure 6.4e Parameter Estimate for a_9 and Error with Variable Q Matrix

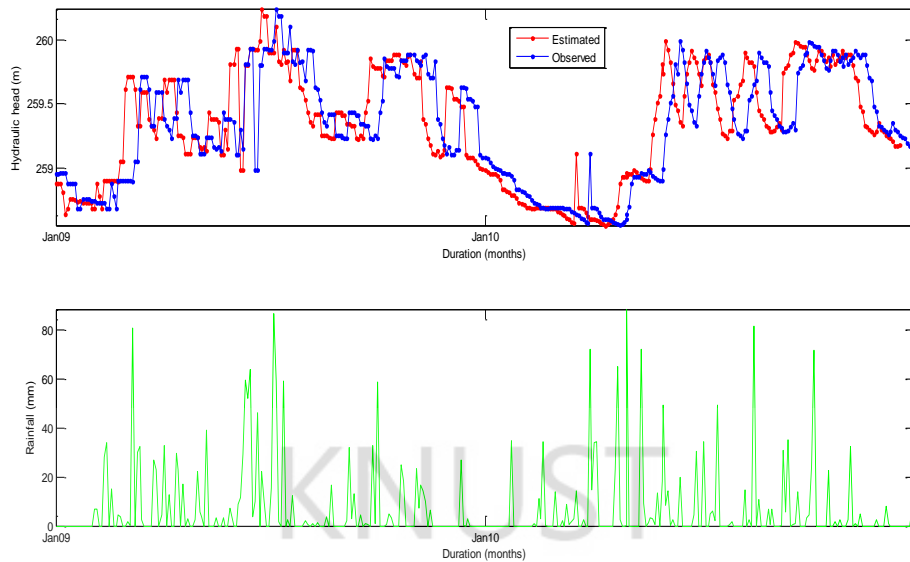


Figure 6.5 Rainfall and Observed and Simulated Watertable Level During the Years 2009 and 2010 for Previous Seven Days Rainfall, Q = Variable

Table 6.3 Recharge Values Based on the Seven Days Previous Rainfall

PZ	Sy	Fraction of rainfall (α)							Total	Recharge	% of Rainfall
		a_1	a_2	a_3	a_4	a_5	a_6	a_7			
P1	0.15	0.07	0.045	0.02	0.02	0.005	0.008	0.004	0.172	0.0258	2.58
P2	0.15	0.078	0.06	0.12	0.07	0.02	0	0.048	0.396	0.0594	5.94
P3	0.15	0.04	0.025	0.03	0.015	0.01	0.02	0	0.14	0.021	2.1
P4	0.15	0.02	0.02	0.03	0.03	0	0.003	0.001	0.104	0.0156	1.56
P5	0.15	0.03	0.04	0.02	0.03	0	0	0	0.12	0.018	1.8
P6	0.15	0.11	0.05	0.03	0.05	0.01	0.01	0.001	0.211	0.03165	3.165
P7	0.15	0.2	0.085	0.05	0.09	0.02	0.01	0	0.455	0.06825	6.825
P8	0.15	0.048	0.06	0.047	0.055	0.05	0.03	0.03	0.32	0.048	4.8
P9	0.15	0.085	0.14	0.09	0.11	0.11	0.04	0.02	0.595	0.08925	8.925
P10	0.15	0.095	0.04	0.09	0.055	0.01	0.03	0.01	0.33	0.0495	4.95
P11	0.15	0.01	0.06	0.01	0.03	0.01	0.01	0.02	0.15	0.0225	2.25
P12	0.15	0.12	0.05	0.098	0.15	0.55	0.075	0.07	1.113	0.16695	16.695
P13	0.15	0.085	0.045	0.02	0.025	0.008	0.005	0.01	0.198	0.0297	2.97
P14	0.15	0.1	0.15	0.18	0.18	0.13	0.06	0.045	0.995	0.14925	14.925

PZ-Piezometers, Sy-Specific yield

The estimated parameters for the period are substituted into Equation (24) and Equation (24) becomes:

$$y_k = 0.078R_k + 0.06R_{k-1} + 0.12R_{k-2} + 0.07R_{k-3} + 0.02R_{k-4} + 0R_{k-5} + 0.048R_{k-6} + 0.93y_{k-1} + 3.4 \dots \dots \dots (25)$$

It can be deduced from Figure 6.4 and Equation (25) that a reasonable amount of recharge took place during the first three days; there was a drop in the watertable level after the 5th day of rainfall and that the fraction of rainfall that actually reaches the watertable could be calculated from the steady-state gain of Equation 25. If one assumes a unit rainfall, then the impact of rain to the change in watertable level will be:

$$\Delta h_i = 0.078 + 0.06 + 0.12 + 0.07 + 0.02 + 0 + 0.048 = 0.396 \text{ m}$$

This implies $\alpha = \Delta h \times Sy$; therefore $\alpha = 0.396 \times 0.15 = 0.0594$

Then the groundwater recharge for the Besease Wetland, with previous rainfall to the order of seven days ranges between 1.56 % for P4 and 16.695 % for P12 of the incident rainfall.

6.3 Conclusions

The Kalman filter method was used to estimate groundwater recharge due to rainfall to an unconfined aquifer with a prior knowledge of the rainfall and history of watertable levels. From the field studies conducted at the inland valley bottom of Besease, it shows that the assumption that, the time variant parameters of the rainfall parameters with different weightages is more appropriate and realistic than the time invariant assumptions, also the time variant parameters with equal weight gives a considerable variation in the parameter values. The infiltration factor between the years 2009 and 2010 varied between 0.0 % and 16.7 % of the rainfall. The lowered

estimated water levels during the dry periods suggest smaller infiltration factor and therefore must be taken into account for the estimation of safe yields from aquifers.

Previous studies by Viswanathan (1983) used one day recharge which was unrealistic; therefore a 7 day rainfall which is more realistic was used in this model.

KNUST



CHAPTER SEVEN

HYDROCHEMISTRY OF THE BESEASE INLAND VALLEY BOTTOM

7.1 Introduction

Human and ecological use of groundwater depends on ambient water quality. The concentration and composition of dissolved constituents in water actually determine its quality for irrigation use. Quality of water is an important consideration in any appraisal of salinity or alkali conditions in an irrigated area. Much work has been done on quality of irrigation water (Opoku-Duah *et al*, 2000; Kankam-Yeboah *et al*, 1997; Odeh *et al*, 2009) to assess its suitability for irrigation, industrial and domestic purpose. The drastic increases in population, modern land use applications (agricultural and industrial), and increase demand for water supply has increase pressure on the globally essential groundwater resources in terms of both its quality and quantity (Dar, 2011). Since physico-chemical composition of groundwater is a measure of its suitability as a source of water for agriculture (irrigation), industrial and domestic purposes, it was necessary to evaluate the groundwater quality in studies aimed at assessing irrigation water.

7.2 Water Sampling

Water samples for chemical analysis were collected from installed piezometers in April 2010. Three water samples were collected in clean plastic bottles. At the time of sampling, bottles were thoroughly rinsed two to three times with the groundwater to be sampled. Samples collected were, stored in cooler boxes and transported to the laboratory where it was filtered using 0.45 millipore filter paper and acidified with nitric acid (Ultrapure Merck Brand) for cation analyses. For anion analyses, these samples were stored below 4°C. Major cations like Ca²⁺ and Mg²⁺ were analysed

titrimetrically, using standard (0.02 N EDTA) and E.B.T indicator. Na^+ and K^+ were determined using flame photometer (Genway, PFP7). The chemical analysis was carried out as per standard procedures given in APHA (1995). HCO_3^- and Cl^- were determined by titrimetric method. Colorimetric method was employed to determine $\text{NO}_3^- \text{ N}$.

7.3 Results and Discussions

7.3.1 Chemical Constituents of Groundwater Samples

Table 7.1 Chemical Constituent of Groundwater

Location	pH	ECEw ($\mu\text{S}/\text{cm}$)	Ca^{2+}	Mg^{2+}	Na^+	K^+	HCO_3^-	$\text{NO}_3^- \text{ - N}$	SO_4^{2-}	Cl	SAR
P 5	7.1	242.3	48	13	11.6	23.8	160	0.7	0.45	0.65	0.54
P 14	6.8	638	22.4	9.72	19.3	26.3	360	1.5	0.39	0.54	1.205

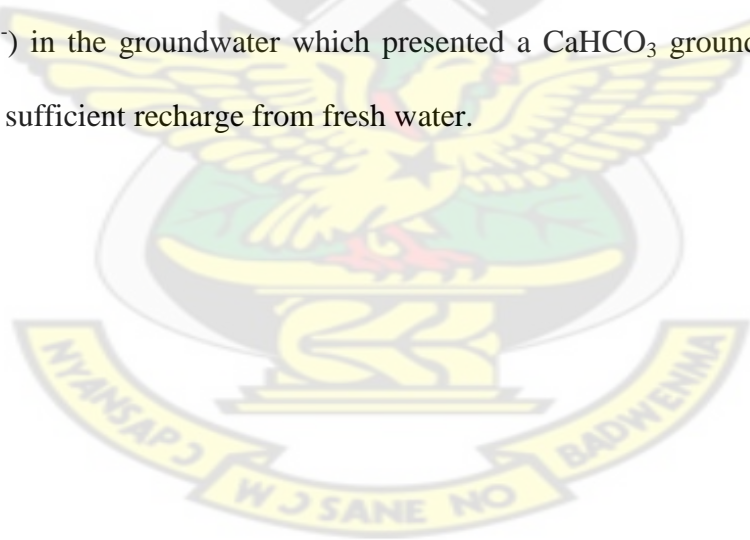
7.3.2 Hydrochemistry

EC of groundwater in the valley was $242\mu\text{S}/\text{cm}$ at site P5 and $638\mu\text{S}/\text{cm}$ at site P14. The higher value of EC at P14 suggests the enrichment of salt due to possible evaporation and groundwater flow direction effect and additional leaching derived from anthropogenic sources. Bicarbonate represents the major sources of alkalinity. Bicarbonate was slightly higher indicating a contribution from carbonate weathering process. High nitrate at P14 suggest greater mineralization of plant matter that has been buried under seasonal alluvial deposition.

7.3.3 Graphical Representation of Hydrochemical Data

Groundwater geochemical evolution can be understood by plotting the major cations and anions concentration on the piper trilinear diagram developed by Piper (1944).

The piper diagram combines three distinct fields for plotting, two triangular fields at the lower left and lower right respectively and an intervening field. Each apex of the triangle represents a 100 % concentration of one of three chemical constituents. Major ions are plotted in the two base triangles of the diagram as cation and anion percentages milligram per litre. The overall cations and anions are each considered as 100 %. The overall characteristic of the water is represented in the diamond-shaped field by projecting the position of the plots in the triangular fields. Different types of groundwater can be distinguished by their plotting position, occupying certain sub-areas of the diamond-shaped field. Piper–trilinear plots were made for the samples collected during April visits. A perusal of hydrochemical character from Piper Trilinear Diagram (Fig 7.1) showed that alkaline earths (Ca^{2+} and Mg^{2+}) exceeded alkalis (Na^+ and K^+) and weak acids (HCO_3^- and CO_3^{2-}) exceeded strong acids (Cl^- and SO_4^{2-}) in the groundwater which presented a CaHCO_3 groundwater type which indicated sufficient recharge from fresh water.



EXPLANATION

- P5
- ▲ P14

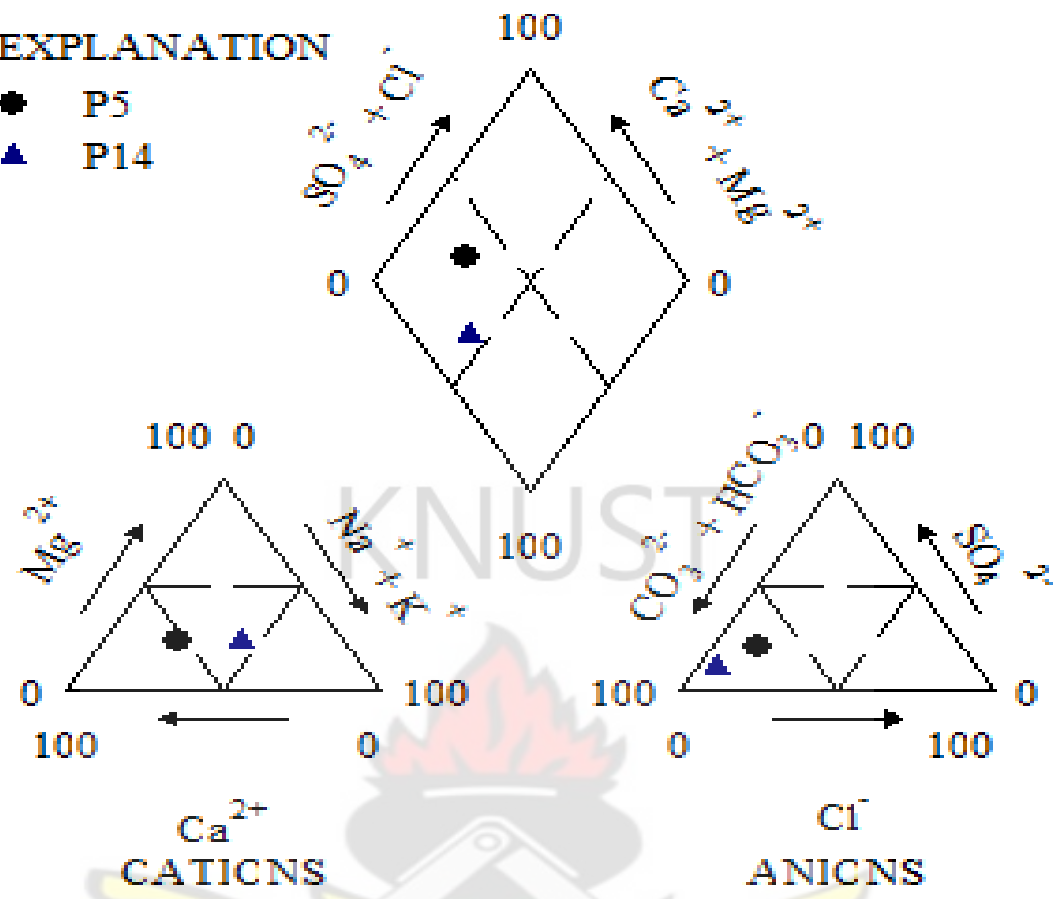
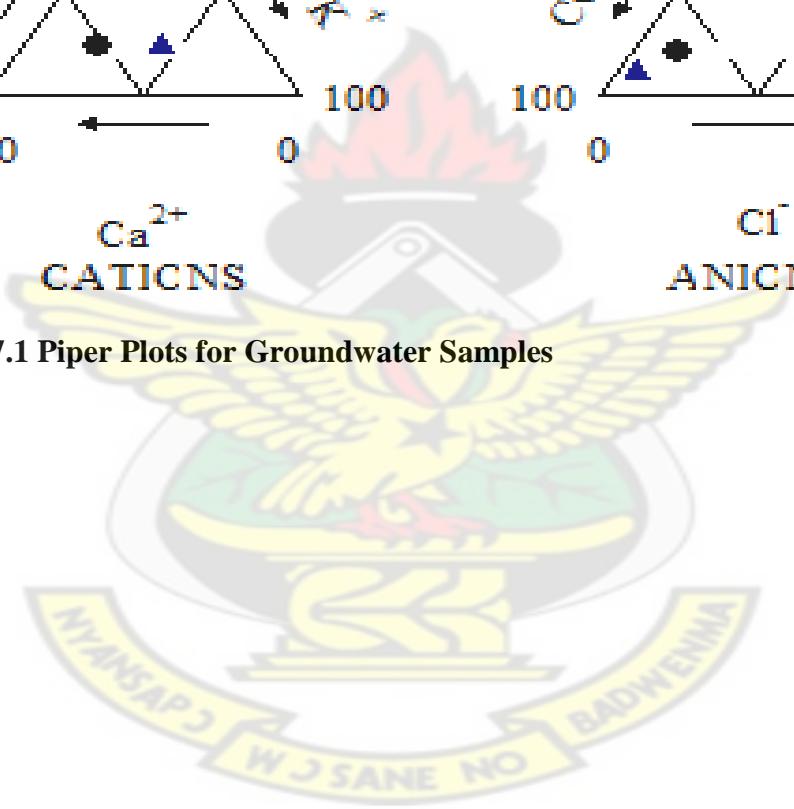


Figure 7.1 Piper Plots for Groundwater Samples



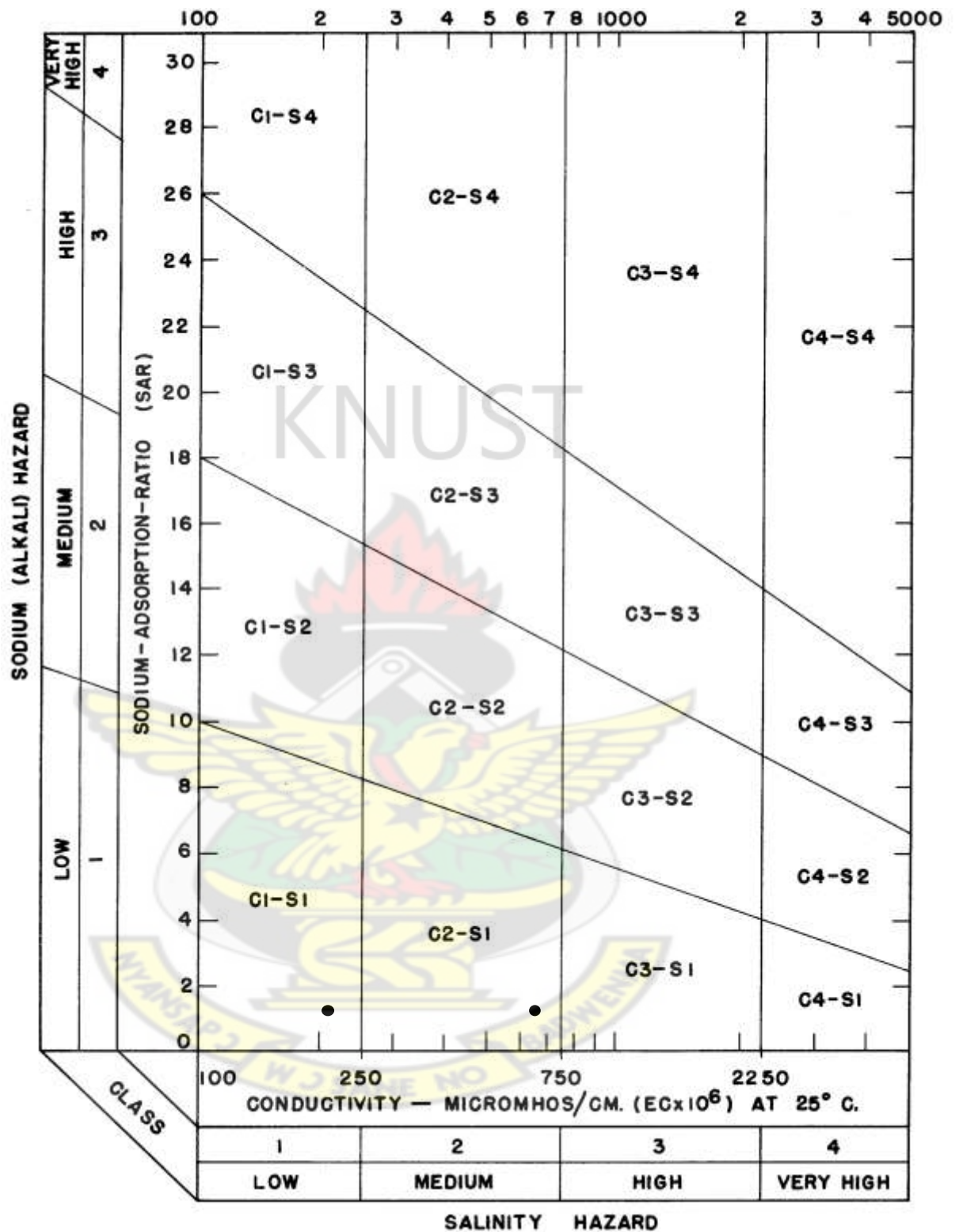


Figure 7.2 US Salinity Diagram for Groundwater Samples at Besease Inland Valley Bottom

7.4 Groundwater Quality Analysis for Irrigation

Suitable irrigation practices are invariably influenced by water quality, soil types and cropping practices. The important chemical constituents that affect the suitability of water for irrigation are the EC and Na⁺. Higher salt content in irrigation water causes an increase in soil solution osmotic (Ayers and Westcot, 1994). Excessive sodium content relative to calcium and magnesium reduces the soil permeability and thus inhibits the supply of water needed for the crops (Kumar *et al*, 2007). Na has the ability to disperse the soil, when present above a certain threshold value relative to the concentrations of total dissolved salts. Osmotic activity is reduced by excess sodium which interferes with the absorption of soil water and nutrient. Irrigation water could be a source of excess sodium in the soil solution and it should be evaluated as such.

SAR is expressed as:

$$SAR = \frac{Na^+}{\sqrt{\left\{ \frac{Ca^{2+} + Mg^{2+}}{2} \right\}}}$$

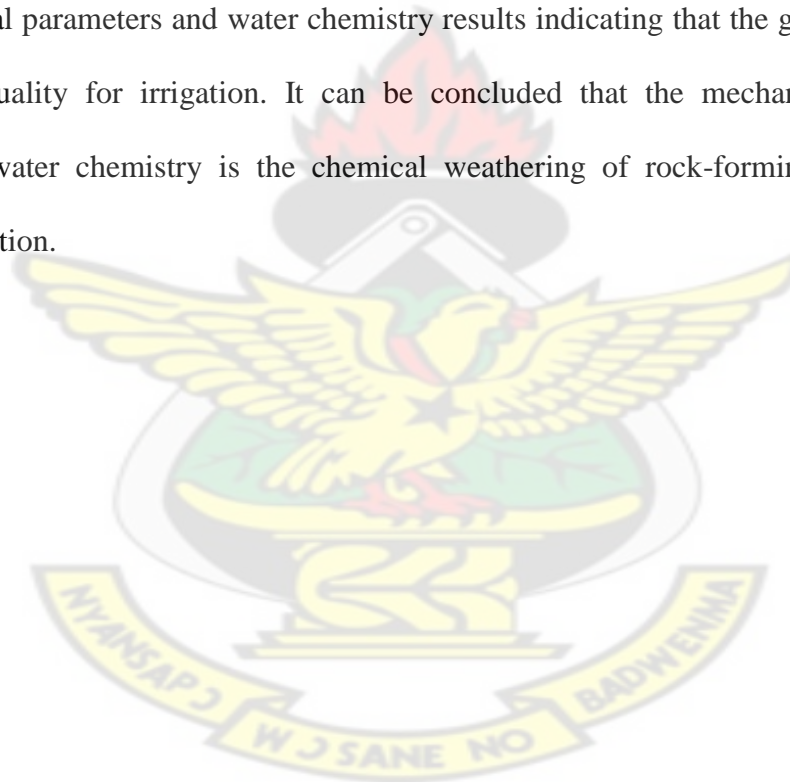
Where the ionic equations are expressed in meq/l.

The hydrochemical data plotted on the US salinity diagram (Fig 7.2) proposed by US Salinity Laboratory Staff (1954) groundwater sample from P14 fell in the field of C2-S1, indicating water of medium salinity and low sodium, which can be used for irrigation in almost all types of soil with little danger of exchangeable Na⁺. Also groundwater sample from P5 fell under C1-SI, indicating water of low salinity and low sodium content, which could be used for irrigation in all types of soils. A rise in conductivity values may reduce soil permeability especially if inadequate drainage facilities exist at the Besease site. The pH values at the Besease Wetlands exhibit slightly less acidic and alkaline (Table 7.1) behaviour which shows that groundwater

is nearly neutral with average value 6.95. Groundwater of this pH level is considered suitable for irrigation.

7.5 Conclusions

An attempt to study the quality of groundwater revealed that alkaline earths (Ca^{2+}) exceeded alkalis (Na^+) and weak acids (HCO_3^-) exceeded strong acids (SO_4^{2-}) in groundwater thus giving a CaHCO_3 groundwater type. It was found out that the dominant HCO_3^- and Ca^{2+} indicated that recharging water is of limestone aquifer. Analysis of groundwater from the two piezometers showed an overlap of the physico-chemical parameters and water chemistry results indicating that the groundwater is of good quality for irrigation. It can be concluded that the mechanism controlling groundwater chemistry is the chemical weathering of rock-forming minerals and evaporation.



CHAPTER EIGHT

WATERTABLE FLUCTUATION AND INLAND VALLEY BOTTOMS CLASSIFICATION

8.1 Introduction

Wetlands hold a lot of water in its phreatic zone which alternate under variable recharge conditions from rainfall, runoff from uplands and rivers and seepage from streams. In the wet seasons watertables fluctuate at or close to the ground surface when rainfall inputs are high. However, watertables fluctuate at lower depths in the dry season and at times piezometers and wells go dry. West African inland valley bottoms which are used for crop production receives surface water through canal irrigation in the dry season and watertables which is expected to fall would be rising due to induced groundwater recharge from the canal. On the other hand, watertable which is expected to rise would be observed falling under a considerable groundwater abstraction due to pumping. The watertable fluctuations even under normal conditions of dry and wet periods or when subjected to different management scenarios depicts different forms and shapes of piezometric and well hydrographs which can be used to classify wetlands hydrologic regimes. Raj (2004) classified well hydrographs in wetlands based on their shapes and forms from slopes made by watertable fluctuations of the wells over more than one hydrological cycle in south eastern Peninsular India. Raj (2004) indicated that the differences in the shapes of the hydrographs were attributed to changes in the climatological pattern, reflection of the underlying aquifer characteristics and lithology and also management practices. Ogban and Babalola (2009) also classified inland valley bottoms on the basis of their drainage densities according to their watertable depths in the dry season in Ayepe, South Western

Nigeria as design criteria for crop production. Studies during this research have led to the introduction of classes (Section 8.44) which are similar to that of Ogban and Babalola (2009) for the Besease Wetlands.

8.2 Piezometric Hydrograph

8.2.1 Shapes and Classifications of Piezometric Hydrographs

A two-year measured watertable fluctuations were plotted on a reference scale of months on the x-axis and hydraulic head on the y-axis (Fig 8.2). The x-axis was divided into one month periods. Hydrographs plotted to this scale were divided into monthly segments and the slope of each segment was then used as a basic element for classification of hydrographs. Slopes are classified as flat (segment's inclination $< 20^\circ$), obtuse (segment's inclination between 20° and 45°), acute (segment's inclination between 45° and 80°), right angled (segment's inclination between 80° and 90°) and homoclinal (when the hydrograph cannot be divided into rising and falling segments and are either rises or falls during one complete water year). Homoclinal segments showing a rise are suffixed as rising, while homoclinal segments that show a fall are referred to as homoclinal falling. Fig. 8.1 shows the elements of this classification. Slopes joining at a point would either have the same rising and falling segment which can be acute-acute or different shapes in the form of acute-obtuse, obtuse-flat and right angled-flat. Slopes forming these segments were counted for each month and grouped under flats, obtuse, acute and right angled segments.

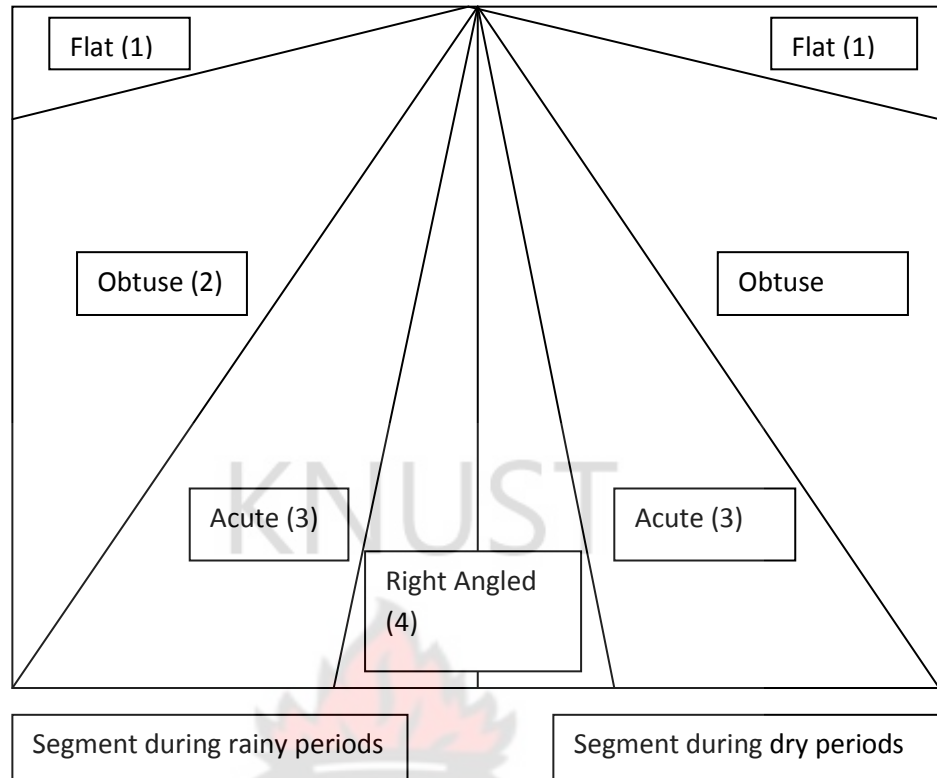
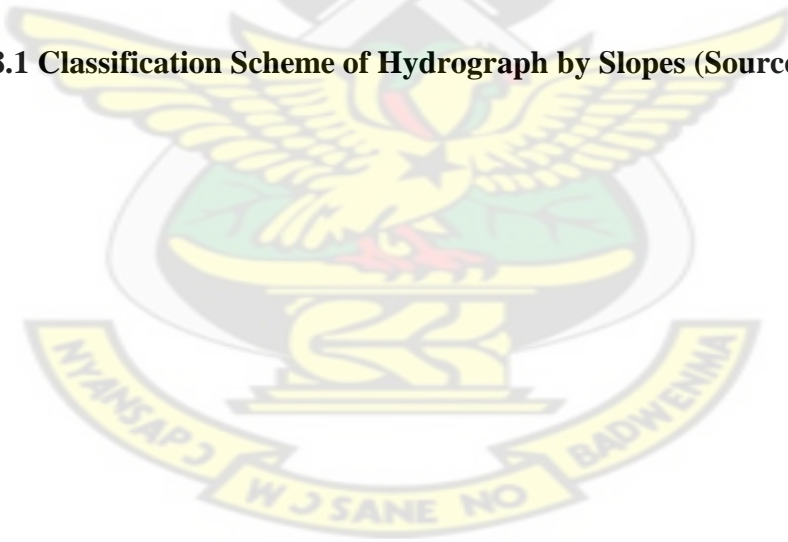


Figure 8.1 Classification Scheme of Hydrograph by Slopes (Source: Raj, 2004)



8.3 Results and Discussions

8.3.1 Results

8.3.1.1 Segmented Watertable Slopes for Different Piezometers

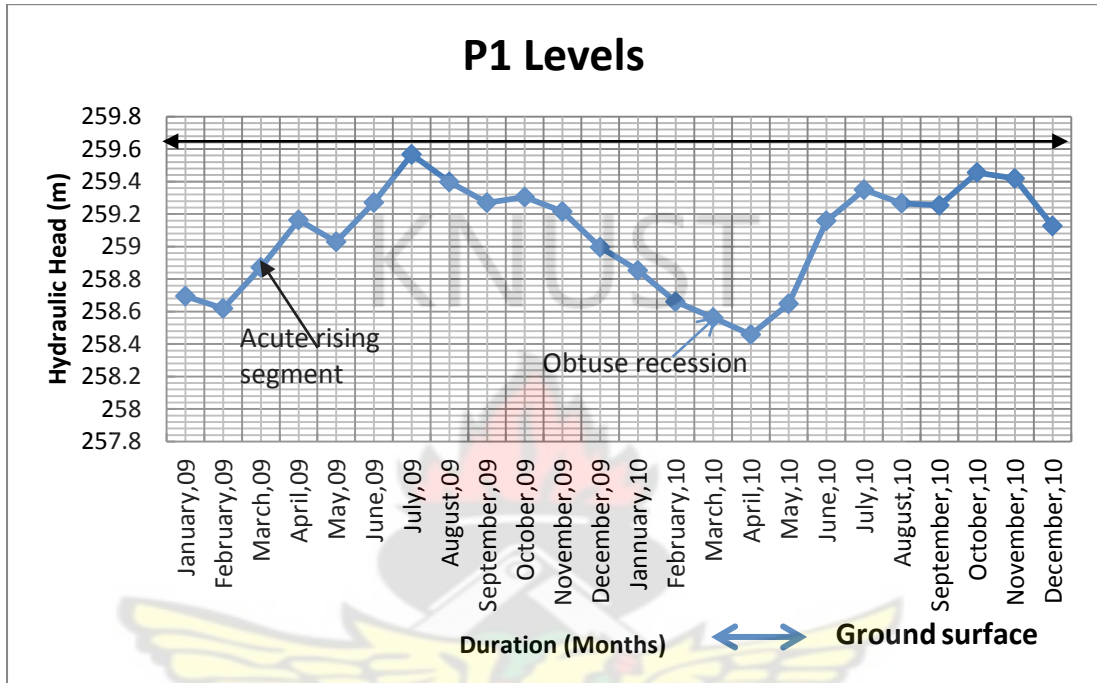


Figure 8.2a Hydrograph of P1 dominated by Acute Slopes

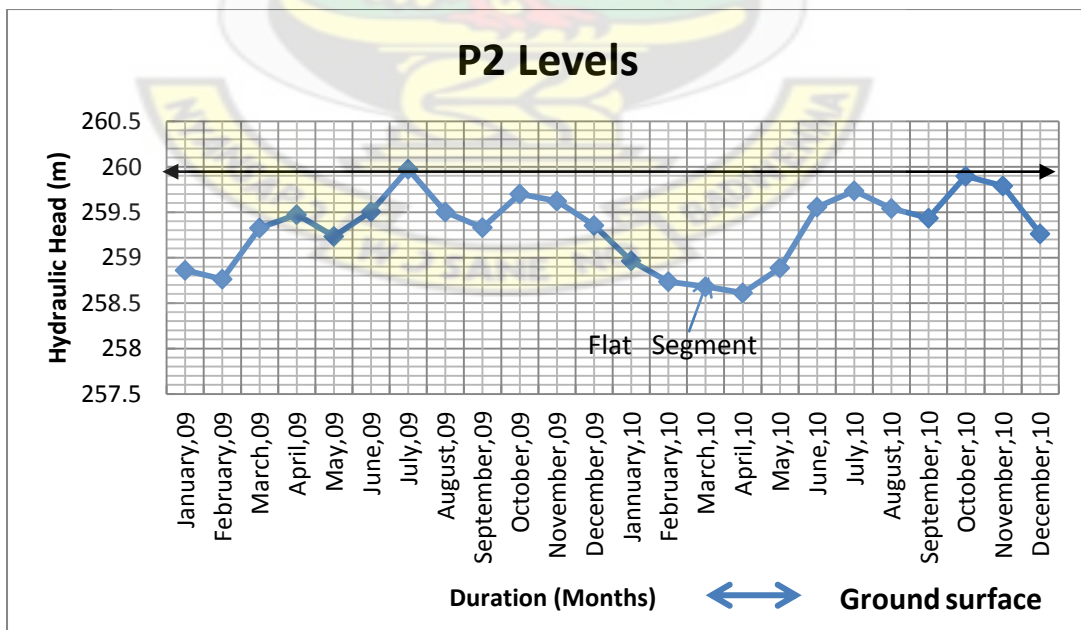


Figure 8.2b Hydrograph of P2 dominated by Acute Slopes

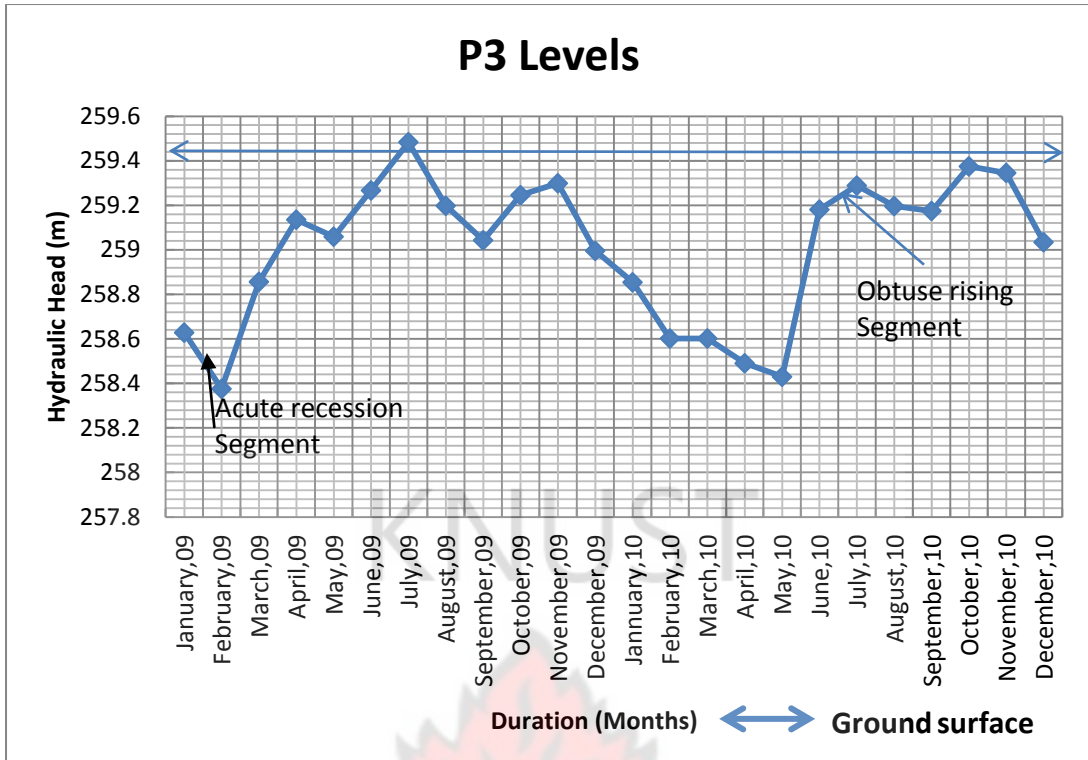


Figure 8.2c Hydrograph of P3 dominated by Acute Slopes

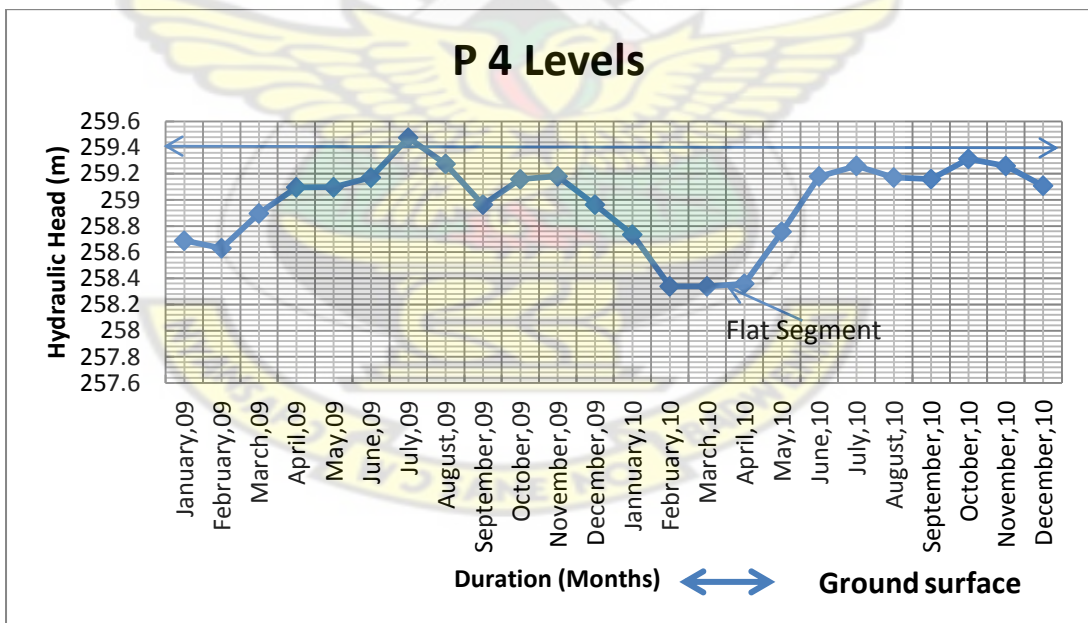


Figure 8.2d Hydrograph of P4 dominated by Acute Slopes

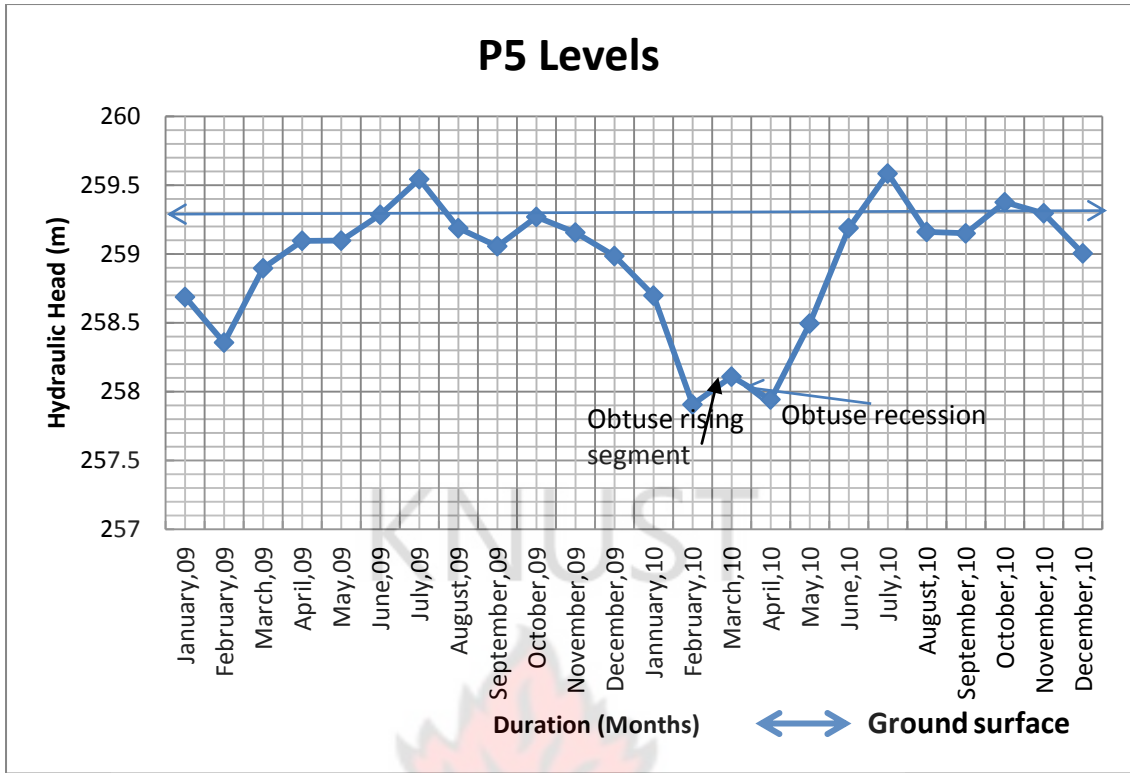


Figure 8.2e Hydrograph of P5 dominated by Acute Slopes

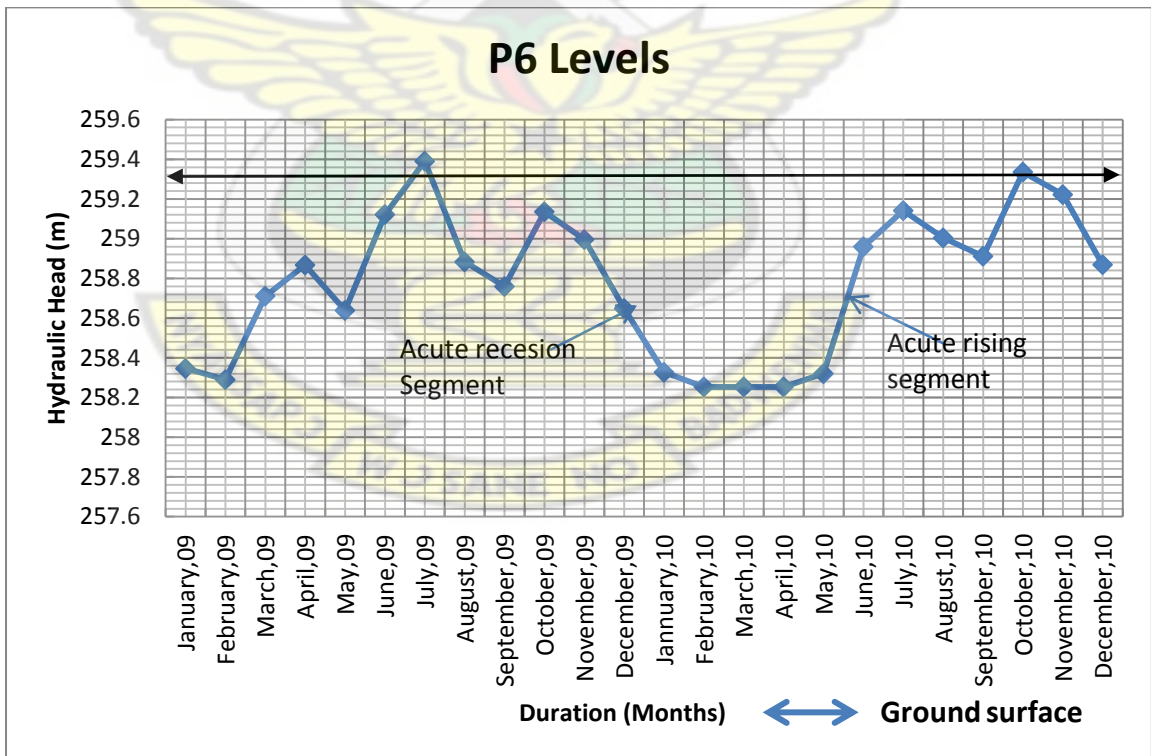


Figure 8.2f Hydrograph of P6 dominated by Acute Slopes

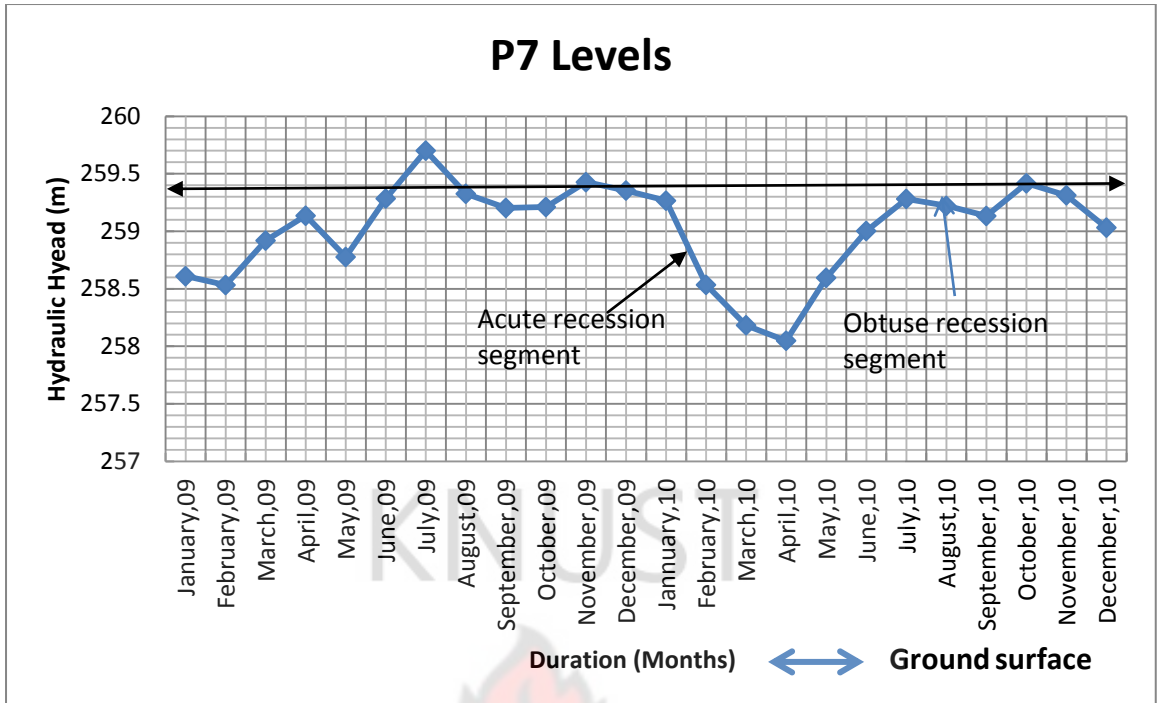


Figure 8.2g Hydrograph of P7 dominated by Acute Slopes

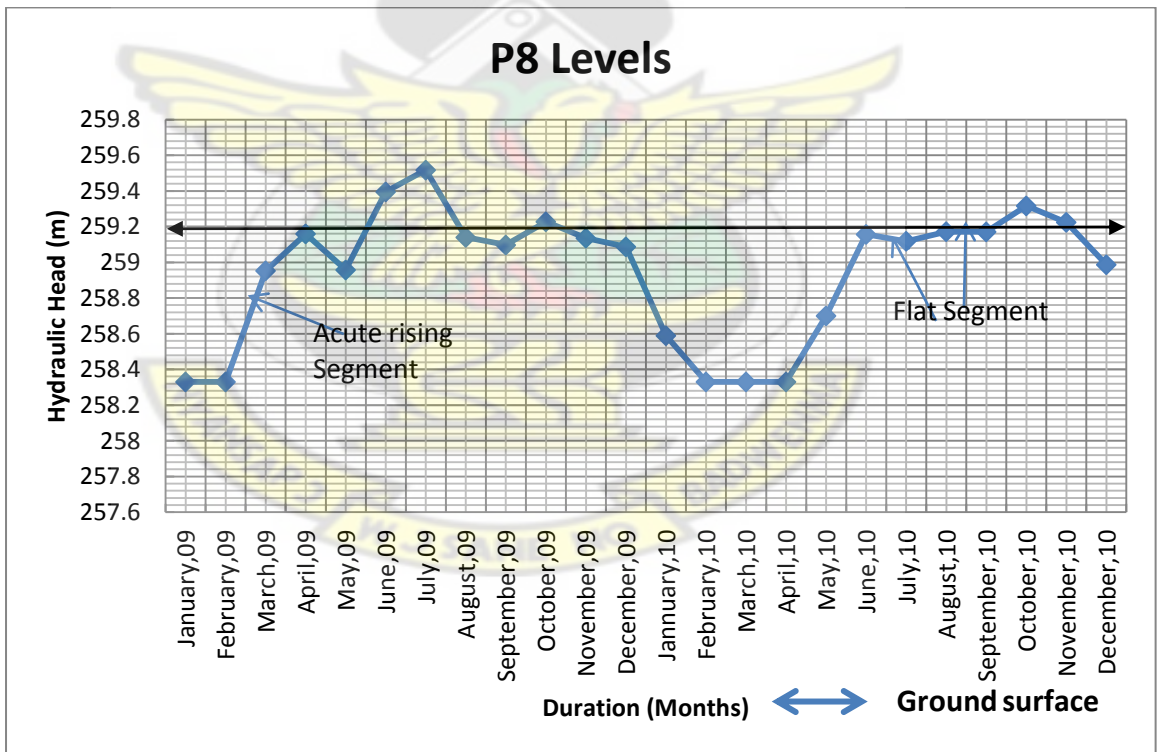


Figure 8.2h Hydrograph of P8 dominated by Acute Slopes

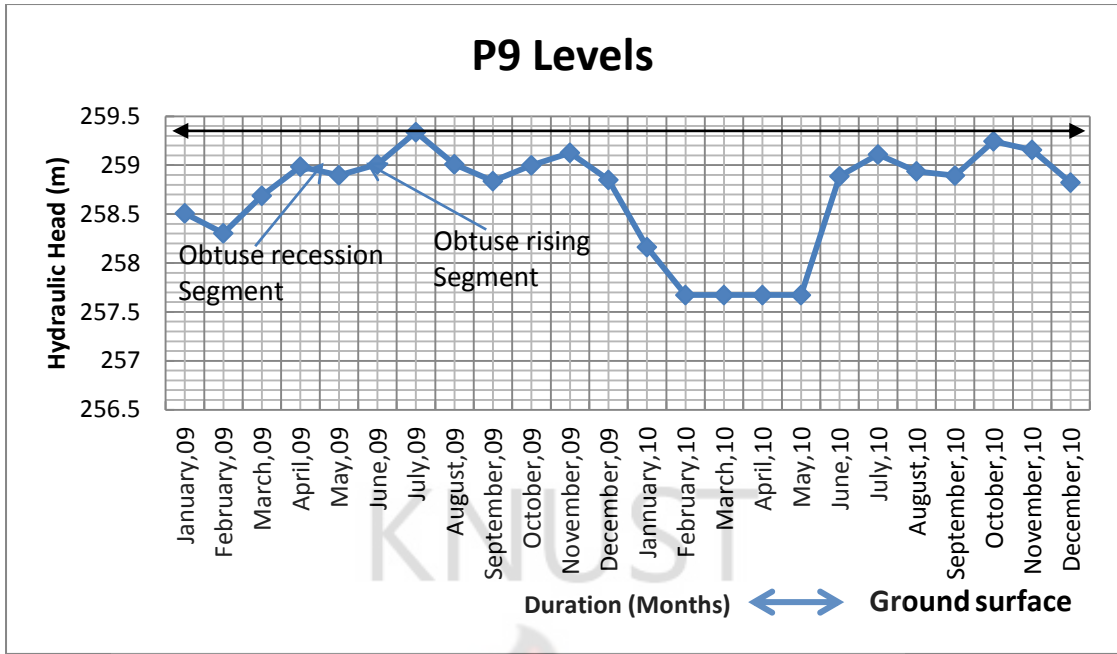


Figure 8.2i Hydrograph of P9 dominated by Acute Slopes

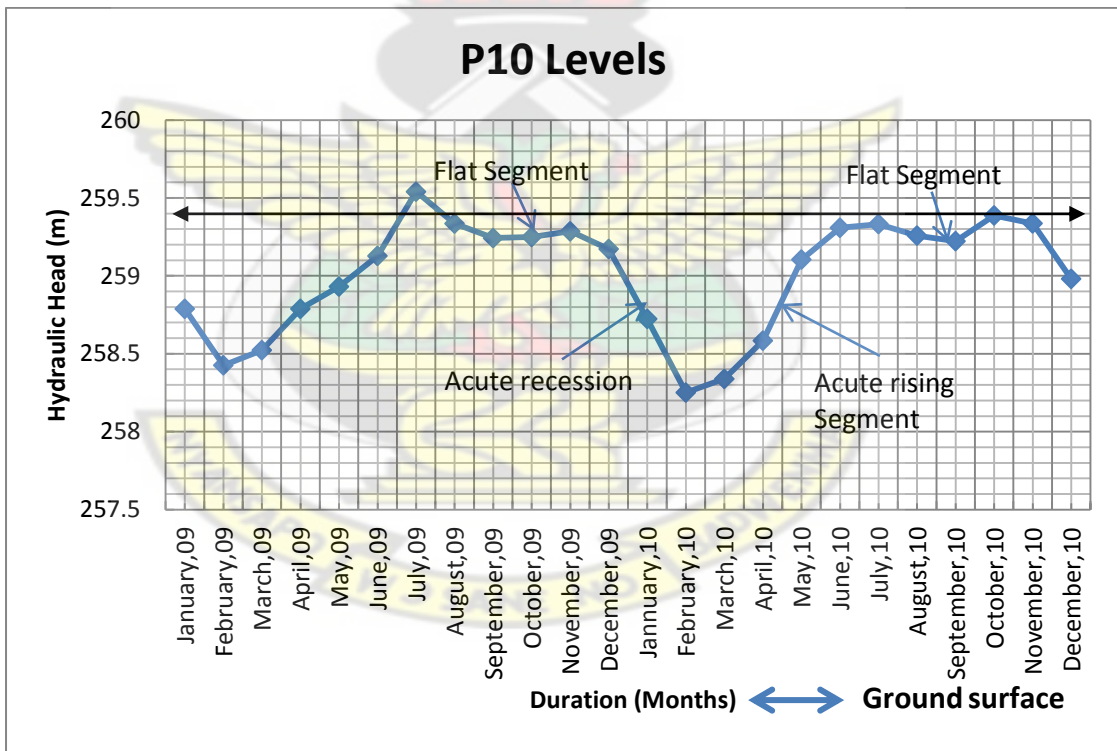


Figure 8.2j Hydrograph of P10 dominated by Acute Slopes

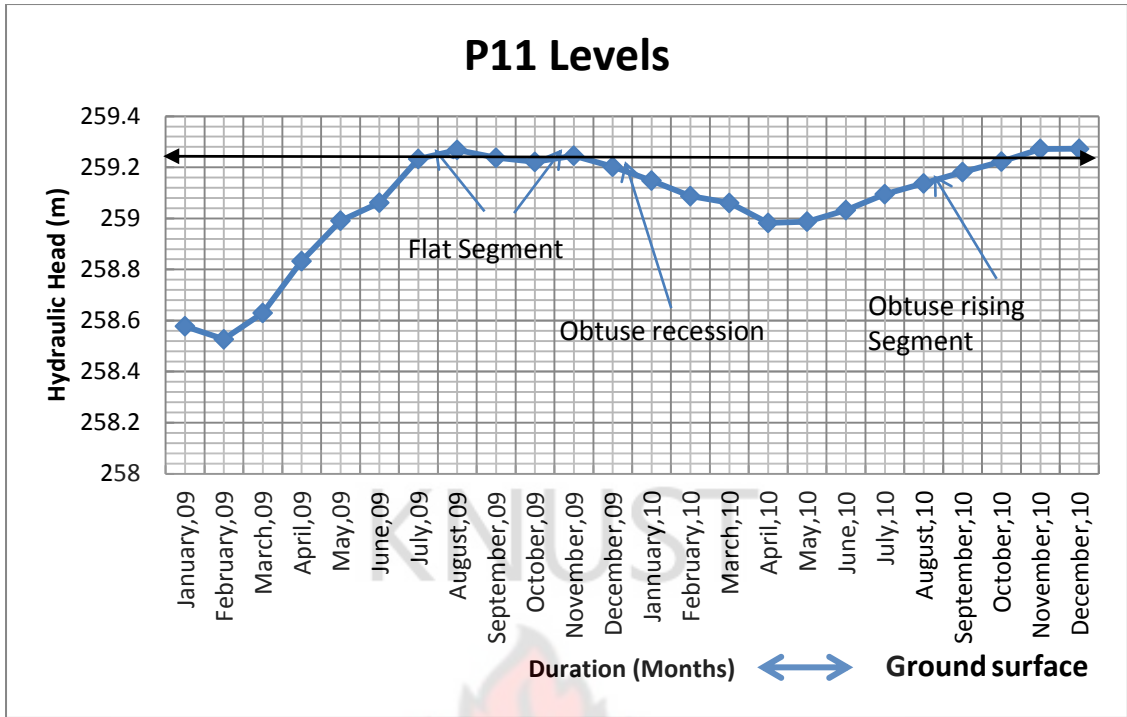


Figure 8.2k Hydrograph of P11 dominated by Obtuse Slopes

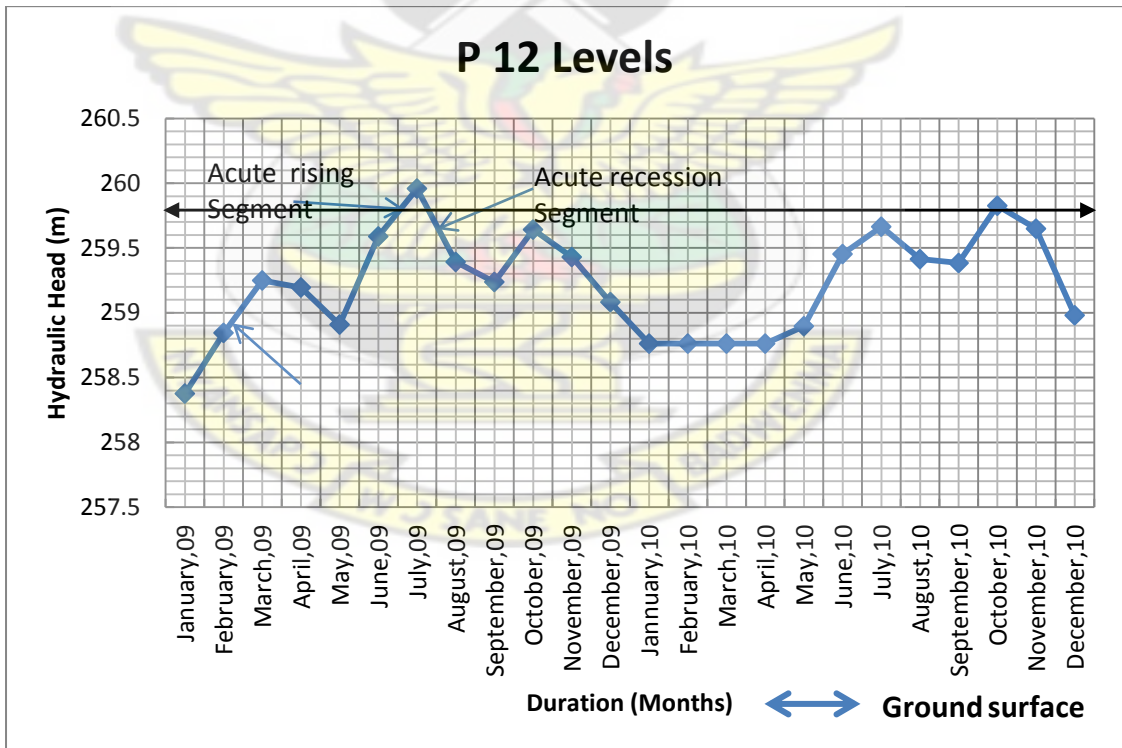


Figure 8.2l Hydrograph of P12 dominated by Acute Slopes

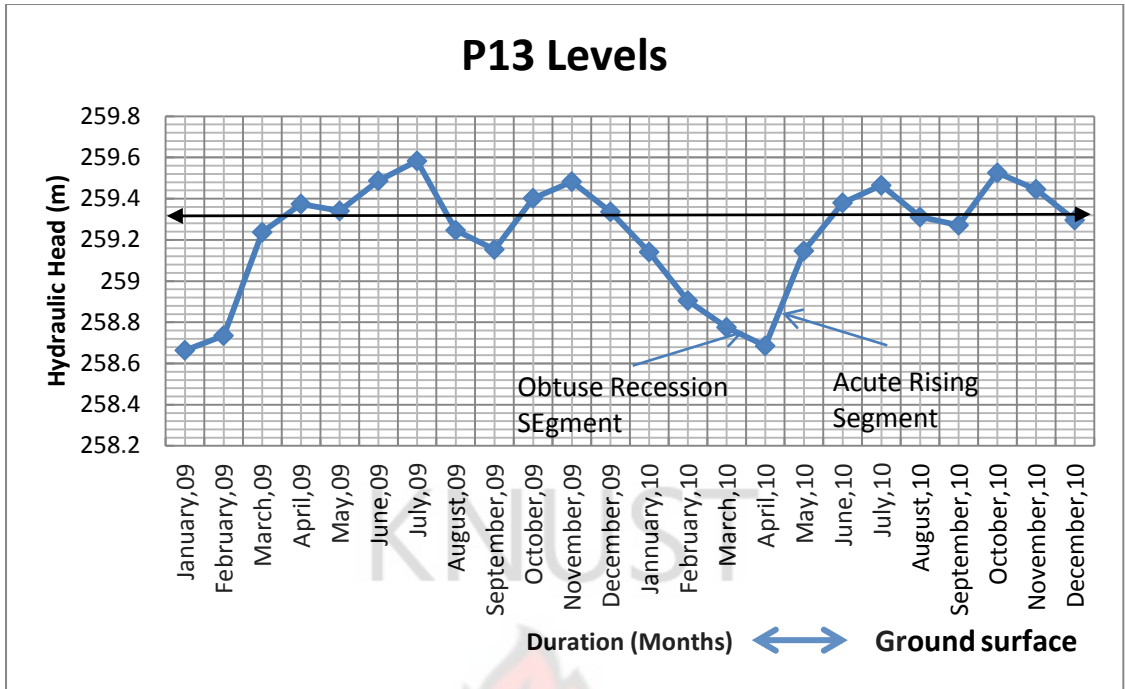


Figure 8.2m Hydrograph of P13 dominated by Acute Slopes

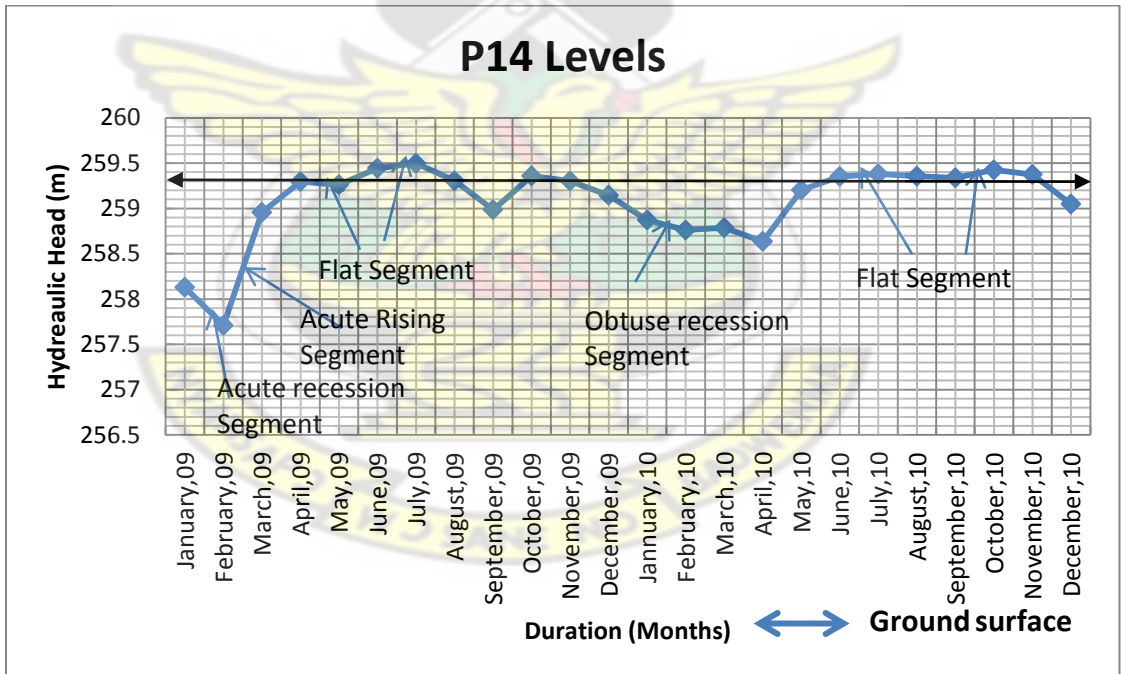


Figure 8.3n Hydrograph of P14 dominated by Flat Slopes

Table 8.1 Percentages of Slopes Exhibited by the Hydrographs

Piezometer	Acute	Obtuse	Flat	Right-angled
P1	52	35	13	-
P2	57	30	13	-
P3	48	35	13	4
P4	57	17	26	-
P5	43	48	9	-
P6	57	43	0	-
P7	52	35	13	-
P8	50	25	25	-
P9	52	43	5	-
P10	44	30	26	-
P11	13	57	30	-
P12	75	15	10	-
P13	61	35	4	-
P14	30	30	40	-

8.3.1.2 Slopes of Piezometric Hydrograph

Results from Table 8.2 shows that most of the piezometers had their monthly slopes dominated by the acute segment followed by the obtuse segment, flat segment and right-angled segment. There were also sharp rises of water in the months of March in 2009 and May in 2010 with acute and right-angled segments. Piezometers experienced an acute rising–acute recession form of segment were mostly observed in the quarter of June–August indicating a high recharge surge in June and low or no recharge in August which also reflects the rainfall pattern. This was noticed in 2009 much than 2010. Obtuse rising–Obtuse recession segments were present in months with moderate rainfall and not too intense evaporation such as April. Flat segments were visible in the months of August–September in the 2010 water year. P11–P14 had the lowest acute form of hydrograph representation of 13% and 30% respectively. P12 and P13 had the highest form of acute slopes representing 70% and 61%. The highest obtuse segment of 57% was obtained at P11 and the lowest was recorded at P4 and P12 respectively (Table 8.1). The highest form of flat segment was recorded at P14

representing 39% of the slopes in the hydrographs followed by P10 and P4. P3 was the only piezometer which showed a right-angled segment slope. Summing the obtuse and the flat segments revealed P11 and P14 recording 87% and 70% respectively as the highest slopes from the hydrograph presentation. However, P12 and P13 had the lowest form of the combination of obtuse and flat of 30% and 39% respectively. The piezometric point P12 which is closer to the river became empty in most of the dry season.

8.4 Discussions

8.4.1 Hydrograph Representation

Comparison of the hydrographs provides an insight into the nature of the aquifer (Raj, 2004). The most common form of the hydrograph is the acute-obtuse slopes of the quarters. The acute slopes suggest a higher fluctuations surge from a high rainfall records while that of obtuse indicates a lower fluctuation also from a moderate rainfall. Right-angled rising segments or departures towards steeper-rising segments occur due to high rainfall in a short duration, either in one spell or in several closely spaced precipitation events (Raj, 2004). The shape of the rising (raining) limb is influenced by the intensity, interval and duration of precipitation. Rainfall appears to primarily determine the shape of the rising limb, as even a hydrograph of a borehole in a good aquifer in an alluvial tract shows an acute or right-angled (steep) rising limb during a period of particularly good rainfall and conversely well hydrographs tend to be obtuse in a poor raining year which is also a characteristic of the aquifer. A higher percentage acute recession slope segments with either acute rising segments or right-angled rising segments are due to relatively poor unconfined aquifers. These are observed in aquifers comprising weathered residual of vispar, gneisis and shale which gives off gritty or coarse grained sand. The dominant Flat segments slopes are noted

in aquifers with low hydraulic conductivity, high silt and clay, and low topographic site of the study area (Appendix 1) and aquifers with granitic sandstones rocks that weathers to give fined grained sand. The dominant obtuse recession and rising slopes reflects characteristics like that of the flat segment which is often accompanied by poor rainfall amount in a water year. Also linear recession in the flat segment slopes could be due to rapid discharge from the aquifer. In the drying periods, the dominant recession slope segment was the acute which suggest a sharp decrease and a higher fluctuation depth and in most cases leads to the drying of the borehole.

8.4.2 Watertable Slopes Segment Fluctuation and Areal Extent

The small size of the IVBs is attributed to deeper incision of the landscape and convex nature of the valleys. The amount of water flowing into the valley depends not only on rainfall amount but also on the catchment size characteristics. Killian and Teissier (1973) have reported that water capture would be too small for a catchment size less than 400 ha. Therefore the extent of the study area of 72 ha suggest that much of the precipitation runs off the surface resulting in flooding of shallow depth and short duration. However, despite the topographic condition and the high drainage density and texture, the rainwater does infiltrate and readily recharges the groundwater, causing a sharp rise in the regional groundwater table and seepage flows, resulting in the seasonal or perennial wetness condition which prevails in Inland Valley Bottoms (Ogban and Babalola, 2009).

8.4.3 Watertable Fluctuation and Classification of Inland Valley Bottom

Time series of the hydrograph shows seasonal variations in the observations among the piezometers of the study sites. About 14 % of the area had their monthly slopes 13-30% of the acute segment. This was observed in P11 and P14. Also 14% of the area had their slopes ranging between 40-45% acute segment which occurred in P10

and P 5. However, 72 % of the monthly slopes had their acute slopes greater than 45 % in the areal domain. It can be explained that most of the piezometric areas dominated by acute forms become relatively dry during the dry season; they may, however, still have some water to support crops. This result also point to some management practices in Inland valley bottoms in developing them for crop production. Figures 8.2k and 8.2n shows that the watertable (WT) is at or near the soil surface for more than 6 months in the valley system of this IVBs with the monthly segment slopes dominated by obtuse and flat forms of 70-87%. This also indicates that with higher records of monthly rainfall amount, watertable would fluctuate near the ground surface for a longer period of time in the wetlands. According to Ogban and Babalola (2009) high watertables fluctuating near the ground surface are also attributed to poor surface and subterranean drainage outlets. Hekstra and Andriess (1993) and Andriess (1986) have reported that IVBs in the West African sub-region have excellent conditions for more than one crop growing season (150 days or more) especially wetland crops, e.g. rice. It can be inferred that this wetland holds a rich potential for food production owing to the availability of water coupled with the fertile nature of inland valley bottoms. On the other hand, watertable recedes at the beginning of the dry season which varies in the inland valley system accounting for high evapotranspiration rates. Effective cultivation can be enhanced by planting upland crops like maize, cassava, sweet potato and vegetable crops specifically when the watertable (Figure 8.2) has attained its mean lowest depth in February. The process of high evaporation and increased internal drainage reduces the pore water pressure and this extends or pushes the phreatic surface downwards and improves aeration for crops with aerobic edaphic requirements.

Thus, a rise in the level of the WT decreases the zone of unsaturation, increases the pore water pressure, reduces the hydraulic gradient and increases the drainage load, and creates waterlogging conditions that inhibit cultivation and crop growth for dryland crops but enhances rice cultivation. On the other hand, the receding watertable reduces waterlogging conditions, or creates unsaturated conditions or re-establishes the agricultural zone of the soils for dryland crops. These alternating conditions explain the alternate fallow and farming in the IVBs (Ogban and Babalola, 2009). Consequently, the descending of the phreatic surface in the dry season is a critical predictive criterion because it defines the effective rooting depth (ignoring the extent of the capillary fringe), the soil water storage depth and drainage requirements, and a distinguishing characteristic for classifying the Inland valley bottoms into soil and water management regimes (Ogban and Babalola , 2009). Three hydrological regimes have been developed to classify this wetland. The regimes are:

- WTF Class I Acute slopes segment varying from 0–30%,
- WTF Class II acute slopes segment varying from 30-45%
- WT Class III > 45%.

The distinguishable factors describing the fluctuation classes are their acute segment slopes, the height of the watertable, duration of high watertable and their suitability for crop production which are further discussed.

8.4.4 Watertable Fluctuation Classes

Watertable Fluctuation Class I

1. Acute slopes segment < 30 % (0-30) %
2. Watertable is close to the ground surface and the soil is always wet through the water year,
3. Duration of high watertable is about 8 months

4. It is suitable for year round crop production, preferably rice.

Watertable Fluctuation Class II

Acute slopes segment ranges 30–45%

Water table is intermediate between the ground surface and the base of the borehole and piezometric watertable recuperates in March in the dry season. Duration of high watertable is about 4 months suitable for wetland (rainy season) and dryland (dry season) crop production but with little soil and water conservation getting to the latter part of the dry season using residue mulch in the middle of the dry season for roots to follow the receding WT.

Watertable Fluctuation class III

Acute slopes segment > 45%

Watertable is close to the ground in the wet seasons and most of the piezometric watertable recuperates in April throughout the water year. Duration of high watertable is about two months and is suitable for wetland (rainy season) and dryland (dry season) crop production but with soil and water conservation using residue mulch together with early planting for roots to follow the receding WT.

8.5 Conclusions

Development of IVBs of unconfined aquifers especially in the Besease wetlands for crop production has been classified into three hydrological regimes based on the intensity of their acute slope segments of the watertable fluctuations. Most of the area studied is within WTF Class III. The regimes are:

- WTF Class I for Acute slope segments varying from 0–30% (<30%)
- WTF Class II for acute slope segments varying from 30% - 45% and
- WT Class III > 45 %.

The results show that most of the piezometric areas which are dominated by acute forms become relatively dry during the dry season; they may, however, still have appreciable water to support crops. It was also revealed that a rise in the level of the WT decreases the zone of unsaturation, increases the pore water pressure, reduces the hydraulic gradient and increases the drainage load, and creates waterlogging conditions that inhibit cultivation and crop growth for dryland crops but rather enhances rice cultivation. It is concluded that a controlled watertable will offer a distinguishing criterion for the development of IVBs for a year round crop production.



CHAPTER NINE

GROUNDWATER FLOW MODELLING USING MODFLOW

9.1 Introduction

Modelling groundwater flow is a way of evaluating groundwater resources to understand why a flow system is behaving in a particular observed manner to predict how a flow system is behaving by employing different stress scenarios in a modelling process. Groundwater models simulate the hydraulic head and flows and can be either physical or mathematical (Mckee and Clarck, 2003, Asim, 2005). There are several ways of classifying groundwater flow models, and these can either be steady state or transient and with one, two or three spatial dimensions. The steady state represents conditions where the inflows and outflows to the model are constant with time (Anderson and Woessner, 1992). This chapter focuses on the simulation of groundwater flow system at the Besease inland valley using groundwater flow modelling. The aquifer system was modelled using PMWIN assuming steady and transient conditions (Chiang and Kinzelbach, 2001). The watertable fluctuation method was employed to estimate the recharge. A combination of trial and error and automatic methods were used to calibrate the models using the observed hydraulic heads. The transient calibration was used to simulate potential future water use scenarios.

9.2 Conceptual Model

A groundwater conceptual model is a pictorial representation of the groundwater flow system incorporating all available geological and hydrogeological data into a simplified block diagram or cross section. Simplification in the modelling process is necessary but over simplification may lead to a model that lacks the required

information, while under simplification may result in the lack of data required for model input. Briefly, a conceptual model describes the hydrologic system with respect to aquifer properties, flow characteristics and boundary conditions. According to Anderson and Woessner (1992) there are three steps in building a groundwater conceptual model:

- Defining hydrostratigraphic units (Appendix 1)
- Preparing a water budget and
- Defining the flow system.

Moreover the conceptual model is very much important to establish the model framework i.e. dimension type of model as well as selection of model codes. The system was conceptualized for simplicity by incorporating all important features and processes with simplifying assumptions on the topography, soil, landuse, and hydrology of the area. Further it incorporates geological data and various hydrologic measurements such as water levels and rainfall data. The conceptual system of the wetland is shown in Fig 10.1:

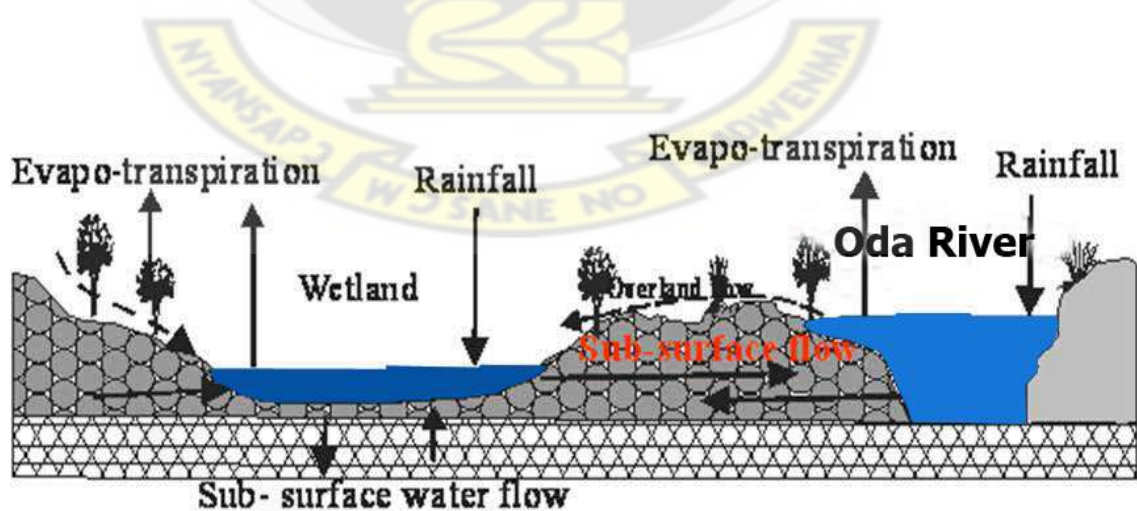


Figure 9.1 Conceptual Diagram of Besease Inland Valley Bottom Study Site

9.3 Layer Type and Boundary Conditions

Two layer types for this study were defined, namely:

Type 1-The layer is strictly unconfined and can be applied for the uppermost part of a model. Specific yield is used to calculate the rate of change in storage for this layer type. During a flow simulation, transmissivity of each cell varies with the saturated thickness of the aquifer.

Type 3-A layer of this type is fully convertible between confined and unconfined. Confined storage coefficient (specific storage \times layer thickness) is used to calculate the rate of change in storage if the layer is fully saturated, otherwise specific yield will be used. During a flow simulation, transmissivity of each cell varies with the saturated thickness of the aquifer. Vertical leakage from above is limited if the layer desaturates.

Three boundary conditions can be applied to cells in a finite difference grid such as Modular 3-Dimensional Groundwater Flow Model (MODFLOW) including (a) Dirichlet, (b) Neuman and (c) Cauchy

(a) Dirichlet condition: the head at the boundary is known, examples are the watertable in an unconfined aquifer, or a river or lake in contact with an unconfined aquifer, all under steady conditions. In a natural hydrological system, an aquifer may continue onwards past the boundary and therefore must be accounted for by placing a fixed or a specified head cell or cells in which the allocated head is known.

(b) Neuman conditions: the flux across a boundary is specified, examples include no flow boundaries between geological units, interactions between groundwater and surface water bodies, springflow, under flow and seepage from bedrock into alluvium. The most commonly applied form of a Newman boundary is a no flow or impermeable boundary, often occurring between a highly permeable unit and a unit of

much lower permeability. A difference in hydraulic conductivity of two orders of magnitude or greater between two adjacent units is sufficient to justify placement of a no flow boundary as this contrast in permeability causes refraction of flow lines such that flow in the higher conductivity layer is essentially horizontal and flow in the lower conductivity unit is essentially vertical (Anderson and Woessner, 1992).

(c) Cauchy condition: the flux across the boundary is dependent on the magnitude of the difference in head across the boundary, with the head on one side of the boundary being input to the model and the head on the other side being calculated by the model. Example of Cauchy boundary include leakage from a surface water body where the flux is dependent on the difference in elevation between the surface water and groundwater level and the vertical hydraulic conductivity of the boundary; and evapotranspiration where the flux is proportional to the depth of the watertable in an unconfined aquifer. A Cauchy boundary has the advantage over a Neuman boundary in that its flux can be calculated by the model if given sufficient input data.

9.4 Model Boundaries

Boundary conditions have great influence on the computation of flow velocities and heads within the model area. In MODFLOW, boundary conditions need to be specified, and there is an array of codes for each cell. In the boundary condition (IBOUND), a positive value in the array defines an active cell (the hydraulic head is computed), a negative value defines a fixed-head cell (the hydraulic head is kept fixed at a given value), and the value 0 defines an inactive cell (no flow takes place within the cell). Specifying a boundary condition, the use of 1 implies active cells, 0 inactive cells and -1 fixed-head cells. If a fixed-head cell is specified, the initial hydraulic head remains the same throughout the simulation. A fixed-head boundary supplies a continuous amount of water and is specified whenever an aquifer is in direct hydraulic

contact with a river, or a reservoir (wetland) if the water level is known. The west side (Fig 9.5) of the model domain having contact with the river was assumed to be a no-flow boundary. This chosen boundary condition was also duplicated to the north and south of the model area. Flow along the eastern boundaries was specified as constant head. During the modelling these conditions were varied among the three boundary conditions to achieve an optimum fit.

9.5 Model Code Selection

The modelling code is the computer programme that contains algorithms to numerically solve the mathematical model. Most modelling codes in common use today also have a graphical user interface for the pre- and post-processing of modelling data.

The mathematical model is the basic hydraulic equation that governs the flow of groundwater in the saturated zone. It is a partial differential equation in time and three-dimensional space. The conceptual model and the hydrogeological framework data together help to define the boundary conditions for the solution of the mathematical model. The hydrogeological stresses complete the boundary condition definition, and provide the temporal and spatial data for the solution of the hydraulic equation.

A modelling code can be thought of as a very complex, three-dimensional, interactive database, with time variability, because it incorporates the following:

the means to input data to describe the model domain and hydrologic stresses in space and time,

the numerical algorithms to solve the mathematical model (hydraulic equation of groundwater flow) and

the means to output the results of the simulation.

9.6 Numerical Model

The selected code for the numerical model was Processing MODFLOW for Windows (PMWIN) version 5.3 (Chiang and Kinzelbach, 2001) as code environments for data input and output management. The partial differential equation (Equation 9.1) describing the groundwater flow is solved numerically for each discrete cell in the defined grid. The equation solved in MODFLOW is a combination of a three dimensional Darcy's law and the mass balance equation:

$$\frac{\partial}{\partial x} \left(K_{XX} \frac{\partial h}{\partial x} \right) + \frac{\partial}{\partial y} \left(K_{YY} \frac{\partial h}{\partial y} \right) + \frac{\partial}{\partial z} \left(K_{ZZ} \frac{\partial h}{\partial z} \right) - w = S_c \frac{\partial h}{\partial t} \dots \dots \dots 9.1$$

Where,

hydraulic head, h (m), is the dependent variable. The hydraulic conductivity is represented here in the three directions (x, y and z) K_{XX} , K_{YY} , and K_{ZZ} (m/day), S_c , specific storage (dimensionless) and w (l/day) represents the general source/sink per volume of the aquifer. If W is positive then water is leaving the system and if it is negative water is entering the system, t (days) stands for time. If the problem is steady-state, there is no time variant parameter and the right side of the equation vanishes (Anderson and Woessner 1992).

9.7 Spatial Descritisation

Descritisation of the model domain plays an important role in the cause of the modelling. The model region was made up of two layers and was divided into grids, the layers which had 65 columns and 38 rows using the 10×10 m grid cell spacing resulting in 247000 grid cells and this was used to represent the entire model area of 72 ha. Cells in the no flow boundary region were defined as inactive using the I

BOUND array in MODFLOW. The total number of active grid cells in the model was 90400 cells.

9.8 Aquifer Geometry

The surface topography was derived from a survey carried out over the area and the aquifer extent was also made based on the available details of the piezometers. The mean thickness of the top unconfined layer is 2.3 m of the study site. The second layer below has a thickness of 1.2 m, specified on the basis of a geological formation which enhances transmission of water.

9.9 Recharge

Recharge is limited to some extent by behaviour of the sedimentary and geological system that underlies the Besease Wetland site. This serves as a partitioning force that controls sub-surface recharge or water movement (Fox *et al.* 1998). In typical model applications recharge can be defined as homogeneously as percentage of yearly average rainfall or calibration as an unknown parameter. In MODFLOW, recharge is normally estimated and entered as input values into the recharge package. The boundary condition in the MODFLOW groundwater model is effectively represented by specifying net bottom flux of watertable fluctuation as a recharge flux. For the two year period (730 days) a recharge of 753.8 mm (28.3 %) of the bi-annual rainfall was specified (Figure 9.2) as input into the model and was applied uniformly over the model domain. The method excludes the evapotranspiration of the groundwater, the value obtained from the method was used for the model.

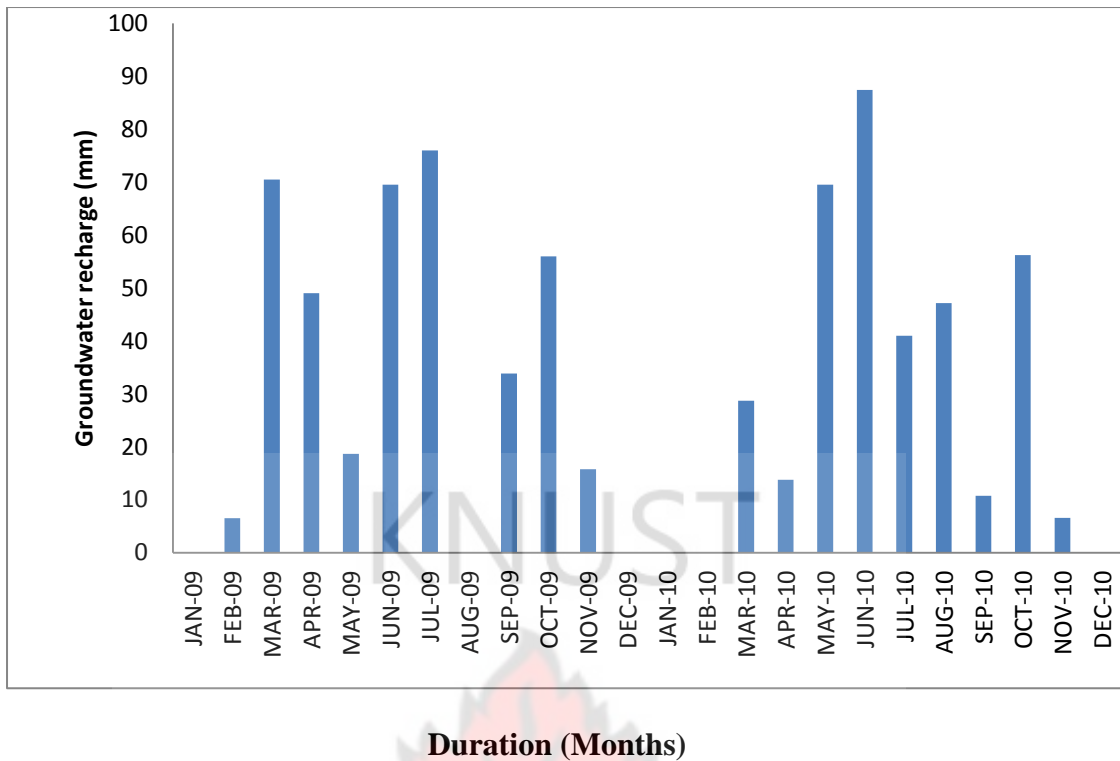


Figure 9.2 Monthly Recharge from Watertable Fluctuation

9.10 Hydraulic Conductivity

Initial values of hydraulic conductivity at the Besease valley aquifer was evaluated from falling head test and mini disc infiltrometer test. The values were used as initial parameter values for the model. Two hydraulic conductivity layers were specified. For the top layer, due to spatial heterogeneity of vertical hydraulic conductivity, a range of 0.02-0.039 m/day was specified. A range of 0.2-0.39 m/day was specified as the horizontal conductivity of the top layer. For the bottom layer, an arbitrary value of 0.07 m/day which best suited the model during calibration was specified for both vertical and horizontal hydraulic conductivities because of lack of data on the layer.

9.11 River Package

Whenever there is a hydraulic contact between a wetland aquifer and a river, there exist seepage flow into and out of the systems and this connection makes the river

system recharges the wetland aquifer and also can encounter a discharge from the aquifer into the river. The river package (Prudic, 1989) was used to represent the Oda River in the model. The water flow between an aquifer and overlying river is commonly simulated using the river package as follows:

- $QRIV = CRIV (HRIV - h)$ for $h > RBOT$
- $CRIV = (HRIV - RBOT)$ for $h \leq RBOT$

$$CRIV = \frac{KLW}{M} \quad 9.2$$

Where:

$QRIV$ = rate of leakage between the river and aquifer $[L^3T^{-1}]$

$CRIV$ = hydraulic conductance of the river bed $[L^2T^{-1}]$

$HRIV$ = head in the river $[L]$

H = head in the cell $[L]$

$RBOT$ = elevation of the bottom of the river bed $[L]$

K = hydraulic conductivity of the river $[LT^{-1}]$

L = length of the river within a cell $[L]$

w = width of the river within a cell $[L]$

M = thickness of the riverbed $[L]$

The Oda River can gain from or contribute water to the floodplain wetland depending on the river stage (Figure 9.3), riverbed conductance and adjacent floodplain aquifer water levels. The river surface elevation data used were measured by the Hydrological

Services of Ghana. The low level of 258.4 m was recorded in January 2009, while September 2010 had the highest reading of 259.6 m.

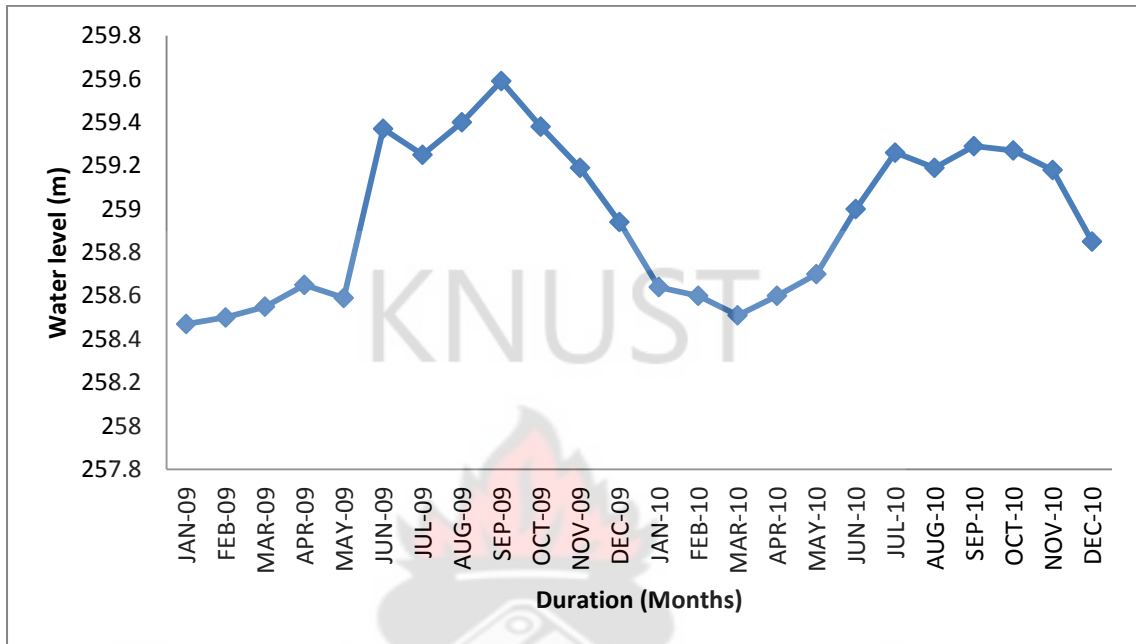


Figure 9.3 River Gauge Heights at Ejisu-Besease Station

Riverbed conductance is a critical parameter in determining the amount of water seepage between the river and underlying aquifer. However, the observed riverbed conductance in the Oda River basin at Besease showed high variability, with differences between the scale at which riverbed conductance was estimated and the scale at which it was applied in the model (Hayashi and Rosenberry, 2002). Riverbed conductance values of between 2.0×10^2 m/day and 2.30×10^2 m/day were assumed and assigned using the hydraulic conductivities of the observed changing bed materials consisting of alluvial deposits, metamorphosed sedimentary and granites outcrops that mostly underlie the riverbed. Data of riverbed thickness and river width were not available to justify adjustment of riverbed conductance on a river-segment basis; therefore, no calibration of riverbed conductance was made during the

modelling process. Digital elevation models for the study area and river depth survey were used to determine the riverbed elevation. A minimum elevation of 257.5 m was approximated and used to adjust the available DEM data. Variations in river water level measured by Hydrological Services, Ghana, were incorporated in the topographic data to derive the monthly gauge level as it relates to the topography. To simulate the lateral flow interaction between wetland and river through the sediment deposits, an assumption about low permeability of the river bed is made to prevent leakage from the riverbed into the underlying aquifer.

9.12 Results and Discussions

9.12.1 Model Calibration

Calibration is the process of adjusting model inputs to achieve the desired degree of correspondence between the model simulations and the natural groundwater flow systems (Anderson and Woessner, 1992). The model was calibrated using both steady and transient mode. The steady state flow simulation was performed to first calibrate model parameters. This was done to obtain a tolerable distribution of the initial hydraulic head. The vertical and horizontal hydraulic conductivity values of the top layer were adjusted to get good fit for conductivities of the layers. For the bottom layer, an arbitrary value was set for both vertical and horizontal hydraulic conductivity, since no hydrogeological data was available (Table 9.1). In addition, effective porosity, specific storage, storage coefficient and specific yield of the subsurface were adjusted to fit the level of fluctuation occurring within the floodplain wetland. The adjustment of the conductivities and other parameters shifted the percent of discrepancy for each time step to be less than one (1%) which means that the model equation has been solved correctly and this agrees with what is mentioned in literature

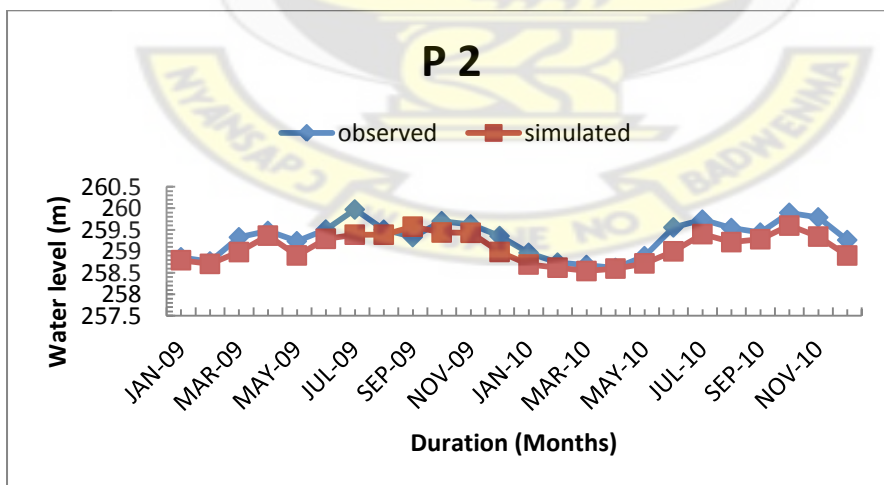
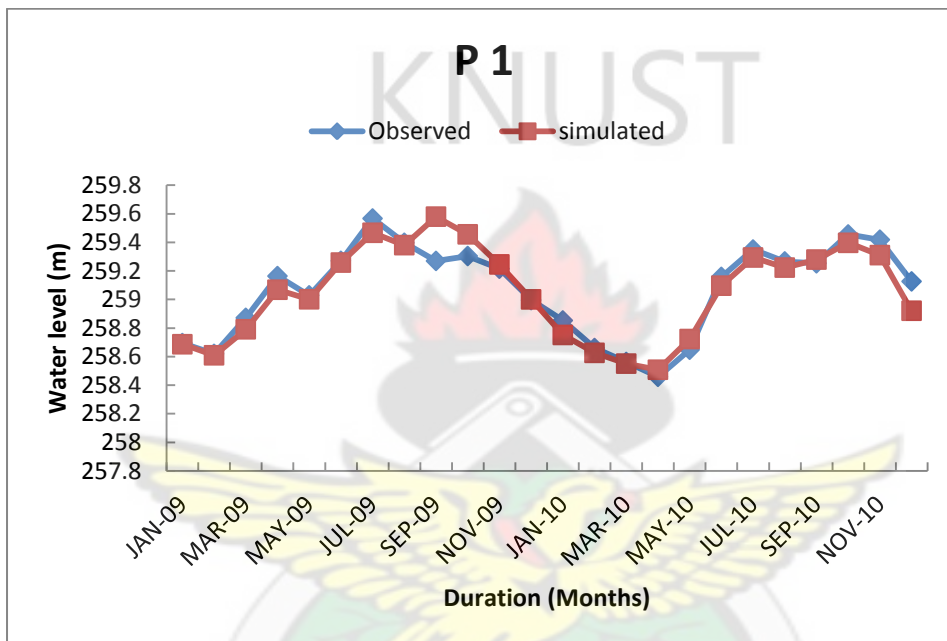
requiring that the mass balance for any time step in a model should have less than 1% discrepancy (Harbaugh, 2005).

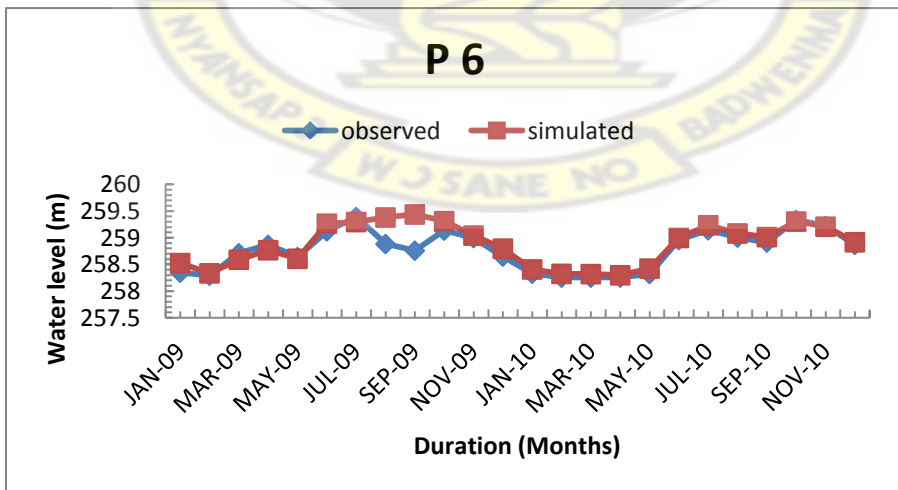
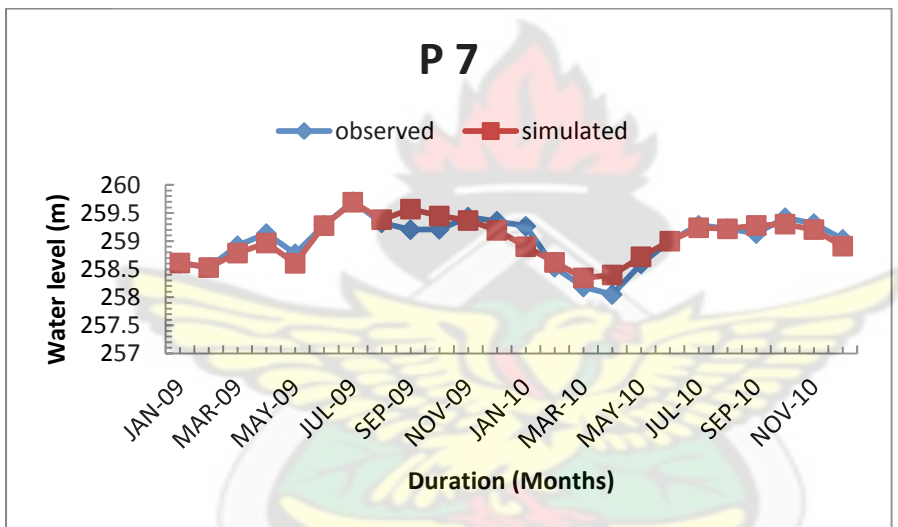
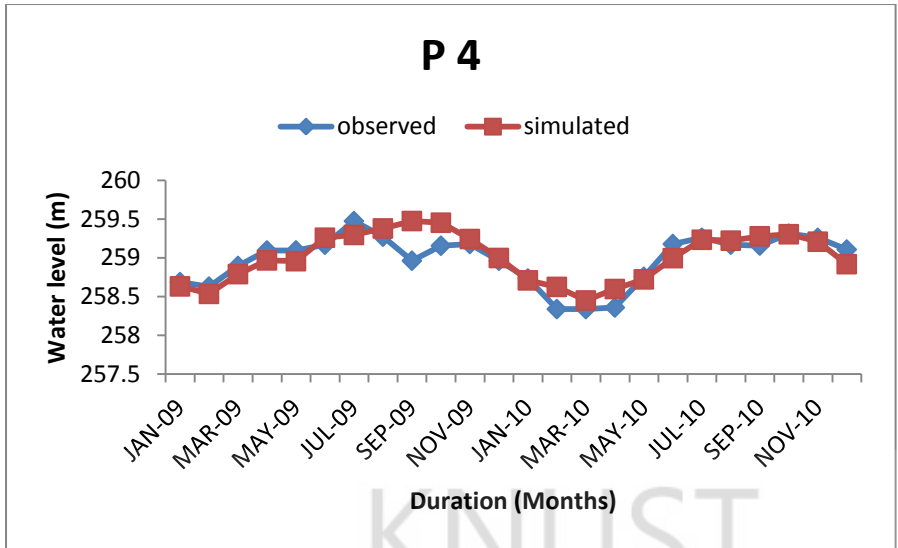
Table 9.1 Adjusted Parameters for the Groundwater Flow Model

Property	Layer 1	Layer 2
Horizontal Hydraulic Conductivity	0.12 - 0.59	0.4
Vertical Hydraulic Conductivity	0.015-0.059	0.07
Effective Porosity	0.20-0.24	25
Specific Yield	0.06 m ³ /d	0.015 m ³ /d
Specific Storage	0.05	0.001
Storage Coefficient	0.01	0.001

The steady state simulation was based on the assumption that the starting hydraulic head from the interpolated hydraulic head of the boreholes and the river in January 2009. For transient calculations of groundwater flow simulation, an initial condition created from the steady state was used. The period September to October 2010 was chosen for the calibration, as detailed hydraulic head measurements were available for this period. The aquifer received 753.83 mm as areal recharge from the watertable fluctuation method. The time step for the two year simulation was divided into 24 stress periods with each stress period representing a month. A time step of 4 days was chosen so that the total time step equals one month while the total simulation time equals 370 days. The output from the model simulation shows monthly flow maps which depends on the variations of the recharge and the river package. The calculated head values for the last step of each stress period were noticed to show slight differences in head contours. Figure 9.4 shows plots of observed and calculated heads for piezometers, for which the calculated head follows the pattern of the observed head. Water levels in the piezometers were always elevated in the rainy season and lower in the dry season. The piezometers in the Besease inland valley were used to

represent sections of the wetlands. The simulated curve generated shows a good fit with observations especially for P1, P2, P4, P5, P6, P7, P12 and P14. The rises in the hydraulic heads of the simulated hydrograph are similar and follow a pattern, while the observed hydraulic head shows some differences. The variability in the observed heads is likely to be as a result of the heterogeneity in the sub-surface aquifer structure.





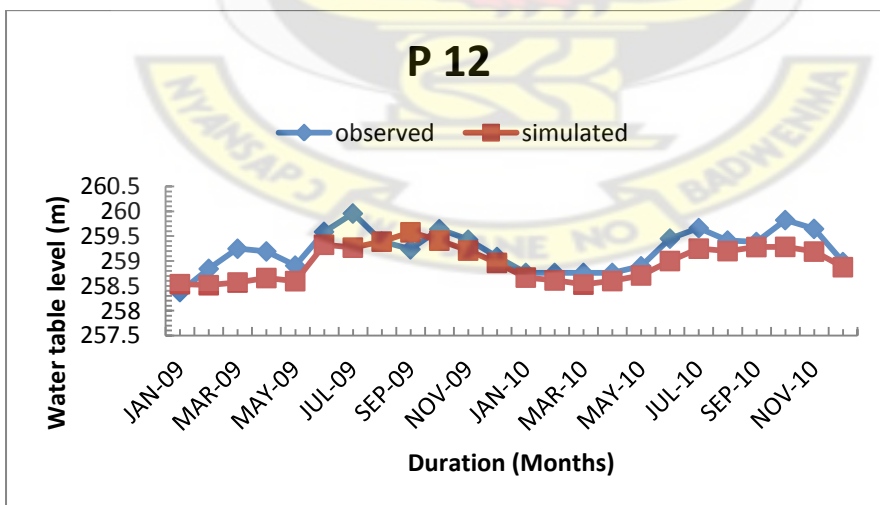
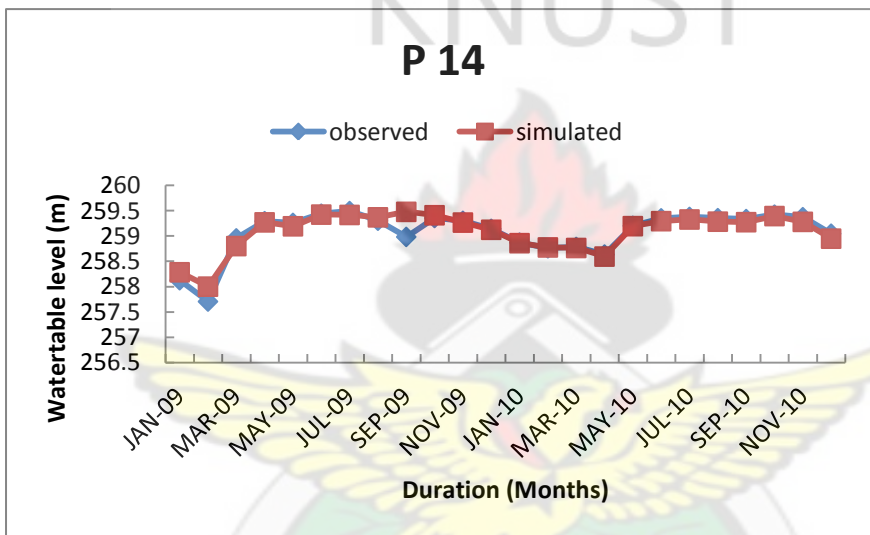
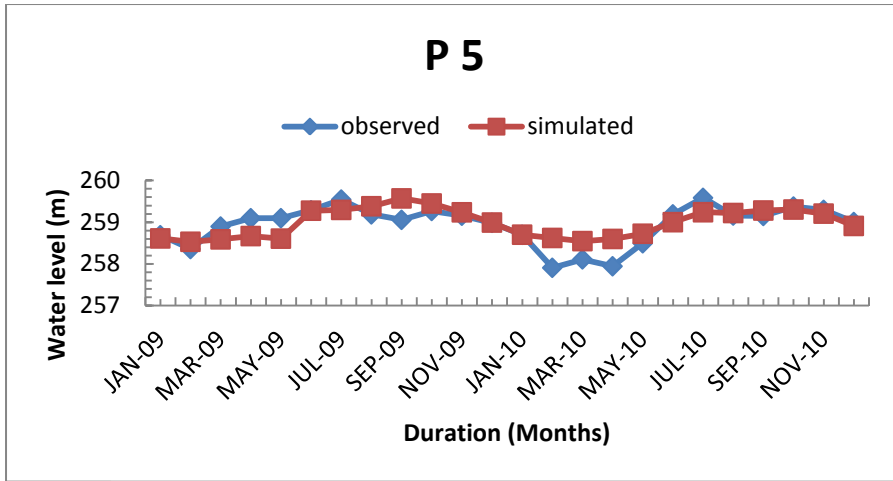


Figure 9.4 Simulated and Observed Heads in the Besease Inland Valley Bottom

The simulation of the sub-surface hydraulic head indicates a systematic variation relative to the Oda River in response to changes in the rainfall pattern in the moist semi-deciduous climatic region. Over the months of January 2009, June 2009, September 2009, October 2009, March 2010, June 2010, August 2010, September 2010, October 2010 and December 2010 (Figure 9.5) distinctive patterns of hydraulic heads were observed.

As depicted in the month of January 2009, where the hydraulic head simulated showed a lowered watertable from 258.5 m to 258.67 m with a difference of 0.17 m. Also in the period of February to March 2010 the hydraulic head experienced in the valley varied between 258.51 m and 258.64 m was below the topographic surface with the lowest in March. The lowering of the watertable in the dry periods even with total rainfall input of 34.9 mm in January 2010 and 49.6 mm in February 2010 replenished the soil moisture deficit but could not reach the watertable to recharge it (Figure 9.3 and Table 9.3). The recorded rainfall input in January and February 2010 could not raise the watertable suggesting that antecedent moisture in the vadoze zone should be taken into consideration in recharge characteristics of unconfined aquifers in response to rainfall events. This also shows that moisture levels in the unsaturated zone holds part of the seasonal replenishment in these unconfined aquifers. In the wet season the precipitation recharge the groundwater by raising the watertable at an average depth of 0.5 m. The wetland became saturated in the months of June and July for both 2009 and 2010 water years. The piezometric watertable rose above the ground surface for all the piezometers except that of P1 and P2 but all the pipes experienced a watertable rise above the ground surface in the month of July. This was evident by the fact that the soil got saturated in most parts of June and July. However, the model under-predicted the simulated hydraulic head in June 2009 with an

estimated head of 259.36 m but over-predicted the hydraulic heads in September 2009 experiencing a simulated head of 259.57 mm and this would be attributed to the accumulated high river stage level in September 2009 (Figure 9.4 and Figure 9.5) which showed some interaction between the Oda River and the inland valley. A bi-direction of sub-surface water flow between the Oda River channel and the wetland hydrologic system is inferred as having a temporal and spatial variation.

KNUST



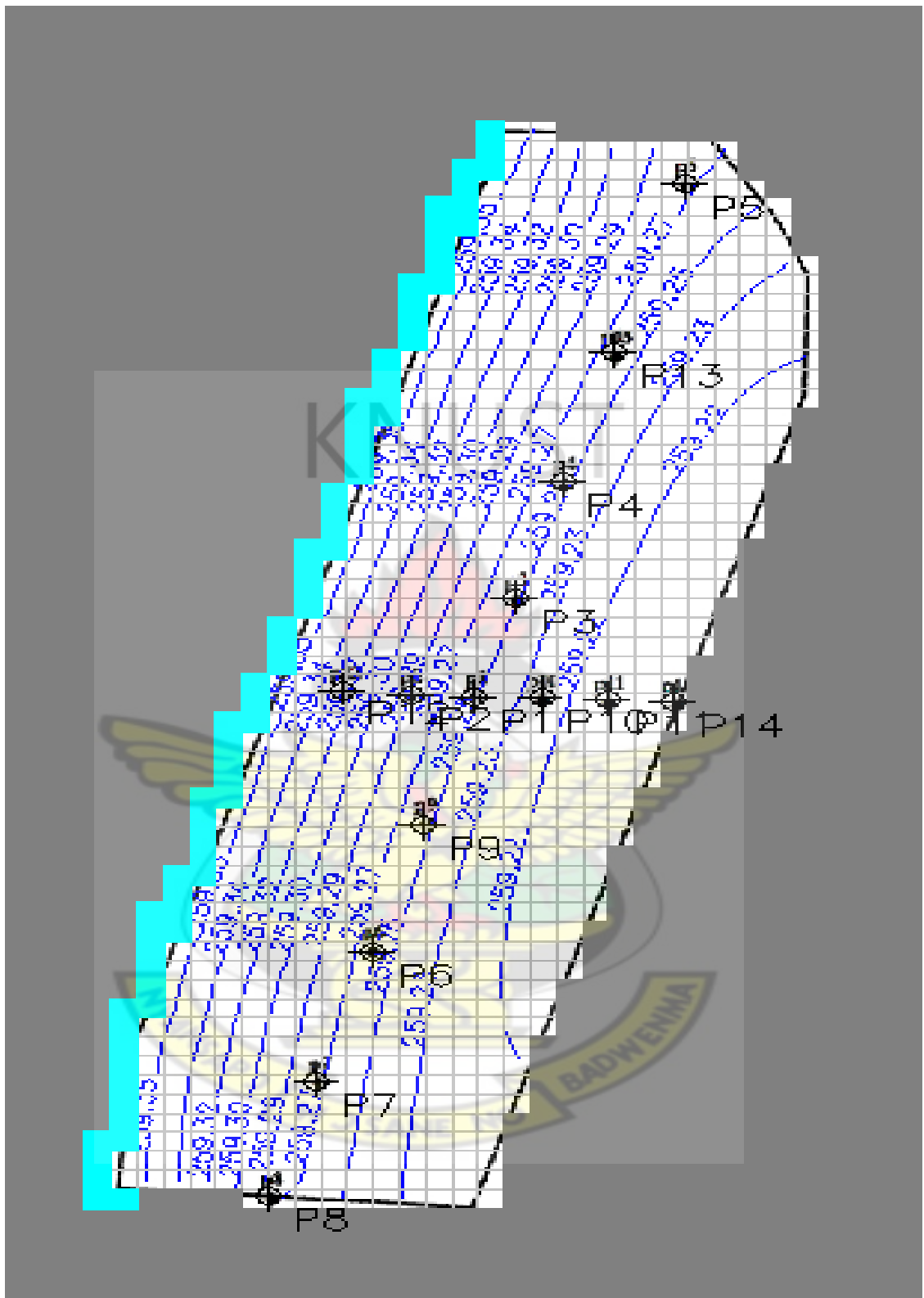


Figure 9.5b Depth of Estimated Hydraulic Head (m) of Inland Valley in June 2009

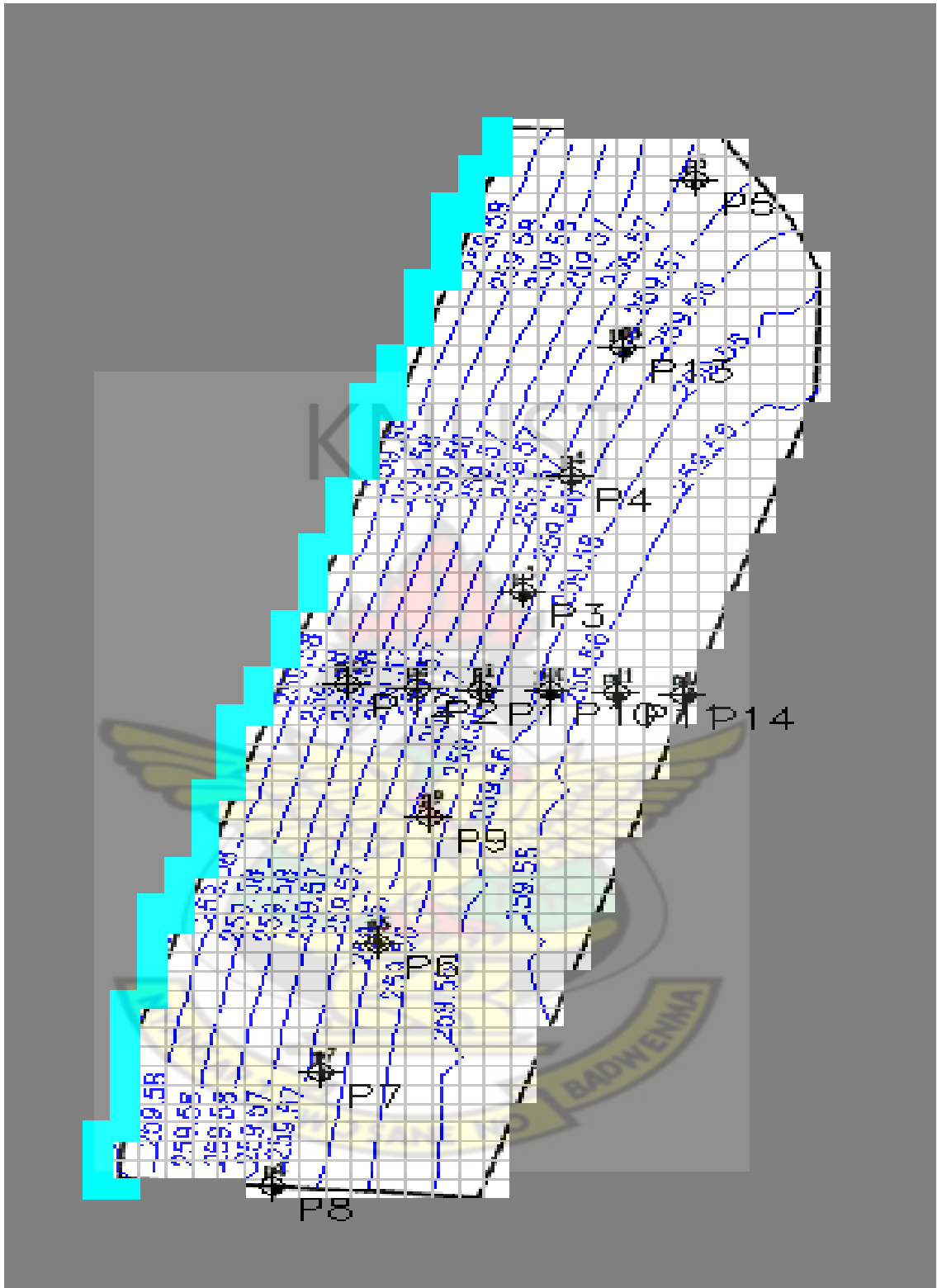


Figure 9.5c Depth of Estimated Hydraulic Head (m) of Inland Valley in September 2009

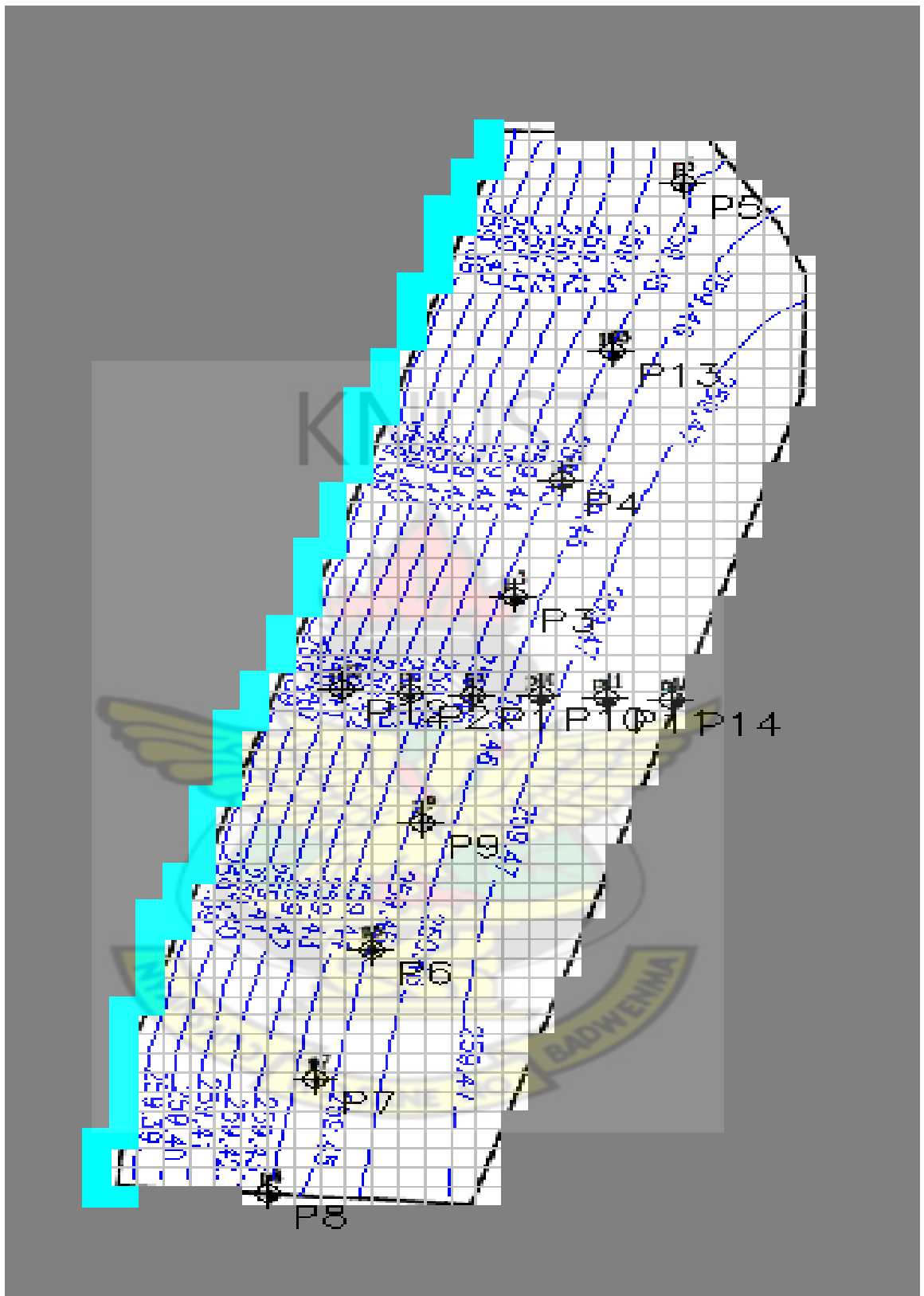


Figure 9.5d Depth of Estimated Hydraulic Head (m) of Inland Valley in October 2009

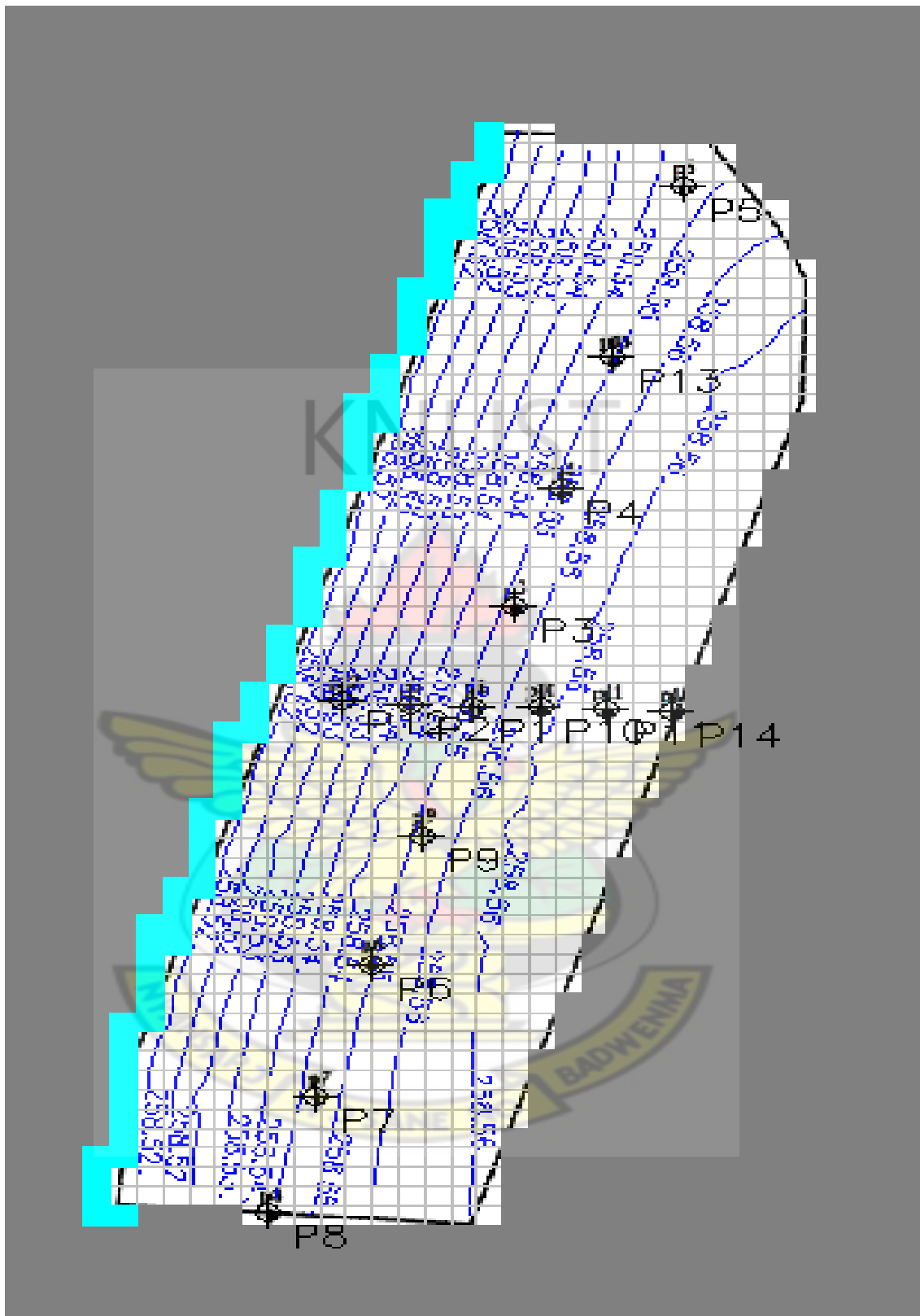


Figure 9.5e Depth of Estimated Hydraulic Head (m) of Inland Valley in March 2010

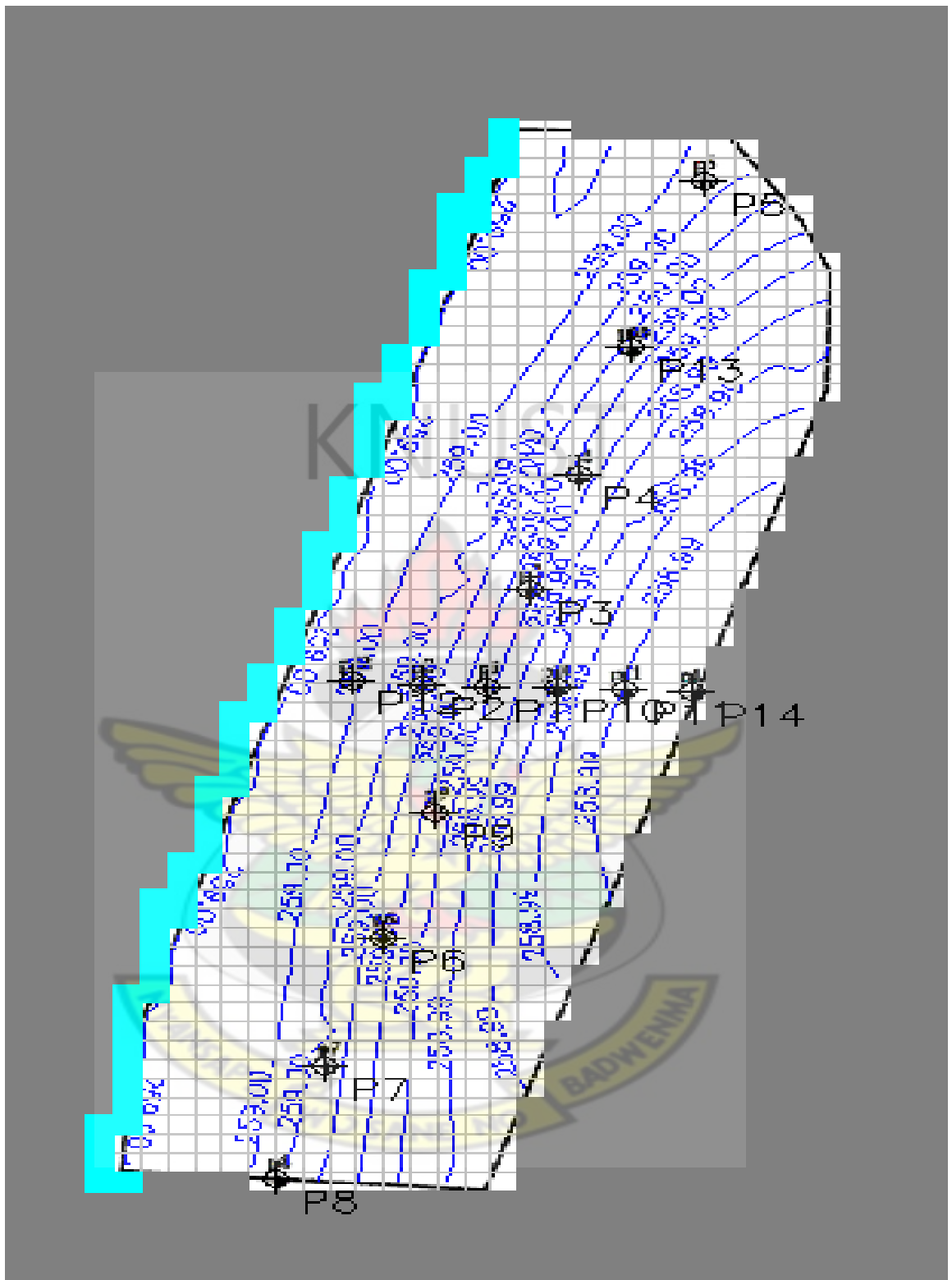


Figure 9.5f Depth of Estimated Hydraulic Head (m) of Inland Valley in June 2010

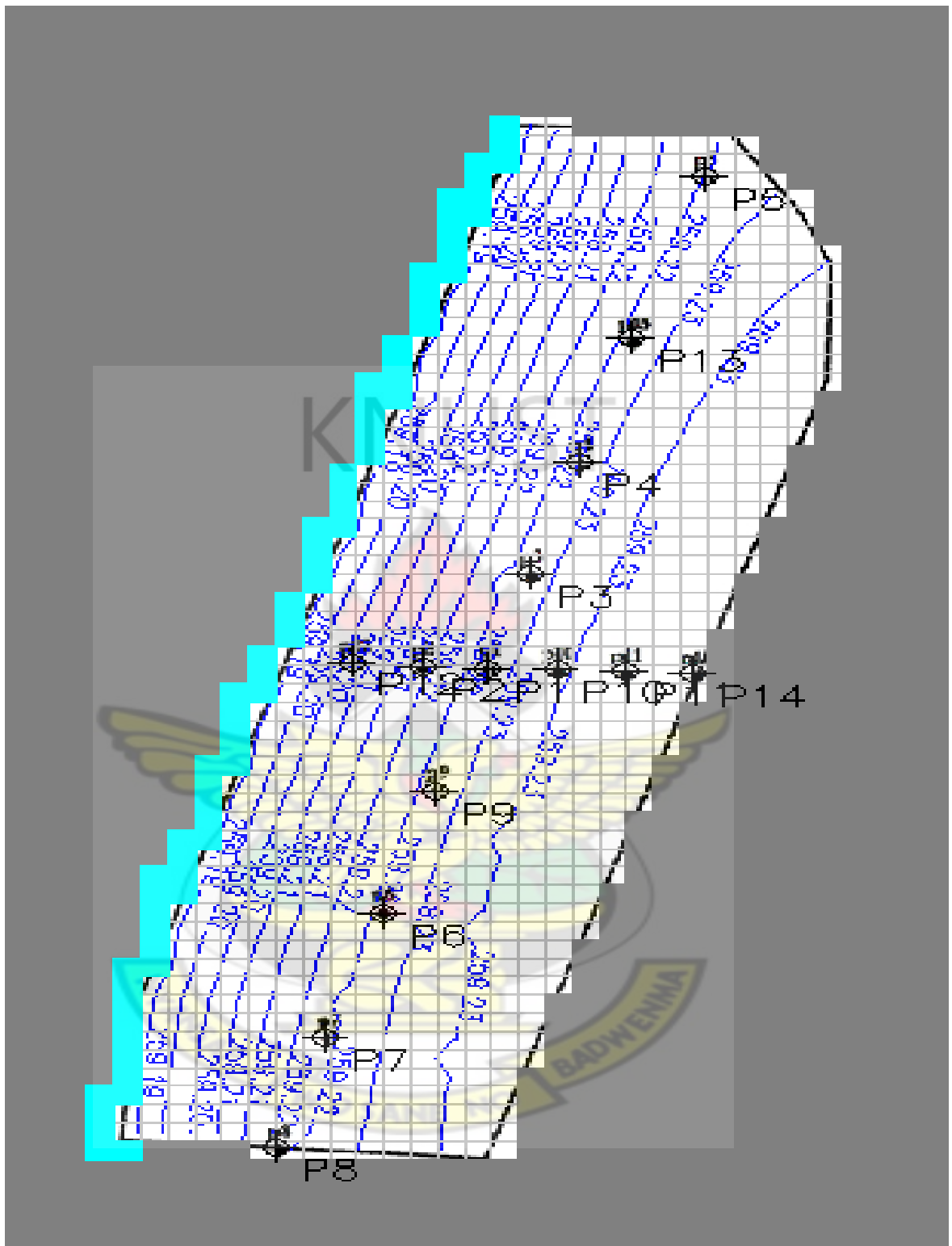


Figure 9.5g Depth of Estimated Hydraulic Head (m) of Inland Valley in August 2010

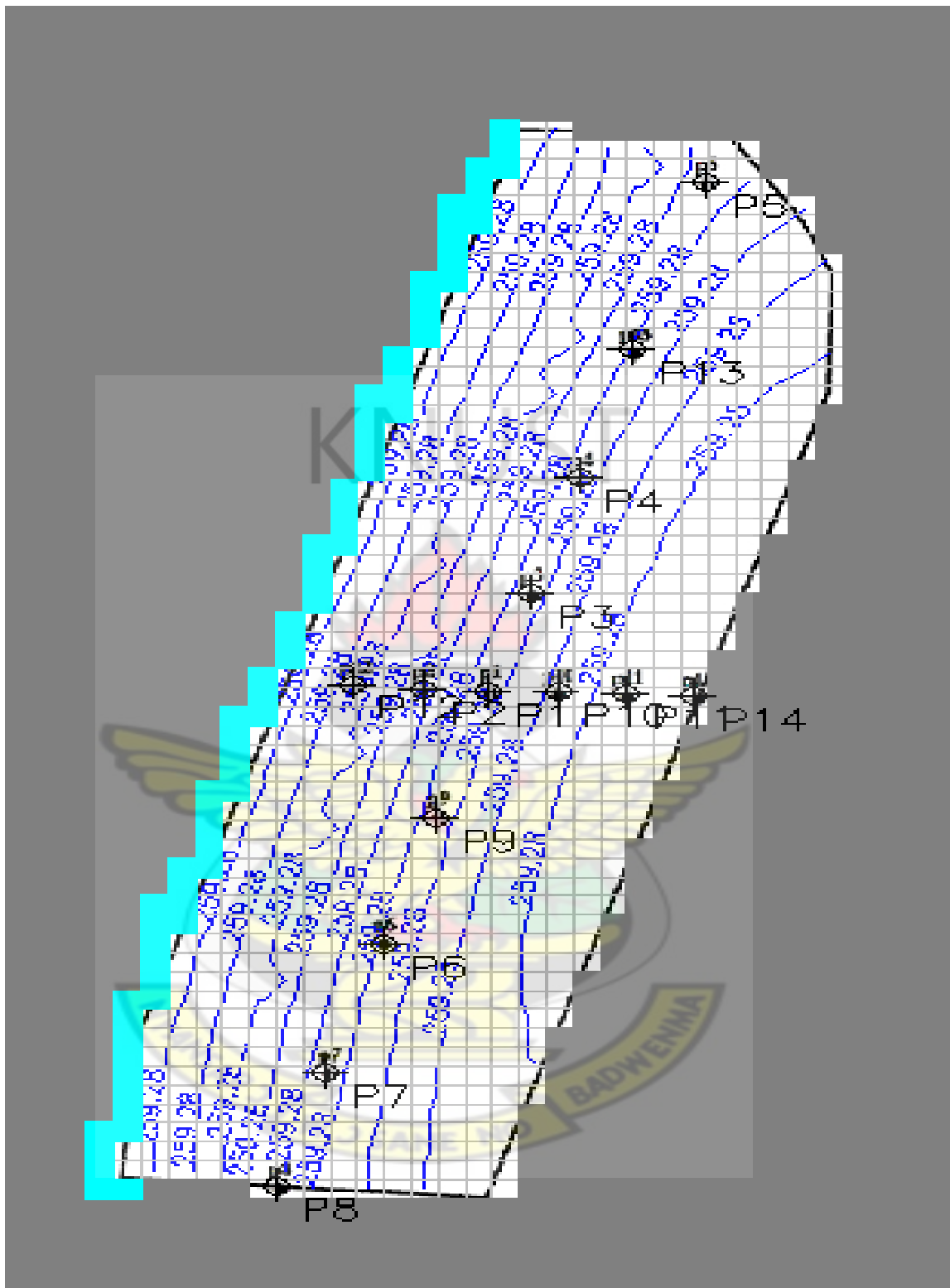


Figure 9.5h Depth of Estimated Hydraulic Head (m) of Inland Valley in September 2010

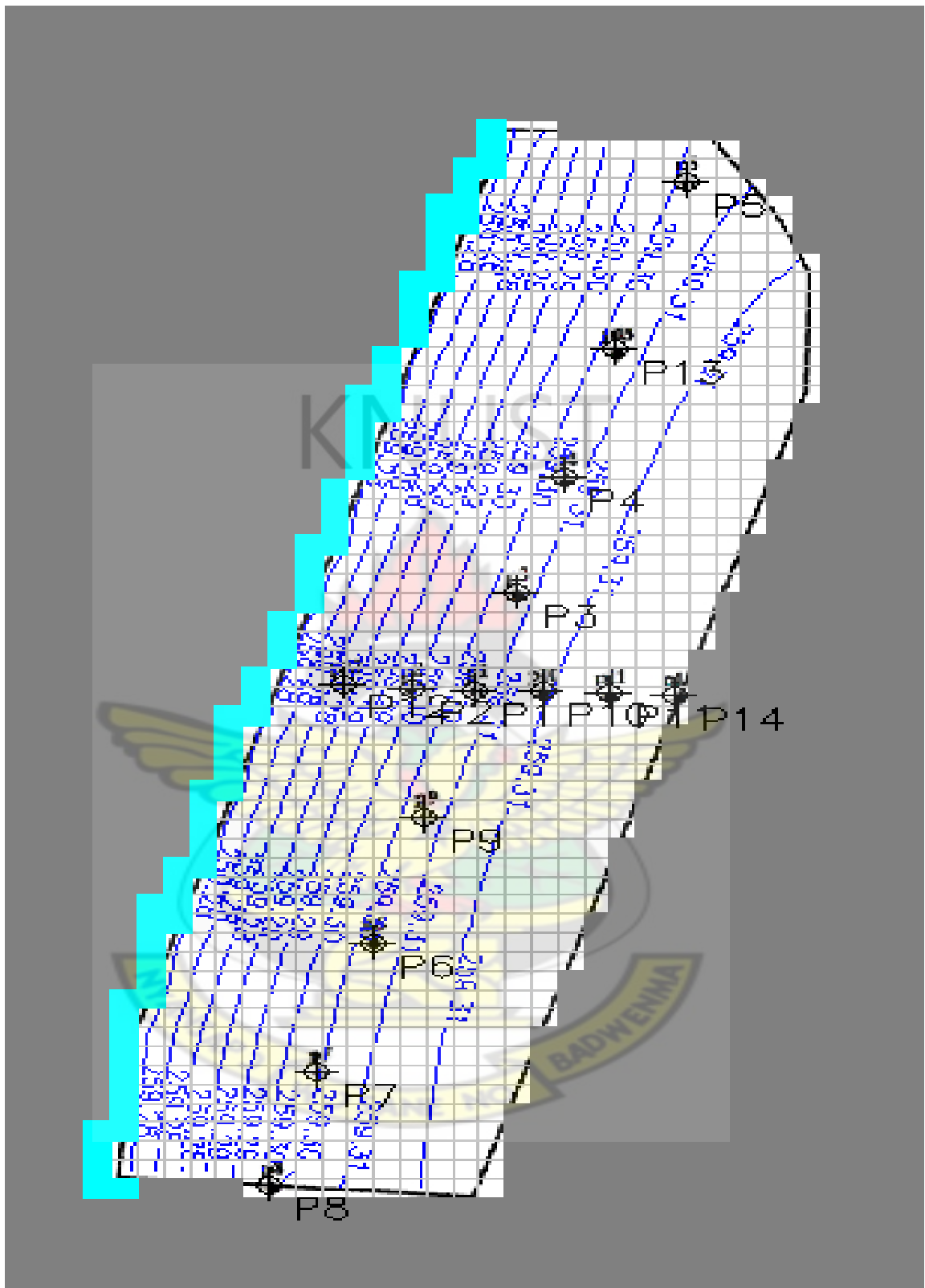


Figure 9.5i Depth of Estimated Hydraulic Head (m) of Inland Valley in October 2010

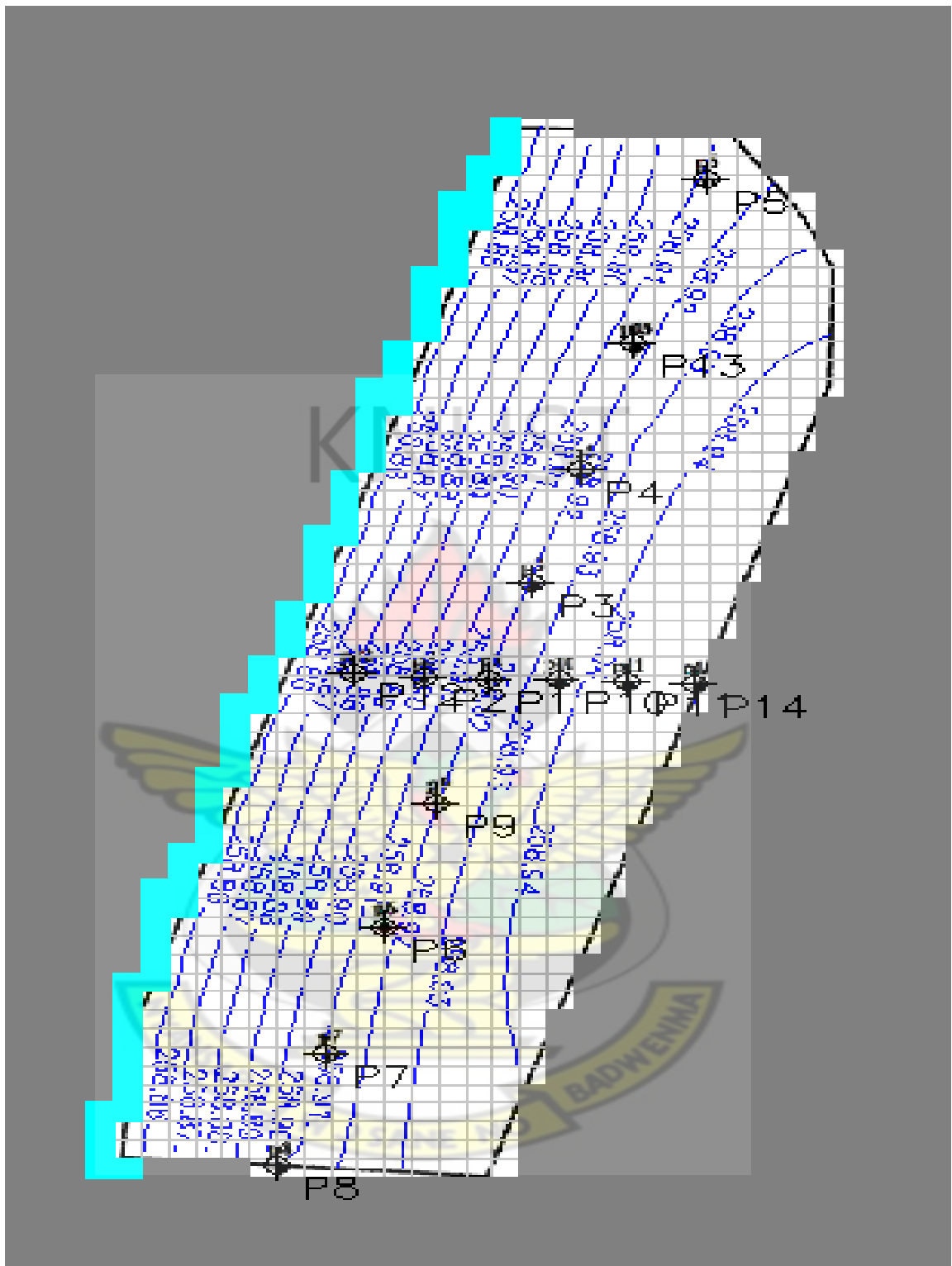


Figure 9.5j Depth of Estimated Hydraulic Head (m) of Inland Valley in December 2010

9.12.2 Model Calibration Evaluation

The results of the calibration were evaluated both quantitatively and qualitatively. The average of the differences between the observed and simulated heads was used to quantify the average error in the calibration. The mean error (ME), the absolute mean error (MAE) and the root mean square error (RMSE) were used to express the average difference between the observed and the calculated heads in Table 9.2.

Table 9.2 Model Fit Statistics for the Transient Run Monthly Values of Observed and Simulated Hydraulic Heads

Piezometer	Observed (m)	Simulated (m)	R ²	ME	MAE	RMSE
P 1	259.0668	259.0509	0.9088	0.016	0.067	0.099
P 2	259.3221	259.0894	0.7984	0.233	0.253	0.293
P 4	258.9821	259.0113	0.7273	-0.029	0.13	0.172
P 5	258.9386	258.9817	0.5474	-0.043	0.239	0.0431
P 6	258.7768	258.8704	0.8056	-0.094	0.126	0.195
P 7	259.0213	259.0242	0.7864	-0.003	0.125	0.167
P 10	259.0099	258.9892	0.7309	0.021	0.15	0.19
P 12	259.2175	258.9686	0.6447	0.249	0.291	0.344
P 14	259.0801	258.9817	0.9045	-0.006	0.084	0.134

The watertable bottom flux used as a recharge estimate resulted in a fit between the simulated hydraulic head and observed sub-surface water level fluctuation. The level of compatibility observed in Table 9.2 gives indication that the model calibration needs to be improved. However, individual piezometers in the wetlands also showed differences between the observed and simulated heads (Table 9.2). Additionally, P1 located within the middle of the wetland and about 66 m away from the Oda River

gave a better fit (ME = 0.016, MAE = 0.067 m and RMSE = 0.099 m). A more accurate calibration will not be justified when given a lack of spatial data, for instance the local flow pattern and hydraulic properties with depth. Also dynamics in phreatic watertable fluctuations, topography and other parameters would be required in more detailed to develop a validated model of the accuracy required for the management of the inland valley in the Ejisu-Besease Oda River Basin

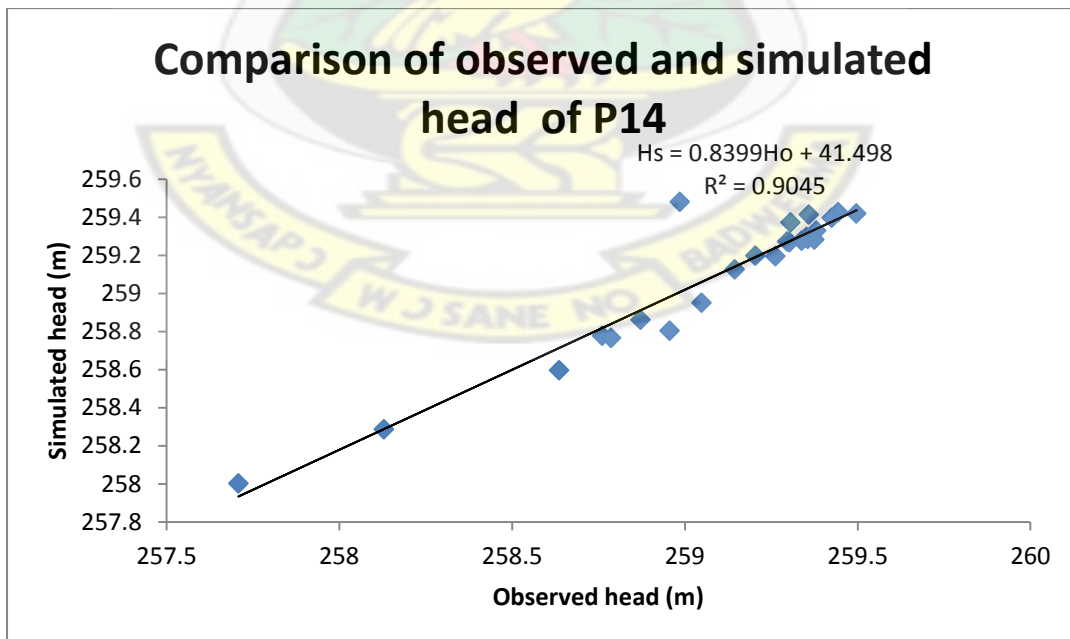
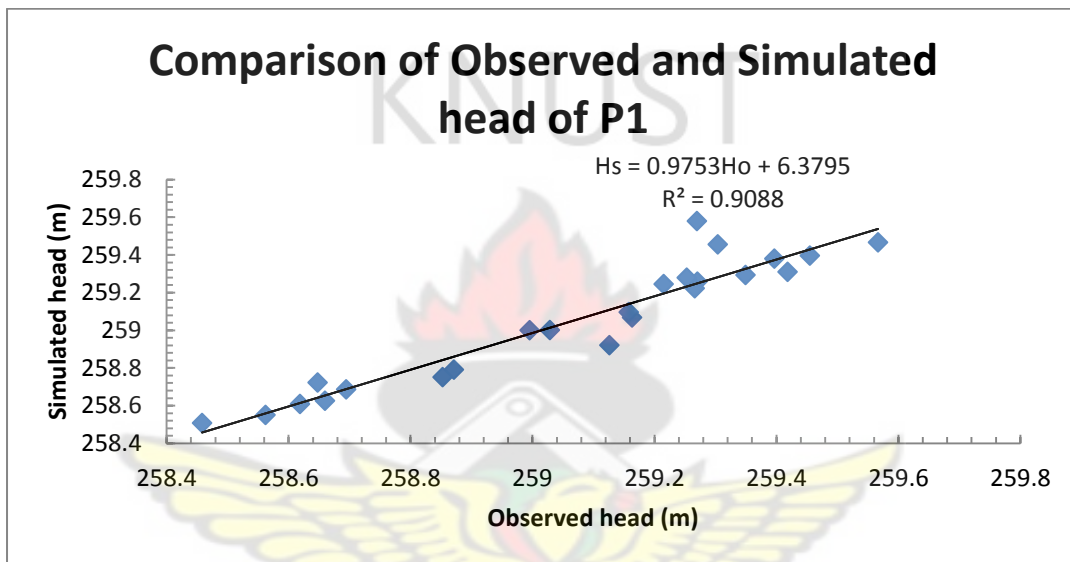


Figure 9.6 Comparison of Simulated and Observed Heads in the Besease Inland Valley Wetland for a Period of two Years (January 2009 to December 2010)

9.12.3 Mass Balance

The calibrated groundwater model produced an estimated groundwater budget for the model domain. The water budget accounts for the sources of water for recharge or discharge of a hydrologic system on monthly basis. The inputs into the model are derived from areal recharge, river leakage into the wetland and storage out of the wetland. River leakage out of the wetland and storage into the wetland are the outputs from the model (Bradley, 2002). The cumulative mass balance at the end of the run period of 24 months (730 days) for the transient model demonstrates the importance of recharge as a water balance input. The model underestimated the recharge of 24.30 mm in June 2009 and this lends credence to the fact that the entire wetland experienced saturation in the middle of the month where the watertable was near or above the ground surface. The storage terms described by MODFLOW in Table 9.3 represent the quantities of water that are either released from storage as the watertable falls and water drains from open pores in the wetland substrate or water that is taken up into storage as the watertable rises and the wetland becomes increasingly saturated (Bradley, 2002). For instance in the month of June 2010 a total amount of 9668.405 m³ moves into storage to saturate the wetland and it was in one of these periods when static water level in all the piezometers rose above the ground surface during field observation but was, however, under predicted by the model (Figure 9.4 and 9.5). The extent, depth, frequency, timing and duration of water ponding at the surface of the wetlands are important parameters controlling the extent of soil moisture for the sustenance of the river. Nyarko (2007) observed that water ponding in the Pwalugu wetland to a depth of 0.65 m as measured during fieldwork in June 2009 was the result of a complex and variable combination of groundwater upwelling and accumulation of rainfall on the saturated surface.

The impact of the dry period lowered the watertable indicating a decrease in aquifer storage. The dry stress periods with low or no recharge (Table 9.3) experienced a low storage input, acted by volume of water released from storage coupled with high active plant evapotranspiration which could not raise the watertable (Figure 9.5). Ransom and Smeck (1986) concluded that the depth to water table was a function of both precipitation and evapotranspiration for seasonally wet soils in southwestern Ohio. For example, the watertable dropped in the Ohio soils during the active growing season because of evapotranspiration, even though this period was normally one of high precipitation. A rise in watertable during late fall and winter were attributed to moderate precipitation and minimal evapotranspiration. Short and long-term precipitation patterns need to be considered for projects that require an assessment of developing wetlands for crop production. Total annual or even seasonal precipitation may not determine the overall watertable fluctuations of a wetland. However, intense but infrequent precipitation events may result in a short-term, elevation in the watertable, but only sustained precipitation during the summer months will maintain elevated watertables (Winter and Rosenberry, 1995).

Data on crop water requirement of dry season cultivated crops and vegetables can be applied to the field to elevate the watertable to an appreciable level otherwise excess water applied or high rainfall variability accounting in the area can cause the watertable to rise above the root zones of the plant due to the high storage capacity of the field depicted from the model (Table 9.3). The values for storage were substantial indicating the temporal variability in the watertable with continuous movement of water to and from storage over an annual cycle (Bradley, 2002). Also the accumulated recharge causes an increase in storage of the subsurface groundwater which can be pumped out from the wetland substrate to sustain dry season cultivation. The monthly

recharge generated suggests a significant contribution of water from the Besease Wetlands into the river. Also there is a form of interaction between the inland valley wetland and the Oda River and this condition vary from period to period depending on the river stage. Over the two year period, influent recharge (ie seepage into the wetlands) was extremely small. In the month of August, 54.42 mm of water leaked into the wetland from the river as against 53.95 mm seeping into the river from the wetland. Seepage from the wetland to the river shows one of the main losses in the volumetric water budget of the valley. However, difference between leakage into and out of the wetland were much reduced as water levels in both the river and the wetland were much high and this was evident in the month of September 2009.

The interaction between the wetland and the river is bi-directional with most of the flow coming out from the wetland which affirms the fact that floodplain wetland serves as moisture buffer and supplies the river with water during flow conditions. A total of 297.91 mm leaked out of the wetland system from November to December 2010 to contribute to the sustenance of the Oda River. In this situation, floodplain wetland contributes as base flow to the Oda River in the dry season.

Table 9.3 Volumetric Water Budget

Stress period 1 (JAN-09)			
FLOW TERM	IN(m³)	OUT(m³)	IN-OUT(m³)
STORAGE	3149.261	0	3149.261
RIVER LEAKAGE	0	3153.419	-3153.419
RECHARGE	0	0	0
SUM	3149.264	3153.419	-4.155
% DISCREPANCY -0.13			
Stress period 2 (FEB-09)			
FLOW TERM	IN(m³)	OUT(m³)	IN-OUT(m³)
STORAGE	3593.3115	24.8589	3568.4526
RIVER LEAKAGE	0.2415	3616.4258	-3616.1843
RECHARGE	45.1305	0	45.1305
SUM	3638.6836	3641.2647	-2.6012
% DISCREPANCY -0.07			

Stress period 3 (MAR-09)			
FLOW TERM	IN(m³)	OUT(m³)	IN-OUT(m³)
STORAGE	3593.3115	314.1565	3279.155
RIVER LEAKAGE	37.8394	3903.9133	-3866.0739
RECHARGE	586.592	0	586.592
SUM	4217.7432	4218.0698	-0.3269
% DISCREPANCY -0.01			

Stress period 4 (APR-09)			
FLOW TERM	IN(m³)	OUT(m³)	IN-OUT(m³)
STORAGE	3593.3115	753.4045	2839.907
RIVER LEAKAGE	202.3504	3987.2871	-3784.9367
RECHARGE	950.4021	0	950.4021
SUM	4746.064	4218.0698	5.3724
% DISCREPANCY 0.11			

Stress period 5 (MAY-09)			
FLOW TERM	IN(m³)	OUT(m³)	IN-OUT(m³)
STORAGE	3919.4312	753.4045	3166.0267
RIVER LEAKAGE	202.3545	4346.7124	-4144.3579
RECHARGE	984.9099	0	984.9099
SUM	5106.6956	5100.1169	6.5787
% DISCREPANCY	0.13		

Stress period 6 (JUN-09)			
FLOW TERM	IN(m³)	OUT(m³)	IN-OUT(m³)
STORAGE	3919.4312	4762.8189	-843.3877
RIVER LEAKAGE	3354.9138	4694.2773	-1339.3635
RECHARGE	2196.9754	0	2196.9754
SUM	9471.3204	9457.0962	14.2242
% DISCREPANCY	0.16		

Stress period 7 (JUL-09)			
FLOW TERM	IN(m³)	OUT(m³)	IN-OUT(m³)
STORAGE	4083.5142	4635.0249	-551.5107
RIVER LEAKAGE	3354.9138	4877.4761	-1522.5623
RECHARGE	2085.3894	0	2085.3894
SUM	9523.8174	9512.501	11.3164
% DISCREPANCY	0.12		

Stress period 8 (AUG-09)			
FLOW TERM	IN(m³)	OUT(m³)	IN-OUT(m³)
STORAGE	5125.7914	5154.1851	-28.3937
RIVER LEAKAGE	4920.043	4877.4761	42.5669
RECHARGE	0	0	0
SUM	10045.8344	10031.6612	14.1732
% DISCREPANCY	0.15		

Stress period 9 (SEP-09)			
FLOW TERM	IN(m³)	OUT(m³)	IN-OUT(m³)
STORAGE	4083.522	6165.915	-2082.393
RIVER LEAKAGE	4646.0684	4877.4761	-231.4077
RECHARGE	2337.0691	0	2337.0691
SUM	11066.6595	11043.3911	23.2684
% DISCREPANCY	0.21		

Stress period 10 (OCT-09)			
FLOW TERM	IN(m³)	OUT(m³)	IN-OUT(m³)
STORAGE	4777.4678	6168.1377	-1390.6699
RIVER LEAKAGE	4646.312	6070.5991	-1424.2871
RECHARGE	2836.448	0	2836.448
SUM	12260.2278	12238.7368	21.491
% DISCREPANCY	0.18		

Stress period 11 (NOV-09)			
FLOW TERM	IN(m³)	OUT(m³)	IN-OUT(m³)
STORAGE	6202.9795	6168.1377	34.8418
RIVER LEAKAGE	7182.76	7193.2388	-10.4788
RECHARGE	0	0	0
SUM	13385.7395	13361.3765	24.363
% DISCREPANCY	0.18		

Stress period 12 (DEC-09)			
FLOW TERM	IN(m³)	OUT(m³)	IN-OUT(m³)
STORAGE	7948.7282	6168.1377	1780.5905
RIVER LEAKAGE	6773.648	8533.458	-1759.81
RECHARGE	0	0	0
SUM	14722.3762	14701.5957	20.7805
% DISCREPANCY	0.14		

Stress period 13 (JAN-10)			
FLOW TERM	IN(m³)	OUT(m³)	IN-OUT(m³)
STORAGE	10240.6693	6168.1377	4072.5316
RIVER LEAKAGE	6064.5794	10116.3428	-4051.7634
RECHARGE	0	0	0
SUM	16305.2487	16284.4805	20.7682
% DISCREPANCY	0.13		

Stress period 14 (FEB-10)			
FLOW TERM	IN(m³)	OUT(m³)	IN-OUT(m³)
STORAGE	10661.4564	6168.1377	4493.3187
RIVER LEAKAGE	6066.5659	10537.3047	-4470.7388
RECHARGE	0	0	0
SUM	16728.0223	16705.4424	22.5799
% DISCREPANCY	0.14		

Stress period 15 (MAR-10)			
FLOW TERM	IN(m³)	OUT(m³)	IN-OUT(m³)
STORAGE	9667.3652	6168.1377	3499.2275
RIVER LEAKAGE	4649.0425	11181.3496	-6532.3071
RECHARGE	3056.9597	0	3056.9597
SUM	17373.3674	17349.4873	23.8801
% DISCREPANCY	0.14		

Stress period 16 (APR-10)			
FLOW TERM	IN(m³)	OUT(m³)	IN-OUT(m³)
STORAGE	9668.4053	6465.6831	3202.7222
RIVER LEAKAGE	4860.6294	11181.7422	-6321.1128
RECHARGE	3148.4558	0	3148.4558
SUM	17677.4905	17647.4253	30.0652
% DISCREPANCY	0.17		

Stress period 17 (MAY-10)			
FLOW TERM	IN(m³)	OUT(m³)	IN-OUT(m³)
STORAGE	9668.4053	7121.2085	2547.1968
RIVER LEAKAGE	5082.9697	11285.2783	-6202.3086
RECHARGE	3682.6283	0	3682.6283
SUM	18434.0033	18406.4868	27.5165
% DISCREPANCY	0.15		

Stress period 18 (JUN-10)			
FLOW TERM	IN(m³)	OUT(m³)	IN-OUT(m³)
STORAGE	9668.4053	8568.0889	1100.3164
RIVER LEAKAGE	5971.1445	11286.7949	-5315.6504
RECHARGE	4250.3984	0	4250.3984
SUM	19889.9482	19854.8838	35.0644
% DISCREPANCY	0.18		

Stress period 19 (JUL-10)			
FLOW TERM	IN(m³)	OUT(m³)	IN-OUT(m³)
STORAGE	9668.4053	9946.5264	-278.1211
RIVER LEAKAGE	6965.4956	11300.1631	-4334.6675
RECHARGE	4646.5679	0	4646.5679
SUM	21280.4688	21246.6895	33.7793
% DISCREPANCY	0.16		

Stress period 20 (AUG-10)			
FLOW TERM	IN(m³)	OUT(m³)	IN-OUT(m³)
STORAGE	9808.4795	9968.3418	-159.8623
RIVER LEAKAGE	6965.6323	11778.6035	-4812.9712
RECHARGE	5008.478	0	5008.478
SUM	21782.5898	21746.9453	35.6445
% DISCREPANCY	0.16		

Stress period 21 (SEP-10)			
FLOW TERM	IN(m³)	OUT(m³)	IN-OUT(m³)
STORAGE	9808.5332	10316.5371	-508.0039
RIVER LEAKAGE	7241.1699	11778.6035	-4537.4336
RECHARGE	5088.5718	0	5088.5718
SUM	22138.2749	22095.1406	43.1343
% DISCREPANCY	0.2		

Stress period 22 (OCT-10)			
FLOW TERM	IN(m³)	OUT(m³)	IN-OUT(m³)
STORAGE	9821.4668	10436.3867	-614.9199
RIVER LEAKAGE	7243.0928	12102.9404	-4859.8476
RECHARGE	5520.6187	0	5520.6187
SUM	22585.1783	22539.3271	45.8512
% DISCREPANCY	0.2		

Stress period 23 (NOV-10)			
FLOW TERM	IN(m³)	OUT(m³)	IN-OUT(m³)
STORAGE	10338.5234	10436.3867	-97.8633
RIVER LEAKAGE	7244.8076	12657.5723	-5412.7647
RECHARGE	5569.7593	0	5569.7593
SUM	23153.0903	23093.959	59.1313
% DISCREPANCY	0.26		

Stress period 24 (DEC-10)			
FLOW TERM	IN(m³)	OUT(m³)	IN-OUT(m³)
STORAGE	13343.4281	10436.3867	2907.0414
RIVER LEAKAGE	11422.1271	14274.0195	-2851.8924
RECHARGE	0	0	0
SUM	24765.5552	24710.4062	55.149
% DISCREPANCY	0.22		

Table 9.4 Cumulative Water Budget for Different Components in the Model Area

Time	Flow Term	Inflow (m ³)	%	Outflow (m ³)	%
1st Year	Storage	52760.98	42.84	49538.39	40.23
	River Leakage	39089.26	31.74	73589.83	59.77
	Recharge	31295.92	25.42	0	0
	Total	123146.15	100	123128.22	100
2nd Year	Storage	50020.39	40.6	48257.54	39.17
	River Leakage	41819.72	33.95	74954.78	60.83
	Recharge	31355.43	25.45	0	0
	Total	123195.55	100	123212.32	100
1st & 2nd Year	Total	246341.7	100	246340.50	100

9.13 Uncertainty and Sensitivity Analysis

Uncertainty in hydrogeologic models can be deduced from the fact that they are not the true reflection of the processes involved, because the condition and data for running the models are not error free. These errors may stem from measurement, scale and calculation errors that are incorporated with the model input. Sensitivity analysis is a measure of uncertainty in the calibrated model caused by uncertainty in the aquifer parameters (e.g. hydraulic conductivity and recharge) and boundary conditions. Geological uncertainty relates to the degree to which the stratigraphy assumed in the model represents the geology of the area. The specific objective of a sensitivity analysis is to understand the influence of various model parameters and hydrological stresses on the aquifer system and to identify the most sensible parameter(s), which will need a special attention in future. Parameter and boundary

condition uncertainty describe the uncertainty in the model from imposed parameters and by characterization of the hydrogeologic conditions along the boundary of the model. During this analysis the calibrated value for the aquifer parameters and the boundary conditions are systematically changed with plausible range (Anderson and Woessner, 1992). In the analysis the magnitude of change in estimated heads from the calibrated solutions was used as a measure of the sensitivity of the model to that specific parameter.

To determine the calibrated solution's sensitivity to the aquifer properties hydraulic conductivity, specific yield were varied in turn by multiplier factors of 0.4, 0.6, 0.8, 1.2 and 1.4 for the two layers. Specific storage was varied by an order of magnitude each way from the calibrated value in order to see a significant alteration. Only one parameter was varied at a time in order to quantify the effect of the changes of the solution and any effect were evaluated by the same statistical methods used to evaluate the model calibration such as the RMSE. The model is highly sensitive to increase in hydraulic conductivity and insensitive to decrease in hydraulic conductivity which produced a lower RMS error (Figure 9.7).

Also for specific yield the multipliers of 1.2 and 1.3 produced a RMS error greater than the calibrated value (Figure 9.8) while for other variables specific yield decreases as RMS error decreases which showed that the model is insensitive to decrease in specific yield. For specific storage the variables 0.0005 and 0.00001 for layers 1 and 2 respectively plots slightly below the value of 0.005 and 0.0001 for the calibrated model while the other variables 0.05 and 0.001 for layers 1 and 2 produced a much higher RMS error.

The sensitivity of the calibrated model to variations in hydraulic conductivity and specific yield which were increased and decreased by a multiplying factor show that these aquifer variables were within realistic bounds for sandy loam and silty sands at Besease Wetlands. The specific yield and specific storage which exhibited lower RMS errors than their calibrated values indicate that the aquifer material has a specific yield values of 0.024 and 0.006 and specific storage values 0.0005 and 0.00001 for layers 1 and 2 than the calibrated values. The lower specific yield values which produced a RMSE lower than the calibrated values of 0.06 and 0.015 for the two layers may suggest that the aquifer material is less sandy.

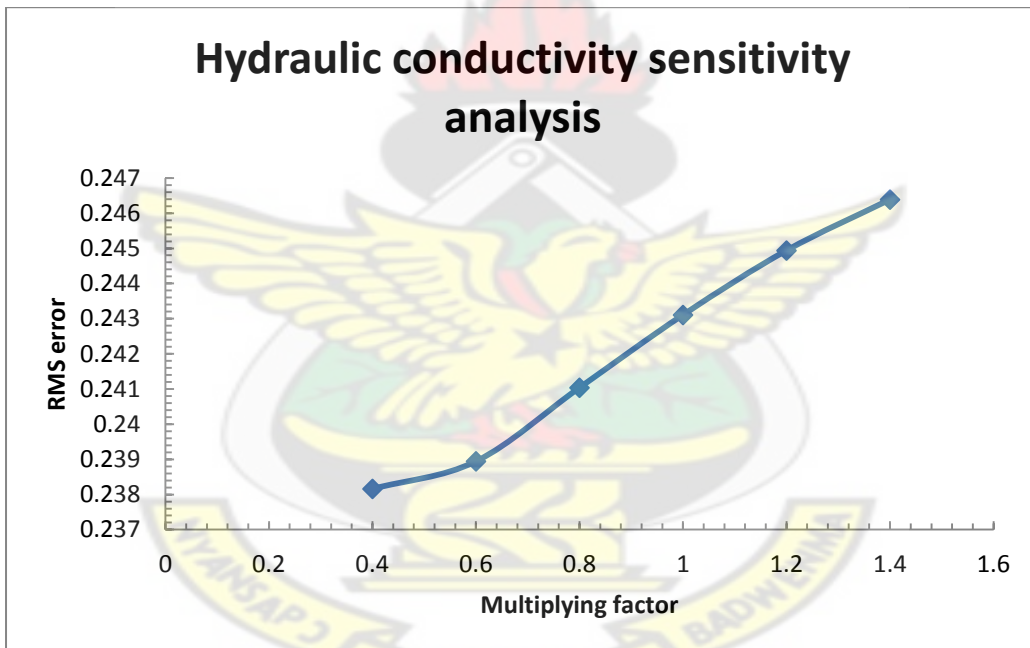


Figure 9.7 Graph of Sensitivity Analysis for Hydraulic Conductivity

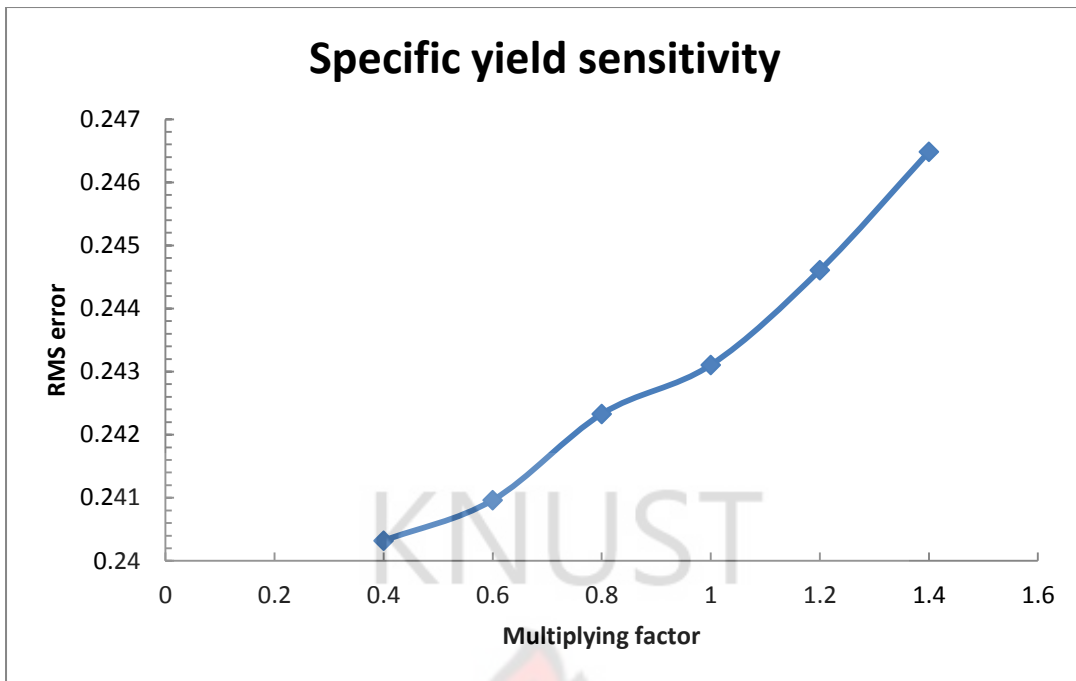


Figure 9.8 Graph of Sensitivity Analysis for Specific Yield

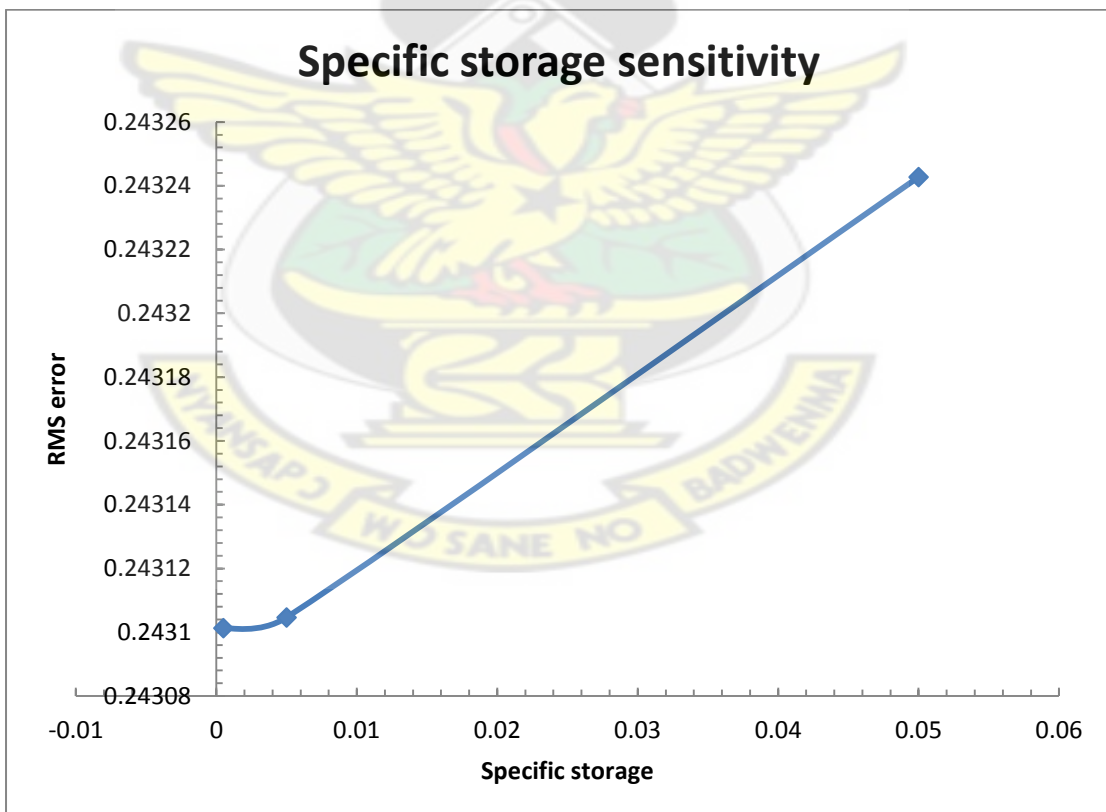
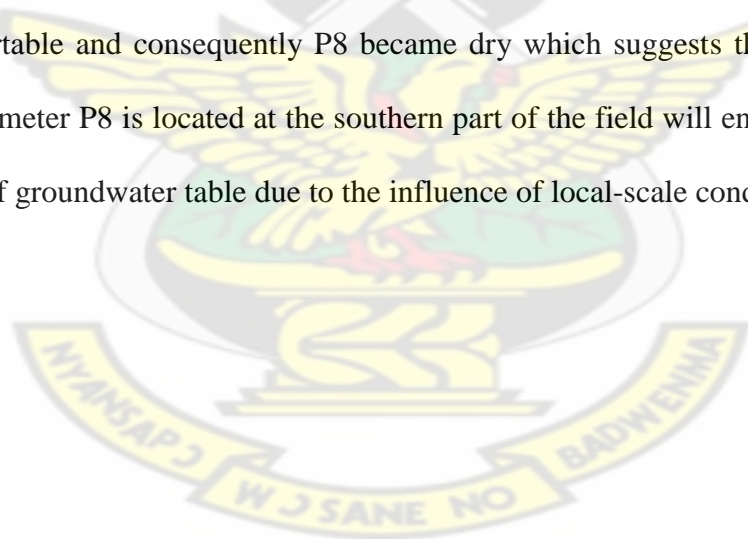


Figure 9.9 Graph of Sensitivity Analysis for Specific Storage

9.14 Groundwater Flow Prediction

A groundwater flow model may be used to predict future flow conditions, such simulation estimates the hydraulic response of an aquifer, and also it can forecast the pumping rate required to monitor the hydraulic heads. Pumping strategy is a set of spatially and possibly temporary distributed rate of extracting water from the aquifer (Parelda, 2004), Hydraulic heads for 2012 were predicted and in the transient simulation there were two stress periods, one for dry period of 240 days when pumping is occurring and no recharge and the other for the wet period of 120 days when there is recharge only. Four (4) wells were distributed to the model domain (Fig 9.10). Water is extracted from the wells at a discharge rate of 100 m³/day. Figs 9.10 and 9.11 show the calculated head distribution after two (2) years with pumping wells and without pumping wells respectively. The predictive scenario shows a decline in the watertable and consequently P8 became dry which suggests that the area where the piezometer P8 is located at the southern part of the field will encounter a seasonal decline of groundwater table due to the influence of local-scale conditions.



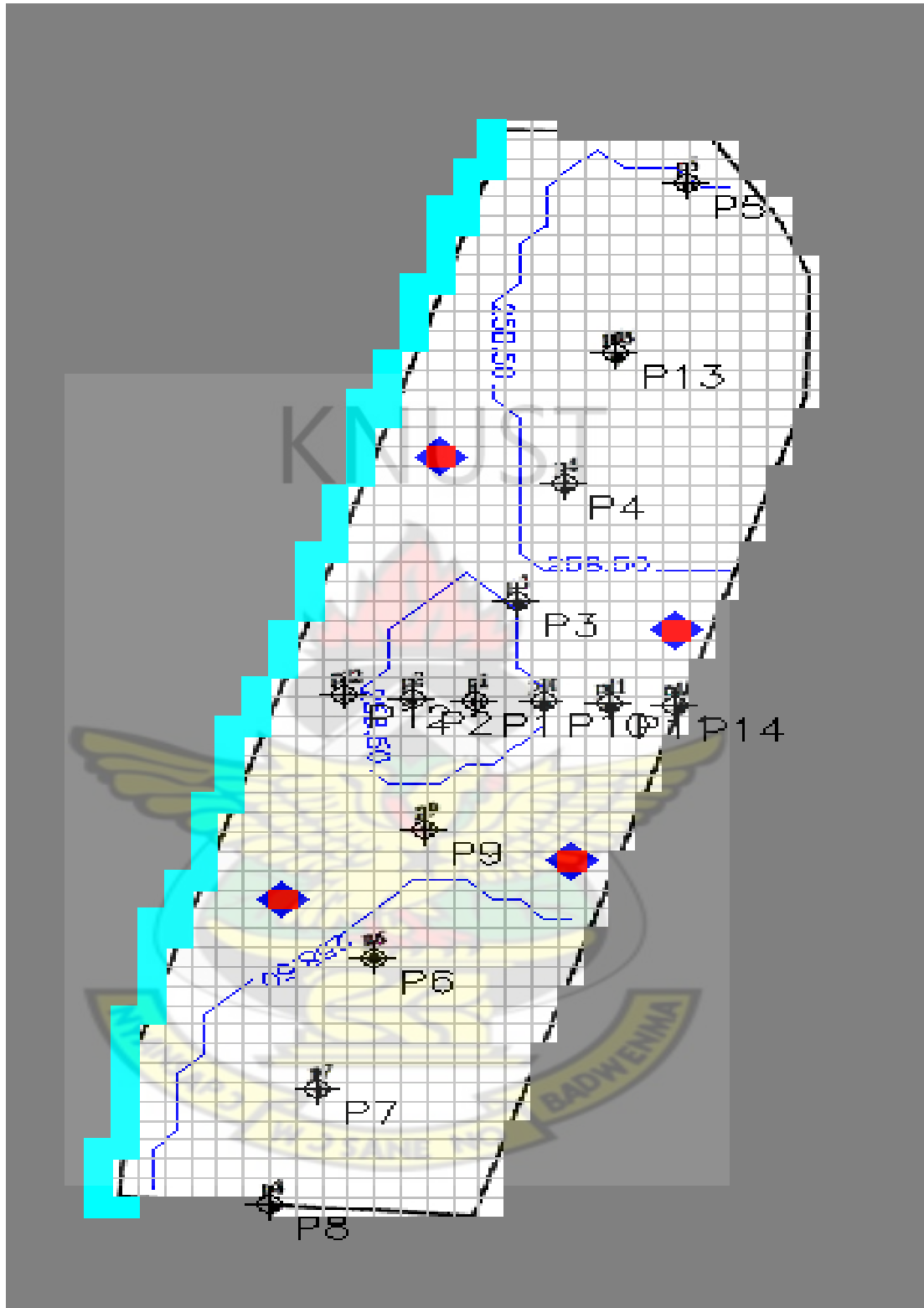


Fig 9.10 Calculated Heads (m) for the Dry Period

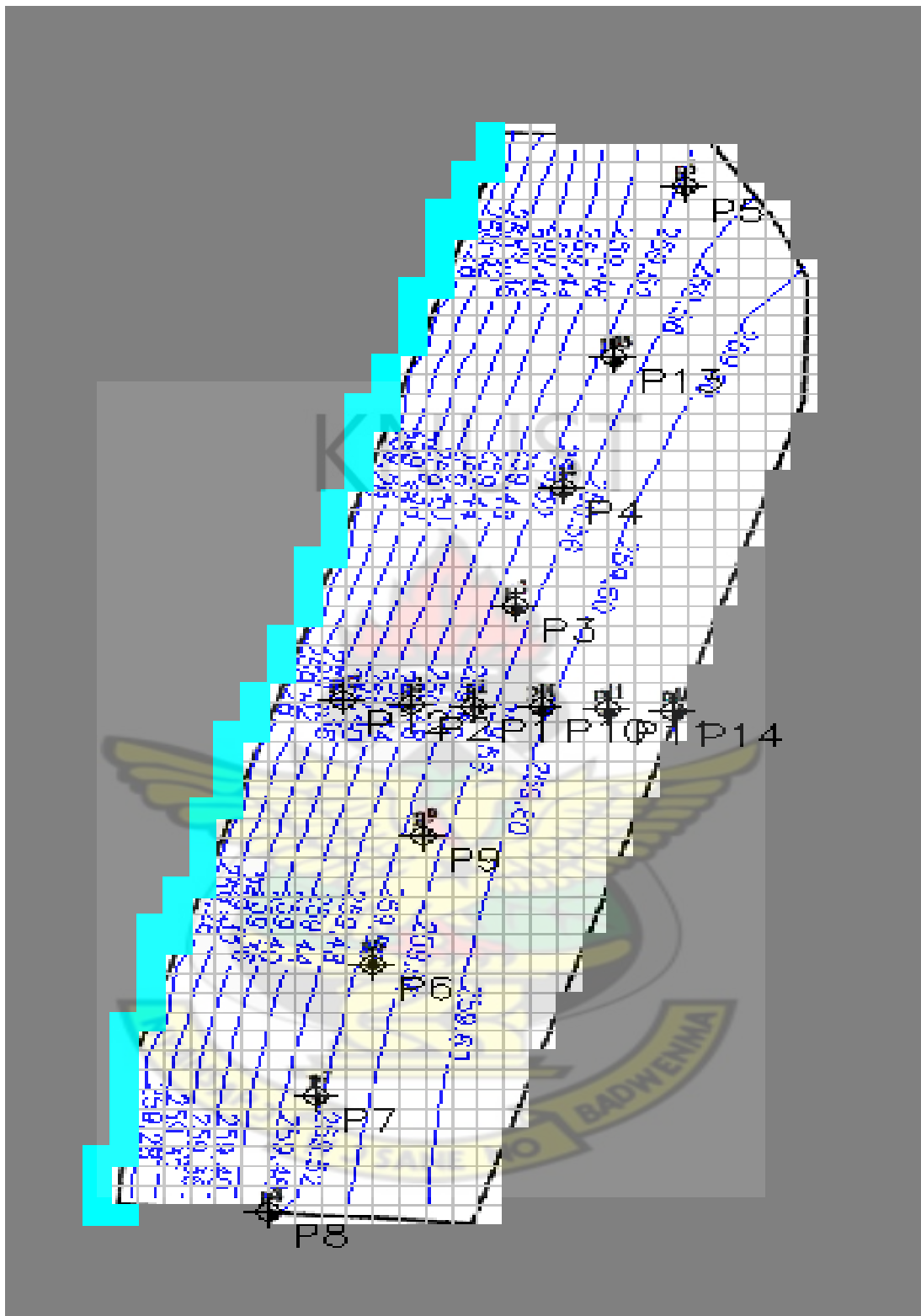


Figure 9.11 Calculated Heads (m) for the Wet Period

9.15 Conclusions

An initial conceptual hydrogeological model of the Oda river basin in Besease with unconfined, semi-confined, two-layered aquifer was developed with differing hydraulic characteristics. The calibrated MODFLOW model was more acceptable with an average root mean square error (RMSE) of 0.099 m and 0.134 m, MAE of 0.067 m and 0.084 m and an average ME of 0.016 m and -0.006 m for P1 and P14 respectively. The Water Table Fluctuation method used as an estimate of groundwater recharge gave a better fit between the simulated hydraulic head and observed subsurface water level fluctuation. For this inland valley bottom, the relationship between the valley bottom and the Oda River showed that the river level represents a base level to which the valley bottom watertable adjusts. From the water budget produced by the model it was noticed that in the month of June 2010 a total amount of 9668.405 m³ moves into storage to saturate the wetland. It was found out from the results that a decline in simulated hydraulic height showed a decrease in storage in the monthly dry stress periods is a critical predictive criterion because it defines the effective rooting depth (ignoring the extent of the capillary fringe), the soil water storage depth and drainage requirements, re-establishes the dry season agricultural unsaturated zone and a distinguishing characteristic for classifying the inland valley bottoms into soil and water management regimes.

CHAPTER TEN

GENERAL CONCLUSIONS AND RECOMMENDATIONS

10.1 Introduction

The potential of water in wetlands for irrigation is a prerequisite for the development of wetlands for crop production. The irrigation potential of wetlands was assessed by analysing the hydrodynamics of the valley bottom through a groundwater flow modelling process using MODFLOW and Kalman Filter.

10.2 Conclusions

The saturated hydraulic conductivity was high at the soil profile pit P1-P2 which was at a higher elevation. However, a lower saturated hydraulic conductivity which was experienced at profile pit P11-P14 at a lower elevation with characteristic fine textured soils indicated a small water intake. Also possible elongation of water level ponding at P7-P8 and P11-P14 with low infiltration rates of 0.06 cm/min and 0.02 cm/min showed an increase in water storage that is ideal for rice production. The higher EC observed at P11-P14 may be due to possible groundwater discharge and evaporation associated with the area. The SAR observed from the four sampling points showed the valley system suitability for crop production. Analysis of the groundwater chemistry revealed that alkaline earths (Ca^{2+}) exceeded alkalis (Na^+) and weak acids (HCO_3^-) exceeded strong acids (SO_4^{2-}) in groundwater which presented a CaHCO_3 groundwater type which showed that groundwater is of limestone aquifer. Results from the three months successive periods of the Watertable Fluctuation Method show that the May-July period in 2009 experienced a minimal recharge (7.8%) because water levels were already near or at ground surface as a result of high

rainfall in the period. The slopes of the watertable fluctuations for each month were used to distinguish the inland valley bottom into hydrological classes namely:

- WTF Class I for Acute slope segments varying from 0–30%
- WTF Class II for acute slope segments varying from 30–45% and
- WT Class III > 45 %.

Analysis carried using the Kalman Filter model showed that the assumption that, the time variant parameters of the rainfall parameters with different weightages is more appropriate and realistic than the time invariant assumptions and the time variant parameters with equal weightage gives a considerable variation in the parameter values.

The dynamics of the surface and subsurface water inflows and outflows of the wetland setting influences the spatial and temporal patterns of the watertable configuration. Therefore, understanding these hydrological changes is paramount for effective management of the integrated water resources in the Ejisu-Besease Oda River Basin of Ghana. Spatial data at the site hampered the development of a fully calibrated model. The simulated groundwater heights which showed a fluctuation of one (1) m at the end of the simulated stress periods indicated that an appropriate irrigation method could be adopted to raise the watertable to saturation to ensure a year round rice production or the watertable could be raised to an optimum height to sustain vegetable production in the dry season.

10.3 Suggestions for Practicalising Research Results

1. Owing to the high storage capacity of the wetlands, groundwater can be pumped out of the wetland substrate to sustain dry season dry season cultivation.
2. A well could be dug at P 14 to irrigate the field and because of the characteristic low topographic height of site P 14, there would be possible irrigation return flow to this point as drainage water which must be treated before reuse.
3. IVBs that exhibit the characteristics of WTF Class I could be used for year round rice cultivation.
4. Also sites that exhibit characteristics of WTF Class II and WTF Class III could be developed for both wet and dry season crop production with controlled irrigation and soil and water conservation methods

10.4 Recommendations

A number of recommendations are put forward for further studies based on the research done.

The accuracy of groundwater recharge estimation is very important when assessing the safe yield of an aquifer. The accuracy of the groundwater recharge estimation could be improved through further research.

There is the need to incorporate GIS, satellite imagery and remote sensing into the groundwater flow modelling to improve upon the modelling process in further studies.

Further studies should also be carried out to perform irrigation experiments on various irrigation methods for efficient water use such as controlled groundwater irrigation for rice cultivation with no ponding.

The model developed in this study should be used as a framework for further future modelling efforts of the basin studied.

The prediction scenarios are under the constraint of lack of long-term data. It is therefore recommended that a large number of data sets should be collected at various time and areal scales from the Besease Wetlands. This could be done for wetlands in other agro-ecological zones in Sub-Saharan Africa.



REFERENCES

- Adamowski, K., Dalezios, R.S. and Gingras, D. 1986. A comparison of parameter estimation procedures in groundwater level modelling. Conjective Water Use (Proceedings of the Budapest Symposium). IAHS Publ. no. 156.
- Agyare, W.A. 2004. Soil characterization and modeling of spatial distribution of saturated hydraulic conductivity at two sites in the Volta Basin of Ghana. PhD.Thesis. Ecology and Development Series No. 17.
- Allen, R. G., Pereira, L. S., Raes, D. and Smith, M. M. 2006. Crop Evapotranspiration, guidelines for computing crop water requirements. FAO Irrigation and Drainage paper No. 56, 307 P.
- Allison, G.B. 1988. A review of some of the physical, chemical and isotopic techniques available for estimating ground water recharge. In: Simmers, I. (Ed.), Estimation of Natural Ground Water Recharge. Reidel, Dordrecht, pp. 49–72.
- Amer, S.A. 1983. The study and improvement of soil productivity under plastic tunnels and open field conditions. Technical Report No. AG:NECP/BAH/501/KUW., FAO, Rome.
- Anderson, M.P. and Woessner, W. W. 1992. Applied groundwater modeling: simulation of flow and advective transport. 381. pp. Academic press, San Diego, CA.
- Anderson. T. 1997. Part iii: Southern Perspectives Chapter 6: Wetlands Management in Ghana. Document(s) 8 of 16. Cited 15 November 2007 from [http:// www.idrc.ca](http://www.idrc.ca).

- Andriessse, W., Windmeijer, P.N. and Van Duivenbooden, N. 1993. Agro-ecological characterization of inland valleys in West Africa. Pages 133-145 in: *Proceedings first Annual Workshop of Inland Valley Consortium*. WARDA, Bouake, Côte d'Ivoire, 8-10 October 1993. Productivity declines in irrigated rice systems of tropical Asia.
- Andriessse, W. 1986. Wetlands in sub-Saharan Africa: area and distribution. In: *The Wetlands and Rice in Sub-Saharan Africa*. International Institute of Tropical Agriculture (IITA), Ibadan, Nigeria, pp. 15–30.
- Annan-Afful, E., Masunaga, T. and Wakatsuki, T. 2005. Soil Properties Along the Toposequence of an Inland Valley Watershed under Different Land Uses in the Ashanti Region of Ghana', *Journal of Plant Nutrition*, 28: 1, 141 — 150
- APHA. 1995. Standard methods for the examination of water and wastewater, 19th edn. American Public Health Association, Washington, D.C., 1467 pp
- Armstrong, A. 2000. DITCH: a model to simulate field conditions in response to ditch levels managed for environmental aims. *Agriculture, Ecosystems and Environment* 77: 179-192.
- Armstrong, A. and Rose, S. 1999. Ditch water levels managed for environmental aims: effects on field soil water regimes. *Hydrology and Earth System Sciences* 3(3): 385-394.
- Armstrong, A. and Rose, S. 1998. Managing water for wetland ecosystems: a case study. In 'European wet grasslands: biodiversity, management and restoration', Joyce, C.B., Wade, P.M. (eds.), p201-216, John Wiley & Sons, Chicester.

Asim, M. 2005. Hydrochemical Characterization and Numerical Modeling of Groundwater Flow in a part of the Himalayan Foreland Basin PhD. Thesis unpublished. Kent State University. 243pp

Ayers, R. S. and Westcot, D. W. (1994). Water quality for agriculture, FAO Irrigation and Drainage Paper; 29 Rev.1.

Bates, P. D., Stewart, M. D., Desitter, A., Anderson, M. G., Renaud, J. P., and Smith, J., 2000. Numerical simulation of floodplain hydrology. *Water Resources Research*, 36(9) 2517-2529.

Beekman, H.E. and Xu, Y. 2003. Review of ground water recharge estimation in arid and semiarid Southern Africa. Council for Scientific and Industrial Research (South Africa) and University of the Western Cape Report. Johnson, A.I., U.S Geological Survey Water-supply paper 1662-D, 1967, 74 p.

Bendjoudi, H., Weng, P., Guérin, R. and Pastre, J.F. 2002. Riparian wetlands of the middle reach of the Seine river (France): historical development, investigation and present hydrologic functioning. A case study. *Journal of Hydrology* 263: 131-155.

Bonell, M., and Balek, J. 1993. Recent Scientific Development and Research Needs in Hydrological Processes of Humid tropics: 167-260. In: Bonell M, Hufschmidt MM, Gladwell JS (eds) *Hydrology and water management in the humid Tropics: Hydrological research issues and strategies for water management*. Cambridge University Press, Great Britain.

Bradford, R. B., and Acreman, M. C. 2003. Applying MODFLOW to wet grassland in-fieldhabitats: a case study from the Pevensey Levels, UK. *Hydro Earth Syst Sc* 7 (1): 43–55.

- Bradley, C. 1996. Transient modelling of water-table variation in a floodplain wetland, Narborough Bog, Leicestershire. *Journal of Hydrology* 185: 87-114.
- Bradley, C. 2002. Simulation of the annual water table dynamics of a floodplain wetland, Narborough Bog, UK. *Journal of Hydrology* 261: 150-172.
- Bradley, C. and Gilvear, D.J. 2000. Saturated and unsaturated flow dynamics in a floodplain wetland. *Hydrological Processes* (14):2945-2958.
- Brown, T.N., Johnston, C.A. and Cahow, K.R. 2003. Lateral flow routing into a wetland: field and model perspectives *Geomorphology* 53:11– 23.
- Burt, T.P. and Haycock, N.E. 1996. Linking floodplains to rivers. In: Anderson, M.G., Walling, D.E., Bates, P. (Eds.), *Floodplain Processes*, Wiley, New York, pp. 461–492.
- Burt, T. P., Bates, P. D., Stewart, M. D., Claxton, A. J., Anderson, M.G. and Price, D. A. 2002. Water table fluctuations within the floodplain of the River Severn, England. *Journal of Hydrology* **262**, 1-20.
- Burrow, M. K. A. 1990. Wetland Development and Management. Proceedings on Workshop on Technical cooperation Network in Wetland Development and management in Banjul and sponsored by FAO/Gambia Government.
- Caro, R. and Eagleson, P.S. 1981. Estimating aquifer recharge due to rainfall. *J. Hydrol.*, 53: 185-211.
- Casanova, M., Messing, M. and A. Joel. 2000. Influence of slope gradient on hydraulic conductivity measured by tension infiltrometer. *Hydrological processes* 14: 155-164.

- Cassman, K.S., Olk, D., Ladha, Re.chardt, J., Doberman, W. A. and Singh, U. 1998. Opportunities for increased nitrogen-use efficiency for improved resource management in irrigated rice systems. *Field Crops Research* 56: 7-19
- Chiang, W.H. and Kinzelbach, W. 2001. *Processing MODFLOW for Windows: A Simulation System for Modelling Groundwater Flow and Pollution.*
- Dar. M,A., Sankar. K. and Dar. I.A. 2011. Major ion chemistry and hydrochemical studies of groundwater of parts of Palar river basin, Tamil Nadu, India. *Environ Monit Assess.* 176: 621–636
- Delin G. N., Healy, R.W., Lorenz, D. L. and Nimmo, J. R. 2007. Comparison of local-to regional scale estimates of ground-water recharge in Minnesota, USA. *Journal of Hydrology*, Volume 334, Issues 1-2, pp. 231-249.
- Dutt, G. R., Pennington, D. A. and Turner. Jr. F. 1984. Irrigation as a solution to salinity problems of river basins. In: *Salinity in Watercourses and Reservoirs*, R.H. French (ed) Ann Arbor Science, pp. 465–472.
- Eigbe, U., Beck, M. B., Wheeler, H.S. and Hirano. F. 1998. Kalman filtering in groundwater flow modelling: problems and prospects. *Stoch Hydrol Hydraul.*12:15–32.
- FAO. 1995. *Irrigation in Africa in figures / L'irrigation en Afrique en chiffres.* FAO Water Report 7. Rome. 336 p.
- Foster, S. S. D. 1988. Quantification of ground water recharge in arid regions: a practical view for resource development and management. In: Simmers, I. (Ed.), *Estimation of Natural Ground Water Recharge.* Reidel, Dordrecht, pp. 323–338.

Fox, D. M., Le Bissonnais, Y. and Bruand, A. 1998. The effect of ponding depth on infiltration in crusted surface depression. *Catena* 32:87-100

Fresco, L.O. 1994. Imaginable Futures: A contribution into thinking about Landuse Planning In the future of the land. Fresco. L. Stroosnjider, L. Bouma, J., Van Keulen, H (eds) John Wiley and Sons Ltd.

Geiger, P. J. and J. P. Hardy. 1971. Total carbon by dry combustion. In *Methods of soil analysis*, Part 2, No. 9, eds. A. L. Page, R. H. Miller, and D. R. Keeney, 543–553. Madison, Wisconsin: ASA/SSSA.

German, P. and Beven. K. 1981. Water flow in soil macropores. I. An experimental approach, *J. Soil Sci.* 32:1-13.

Gilman, I. C. 1994. Hydrology and Wetland Conservation. Wiley, Chichester, 101 pp.

Gilvear, D. J., Andrews, R. J., Tellam. H., Lloyd, J.W. and lerner. D.N. 1993. Quantification of the water balance and hydrogeological processes in the vicinity of a small groundwater-fed wetland, East Anglia, UK. *J.Hydrol.*, 144: 311-334.

Gomes, F., Marques, M.R., Mafalacusser, J. and Brito, R. 1998. Wetlands for Agricultural Development, Mozambique Country Report. Expert Consultation on Wetlands Classification for Agricultural Development in Eastern and Southern Africa, 03-06/12/1997. Harare, Zimbabwe.

Goswami, M.N., Prasad , R., Sarkar, M.C. and Singh, S. 1986. Studies on the effect of green manuring in N economy in a rice wheat rotation using N-15 techniques. *Journal of Agricultural Sciences.* 111:413-417

Gupta, B. L. and Gupta, A. 1999. Engineering hydrology. Standard publishers distributors. Delhi. 380pp.

Hall, D.W. and Risser, D. W. 1993. Effects of agricultural nutrient management on nitrogen fate and transport in Lancaster county, Pennsylvania. *Water Resour Bull* 29:55–76.

Harbaugh, A. W. 2005. MODFLOW 2005. The U.S. Geological Survey Modular Ground-Water Model the Groundwater Flow Process, Techniques and methods 6-A16. U.S. Geological Survey, 206 P.

Hayashi, M. and Rosenberry, D.O. 2002. Effects of ground water exchange on the hydrology and ecology of surface water. *Ground Water* 40:309–316.

Healy, R.W. and Cook, P, G. 2002. Using groundwater levels to estimate recharge. *Hydrogeol J* 10(1):91–109

Hekstra, P, and A. Andriessse. 1983. Wetland Utilization Research Project. West Africa. Phase 1. The Inventory. Vol. 11. The Physical Aspects. International Institute of Land Reclamation and Development (ILRI) and Soil Survey Institute (STIBOKA), Wageningen, The Netherlands, 78 pp.

Hendrickx, J.M.H. and Walker, G.R., 1997. Recharge from precipitation. In: Simmers I (ed) Recharge of phreatic aquifers in (semi-)arid areas. IAH Int Contrib Hydrogeol 19. AA Balkema, Rotterdam, pp 19–111.

Henry, J.L and T.J. Hogg. 2002. Evaluation of the effects of Irrigation on Soil Chemical Properties. Canada-Saskatchewan Irrigation Diversification Centre. Agriculture and Agri food, Canada.

- Hillel, D. 1998. Environmental Soil Physics. Academic Press, San Diego, CA.
- Howeler, R. H. 1973. Iron-induced orange disease of rice in relation to changes in physicochemical changes in a flooded Oxisol. Soil Science Society of America Proceedings, 898 – 903.
- IFPRI. 1995. Water resources development in Africa: a review and synthesis of issues, potentials and strategies for the future. Report prepared for FAO by Rosegrant, M., Perez, W. and Nicostrato, D. International Food Policy Research Institute, Washington. 111 p
- IITA. 1982. Automated and semi-automated methods of soil and plant analysis manual, series No.7. IITA, Ibadan, Nigeria
- IITA (International Institute of Tropical Agriculture, Ibadan, Nigeria). 1979. Selection methods for soil and plant analysis, Manual Series No. 1. Ibadan, Nigeria: IITA.
- Ingram, H.A.P. 1983. Hydrology. In: A.J.P. Gore (Editor), Ecosystems of the World, 4A, Mires, Swamp, Bog, Fen and Moor. Elsevier, Amsterdam, pp. 67-158.
- IRRI (International Rice Research Institute). 1978. Proceedings of the workshop on the genetic conservation of rice. IRRI-IBPGR, Los Baños, Philippines. 54 p.
- Jamin, J.Y. and W. Andriessse. 1993. Discussion synthesis. Pages 8-16 in: Proceedings first Annual Workshop of Inland Valley Consortium. WARDA, Bouake, Côte d'Ivoire, 8-10 October, 1993.
- Janssen, G. and Hemke, K. 2004. Ground water models as civil engineering tools, FEM_MODFLOW, Karlovy Vary, Czech Republic.

- Johnson, A. I. 1967. Specific yield – compilation of specific yields for various materials. US Geol Surv Water-Supply Paper 1662-D, 74 pp
- Johnson, T. J. and Bernard, E. 1984. Crop alternatives to carrots on a sphagnum peat soil. Adaptive research reports 1984 / Rapports de recherches sur l'adaptation. NBDARD; 1984: 68-69.
- Kankam Yeboah, K., Duah, A. A., and Mensah, F. K., 1997. Design and construction of Hund Dug wells at Besease Technical report, Water Research Institute (CSIR), Accra, Ghana. 16 pp.
- Kawaguchi, K. and Kyuma, K. 1977. Paddy soils of tropical Asia, their material nature and fertility. Honolulu, Hawaii: The University Press of Hawaii.
- Killian, J. and Teisseir, J. 1973. Methodes d'investigation pour l'analys culture et le classement des bas-fonds dans quelques regions de l'Afrique de l'ouest. Propositions de classification d'aptitudes de terres á riziculture. L'Agronomie Tropicale 28(2):156-171.
- Klute, A. and Dirkson, C. 1986. Hydraulic conductivity and diffusivity: Laboratory methods. In: Klute A (ed) Methods of soil analysis-Part I. American Society of Agronomy, Madison, USA.
- Krasnostein, A. L. and Oldham, C. E. 2004. Predicting wetland water storage. Water Resour Res 40(10): W10203.1-W10203.12.
- Krause, S. and Bronstert, A. 2005. An advanced approach for catchment delineation and water balance modelling within wetlands and floodplains. Advances in Geosciences, 5:1-5.

Kumar, M., Kumari, K. and Ramathan. A. I. 2007. A comparative evaluation of groundwater suitability for irrigation and drinking purposes in two intensively cultivated districts of Punjab, India. *Environ Geol* (2007) 53:553–574.

Kyei-Baffour, N. and Agodzo, S.K. 1996. Development and management of wetlands. *JUST* 16(3): 3-6

Lerner, D.N., Issar, A. and Simmers, I. 1990. A guide to understanding and estimating natural recharge. Int. Contribution to hydrogeology, I.A.H. Publication, 8, Verlag Heinz Heisse, 345 p.

Lucassen, E.C.H.E.T., Smolders, A.J.P., Van Der Salm, A.L. and Roelofs., J.G.M. 2004. High groundwater nitrate concentrations inhibit eutrophication of sulphate-rich freshwater wetlands. *Biogeochemistry* 00: 249-267.

Mansell, R. S., Bloom., S. A., and Sun., G. 2000. A model for wetland hydrology: description and validation. *Soil Science* 165(5): 384-397.

Maréchal, J.C., Dewandel, B.S., Ahmed., Galeazzi, L. and Zaidi, F. K. 2006. Combined estimation of specific yield and natural recharge in a semi-arid groundwater basin with irrigated agriculture. *Journal of Hydrology* 329:281-293.

Marneweck, G. C. and Batchelor, A. L. 2002. Wetland classification , mapping and inventory. In *Ecological and economic evaluation of wetlands in the Upper Olifants River Catchment*. Eds R W Palmer, J Turpie, GC Marneweck & A L Batchelor. Water Research Commission Report, Rept Number 1162/1/02. Pretoria.

- Martin, N. 2006. Development of a water balance for the Atankwidi catchment, West Africa A case study of groundwater recharge in a semi-arid climate. PhD.Thesis. Ecology and Development Series No. 41,
- Matsumoto, N. 1992. Regression analysis for anomalous changes of groundwater level due to earth quakes. *Geophys. Res. Lett.*, 19(12): 1193-1196.
- McLean, E. O. 1965. Aluminium. In *Methods of soil analysis, Part 2, No. 9*, eds. A. L. Page, R. H. Miller, and D. R. Keeney, 978–998. Madison, Wisconsin: ASA/SSSA.
- Mckee, P. W. and Clark. B . R. 2003. Development and Calibration of a Ground-water Flow Model for the Sparta Aquifer for the southeastern Arkansas and North Central Louisiana and Simulated Response to Withdrawals 1998-2027, U.S. Geological Survey Water-Resources Investigations Report 03-4132.80P.
- Meinzer, O. E. 1923. The occurrence of groundwater in the United States with a discussion of principles. *US Geol Surv Water- Supply Pap* 489, 321 pp.
- Menz, G., and Bethke, M., 2000. Regionalisation of the IGBP Global Land Cover Map for Western Africa (Ghana, Togo and Benin). In: *Proceedings of the 20th EARSeL-Symposium*, June 2000, Dresden, 6p
- Mitsch, W. J. and J. G. Gosselink. 2000. *Wetlands*. Third Edition. Wiley & Sons, New York, 920 pp.
- Moormann, F. R., W. J. Veldkamp and J. C. Ballaux. 1977. The growth of rice on a toposequence — a methodology. *Plant Soils*. 48 p.

Mulligan, M. 2004. Modelling and model building, In: Wainwright J, Mulligan M (eds) Environmental modeling: finding simplicity in complexity. John Wiley, West Sussex, England.

NRC. 1995. Wetlands, Characteristics and Boundaries. National Academy Press, Washington.

Nyarko, B. K. 2007. Floodplain wetland-river flow synergy in the White Volta River basin, Ghana. Ecology and Development Series Bd. 53.

Obropta., C, Kallin., P, Mak, M. and Ravit, B. 2006. Modeling Urban Wetland Hydrology for the Restoration of a Forested Riparian Wetland Ecosystem. Urban Habitats, 5 (1):166-174.

Obuobie, E. 2008. Estimation of groundwater recharge in the context of future climate change in the White Volta River Basin, West Africa. PhD. Thesis. Ecology and Development Series No. 41,

Odeh, T., Salameh. E., Schirmer, M. and Strauch, G. 2009. Structural control of groundwater flow regimes and groundwater chemistry along the lower reaches of the Zerka River, West Jordan, using remote sensing, GIS, and field methods. Environ Geol. 58, 1797–1810.

Ogban, P. I. and Babalola, O. 2009. Characteristics, classification and management of Inland valley bottom soils for crop production in subhumid southwestern Nigeria. Journal of Tropical Agriculture, Food, Environment and Extension. 8:1-13

Opoku-Duah. S., Kankam Yeboah. K. and Mensah, E. K. 2000. Determination of water requirements for producing irrigated rice and other crops in the Afram river valley bottom, Ghana J. Sci, 40: 15-24.

- Owen, C.R. 1995. Water budget and flow patterns in an urban wetland. *Journal of Hydrology* 169(1): 171–187.
- Pareta, R.C. 2004. *Optimisation Modelling for Groundwater and Conjunctive Water Policy*. Water dynamic laboratory, Utah State University Foundation. Utah State University. 191 pp
- Penman, H. L. 1963. *Vegetation and hydrology*. Tech. Comment No. 53, Commonwealth Bureau of Soils, Harpenden, England.
- Penney, B. G., Cox, D. C., Gallagher, C. A. and Salter, A. M. 1991. Vegetable crop research on peat soil – 1991 report. *Agriculture Canada*: 26.
- Piper, A. M. 1944. A graphic procedure in the geochemical interpretation of water analysis. *Trans. Am. Geophys. Union*, 25: 914-923
- Prickett, T. A. 1965. Type-curve solution to aquifer tests under water-table conditions. *Ground Water* 3:5-14.
- Prudic, D. E. 1989. Documentation of a computer program to simulate stream-aquifer relations using a modular, finite-difference, ground-water flow model: U.S. Geological Survey Open-File Report 88-729,113.
- Raj, P. 2004. Classification and interpretation of piezometer well hydrographs in parts of southeastern peninsular India. *Environmental Geology* 46:808–819.
- Rasmussen, W. C. and Andreasen, G. E. 1959. Hydrologic budget of the Beaverdam Creek Basin, Maryland. *US Geol Surv Water- Supply Pap* 1472: 106 p

Ransom, M. D. and Smeck. N. E. 1986. Water table characteristics and water chemistry of seasonally wet soils of southwestern Ohio. *Soil Science Society of America Journal* 50:1281–1289.

Rayment, A. F. 1993. Peat development in Newfoundland : an historic overview . Newfoundland peat opportunities - an international conference; Corner Brook, Newfoundland. Newfoundland and Labrador Peat Association; section 7: 1-11.

Reichle, R. H., McLaughlin, D. B. and Entekhabi, D. 2002. Hydrologic data assimilation with the ensemble Kalman filter. *Monthly Weather Rev* ;130:103–14.

Rennolls, K., Carnell, R. and Tee, V. 1980. A Descriptive model of the relationship between rainfall and Soil water table. *J. Hydrol.*, 47: 103-114.

Risser, D. W., Gburek, W. J. and Folmar, G. J. 2005. Comparison of methods for estimating ground-water recharge and base flow at a small watershed underlain by fractured bedrock in the eastern United States. *US Geol Surv Sci Invest Rep* 2005–5038.

Roulet, N.T. 1990. Hydrology of a headwater basin wetland: groundwater discharge and wetland maintenance. *Hydrol. Processes*, 4: 387-400.

Sanchez, P. A. 1976. Properties and management of soil in the tropics. New York: Wiley.

Sandwidi, W.J.P. 2007. Groundwater potential to supply population demand within the Kompienga dam basin in Burkina Faso. PhD Thesis. Ecology and Development Series, No. 54. Cuvillier Verlag Göttingen. 160pp

- Savva, A.P., Karam, R., Thanki, S.B., Fathi, M. and Awartani M. 1981. Irrigation practices in relation to crop response, water use, and soil salinity. FAO/UNDP/United Arab Emirates. April 1981. 37 p.
- Scanlon, B .R., R.W. Healy. and P. G. Cook. 2002. Choosing appropriate techniques for quantifying groundwater recharge. *Hydrogeology Journal*.10 (1):18–39
- Schot, P. P., Dekker, S. C. and Poot, A. 2004. The dynamic form of rainwater lenses in drained fens. *Journal of Hydrology* **293**: 74-84.
- Seneviratne, A. A. 2007. Development of steady state groundwater flow model in lower Walawala basin-Sri Lanka Integrating GIS remote sensing and numeric groundwater modeling) MSc. Thesis.
- Serrano, S.E. and Unny, T.E. 1987. Predicting groundwater flow in a phreatic aquifer *J. Hydrol.*, 95: 241-268.
- Setter, T.L., Ingram, K.T., Tuong, T.P. 1995. Environmental characterization requirement for strategic research in rice grown under adverse conditions of drought, flooding, or salinity. Pages 3-18 in: *Rainfed lowland rice: Agricultural Research for High-Risk Environment*. Edited by K.T. Ingram, IRRI.
- Sharma, M. L.1989. Groundwater recharge. Balkema, Rotterdam, 323 pp
- Sibanda, T . C., Johannes. N. and Uhlenbrook, S. 2009 Comparison of groundwater recharge estimation methods for the semi-arid Nyamandhlovu area, Zimbabwe. *Hydrogeology Journal* 17 (6).pages
- Siegel, D.I. 1988. The recharge-discharge function of wetlands near Jueau, Alaska: Part I. Hydrogeological investigations. *Ground Water* 26, no. 4: 427-434.

Simmers, I. ed. 1988. Estimation of natural groundwater recharge. NATO ASI Series C 222. Reidel, Dordrecht, 510 pp

Simmers, I. ed. 1997. Recharge of phreatic aquifers in semi-arid areas. Balkema, Rotterdam, 277 pp.

Šimúnek, J., Šejna, M. and van Genuchten, M.Th. 1999. The HYDRUS-2D software package for simulating water flow and solute transport in two-dimensional variably saturated media (version 2.0). U.S. Salinity Laboratory, Riverside, California.

Sinha, B.P. and Sharma, S.K. 1988. Natural groundwater recharge estimation methodologies in India: Estimation of Natural Groundwater. Dordrecht: Reidel. 301-311.

Smakhtin, V. U. and S. C. Piyankarage. 2003. Simulating hydrologic reference condition of coastal lagoons affected by irrigation flows in southern Sri Lanka. *Wetlands* 23:827–834.

Smyth, A.J. and Montgomery, R. F. 1962. Soils and Landuse in Central Western Nigeria. Government Printers, Ibadan, Nigeria, 265 pp.

Sobieraj, J.A., Elsenbeer, H. and Cameron, G. 2004. Scale dependency in spatial patterns of saturated hydraulic conductivity. *Catena*, 55: 49–77.

Sophocleous, M. A. 1991. Combining the soil water balance and water-level fluctuation methods to estimate natural ground water recharge: practical aspects. *Journal of Hydrology* 124: 229–241.

Sophocleous, M. and Perry, C. A. 1985. Experimental studies in natural groundwater – recharge dynamics: the analysis of observed recharge events. *J Hydrol* 81: 297–332

Stephenson, C.R. and Zuzel, J. F. 1981. Groundwater recharge characteristics in a semi arid environment of southwest Idaho. *Journal of Hydrology* Vol 53. pp 213-227.

Su, M., Stolte, W. J., and van der Kamp, G. 2000. Modelling Canadian prairie wetland hydrology using a semi-distributed streamflow model. *Hydrological Processes* **14** : 2405-2422.

Sui, D. Z. and R.C. Maggio.1999. Integrating GIS with hydrological modeling: practices, problems, and prospects *Computers, Environment and Urban Systems* 23 33-51

Takatert, N., Sánchez-Pérez, J. M. and Trémolières, M. 1999. Spatial and temporal variations of nutrient concentration in the groundwater of a floodplain: effect of hydrology, vegetation and substrate. *Hydrological Processes* **13**: 1511-1526.

Thompson, J. R., Sørensen, H. R., Gavin, H. and Refsgaard, A. 2004. Application of the coupled MIKE SHE/MIKE 11 modelling system to lowland wet grassland in southeast England. *Journal of Hydrology* 293: 151-179.

Todd., D. K. 1980. *Groundwater hydrology*, 2nd edn. Wiley, New York, 535 pp

USE PA. 2007. *Water: Wetlands –Wetland Types*. Available at http://water.epa.gov/type/wetlands/types_index.cfm cited on 23rd November, 2007

USGS. 1974. *Quality of surface waters of the United States Water Supply Papers* Nos. 2145-2150.

USSLS. 1954. *Diagnosis and improvement of saline and alkali soils*. USDA, USA

Van Genuchten, MTh. 1978. Numerical solutions of the one-dimensional saturated-unsaturated flow equation. Research Report 78- WR-09. Water Resources Program, Department of Civil Engineering, Princeton University.

Van't Leven, J. A. and Haddad, M. A. 1968. Surface irrigation with saline water on a heavy clay soil in the Medjerda Valley, Tunisia. Institute for Land and Water Management Research, Technical Bulletin No. 54. Netherlands J. Agriculture, Wageningen 15: 281–303.

Viswanathan, M.N. 1983. Recharge characteristics of an unconfined aquifer from the rainfall water-table relationship. *J. Hydrol.*, 70: 233-250.

Vogel, H. J. Hoffmann, H., Leopold, A. and Roth, K. 2005. Studies of crack dynamics in clay soil II. A physically based model for crack formation *Geoderma* 125:213-223.

Wakatsuki, T., Y. Shinmura, E. Otoo. and Olaniyan, G. U. 1998. African-based sawah systems for the integrated watershed management of small inland valleys in West Africa. In *Institutional and technical options in the development and management of small-scale irrigation*, 56–77. Tokyo, Japan: FAO, MAFF Japan, Japan FAO Association.

Watson, K.W. and Luxmoore, R. J. 1986. Estimating macroporosity in a forest watershed by use of a tension intiltrometer. *Soil Sci. Sec. Am. J.*, 50: 578-582.

Wheeler, B.D. 1999. Water and plants in freshwater wetlands. in "Eco-hydrology:Plants and water in terrestrial and aquatic environments", A.J. Baird, R.L. Wilby (Eds.), p 127-180, Routledge, London.

Wilcox, D.A., 2002. Wetland. Available at Microsoft Encarta Reference Library.

[http:// www.ukm.my/ahmadukm/images](http://www.ukm.my/ahmadukm/images). Cited on 15th December, 2007.

Windmeijer, P. N. and Andriessse W. 1993. Inland valleys in West Africa: An agro-ecological characterization of rice-growing environments, Publication 52. Wageningen, Netherlands: ILRI.

Winter, T. C. and Rosenberry, D. O. 1995. The interaction of ground water with prairie pothole wetlands in the Cottonwood Lake area, east-central North Dakota, 1979–1990. *Wetlands* 15:193–211.

Young, P.C. 2001. Database mechanistic modeling and validation of rainfall-flow processes. In Zhang, Y.K. and K.E. Schilling. (2006). Effects of land cover on water table, soil moisture, evapotranspiration, and groundwater recharge: A Field observation and analysis.

Young, P.C. 1974. Recursive approaches to time series analysis. *The institute of Mathematics and its applications – Buletin*. May-June. pp 209-224.

Zhang, R. 1997. Determination of soil sorptivity and hydraulic conductivity from the disk infiltrometer. *Soil Sci. Soc. Am. J.* 61: 1024-1030.

APPENDICES

Appendix A

5.2 Soil Physical Properties

Table 5.1 Particle Size Analysis for the Besease Inland Valley Bottom Site

Profile pit -P11-P14				
Depth of Soil	% Sand	% Silt	% clay	Texture
0-10	31.58	56.42	12	Silt Loam
20-30	17.54	60.46	22	Silt Loam
20-30	38.32	44.58	16.8	Loam
30-40	51.94	36.06	12	Loam
40-50	45.58	36.22	18.2	Loam
50-60	63.9	24.1	12	Sandy Loam
60-70	76.38	17.42	6.2	Loamy Sand
70-80	87.32	10.28	2.4	Sandy

Profile pit -P1-P2				
Depth of Soil	% Sand	% Silt	% clay	Texture
0-10	63.04	34.96	2	Sandy Loam
20-30	62.06	35.74	2.2	Sandy Loam
20-30	63.34	31.66	5	Sandy Loam
30-40	63.92	29.88	6.2	Sandy Loam
40-50	61.76	31.84	6.4	Sandy Loam
50-60	60.14	31.86	8	Sandy Loam
60-70	59.34	32.66	8	Sandy Loam
70-80	65.6	28.2	6.2	Sandy Loam
80-90	80.58	17.42	2	Loamy Sand
90-100	87.58	10.42	2	Sand
100-110	95.12	2.88	2	Sand
110-120	96.69	1.04	2	Sand
120-130	97.76	0.24	2	Sand

Profile pit -P7-P8

Depth of Soil	% Sand	% Silt	% clay	Texture
0-10	17.2	69.2	13.6	Silt Loam
20-30	15.84	65.96	18.2	Silt Loam
20-30	21.02	60.98	18	Silt Loam
30-40	27.16	50.74	22.1	Silt Loam
40-50	31.38	45.62	23	Loam
50-60	34.96	47.84	17.2	Silt Loam
60-70	40.82	42.18	17	Loam
70-80	45.68	40.42	13.9	Loam
80-90	59.64	35.36	5	Sandy Loam
90-100	84.74	13.26	2	Loamy Sand

Profile pit -13-P14

Depth of Soil	% Sand	% Silt	% clay	Texture
0-10	65.22	32.78	2	Sandy Loam
20-30	64.18	31.82	4	Sandy Loam
20-30	59.96	34.04	4	Sandy Loam
30-40	57.04	37.16	5.8	Sandy Loam
40-50	56.34	34.46	9.2	Sandy Loam
50-60	55.74	35.86	8.4	Sandy Loam
60-70	56.84	34.76	8.4	Sandy Loam
70-80	56.84	34.76	8.4	Sandy Loam
80-90	57.38	33.82	8.8	Sandy Loam
90-100	54.38	39.82	5.8	Sandy Loam
100-110	54.68	39.52	5.8	Sandy Loam
110-120	60.76	33.44	5.8	Sandy Loam
120-130	62.96	33.84	3.2	Sandy Loam

6.5 Horizontal Hydraulic Gradient between Selected Piezometers in Besease Wetland Site

Months	P2 & P1	P2 & P10	P2 & P14	P2 & P13	P3 & P 11	P7 & P11
January 09	0.00497	0.001078	0.005488	0.0010792	0.000592	0.00015987
February 09	0.004327	0.00506	0.00792	0.0001535	-0.00178	0.000033
March 09	0.013646	0.012053	0.002776	0.0004879	0.002672	0.00146983
April 09	0.009291	0.010276	0.001326	0.0005424	0.003571	0.0015353
May 09	0.006156	0.004545	-0.00021	-0.000589	0.000802	-0.0010877
June 09	0.007021	0.005655	0.000456	0.00009461	0.002419	0.0011313
July 09	0.012177	0.006486	0.003574	0.0021397	0.002958	0.00237629
August 09	0.003135	0.002485	0.001468	0.0013993	-0.00083	0.00029437
September 09	0.001826	0.001323	0.002591	0.0009752	-0.0023	-0.0001741
October 09	0.011877	0.006761	0.002558	0.0016348	0.000281	-0.000052
November 09	0.012222	0.005054	0.002399	0.0007679	0.000629	0.00092169
December 09	0.010763	0.002727	0.001572	0.0000974	-0.00244	0.00077146
January 10	0.003348	0.003614	0.000694	-0.000972	-0.00347	0.00059839
February 10	0.002282	0.007281	-0.00019	-0.000931	-0.00573	-0.0028082

Appendix B

Computer Programme Used for the Research

MATLAB 7.8.0 (2009a)

Codes for Kalman Filtering Scheme based on the present day rainfall

```
%% State - Space Equations
% State equation is given by  $x = Fx + wk$ 

% Observation Equation is  $y = Hx + vk$ 

% where the observation time step is different from the integration
% time step

%%
%% initialization
%*****
*****

%definition of time steps
duration = 365; %length of experiment
dt = 1; %time step between observations (equivqlent to 48 hours)
delta_t = (2/48); %Integration time step (equivqlent to 2 hours)

%Coefficient matrices`
F = [1 0 0;0 1 0;0 0 1]; %state matrix

%definition of parameters
xo = [0.05;0.05;0.05];
xdim = 3; ydim = 1;

Rk = 0.002; %
%C = [0 0.01 0];
%Qk = diag(C);
Qk = 0.01*eye(xdim);
%Pk = 500*ones(xdim);
Pk = 500*eye(xdim);
%}

x = xo;
xtrue = [ ];
ztrue = [ ];

%%
```

```

%% Generating the truth
% *****
% {-
for t = 0:dt:duration
    %prediction of true state
    for int = 0:delta_t:dt
        x = F*x + sqrt(Qk)*randn(xdim,1);
    end
    xtrue = [xtrue x];

    %predicting the truth (observation)
    % y = H*x + sqrt(Rk)*randn(ydim,1);
    % ztrue = [ztrue y];
end
% }

% {-
ztrue = load('Groundwater height.txt');
% }

%%
%% Kalman Filtering
% *****
% *****
load('stream.txt')
mydate = stream(:,1:3);
grounddate = datenum(mydate);
load('river.txt')
yourdate = river(:,1:3);
workdate = datenum(yourdate);
est_x = [ ];
uncertainty = [ ];
track_Pk = [ ];
x_est = x0;
M = [ ];
errM = [ ];

for t = 2:length(ztrue)

    for int = 1:length(0:delta_t:dt)
        %prediction of true state
        x_est = F*x_est;

        %prediction of covariance matrix
        Pk = F*Pk*F' + Qk;
        track_Pk = [track_Pk diag(Pk)];
    end

    %measurement operator

```

```

H = [ztrue(t-1,1) ztrue(t,2) 1];

%predicting the Kalman Gain
Kk = Pk*H'*inv(H*Pk*H' + Rk);

%update the state estimate
x_est = x_est + Kk*(ztrue(t) - H*x_est);
est_x = [est_x x_est];

%update covariance matrix
Pk = (eye(xdim) - Kk*H)*Pk;
uncertainty = [uncertainty diag(Pk)];
M(:,t-1) = H * est_x(:,t-1);
errM(:,t) = (ztrue(t,1) - M(:,t-1));
% errM(:,t)=sqrt(sum(ztrue(t,1)(:)-M(:,t)(:)).^2)/numel(ztrue(t,1));
%errM(:,t) = sqrt(mean((ztrue(t,1)(:)-M(:,t)(:)).^2));
track_Pk = [track_Pk diag(Pk)];
end

%% Plots of the truth
%*****
*****

%{-
figure(1)
plot(grounddate,est_x(1,:))
datetick('x',12),axis tight
xlabel('months')
ylabel('A1')

figure(2)
plot(grounddate,est_x(2,:))
datetick('x',12),axis tight
xlabel('months')
ylabel('A2')

figure(3)
subplot(2,1,1)
plot(grounddate,est_x(3,:))
datetick('x',12),axis tight
xlabel('months')
ylabel('A3')
subplot(2,1,2)
plot(workdate,errM(1,:), 'r')
datetick('x',12),axis tight
xlabel('months')
ylabel('error (m)')

```

```

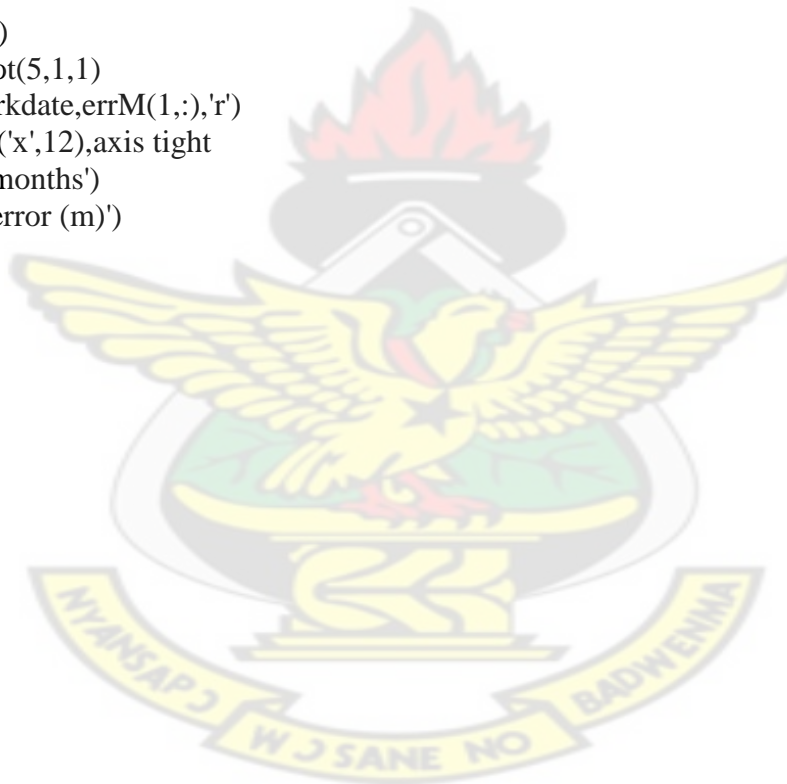
figure(5)
subplot(2,1,1)
plot(grounddate,M(1:,:),'r.-')
datetick('x',12),axis tight
hold on
plot(workdate,ztrue(:,1),'b.-')
datetick('x',12),axis tight
legend('Estimated','Observed')
xlabel('months')
ylabel('Hydraulic head (m)')
subplot(2,1,2)
plot(workdate,ztrue(:,2),'g')
datetick('x',12),axis tight
xlabel('months')
ylabel('Rainfall (mm)')

```

```

figure(6)
%subplot(5,1,1)
plot(workdate,errM(1:,:),'r')
datetick('x',12),axis tight
xlabel('months')
ylabel('error (m)')
%}

```



Appendix C

Modification of Original Kalman Filter Computer Programme by Researcher for Previous Seven Days

MATLAB 7.8.0 (2009a)

Codes for Kalman Filtering Scheme based on the previous seven days rainfall

```
%% State - Space Equations
% State equation is given by  $x = Fx + wk$ 

% Observation Equation is  $y = Hx + vk$ 

% where the observation time step is different from the integration
% time step

%%
%% initialization
% *****
*****

% {-
% definition of time steps
duration = 365; % length of experiment
dt = 1; % time step between observations (equivqlent to 48 hours)
%n = 730 ; % length of simulation
delta_t = (2/48); % Integration time step (equivqlent to 2 hours)

% definition of parameters
xo = [0.05;0.05;0.05;0.05;0.05;0.05;0.05;0.05];
xdim = 9; ydim = 1;
F = eye(xdim); % state matrix
Rk = 0.002; % Nin_noise_m^2;
C = [0.02 0.01 0.01 0.01 0.001 0.001 0.001 0.0 0.00001];
Qk = diag(C);
%Qk = 0.00*eye(xdim);
%Pk = 500*ones(xdim);
Pk = 500*eye(xdim);
% }

x = xo;
xtrue = [ ];
ztrue = [ ];

%%
```

```

%% Generating the truth
% *****
% { -
for t = 0:dt:duration
    %prediction of true state
    for int = 0:delta_t:dt
        x = F*x + sqrt(Qk)*randn(xdim,1);
    end
    xtrue = [xtrue x];

    %predicting the truth (observation)
    % y = H*x + sqrt(Rk)*randn(ydim,1);
    % ztrue = [ztrue y];
end
% }

% { -
ztrue = load('Groundwater height.txt');
% }

%%
%% Kalman Filtering
% *****
% { -
load('spring.txt')
mydate = spring(:,1:3);
juliandate = datenum(mydate);
load('river.txt')
yourdate = river(:,1:3);
workdate = datenum(yourdate);
est_x = [ ];
uncertainty = [ ];
track_Pk = [ ];
x_est = xo;
M = [ ];
errM = [ ];
for t = 7:length(ztrue)

    for int = 1:length(0:delta_t:dt)
        %prediction of true state
        x_est = F*x_est;

        %prediction of covariance matrix
        Pk = F*Pk*F' + Qk;
        track_Pk = [track_Pk diag(Pk)];
    end

    %measurement operator

```

```
H = [ztrue(t,2) ztrue(t-1,2) ztrue(t-2,2) ztrue(t-3,2) ztrue(t-4,2) ztrue(t-5,2) ztrue(t-6,2) ztrue(t-1,1) 1];
```

```
%predicting the Kalman Gain
Kk = Pk*H'*inv(H*Pk*H' + Rk);
```

```
%update the state estimate
x_est = x_est + Kk*(ztrue(t) - H*x_est);
est_x = [est_x x_est];
```

```
%update covariance matrix
Pk = (eye(xdim) - Kk*H)*Pk;
uncertainty = [uncertainty diag(Pk)];
M(:,t-6) = H * est_x(:,t-6);
errM(:,t-6) = (ztrue(t,1) - M(:,t-6));
track_Pk = [track_Pk diag(Pk)];
```

```
end
```

```
%%
%% Plots of the truth
%*****
*****
```

```
%{-
figure(1)
subplot(2,1,1)
plot(juliandate,est_x(1,:))
datetick('x',12),axis tight
xlabel('months')
ylabel('A1')
subplot(2,1,2)
plot(juliandate,est_x(2,:))
datetick('x',12),axis tight
xlabel('months')
ylabel('A2')
```

```
figure(2)
subplot(2,1,1)
plot(juliandate,est_x(3,:))
datetick('x',12),axis tight
xlabel('months')
ylabel('A3')
subplot(2,1,2)
plot(juliandate,est_x(4,:))
datetick('x',12),axis tight
xlabel('months')
ylabel('A4')
```

```
figure(3)
```

```

subplot(2,1,1)
plot(juliandate,est_x(5,:))
datetick('x',12),axis tight
xlabel('months')
ylabel('A5')
subplot(2,1,2)
plot(juliandate,est_x(6,:))
datetick('x',12),axis tight
xlabel('months')
ylabel('A6')

```

```

figure(4)
subplot(2,1,1)
plot(juliandate,est_x(7,:))
datetick('x',12),axis tight
xlabel('months')
ylabel('A7')
subplot(2,1,2)
plot(juliandate,est_x(8,:))
datetick('x',12),axis tight
xlabel('months')
ylabel('A8')

```

```

figure(5)
subplot(2,1,1)
plot(juliandate,est_x(9,:))
datetick('x',12),axis tight
xlabel('months')
ylabel('A9')
subplot(2,1,2)
plot(juliandate,errM(1,:),'r')
datetick('x',12),axis tight
xlabel('months')
ylabel('error (m)')

```

```

figure(8)
subplot(2,1,1)
plot(juliandate,M(1,:),'r.-')
datetick('x',12),axis tight
hold on
plot(workdate,ztrue(:,1),'b.-')
datetick('x',12),axis tight
xlabel('months')
ylabel('Hydraulic head (m)')
legend('Estimated','Observed')

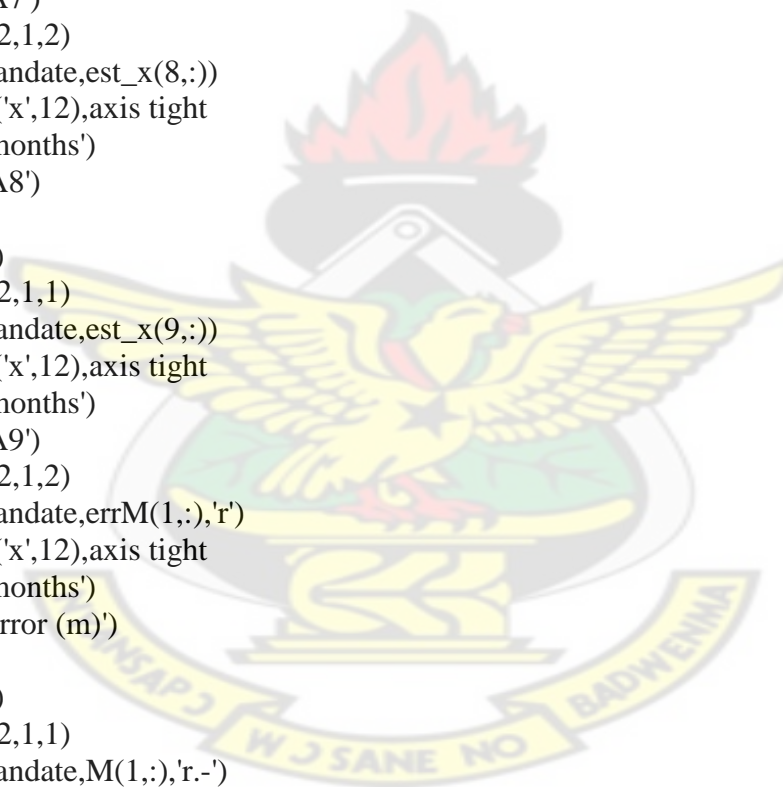
```

```

subplot(2,1,2)
plot(workdate,ztrue(:,2),'g')
datetick('x',12),axis tight
xlabel('months')

```

KNUST



```
ylabel('Rainfall (mm)')  
  
figure(9)  
%subplot(5,1,1)  
plot(juliandate,errM(1,:), 'r')  
datetick('x',12),axis tight  
xlabel('months')  
ylabel('error (m)')  
% }
```

KNUST

